Vol. 96 No. 2 February 1, 1978
Completing Vol. 96

ISSN 0003-2670

ANALYTICA CHIMICA ACTA

International journal devoted to all branches of analytical chemistry

ELSEVIER SCIENTIFIC PUBLISHING COMPANY

ANALYTICA CHIMICA ACTA

International journal devoted to all branches of analytical chemistry
Revue internationale consacrée à tous les domaines de la chimie analytique
Internationale Zeitschrift für alle Gebiete der analytischen Chemie

PUBLICATION SCHEDULE FOR 1978 (incorporating the section on Computer Techniques and Optimization).

	J	F	M	A	M	J	J	A	S	O	N	D
Analytica Chimica Acta	96/1	96/2	97/1	97/2	98/1	98/2	99/1	99/2	100	101/1	101/2	102
Section on Computer Techniques and Optimization			103/1			103/2			103/3			103/3

Scope. *Analytica Chimica Acta* publishes original papers, short communications, and reviews dealing with every aspect of modern chemical analysis, both fundamental and applied. The section on *Computer Techniques and Optimization* is devoted to new developments in chemical analysis by the application of computer techniques and by interdisciplinary approaches, including statistics, systems theory and operation research.

Submission of Papers. Manuscripts (three copies) should be submitted to:
for *Analytica Chimica Acta:* Dr. A.M.G. Macdonald, Department of Chemistry, The University, P.O. Box 363, Birmingham B15 2TT, England;
for the section on *Computer Techniques and Optimization:* Dr J.T. Clerc, Laboratorium für Organische Chemie, Swiss Federal Institute of Technology, Universitätstrasse 16, CH-8092 Zürich, Switzerland.

Information for Authors. Papers in English, French and German are published. There are no page charges. Manuscripts should conform in layout and style to the papers published in this Volume. Authors should consult Vol. 93, p. 379 for detailed information. Reprints of this information are available from the Editors or from: Elsevier Editorial Services Ltd., Mayfield House, 256 Banbury Road, Oxford OX2 7DE (Great Britain).

Reprints. Fifty reprints will be supplied free of charge. Additional reprints (minimum 100) can be ordered. An order form containing price quotations will be sent to the authors together with the proofs of their article.

Advertisements. Advertisement rates are available from the publisher.

Subscriptions. Subscriptions should be sent to: Elsevier Scientific Publishing Company, P.O. Box 211, Amsterdam, The Netherlands. The section on *Computer Techniques and Optimization* can be subscribed to separately.

Publication. *Analytica Chimica Acta* (including the section on *Computer Techniques and Optimization*) appears in 8 volumes in 1978. The subscription for 1978 (Vols. 96–103) is Dfl. 1000.00 plus Dfl. 120.00 (postage) (Total approx. US $457.14). The subscription for the *Computer Techniques and Optimization* section only (Vol. 103) is Dfl. 125 plus Dfl. 15.00 (postage) (Total approx. US $57.14). Journals are sent automatically by air mail to the U.S.A. and Canada at no extra cost and to Japan, Australia and New Zealand for a small additional postal charge. All earlier volumes (Vols. 1–87) are available at Dfl. 115.- (plus postage).

Claims for issues not received should be made within three months of publication of the issue, otherwise they cannot be honoured free of charge.

Printed in The Netherlands

Sulfur, Energy, and Environment

BEAT MEYER, *Chemistry Department, University of Washington, Seattle, U.S.A.*

This interdisciplinary book describes the properties of sulfur and deals with those aspects of production, use and recovery of sulfur which are important in relation to energy production and environmental protection. Supported by 94 figures, 72 tables and 1500 references, the 15 chapters present a short introduction, a critical review and a reference guide in 14 major areas of the field. A large number of topics are highlighted, such as sulfur based materials and their potential for future utilization, problems of waste and legislation at the interface of scientific and societal concern, and the extensive use of sulfur in agriculture and food preparation. In addition to presenting trends in energy uses, sources, and technology, and trends in the supply and demand of sulfur compounds, the concluding chapter discusses the relationship between scientific initiative and industrial and public demands.

Designed for specialists and non-specialists, this book will serve as a valuable reference guide for scientists, engineers, civil servants, managers, political and social scientists, and lawyers connected with practical or theoretical work involving sulfur.

CONTENTS: **Chapters 1. Introduction. 2. History. 3. Properties.** Elemental Sulfur. Hydrogen Sulfide, Polysulfides, and Sulfanes. Sulfur Oxides and Oxyacids. Corrosion. **4. Analytical Chemistry.** Quantitative Analysis of Total Sulfur. Qualitative Analysis. Sulfur Isotopes. Impurities in Elemental Sulfur. **5. Occurrence and Sources of Sulfur.** Natural Deposits. Secondary Sources. **6. The Sulfur Cycles.** The Global Sulfur Cycle. Hydrosphere. Atmospheric Sulfur Budget. The Anthropogenic Sulfur Cycle. **7. Sulfur Production.** Production of Elemental Sulfur. By-Product Sulfur. **8. Recovery from Combustion Gases.** Coal Combustion Chemistry. Abatement Methods. Abatement Chemistry. **9. Environmental Control and Legislation.** Waste, Disposal, and Education. Air Pollution Legislation. **10. Medical Use and Health Effects.** Elemental Sulfur. Hydrogen Sulfide. Sulfides. Thiosulfate. Polythionates. Sulfite. Sulfur Dioxide. **11. Sulfur in Agriculture and Food.** Sulfur in Agriculture. Sulfur as Fungicide and Insecticide. Sulfur in the Food Industry. **12. Industrial Uses of Sulfur and Its Compounds. 13. Sulfur Polymers.** Polymeric Elemental Sulfur. Inorganic Polymers. Organic Polymers. Polymer Mixtures and Blends. **14. Sulfur Containing Materials.** Sulfur-Asphalt. Sulfur-Concrete. Sulfur Foam. Cardboard. Wood-Sulfur Products. Batteries. Sulfur Impregnated Ceramics. Application of Sulfur Compositions. **15. Future Trends.** Sulfur, Energy, and Environment. Chemistry, Government, and Education. Conclusions. **Appendix. Bibliography. Author Index. Subject Index.**

June 1977 xii + 448 pages US $39.60/Dfl. 97.00 ISBN 0-444-41595-5

The Dutch guilder price is definitive. US $ prices are subject to exchange rate fluctuations.

ELSEVIER

P.O. Box 211, Amsterdam
The Netherlands
52 Vanderbilt Ave
New York, N.Y. 10017

Special Topics in Electrochemistry

edited by P. A. ROCK, *Department of Chemistry, University of California, U.S.A.*

In the last decade the field of electrochemistry has undergone rapid expansion. Several factors have contributed to this expansion but the major ones are undoubtedly the energy shortages, the desire for higher quality environments, and the greatly expanded efforts to understand bioelectric phenomena. Because of the rapid expansion of research efforts in electrochemistry, significant gaps have developed between the coverage of electrochemistry in existing chemistry textbooks and the research literature. The aim of this book is to bridge these gaps in several of the subfields of electrochemistry.

The material in this book is based mainly on papers presented at the Symposium entitled "Teaching of Electrochemistry" which was held on August 31, 1976 at the 172nd ACS Meeting in San Francisco, California. The symposium was sponsored by the Division of Chemical Education, Inc.

The level of presentation and the extent of the coverage of the various topics have been designed especially for senior and first-year graduate students who wish to survey the various research areas of contemporary electrochemistry. This work is also intended for chemistry teachers who wish to update and expand the coverage of electrochemistry in their courses.

CONTENTS: 1. Advanced Electrochemical Energy Systems *(L. R. McCoy).* 2. Photovoltaic Phenomena in Electrochemical Cells *(H. Gerischer).* 3. Electrochemical Synthesis *(Charles K. Mann and Margaret R. Asirvatham).* 4. Electrochemical Cells Without Liquid Junction *(Peter A. Rock).* 5. Species-Selective Electrochemical Sensors *(Peter A. Rock).* 6. Mechanisms of Electrochemical Oscillations *(Joel Keizer).* 7. Electrochemistry of Nerves *(Walter J. Moore).* 8. Theory and Applications of Electron Transfers at Electrodes and in Solution *(R. A. Marcus).* 9. On the Theory of Overvoltage for Electrode Processes Possessing Electron Transfer Mechanism *(R. A. Marcus).* 10. Electrostatic Free Energy and Other Properties of States Having Non-Equilibrium Polarization: Electrode Systems *(R. A. Marcus).*

Sept. 1977 viii + 224 pages US $39.50/Dfl. 97.00 ISBN 0-444-41627-7

ELSEVIER

P.O. Box 211, Amsterdam
The Netherlands
52 Vanderbilt Ave
New York, N.Y. 10017

The Dutch guilder price is definitive. US $ prices are subject to exchange rate fluctuations.

7058

Analytica Chimica Acta, 96 (1978) 229—241

THE DETERMINATION OF CADMIUM, COPPER, IRON, LEAD AND ZINC IN AEROSOLS BY ATOMIC-ABSORPTION SPECTROMETRY

P. GELADI and F. ADAMS*

Department of Chemistry, University of Antwerp (U.I.A.), 2610 Wilrijk (Belgium)

(Received 2nd September 1977)

SUMMARY

The determination of five elements in filter papers loaded with air particulate matter has been investigated. After a wet destruction of about 10 cm^2 of filter material by a standard procedure, analysis was carried out with a flame atomic absorption method for zinc and a flameless procedure for Cd, Cu, Fe and Pb. Furnace program parameters for each of the elements in different acid solutions are reported. The interferences of some common anions and the most abundant cations in aerosol material are described. For some urban and industrial samples, the results are compared with those obtained by energy-dispersive x-ray fluorescence. Accuracy was checked against standard samples.

Many natural and industrial processes and activities generate particulate air pollution. For the characterization of the air particulate matter in a number of urban and industrial environments a combination of energy-dispersive x-ray fluorescence [1] and atomic absorption spectrometry is used. The present paper describes the determination of Cd, Cu, Fe, Pb and Zn. The atomic-absorption spectrometric determination of aluminium has already been reported [2].

The elements in the environment can be classified, according to their toxicity, as harmless, toxic and very abundant, and toxic but rare [3]. Iron is classified among the harmless and necessary elements, while Cd, Cu, Pb and Zn are classified as toxic and abundant. This is especially true for cadmium and lead, which are no use to human metabolism. For air particulate matter, lung hazards are considered to exist for all five of the above-mentioned elements [4].

Emission spectrometry [5], x-ray fluorescence [1], neutron activation analysis [6] and atomic-absorption spectrometry [7] have been used for the determination of trace elements in airborne particulate matter collected on different types of filter media. Recently, atomic-absorption spectrometry has often been applied [8—14], despite its drawback of being a mono-element technique.

For the destruction of the samples, different types of acid mixtures in combination with low- and high-temperature ashing may be used. For the present work, the nitric—perchloric acid digestion method issued by the

Belgian Institute of Standardization [15], was adopted as being most convenient. This procedure gives a quick and complete destruction of the filter paper and the organic material on it without losses of volatile elements such as Cd, Pb and Zn. The solution obtained can be used for the determination of Cd, Cu, Fe, Pb, Zn and possibly also Mn and Ni.

For the final analysis, the well-established flame procedures are relatively easy and free from interferences; the flame determination of the five elements could be readily adapted from existing literature information. The flameless procedures are more sensitive and consume less sample, but the manufacturers' specifications and literature information are inadequate, so that the whole procedure had to be checked carefully. The furnace programs had to be established and especially the ashing and atomization conditions had to be optimized. The problems of pre-atomization losses and atomization yield have been discussed by several workers [16—20]. Various attempts have been made [21—25] to analyse the problems and provide suitable solutions. The present work was directed towards providing practical solutions to the problems of furnace programming without going too far into theoretical considerations. Other severe problems include the interferences which might arise. These interferences are usually subdivided into groups such as spectral line broadening, ionization, matrix, background, chemical and non-atomic absorption. A more practical approach can be based on the most abundant elements present in aerosols and on the acids used without attempts to classify the interferences, which are usually the sum of many different complex phenomena e.g. [26, 27].

Particular attention was paid to the establishment of calibration graphs and to the choice between calibration graphs and standard addition. A compromise was found between standard addition, which gives good results but is time-consuming, and the calibration curve method, which is faster but subject to errors because samples and standard solutions may differ considerably in composition. A more practical method is to take a number of standards through the decomposition procedure. Several different calibration standards were analyzed carefully for the assessment of accuracy. For routine analysis of urban and industrial aerosols, some comparisons are given between flame and flameless a.a.s. and energy-dispersive x.r.f.

EXPERIMENTAL

Apparatus

A Perkin-Elmer 503 atomic-absorption spectrometer was used, in combination with a PE HGA-74 graphite furnace atomizer. Absorbances were read as peak height from a Hitachi-Perkin-Elmer 56 strip-chart recorder and from the built-in peak-read device of the spectrometer. The furnace was flushed with argon (l'Air Liquide N46) at a flow rate of 300 ml min^{-1} internally and 900 ml min^{-1} externally. The gas flow could be changed during the atomization stage to increase sensitivity, by means of the stopped (Gas-Stop), reduced (Mini-Flow) and continuous flow settings.

Solutions were injected with Eppendorf micropipettes with disposable polypropylene tips. Deuterium background correction was done with a Perkin-Elmer 303-0875 system.

The Perkin-Elmer 503 spectrometer was also used for flame analyses with a 10-cm single-slot burner with acetylene (l'Air Liquide N 25) as fuel and compressed air as oxidant.

The spectral light sources used are listed in Table 1, together with their wavelengths and the conventional sensitivities obtainable with the graphite furnace. For all measurements of sensitivity in this Table, the gas-stop mode was used in the atomization step, except for iron where large concentrations were expected so that high sensitivity was unnecessary. The useful range is defined as the range between the lowest value that can be read easily without scale expansion and the upper limit of linearity; between these limits the precision of the measurements is better than 5%. For the flame, conventional sensitivities are 38 ppb for Cd at 228.8 nm, 79 ppb for Cu at 324.8 nm, 84 ppb for Fe at 248.3 nm, 0.68 ppm for Pb at 283.3 nm and 36 ppb for Zn at 214.0 nm. For the graphite furnace, the volume injected, the wavelength and the gas-flow during atomization can be adjusted to adapt the sensitivity

TABLE 1

Characteristics of spectral light sources

Element	Hollow-cathode lamp	Lamp current (mA)	Wavelength[a] (nm)	Sensitivity[b] (pg)	Useful range (ng)
Cd	PE 303-6016	8	228.8	1.7	0.003—0.100
			326.1	704	
	PE 303-6216[c]	5W	228.8	0.8	0.002—0.080
			326.1	330	
Cu	PE 303-6024	15	324.8	15	0.1—10
	PE 303-6110[d]	30	327.4	30	0.2—20
	PE 303-6103[d]	30	216.5	150	1—50
			222.6	7300	50—2000
Fe	PE 303-6110	30	248.3	88	0.5—20
	PE 303-6103	30	372.0	450	5—100
			344.1	900	10—150
			305.9	12000	20—100
			346.6	9000	100—1000
Pb	PE 303-6039	10	217.0	90	0.25—6
			283.3	175	0.5—10
			261.4	1800	50—1000
			368.4	4500	100—3500
Zn	PE 303-6081	15	214.0	—	—
			307.6	90	1.0—25

[a]The wavelength most often used is underlined. [b]Defined as the amount of material for which $A = 0.0044$. [c]Electrodeless discharge lamp. [d]Multi-element lamps: Cr, Co, Cu, Fe, Mn, Ni for 6106; Al, Ca, Cu, Fe, Mg, Si, Zn for 6110.

as appropriate. For the flame measurement, aspiration speed and burner height must remain optimized for minimal flame noise and only the wavelength can be selected. The 217.0-nm lead line was not used because of possible spectral interferences [28]. The 213.0-nm zinc line is too sensitive for use with the furnace.

Reagents

Standard stock solutions of the elements investigated were prepared from Merck Titrisol (1000 ppm) solutions. For investigations of furnace parameters and interferences, the acids and salts used were of analytical-reagent grade. Suprapur-grade acids were used for destruction of the filter samples, in order to minimize blanks. All dilutions were made with doubly-distilled water from quartz apparatus. Acidified (ca. 0.1 M) dilute solutions could be stored for several weeks without losses. Neutral solutions showed considerable losses by adsorption onto the glass vessels [29]. Dilute solutions were therefore remade regularly.

Sampling procedures

The aerosols were collected on Whatman 41 filter paper (110-mm diameter) with a high-volume sampler as described by Dams and Heindryckx [30], and with a low-volume sampler consisting of a Millipore XX-60-220-50 vacuum pump, a Schleicher and Schüll FP 050/2 (50-mm diameter) filter holder and a Contigea SG6 gas meter. Total loading of the filters was normally between 100 and 5000 $\mu g\ cm^{-2}$ with an average value of 800 $\mu g\ cm^{-2}$.

Procedure for decomposition

About 10 cm^2 of aerosol-loaded filter paper was pre-treated with 7.5 ml of boiling concentrated nitric acid. Then, 5 ml of perchloric acid was added and heating was continued until the solution was clear and colourless. The excess of acid was boiled off and the dry material was redissolved in 2.5 ml of nitric acid and 10 ml of water by gentle heating. The solution obtained was cooled and diluted to 50 ml in a graduated flask. Known amounts of standard and filter paper blanks were taken through the whole procedure. The volumes of acid added for heavily loaded filters can be adapted to the amount of material to be decomposed. The final volume can be reduced when very low concentrations are expected.

Furnace programs

For the five elements investigated, furnace parameters were established for different commonly used acid media. Ashing losses were measured as a function of the ashing temperature, and the atomization yield as a function of the atomization temperature, with all other parameters constant, under the conditions giving the highest sensitivity. The results obtained (Fig. 1) should also be applicable for other wavelengths and gas-flow settings. Usually, the influence of the acid on the atomization yield is small, so that a common

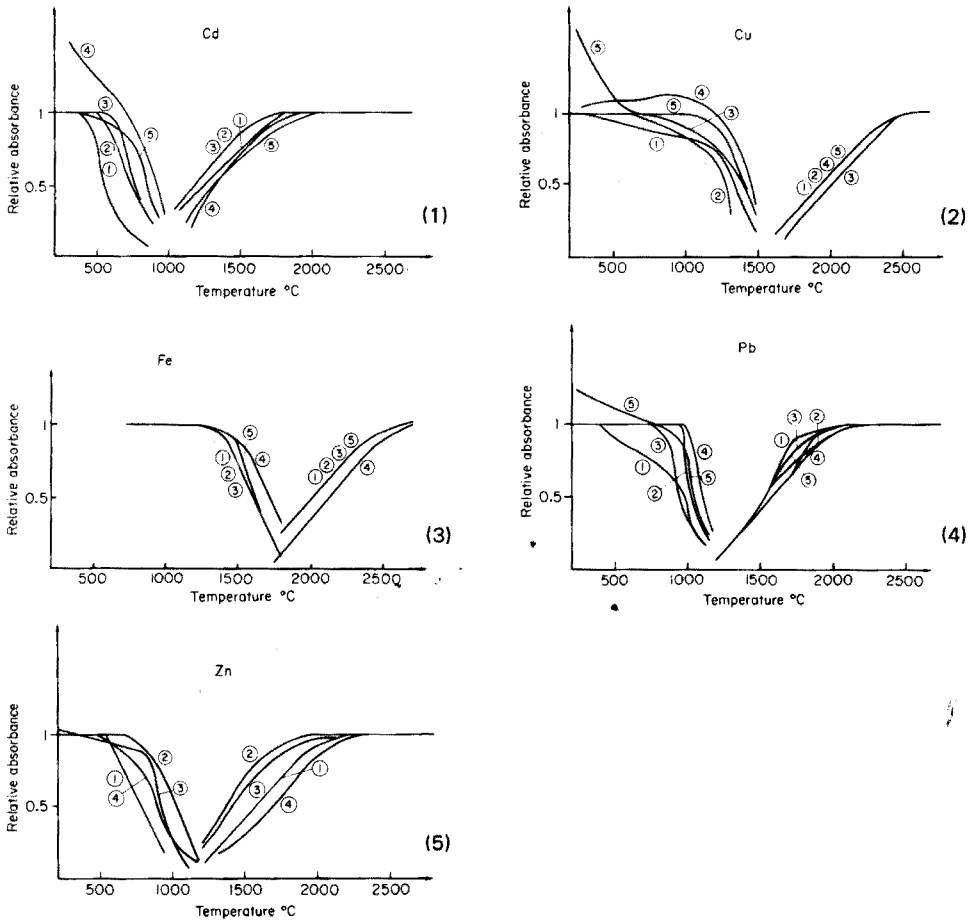

Fig. 1. Ashing and atomization curves for 0.1 N acid solutions: (1) HCl; (2) HNO_3; (3) H_2SO_4; (4) $HClO_4$; (5) H_3PO_4. Cd: 20 μl of 2.5-ppb solution injected. Cu: 20 μl of 0.1-ppm solution injected. Fe: 20 μl of 0.25-ppm solution injected. Pb: 20 μl of 0.1-ppm solution injected. Zn: 20 μl of 10-ppm solution injected; zinc absorption was not measurable in H_3PO_4 solution.

atomization temperature can be found for the different acid media. For the more volatile elements, Cd, Pb and Zn, there is a wide range of possible atomization temperatures but for Cu and Fe the atomization temperature should be close to the maximum temperature of the furnace so that there is little choice. For the ashing step, the effect of the acids varies widely. The choice of a suitable ashing temperature is difficult, but ashing cannot be avoided because acids of high boiling point may volatilize during the atomization step with volatilization of the element to be determined; also, acid fumes may cause light scattering. Figure 2 shows examples of the ashing losses as a function of time at different temperatures for iron in 0.1 N hydrochloric

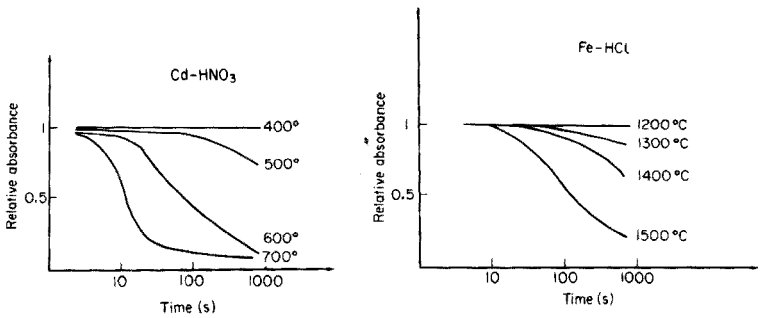

Fig. 2. Ashing losses as a function of ashing time for 2.5 ppb Cd in 0.1 N HNO_3 and for 0.25 ppm Fe in 0.1 N HCl at different ashing temperatures; 20 μl injected.

acid and cadmium in 0.1 N nitric acid. Similar experiments were performed for all five elements in the different acid media. Table 2 shows the maximum temperatures at which no ashing losses occurred as a function of time.

The samples were always dried at 100°C and the drying time (s) was selected as twice the injected volume (μl). Clean-up was done at 2700°C until disappearance of memory effects, usually after 10 s for Cd, Pb and Zn and 15—20 s for Cu and Fe. The different furnace parameters finally adopted are given in Table 3. For the ashing time, the amount of material to be ashed is important. With the prior acid decomposition, an ashing time of 20 s was chosen, because the furnace normally took 5—8 s to reach its preset temperature. The atomization time depends on atomization kinetics. Usually, the peak maximum was reached after 2—5 s, hence an atomization time of 10 s was selected.

Interferences

The possible interferences of the various ions that are most abundant in air particulate matter were studied. Because acids were used for decomposition of samples and for stabilization of dilute solutions, anion interferences were investigated for HCl, HNO_3, H_2SO_4, $HClO_4$ and H_3PO_4. The absorbance loss relative to neutral solutions as a function of acid normality is shown in Fig. 3. For the study of the cation interferences, Na, K, Mg and Pb were added as

TABLE 2

Maximum temperatures (°C) for zero ashing losses as a function of time

Element	HCl	HNO_3	H_2SO_4	$HClO_4$	H_3PO_4
Cd	300	400	500	600	600
Cu	800	800	900	1100	900
Fe	1200	1200	1200	1400	1300
Pb	600	700	700	900	800
Zn	600	700	700	600	—

TABLE 3

Furnace program parameters chosen for routine analysis

Parameter	Cd	Cu	Fe	Pb	Zn
Ashing temperature (°C)[a]	400	800	1200	500	600
Atomization temperature (°C)[b]	2300	2600	2500	2500	2400

[a]20-s ashing time. [b]10-s atomization time.

nitrate and Ca, Al and Fe as chloride up to concentration ratios considerably exceeding the average aerosol composition. The results shown in Table 4 take account of the blanks for the acids and salts added. These results serve simply as a guide to the concentration levels at which errors may intervene if no precautions are taken. All interferences lead to a decrease in the absorption signals except for the influence of lead on copper and aluminium on iron. Deuterium correction is useful in the measurement of atomic absorption signals when non-atomic absorption, e.g. from organic matter, can be expected. In the present case, all organic material was decomposed previously, and there were few interferences from the acids and salts, so that the background correction was of little use.

Construction of calibration graphs

For the determination of the metals under study, three methods were compared: (1) calibration graphs with dilutions from stock solutions; (2) calibration graphs with standards taken through the whole procedure; (3) standard addition on the solutions obtained after decomposition.

For the flame determinations, interferences from the acids used and the elements present in the samples are negligibly small, and the calibration graph method can be used. For the flameless determinations, standard addition is the best method because any interferences are corrected. However, for routine analyses where speed and simplicity are important, a

TABLE 4

Interference of cations

Element	Wavelength nm	Interfering element	Tolerable concentration ratio	Element	Wavelength nm	Interfering element	Tolerable concentration ratio
Cd	228.8	Na	200	Fe	248.3	Al	100
		Mg	10^4			Ca	100
		Al	10^4	Pb	283.3	Mg	20
		K	100			Fe	100
		Ca	10^3				
		Fe	10^3	Zn	307.6	Mg	0.1
		Pb	200			Al	10
Cu	324.8	Na	800			Ca	10
		Pb	20			Fe	0.1

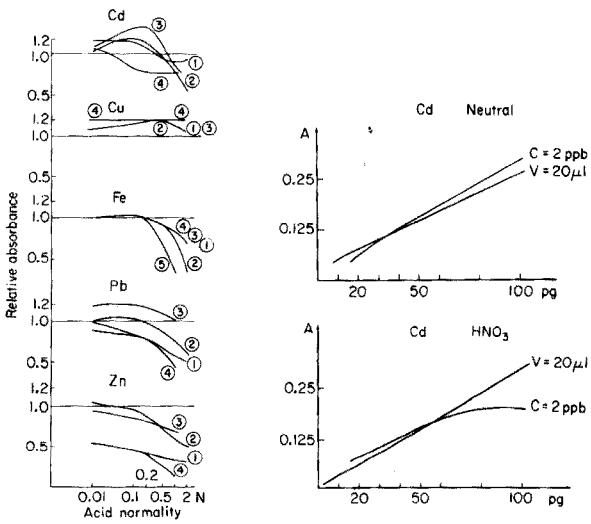

Fig. 3. Interferences of (1) HCl; (2) HNO_3; (3) H_2SO_4; (4) $HClO_4$ and (5) H_3PO_4 on 1 ppb Cd, 50 ppb Cu, 0.2 ppm Fe; 0.5 ppm Pb and 10 ppm Zn; 20 µl injected with furnace parameters as in Table 4. The signal with H_3PO_4 was too irreproducible to be measured, except for Fe.

Fig. 4. Calibration curves for Cd at 228.8 nm in neutral solution and in 1 N HNO_3, with volume and concentration variations. Constant volume (20 µl) or concentration (2 ppb) is indicated.

number of standards should be taken through the whole procedure and the unknown samples compared with them. There is then matching of acid concentrations, though not of interfering element concentrations, between samples and standards.

In flame atomic absorption calibration graphs are constructed after solutions of different concentration have been aspirated. In furnace atomic absorption, calibration data can be obtained either by injecting different volumes of the same concentration, or by injecting the same volume of different concentrations; the first approach is easier. The two methods were compared and some selected results are shown in Fig. 4 for cadmium in neutral and 1.0 N HNO_3 solution. For the other elements comparable calibration curves were obtained. It is apparent that different calibration graphs are obtained for neutral and acidic solutions and that the best graphs are those where the volume is kept constant. The difference with the acidic solutions is caused by the different amounts of acid placed in the furnace when a single concentration is used. Another reason, which is also valid for the neutral solutions, is the difference in distribution of the liquid in the graphite tube. This can result in different shapes of the atomic cloud.

Blanks

An important factor is the blank value of the reagents and materials used. For the water and for the reagents, amounts of 10 ml were concentrated by boiling and the dry residue was dissolved in dilute nitric acid (0.1 N) of previously determined purity. The results for the net concentrations of the elements considered are shown in Table 5. For zinc, the furnace procedure was either too sensitive at 214.0 nm or too insensitive at 307.6 nm, and there was not enough material for a flame determination. The Table shows clearly that very pure reagents and doubly-distilled water are required.

To determine the blank of the filter paper, a whole Whatman 41 filter (110-mm diameter) was decomposed in boiling Suprapur nitric acid and the excess of acid was boiled off. The residue was redissolved in 0.1 N nitric acid and measured. The blanks are shown in Table 6. To determine the blank for the entire decomposition procedure, 10 cm^2 of filter paper, 10 ml of Suprapur HNO_3 and 5 ml of Suprapur $HClO_4$ were used and the solution was diluted to 50 ml with doubly-distilled water. The total blank was also estimated for analytical-grade reagents and normal singly-distilled water. The blank values are given in Table 6. From the data, the amount of

TABLE 5

Blank values for the reagents

Reagent	Grade and source	Element concentration ($\mu g\ l^{-1}$)			
		Cd	Cu	Fe	Pb
Water	Distilled	0.26	1.3	35	0.3
	Double-distilled in quartz	0.23	0.5	12	0.8
HNO_3	Analytical Merck 454	0.14	6.5	110	0.6
	Suprapur Merck 441	0.11	0.4	42	<0.05
$HClO_4$	Analytical Merck 518	2.5	45	6100	6.2
	Suprapur Merck 517	0.13	0.05	140	0.38
HF	Baker 9560	0.5	<0.05	140	0.38

TABLE 6

Blank values for the filter paper and decomposition procedure

Medium	Element concentration in apparent ng cm^{-2}				
	Cd	Cu	Fe	Pb	Zn
Filter paper Whatman 41	<1	2.5	28	2.0	<30
Decomposition procedure with					
"normal" reagents	3.1	38	3350	7.1	—
"pure" reagents	1.8	5.3	200	6.0	—

particulate matter which must be collected in order to exceed the blank effect can be estimated.

These blanks do not, of course, include accidental contaminations during sampling, transport of the filter and the analytical procedure.

RESULTS AND CONCLUSIONS

A large number of urban and industrial aerosol samples and some standard samples were analyzed by the method described above. For the flame measurements, the calibration curves were prepared from stock solutions, while for the flameless measurements a number of standard solutions was taken through the whole decomposition procedure for comparison. Cadmium, which was usually less than 20 ng cm^{-2}, and some copper samples with less than 200 ng cm^{-2}, could not be measured in the flame. For the flameless measurements, difficulties arose for zinc, because the 214.0-nm line is too sensitive and the 307.6-nm line too insensitive, and because interferences occurred for both cations (Mg, Fe) and acids (H_3PO_4). Therefore zinc was always measured in the flame at the 214.0-nm line. For iron, the 248.3-nm line was sometimes too sensitive for the flameless determination, and the 372.0-nm line was then used.

The accuracy and precision were tested for some common standard samples. Table 7 shows the results for the Kodak TEG-50-A gelatin standard [31], the MILAN-aerosol standard [32], spotted filters of the I.A.E.A. AIR-3 intercomparison test [33] and the NBS SRM-1633 coal fly ash [34]. Zinc was determined in the flame, and the other elements in the furnace. The fly ash could not be completely destroyed by the procedure described above, and decompositions with HNO_3/HF and standard addition were applied [2]. The results agree very well with the certified values. The worst deviations are 17% for Cd (fly ash), 8% for Cu (IAEA), 10% for Fe (MILAN), 12% for Pb (MILAN, IAEA) and 8% for Zn (Kodak). The worst standard deviations found were 13% for Cd, 5% for Cu, 5% for Fe, 6% for Pb, and 3% for Zn. The precision and accuracy mentioned are overall values including the decomposition procedure.

A large number of aerosol-loaded filter papers was analyzed by flameless atomic absorption, flame atomic absorption and energy-dispersive x-ray fluorescence as described by Van Espen and Adams [1]. Table 8 gives some typical results. The average deviation between the results of the three methods for 75 samples was 30% for copper, 20% for iron and 18% for lead. For zinc the average deviation between the flame method and x.r.f. was 17%. Fig. 5 shows a comparison of the results obtained by atomic absorption in the flame and x.r.f. for zinc and by flameless atomic absorption and x.r.f. for Cu, Fe, and Pb. There appears to be no bias between the methods, but despite all precautions considerable deviations occasionally occur.

Aerosols are a very complex matrix for analysis. They may contain a large number of elements in widely differing concentrations and variable

TABLE 7

Accuracy tests on reference samples

Sample	Element	Concentration ppm ($\mu g\ g^{-1}$)	
		Found	Certified
Kodak TEG-50-A[a]	Cd	49	54 ± 5
	Cu	49	49 ± 5
	Zn	57	53 ± 4
MILAN[b]	Cd	41.5 ± 5.4	42
	Cu	675 ± 34	673
	Fe	30400 ± 1500	33700
	Pb	5970 ± 210	5350
	Zn	7650 ± 240	7530
IAEA AIR-3[c]	Cd	3.4 ± 0.11	3.6
	Cu	3.9 ± 0.07	3.6
	Fe	200 ± 6	200
	Pb	3.5 ± 0.2	4.0
	Zn	68 ± 1	70
Coal fly ash NBS SRM-1633[a,d]	Cd	1.69	1.45 ± 0.6
	Cu	127	128 ± 5
	Pb	70	70 ± 4
	Zn	214	210 ± 20

[a]A single 250-mg sample was analyzed. [b]Ten 10-mg samples were analyzed; the "certified" results are the averages of independent a.a.s. results. [c]Six filters were analyzed. [d]Destruction with HF and standard addition.

TABLE 8

Comparison between flameless a.a.s. (columns A), flame a.a.s. (columns B) and x.r.f. (columns C) for aerosol-loaded filters: results in ng cm^{-2}

Sample number	Cu			Fe			Pb			Zn	
	A	B	C	A	B	C	A	B	C	B	C
D 09	590	310	400	10800	11800	10700	1250	1600	1410	12700	11900
D 11	500	270	390	5740	5000	4380	2970	2740	2340	17000	14700
D 20	3400	4230	4470	9770	10000	11400	2970	2830	2180	15900	16600
D 24	2100	2310	1760	4280	3200	3410	1000	760	960	6070	6710
D 29	320	270	420	4280	3000	2770	2500	2170	1930	5250	5030

amounts of organic material and silicate base dust. Whereas the organic matter is destroyed by the procedure used, silicates are not. In some cases, it might be necessary to use an HF-based decomposition as used earlier [2] for the determination of aluminium. However, this treatment is inherently more difficult and was not used in the present routine work.

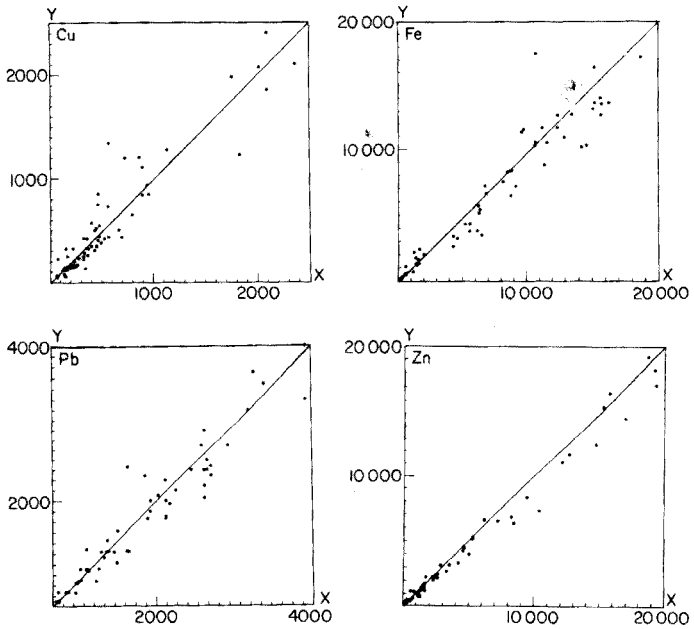

Fig. 5. Comparison of results obtained by x-ray fluorescence (ordinate) and atomic absorption spectrometry by the described procedure (abscissa) for iron, zinc, copper and lead. Concentrations are in ng cm^{-2}.

This research was carried out within the framework of the National Research and Development Program on Environment of the Interministerial Commission for Science Policy. The technical assistance of W. Van Mol for sampling and analysis by a.a.s. is gratefully acknowledged. The x.r.f. analyses were done by P. Van Espen.

REFERENCES

1 P. Van Espen and F. Adams, Anal. Chim. Acta, 75 (1974) 61.
2 A. Pilate, P. Geladi and F. Adams, Talanta, 24 (1977) 512.
3 J. Wood, La Recherche, 7 (1976) 712.
4 M. Winell, Ambio, 4 (1975) 34.
5 A. Sugimae, Anal. Chem., 47 (1975) 1840.
6 R. Dams, K. Rahn and J. Winchester, Environ. Sci. Technol., 6 (1972) 441.
7 J. Hwang, Anal. Chem., 44 (1972) 20A.
8 R. Thompson, G. Morgan and L. Purdue, At. Absorpt. Newsl., 9 (1970) 53.
9 C. Dorn, J. Pierce, P. Phillips and G. Chase, Atmos. Environ., 10 (1976) 443.
10 M. Janssens and R. Dams, Anal. Chim. Acta, 70 (1974) 25.
11 D. Siemer and R. Woodriff, Spectrochim. Acta, Part B, 29 (1974) 269.
12 R. Davison, D. Natusch, J. Wallace and C. Evans, Environ. Sci. Technol., 8 (1974) 1107.
13 J. Hwang and F. Feldman, Appl. Spectrosc., 24 (1970) 371.
14 B. Begnoche and T. Risby, Anal. Chem., 47 (1975) 1041.
15 Belgisch Instituut voor Normalisatie, Document NBN T-94-401 (1976).

16 M. Pinta and C. Riandey, Analusis, 3 (1975) 86.
17 A. Rattonetti, Anal. Chem., 46 (1974) 739.
18 R. Ediger, At. Absorpt. Newsl., 14 (1975) 127.
19 W. Findlay, A. Zdrojewski and N. Quickert, Spectrosc. Lett., 7 (1974) 355.
20 C. Fuller, Anal. Chim. Acta, 62 (1972) 442.
21 D. Segar and J. Gonzales, Anal. Chim. Acta, 58 (1972) 7.
22 K. Sperling, At. Absorpt. Newsl., 14 (1975) 60.
23 J. Aggett and A. Sprott, Anal. Chim. Acta, 72 (1974) 49.
24 B. Welz, Proc. 3rd Int. At. Absorpt. Flame Spectrom. Congr., Paris, 1971, 67.
25 W. Campbell and J. Ottaway, Talanta, 21 (1974) 837.
26 W. Frech and A. Cedergren, Anal. Chim. Acta, 82 (1976) 83.
27 W. Wegscheider, G. Knapp and H. Spitzy, Z. Anal. Chem., 283 (1977) 9.
28 Perkin-Elmer, Document 303-0152, 1973.
29 L. Lewis, Anal. Chem., 40 (1968) 28A.
30 R. Dams and R. Heindryckx, Atmos. Environ., 7 (1973) 319.
31 D. Anderson, J. Murphy and W. White, Anal. Chem., 48 (1976) 116.
32 S. Finzi, Euratom, Ispra, Document 1183, 1973.
33 International Atomic Energy Agency, Report IAEA/RL/42, Dec. 1976.
34 J. Ondov, W. H. Zoller, I. Olmez, N. K. Aras, G. E. Gordon, L. A. Rancitelli, K. H. Abel, R. H. Filby, K. R. Shah and R. C. Ragaini, Anal. Chem., 47 (1975) 1102.

Analytica Chimica Acta, 96 (1978) 243—249

NATURE OF THE INTERFERENCE OF NITRIC ACID IN THE DETERMINATION OF NICKEL AND VANADIUM BY ATOMIC ABSORPTION SPECTROMETRY WITH ELECTROTHERMAL ATOMIZATION

ELIANE M-M. SUTTER and MAURICE J-F. LEROY*

Laboratoire de Chimie Minérale, École Nationale Supérieure de Chimie, 1 rue Blaise Pascal, 67008 Strasbourg, Cedex (France)

(Received 7th August 1977)

SUMMARY

Effects of the concentration of nitric acid in the determination of nickel and vanadium in the presence of other metals by flameless atomic absorption spectrometry have been studied. Specific complexation of the metals in the aqueous phase suppresses the interferences. A method has been developed which allows the use of calibration curves from dilute acidic solutions in the determination of samples with high nitrate concentrations. The method is suitable for solutions reproducing the mineralization of airborne particulates.

Interferences in the determination of nickel and vanadium in slightly acidic aqueous solutions in the concentration range of 50 ng ml^{-1} by flameless atomic absorption spectrometry have been reported [1—6]. However, the determination of these metals in airborne particulates normally involves a mineralization of the sample with nitric acid; depending on the nature of the sample, the quantity of acid used may be important. A study has been made of the effects of the concentration of nitric acid or nitrate ions (1.5×10^{-3}—1.5 M), and of the presence of other metals, on the absorbance by nickel and vanadium.

Concerning the nature of the interference from nitrate ions, the role of their complexing power has been considered. Various complexes of nickel and vanadium exist in solution, and as they may behave differently during the drying and decomposition cycles, the effect on the absorbance of the metals of their specific complexation has been investigated.

EXPERIMENTAL

Apparatus

The IL 455 flameless atomizer and IL 151 atomic absorption spectrophotometer were used. The optimal operating conditions, for nickel and vanadium in 1.5×10^{-3} M HNO_3 are given in Table 1. The argon purge gas was supplied at the manufacturer's recommended rates and all signals were

measured by the peak height technique. Samples (20 μl) were placed in the graphite furnace with an Eppendorf micropipette.

Reagents

The standard solutions of vanadium and cadmium were supplied by Merck (Titrisol); for nickel, iron and lead high-purity metals were dissolved in nitric acid (ultra-pure grade). All dilutions were made with deionized distilled water. For the silica stock solution, silica powder was dissolved in a mixture of hydrofluoric and nitric acids; for calcium and zinc, the nitrates were dissolved directly in deionized distilled water. Working solutions were prepared from the 1 mg ml^{-1} stock solutions. A 0.4% (w/v) DMG solution in ethanol was used; to each sample, aliquots (20-μl) of the DMG solution were added to complex the metal to be determined. The pH adjustments were made with analytical-grade ammonia.

Applications

A synthetic solution reproducing the composition of atmospheric matter was prepared by dissolving metal salts in dilute nitric acid; the composition per litre is given in Table 2. Portions (5 ml) of this solution were placed on polycarbonate membranes (Nucleopore Corp., 47 mm, pore diameter 0.4 μm). These filters were then treated in a Teflon beaker by adding an aliquot (2 ml) of dichloroethane to destroy the membrane structure, followed by 6 ml of concentrated nitric acid. The solution was evaporated on a sand bath; the residue was dissolved in 5 ml of 0.15 M nitric acid to give the solution to which nickel and vanadium were added in known amounts.

TABLE 1

Instrumental parameters for the IL 151 atomic absorption spectrophotometer and IL 455 graphite furnace

	Nickel	Vanadium
Wavelength (nm)	232.0	318.4
Spectral slit width (μm)	40	160
Furnace temperature (°C)[a]		
Dry	200 (20)	100 (25)
Ash	1200 (75)	1000 (60)
Atomize	3000 (5)	3200 (10)

[a]The times (in s) are given in parentheses.

TABLE 2

Composition (g l^{-1}) of the synthetic solution reproducing atmospheric matter

Cd (nitrate)	4×10^{-7}	Cu (chloride)	2×10^{-5}	Mn (chloride)	2×10^{-4}	Mg (nitrate)	2×10^{-4}
Cr (nitrate)	3×10^{-6}	Fe (nitrate)	3×10^{-4}	Mo (metal dissolved in $HCl + HNO_3$)	10^{-6}	Ca (nitrate)	4×10^{-4}
Co (nitrate)	10^{-7}	Pb (sulphate)	2×10^{-4}	Zn (nitrate)	10^{-4}		

RESULTS AND DISCUSSION

Effect of the nitric acid concentration

The variation of the absorbance, as a function of the concentration of nickel or vanadium, for aqueous solutions of constant nitric acid concentration was studied. Figure 1 shows that the variation is linear in the concentration ranges 10—60 ng ml^{-1} for nickel and 20—150 ng ml^{-1} for vanadium. From these results, the composition of the standard solutions can be determined, provided that the nitric acid concentration in the samples is known and constant. However, the curve relative to 1.5 M nitric acid shows that these ions affect strongly the sensitivity and the precision of the method. The loss in performance will be even more pronounced for an aged furnace, since the nitric acid concentration will reduce the lifetime of the pyrolytic coating.

The relation between the addition of other metals to the nitric acid solution and the variation of the absorbance of nickel and vanadium, was studied.

Figure 2 shows the effect of the addition of iron to 1.5×10^{-3} M and 1.5 M nitric acid solutions containing constant concentrations of nickel and vanadium. The effect of iron is of particular interest as it is always present in airborne particulates, generally in amounts several orders of magnitude greater than nickel and vanadium. In slightly acidic medium, concentrations of iron up to 100 ng ml^{-1} enhance the signal from nickel, in agreement with a reported enhancement [4] of 100% in the absorbance of a solution of 50 ng Ni ml^{-1} after the addition of 2500 μg Fe ml^{-1}. However, the behavior of the strongly acidic solutions is different; Fig. 2 shows that the nickel absorbance is lowered markedly by increasing concentrations of iron. For vanadium, the interference from iron up to 100 μg ml^{-1} lowers the absorbance both in dilute and strongly acidic media (Fig. 2). The addition of other metals to nickel solutions shows that the absorbance is unaffected in the concentration range 1.5—50 ng ml^{-1} when silicon, lead, calcium, or zinc is present up to 100 μg ml^{-1} and cadmium up to 500 ng ml^{-1}. From these results, the determination of nickel and vanadium in a series of samples

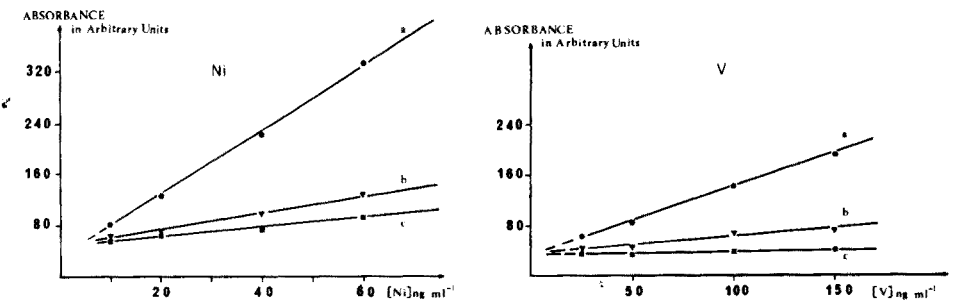

Fig. 1. Absorbance of nitric acid solutions containing nickel or vanadium. (a) 1.5×10^{-3} M HNO_3. (b) 0.75 M HNO_3. (c) 1.5 M HNO_3.

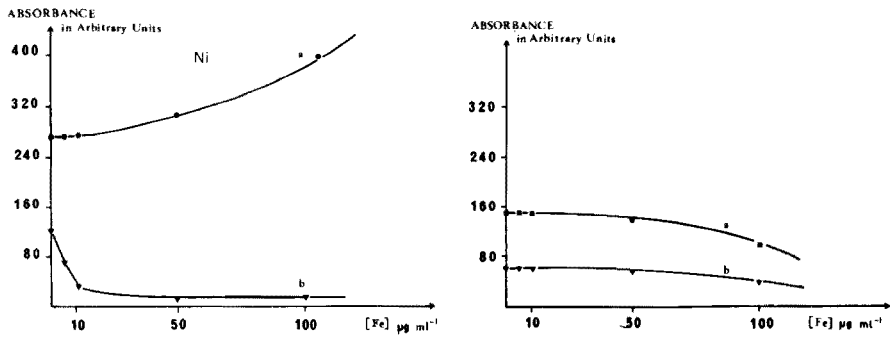

Fig. 2. Effect of the concentration of iron on the absorbance of solutions containing nickel (40 ng ml^{-1}) or vanadium (100 ng ml^{-1}). (a) 1.5 × 10^{-3} M HNO_3. (b) 1.5 M HNO_3.

would require a knowledge of the iron and nitrate concentrations in the standard solutions. The standard additions method, which has been criticized recently [3] cannot be applied to high concentrations of nitric acid since the slope of the calibration curve is very small and the extrapolation to zero signal would be liable to great error.

Effect of the complexation of nickel and vanadium

The selective extraction of metals by an inert solvent is generally used when the method of standard additions is not suitable. However, the extraction yield depends on the parameters of the aqueous solution, i.e. anions, concentrations, pH, etc; if these parameters vary greatly in a series of samples, the method may be unreliable.

In order to understand the influence of the constituents of the aqueous phase on the absorbance of nickel and vanadium, specific complexing agents were added to aqueous solutions of these metals. This complexation in situ should isolate the metals from the matrix and lead to the formation of definite compounds before the drying and decomposition steps.

The effect of the addition of dimethylglyoxime to nickel solutions (40 ng ml^{-1} with the nitric acid concentration varying from 1.5 × 10^{-3} M to 2.25 M, is shown in Figs. 3 and 4. A significant decrease in the interference is obtained for nickel; the signal is independent of the nitric acid concentration and it is possible to use the calibration curve (Fig. 4, curve a) even for high nitric acid concentrations. The effect of nitrate on the absorbance of some metals in flameless atomic absorption has been reported [3, 7]. This effect is often attributed to destruction of the pyrolytic coating of the graphite furnace [6] leading to the inclusion and therefore segregation of the metal in the graphite structure. Another interpretation [8] is based on the presence of nitric acid in the vapour phase at temperatures up to 1000 K [9].

Figure 3 shows that the interference is reduced by the addition of DMG at pH 8, corresponding to the conditions of formation of $Ni(DMG)_2$. The addition of ammonia alone has no correcting effect; the absorbance of nickel

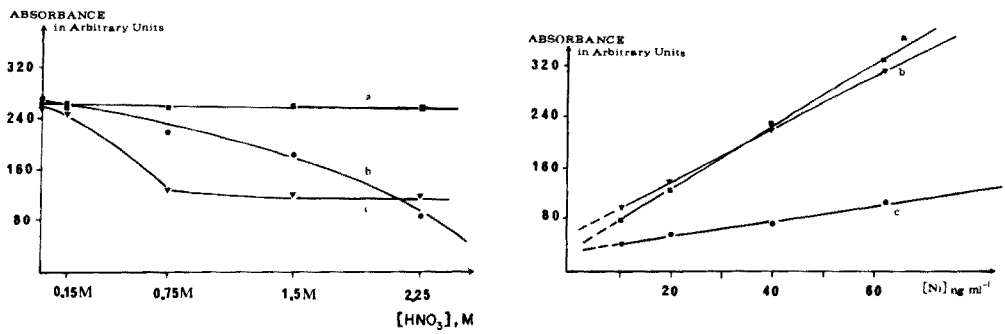

Fig. 3. Effect of DMG on the absorbance of nickel solutions (40 ng ml^{-1}) for different nitric acid concentrations. (a) 0.06×10^{-3} M DMG, pH 8. (b) and (c) without addition of DMG for two different graphite furnaces. For this, and later Figures where DMG is mentioned, 20 μl of a solution of DMG in ethanol were added to 10 ml of aqueous solutions of nickel or vanadium.

Fig. 4. Absorbance of nickel solutions. (a) 1.5×10^{-3} M HNO_3 with or without the addition of DMG. (b) 1.5 M HNO_3 0.06×10^{-3} M DMG, pH 8. (c) 1.5 M HNO_3.

is therefore related to its complexation in the aqueous phase. Some studies [10], particularly of the solid state, have shown that nitrate ions can act as mono or bidentate ligands with respect to nickel: the complexing behavior of these anions during the drying step will be related to the relative concentrations of nickel and nitrate in the aqueous phase. The interference may arise from the existence of several compounds to which would correspond different temperatures of decomposition and atomization; this interpretation is supported by the fact that modifications in the temperature cycles do not correct the interference. The dimethylglyoxime would complex the nickel in solution and this would always lead to the same definite compound after the drying step for any nitrate concentration.

Similar experiments with solutions of vanadium are reported in Figs. 5 and 6. A decrease in the interference from nitric acid is obtained by the addition of ammonia. This result also shows the importance of the complexing power of nitrate ions. At pH 8, the metavanadate ion VO_3^- predominates in solution; this ion cannot coordinate with nitrate, whereas in acidic solution the ions VO_2^+ or VO^{2+} can accept the ligand in their coordination sphere, leading to several types of compound after the drying step.

As for nickel, the pH correction allows the use of the calibration curve (Fig. 6, curve a) for high nitrate concentrations. In these experiments, the interference of iron in the determination of nickel and vanadium is not reduced by the addition of DMG nor by modification of the pH of the aqueous solution. These results can be interpreted in terms of vapor phase or spectral interactions.

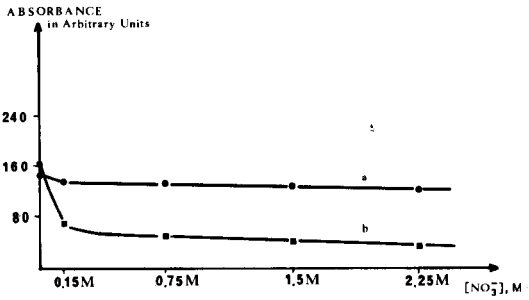

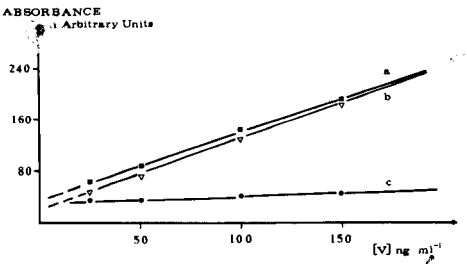

Fig. 5. Effect of ammonia on the absorbance of vanadium solutions (100 ng ml^{-1}) at different nitric acid concentrations. (a) pH 8 with or without the addition of DMG. (b) no addition of ammonia.

Fig. 6. Absorbance of vanadium solutions. (a) 1.5×10^{-3} M HNO_3 with or without the addition of ammonia and DMG. (b) 1.5 M HNO_3 pH 8, with or without the addition of DMG. (c) 1.5 M HNO_3.

Application

The addition of DMG at pH 8 to aqueous solutions of nickel and vanadium was applied to synthetic solutions reproducing the composition of airborne particulates. In these solutions, no interferences from iron are expected as the ratio of the concentrations of iron and nickel is always less than 10^3. The results are reported in Table 3; without the addition of DMG, the values for nickel and vanadium are significantly low. Addition of the complexing agent leads to the order of error expected with this method. Considering the constitution of the aqueous solution, these results support the interpretation in that the interference from nitrate ions is related to their complexing power for nickel and vanadium.

TABLE 3

Application of the method to synthetic solutions

Without DMG					With DMG				
Sample	Ni or V added (ng)	Ni or V found	s_r (ng)	Error (%)	Sample	Ni or V added (ng)	Ni or V found	s_r (ng)	Error (%)
1	Ni: 200	170	15	−15	7	Ni: 200	195	6	−2.5
2	Ni: 300	40	18	−87	8	Ni: 300	307	15	+2.3
3	Ni: 400	355	20	−11	9	Ni: 400	405	7	+1.2
4	V: 300	102	45	−66	10	V: 300	362	60	+20
5	V: 600	239	88	−60	11	V: 600	660	19	+10
6	V: 600	287	96	−52	12	V: 600	513	44	−14

[a] 20 µl of a solution of DMG in ethanol added to each sample.
[b] The calibration curve was obtained from dilute solutions of Ni and V, 1.5×10^{-3} M in nitric acid.

REFERENCES

1 C. W. Fuller, Anal. Chim. Acta, 62 (1972) 442.
2 C. W. Fuller, Proc. Soc. Anal. Chem., 7 (1974) 176.
3 W. Wegscheider, G. Knapp and H. Spitzy, Z. Anal. Chem., 14 (1977) 283.
4 R. B. Cruz and J. C. van Loon, Anal. Chim. Acta, 72 (1974) 231.
5 B. Gandrud and J. C. Marshall, Appl. Spectrosc., 24 (1970) 367.
6 A. Syty, C.R.C. Crit. Rev. Anal. Chem., 4 (1974) 155.
7 J. Smeyers-Verbeke, Y. Michotte, P. Van den Winkel and D. L. Massart, Anal. Chem., 48 (1976) 284.
8 G. Volland, G. Kölblin, P. Tschöpel and G. Tölg, Z. Anal. Chem., 12 (1977) 284.
9 R. E. Sturgeon, C. L. Chakrabarti and C. H. Langford, Anal. Chem., 48 (1976) 1792.
10 C. C. Addison, N. Logan, S. C. Wallwork and C. D. Garner, Q. Rev. Chem. Soc., 25 (1971) 289.

Analytica Chimica Acta, 96 (1978) 251—257

FLAME AND FLAMELESS ATOMIC-ABSORPTION DETERMINATION OF TELLURIUM IN GEOLOGICAL MATERIALS

T. T. CHAO*, R. F. SANZOLONE and A. E. HUBERT

U.S. Geological Survey, Box 25046, Denver, Colorado 80225 (U.S.A.)

(Received 27th September 1977)

SUMMARY

The sample is digested with a solution of hydrobromic acid and bromine and the excess of bromine is expelled. After dilution of the solution to approximately 3 M in hydrobromic acid, ascorbic acid is added to reduce iron(III) before extraction of tellurium into methyl isobutyl ketone (MIBK). An oxidizing air-acetylene flame is used to determine tellurium in the 0.1—20 ppm range. For samples containing 4—200 ppb of tellurium, a carbon-rod atomizer is used after the MIBK extract has been washed with 0.5 M hydrobromic acid to remove the residual iron. The flame procedure is useful for rapid preliminary monitoring, and the flameless procedure can determine tellurium at very low concentrations.

The crustal abundance of tellurium is not known definitely, but recent estimates are generally in the low ppb range [1]. Tellurium tends to form dispersion halos around or above some less mobile ore elements, and its presence in anomalous amounts may indicate targets of mineral potential. Its use as a pathfinder or indicator of certain types of deposits containing Ag, Au, Bi, Ni, Co, W, Sn, Mo, and Cu has been suggested [2]. As the search for concealed ore deposits becomes more intensive and extensive, a sensitive and rapid method for the analysis of tellurium is needed. Recently, several methods capable of determining tellurium in the low ppm or ppb range have been reported [3—7], but these suffer from limitations involving lengthy separation procedures prior to atomic-absorption determination [3, 5], expensive mass spectrometry [7], or interferences by other elements so that either a concentration limit has to be imposed on copper as an interfering element in hydride generation [6], or the method of standard additions has to be used [4].

The atomic-absorption method presented in this paper uses both flame and flameless atomization and fulfils the requirement of being sensitive and rapid with applications in geochemical exploration. It employs a hydrobromic acid—bromine sample digestion followed by extraction of tellurium with MIBK after reduction of iron(III) with ascorbic acid. The flame procedure allows a rapid preliminary monitoring of tellurium in geological materials at a lower limit of 0.1 ppm while the flameless procedure can determine tellurium in the low ppb range.

EXPERIMENTAL

Apparatus

A Varian AA6 atomic-absorption spectrophotometer equipped with an automatic gas control unit, a variable nebulizer, a simultaneous background corrector, and a Westinghouse tellurium electrodeless discharge lamp operated at 8 W with a power supply unit was used. The slit width was 0.5 nm and the wavelength was 214.3 nm. An oxidizing air-acetylene flame was used with burner height, aspiration rate, and position of the glass bead adjusted for maximum sensitivity and minimal noise. A Model 63 carbon rod atomizer was employed for the flameless work in the peak-height mode. Other instrument settings are given in Table 1.

Reagents and standards

Hydrobromic acid —2% bromine solution. Pipet 20 ml of bromine into a 1-l volumetric flask and make up to volume with concentrated hydrobromic acid.

Iron solution, 10% (w/v) in 3 M hydrobromic acid. Dissolve 10 g of Specpure iron powder in concentrated hydrobromic acid, add 1 ml of bromine, and evaporate to dryness. Add 34.2 ml of concentrated hydrobromic acid to the residue, heat gently to effect dissolution, and dilute to 100 ml with water.

Tellurium stock solution (100 $\mu g\ ml^{-1}$). Dissolve 0.125 g of Specpure TeO_2 in 1 l of 3 M hydrobromic acid.

Dilute tellurium standard solutions. Prepare 10, 1, and 0.1 $\mu g\ ml^{-1}$ solutions by serial dilutions of the tellurium stock solution with 3 M hydrobromic acid. The 0.1 μg Te ml^{-1} solution should be prepared daily before use. Prepare working standards for the flame work by pipetting aliquots containing 0, 0.25, 1, 5, 10, 20, and 50 μg Te from the appropriate dilute tellurium standard solutions into 25 × 200 mm culture tubes, and dilute to the 43-ml mark with 3 M hydrobromic acid. Add 0.5 ml of the iron solution to each standard. Prepare working standards for the flameless work by pipetting aliquots containing 0, 0.01, 0.025, 0.05, 0.1, 0.25 and 0.5 μg Te from the appropriate dilute

TABLE 1

Instrument settings for a.a.s.

Condition	Flame	Flameless
Air flow meter	4	—
Acetylene flow meter	0.2	—
Nitrogen flow meter	—	7.5
Dry-voltage setting, ~100°C	—	5.5 (for 35 s)
Ash-voltage setting, ~500°C	—	6.5 (for 15 s)
Ramp atomize, cutoff voltage, ~2100°C	—	8 (at rate 5)

tellurium standard solutions into 25 × 200 mm culture tubes, and dilute to the 43-ml mark with 3 M hydrobromic acid. Add 0.5 ml of the iron solution to each standard.

Procedure for flame method

Weigh 2.500 g of the soil, rock, or stream sediment sample (less than 100-mesh) into a 25 × 150 mm culture tube. Add 15 ml of hydrobromic acid—bromine solution in small portions to prevent vigorous reactions which may be caused by carbonates and organic matter in the sample. Add a further 2 ml of bromine to samples with visible sulfides. Allow the acid to react with the sample for 1 h with occasional vortexing. Place the tube in an aluminum heating block on an oscillating hot-plate preset at 135—140°C. Heat for 30 min (longer for samples containing sulfides) to expel the excess bromine. Dilute the sample solution with 28 ml of water to approximately 3 M hydrobromic acid and mix. Centrifuge and decant the supernatant solution into another 25 × 150 mm tube. To the sample solution, add at least 1 g of ascorbic acid and shake to dissolve until a clear light yellow color appears. Add 1 g of ascorbic acid to each of the tellurium working standards. By pipet add 3 ml of MIBK to the sample and standards, and shake for 2 min on a shaker. Centrifuge to assist the separation of the organic layer. Aspirate the organic extract into the air-acetylene flame and record the absorbance.

Procedure for flameless method

For samples containing less than 0.1 ppm Te, the carbon rod is used in place of the flame for atomization. Treat the sample and tellurium working standards identically, as above, through the step of separation of organic and aqueous layers by centrifugation. Then transfer the contents of the tube to a 60-ml separatory funnel. Drain off the aqueous layer and discard. Add 2 ml of 0.5 M hydrobromic acid to the funnel, and shake for exactly 5 min on a shaker designed for separatory funnels of different sizes [8]. The volume and molarity of the hydrobromic acid washing solution must be rigidly controlled in order to obtain reproducible results. Allow the two layers to separate completely before the aqueous layer is drained off. Transfer the organic extract to a capped glass vial; this is now ready for atomization. Take up a 5-μl portion of the extract with a micropipette. Press the start button on the carbon-rod power supply and inject the extract into the graphite tube in a reproducible manner. Make sure that the tube becomes cool enough (i.e., slightly warm to the touch) before the next injection. This usually takes about 20 s.

When the above method is used, the procedure may be interrupted after decanting the sample solution from the digestion tube following centrifugation. The solution is stable and can be saved for future analysis. Once ascorbic acid has been added, the extraction of tellurium into MIBK should proceed without delay and the analysis should be completed on the same day.

TABLE 2

Tellurium in three USGS standard rocks (ppb determined by the flameless procedure)

Sample	Sample decomposition		Literature values
	$HBr-Br_2$	$HF-HCl-H_2O_2$	
G-2	5	6	5 [7], <3.4 [14]
BCR-1	4	4	4 [7], 0.0 ± 0.4 [6]
GSP-1	22	26	31 [7], 20 [14], 19 [6], 20.8 [5]

RESULTS AND DISCUSSION

Sample decomposition

The hydrobromic acid—bromine digestion has been used previously to dissolve tellurium in geological materials prior to determination by a.a.s. [9, 10]. The efficiency of this digestion was checked against a more complete $HF-HCl-H_2O_2$ digestion [11] of three different rock types. The residue from the $HF-HCl-H_2O_2$ digestion was taken up in 3 M hydrobromic acid and determinations were made by the above procedure. Values of tellurium obtained by both digestions are in good agreement (Table 2). However, if tellurium minerals are occluded in, or protected by, silicates or siliceous materials, sample decomposition involving hydrofluoric acid may be beneficial.

The optimum weight of sample for the digestion specified in the procedure was 2.500 g; larger samples tend to reduce the efficiency of the digestion and give lower tellurium values.

Solvent extraction of tellurium

Tellurium can be extracted from 2—4 M hydrobromic acid into MIBK in the presence of ascorbic acid. Iron suppresses the extraction. However, once 0.05 g of iron (corresponding to 2% iron dissolved from the sample in the digestion) is present in the sample solution, additional amounts of iron do not further suppress the extraction of tellurium into MIBK, provided that sufficient ascorbic acid is added to reduce the iron. Figure 1 shows the effect of variable amounts of iron on the extraction of 10 μg Te into MIBK with and without ascorbic acid; the amount of ascorbic acid added is not critical as long as it is sufficient to reduce the iron present.

Based on the above observations, 0.5 ml of 10% iron solution is added to all the standards along with 1 g of ascorbic acid to compensate for the variable amounts of iron encountered in diverse sample types.

Sensitivity

With the flame procedure described it is possible to determine 0.25—50 μg Te in the MIBK layer. This range corresponds to 0.1—20 ppm in the sample. Dilution of the MIBK extract will extend the range of determination

to levels greater than 20 ppm. The flameless procedure is suitable for determinations of 0.01—0.5 μg Te in the organic extract, equivalent to 4—200 ppb in the sample. Standards for the flameless work are not stable and should be prepared with the samples.

Interferences

Iron causes suppression of absorbance readings in both flame and flameless determinations of tellurium. Ascorbic acid removes this interference in the flame procedure (Fig. 1). The tolerance to iron is much less with the carbon-rod atomizer, and ascorbic acid alone is not sufficient to prevent suppression of the absorbance. Washing the organic extract with 0.5 M hydrobromic acid is necessary to remove the residual iron to maintain the absorbance readings constant at iron levels greater than 0.05 g in the sample solutions (Fig. 2). Without washing, the absorbance decreases with increasing concentrations of iron in the original sample solution and the sensitivity of the flameless procedure is greatly reduced. Absorbance readings obtained after washing are linearly related to concentrations of tellurium, with an absorbance of 0.10 corresponding to 0.50 μg Te in standards (200 ppb in samples).

For both flame and flameless procedures, the tolerance to the presence of iron is remarkable, amounting to 1 g of iron in the sample solution, or 40% iron in the sample; this is equivalent to 57% Fe_2O_3 (Figs. 1 and 2).

Copper does not seem to interfere. The recovery of two levels of tellurium added to GXR-4, which contains 6860 ppm Cu [11], amounts to 94 and 100% (Table 3).

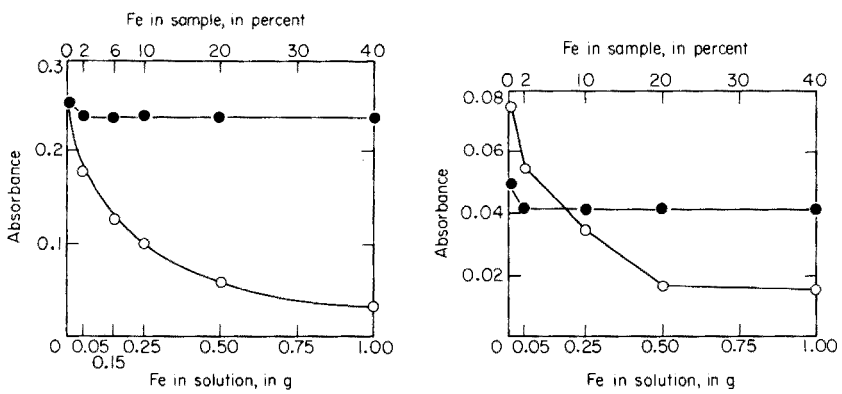

Fig. 1. Effect of various amounts of iron on the absorbance of 10 μg Te by the flame procedure with (●) and without (○) ascorbic acid sufficient to reduce the iron.

Fig. 2. Effect of washing organic extracts of tellurium with 0.5 M hydrobromic acid on absorbance readings given by the flameless procedure. Extracts were obtained from solutions containing 0.2 μg Te and various amounts of iron as described for the flame procedure. ● With 0.5 M HBr washing. ○ Without washing.

One additional interference in the flame procedure is related to molecular absorption and/or light scattering. Analyses were performed on three samples with and without the background corrector. No absorbance was observed for the three samples when the background corrector was used. Without the corrector, values of 0.2, 0.5, and 0.6 ppm Te were obtained. The background corrector is therefore necessary to eliminate the background absorption.

Analytical data

Replicate analyses of three geological materials of varying matrices by the flame procedure gave s_r = 1.2, 1.4, and 2.6% for tellurium concentrations in the range 1—10 ppm. Analyses by carbon-rod atomization of five replicates of two samples (GXR-3, GXR-6) containing tellurium in the ppb range gave s_r = 2.8 and 15.6% (Table 3).

TABLE 3

Replicate analyses (n = 5) of tellurium in various samples

Sample	Material	Atomization	Range[a]	Mean[a]	s_r (%)
GXR-1	Jasperoid	Flame	8.4—9.0	8.7	1.2
GXR-2	Soil	Flame	0.85—0.90	0.88	1.4
GXR-4	Cu mill tailings	Flame	0.96—1.0	1.0	2.6
GXR-3	Fe—Mn deposits	Flameless	7—10	9	15.6
GXR-6	Soil	Flameless	15—16	16	2.8

[a] GXR-1, GXR-2 and GXR-4 in ppm; GXR-3 and GXR-6 in ppb.

TABLE 4

Recoveries of known amounts of tellurium added to different samples (average of duplicate analyses)

Sample	Present (μg)	Added (μg)	Found (μg)	Recovery (%)
Flame procedure (2.5-g sample)				
GXR-1	17.0	5.0	20.0	90.9
GXR-1	17.0	12.5	23.8	80.7
GXR-2	2.3	1.0	3.3	100.0
GXR-2	2.3	2.5	4.8	100.0
GXR-4	2.6	1.0	3.6	100.0
GXR-4	2.6	2.5	4.8	94.1
Flameless procedure				
Greisen, 1 g	0.05	0.025	0.08	106.7
Greisen, 1 g	0.05	0.05	0.12	120.0
Greisen, 2.5 g	0.12	0.05	0.16	94.1
Greisen, 2.5 g	0.12	0.10	0.21	95.5

Three geochemical exploration reference samples [12] that had tellurium contents suitable for determination by the flame procedure were spiked with two levels of tellurium. Two weights of a greisen sample containing tellurium in the ppb range were spiked with fractions of 1 μg of tellurium. The recovery results are presented in Table 4. The average recovery for the flame procedure is 94.3% and that for the flameless procedure is 104.1%.

Three U.S. Geological Survey standard rocks [13] with tellurium values in the ppb range were analyzed by the flameless procedure; the results are compared with those reported in the literature in Table 2.

REFERENCES

1 D. F. Davidson and H. W. Lakin, U.S. Geol. Surv. Prof. Pap., 820 (1973) 627.
2 R. W. Boyle, Geol. Surv. Can. Pap. 74-45 (1974).
3 C. E. S. Davis, W. E. Ewers and A. B. Fletcher, Proc. Aust. Inst. Min. Met., No. 232 (1969) 67.
4 R. D. Beaty, At. Absorpt. Newsl., 13 (1974) 38.
5 J. R. Watterson and G. J. Neuerburg, U.S. Geol. Surv. J. Res., 3 (1975) 191.
6 L. P. Greenland and E. Y. Campbell, Anal. Chim. Acta, 87 (1976) 323.
7 C. L. Smith, J. R. de Laeter and K. J. R. Rosman, Geochim. Cosmochim. Acta, 41 (1977) 676.
8 J. W. Ball and E. A. Jenne, At. Absorpt. Newsl., 10 (1971) 117.
9 H. M. Nakagawa and C. E. Thompson, U.S. Geol. Surv. Prof. Pap., 600-B (1968) B123.
10 R. E. Stanton, Analytical Methods for Use in Geochemical Exploration, J. Wiley, New York, 1976.
11 R. F. Sanzolone and T. T. Chao, Anal. Chim. Acta, 86 (1976) 163.
12 G. H. Allcott and H. W. Lakin, Proc. 5th Int. Geochem. Exp. Symp., (1974) 659.
13 F. J. Flanagan, U.S. Geol. Surv. Prof. Pap., 340 (1976) 131.
14 R. D. Beaty and O. K. Manuel, Chem. Geol., 12 (1973) 155.

Analytica Chimica Acta, 96 (1978) 259—269

SIMULTANEOUS DETERMINATION OF NITROGEN AND LITHIUM BY THERMAL NEUTRON ACTIVATION ANALYSIS

P. N. SHUKLA, B. K. KOTHARI and P. S. GOEL*

Department of Chemistry, Indian Institute of Technology Kanpur, Kanpur 208016 (India)

(Received 21st September 1977)

SUMMARY

The determination of lithium and nitrogen in a variety of materials by thermal neutron activation is described. The nuclear reactions used are $^{14}N(n,p)^{14}C$ and $^{6}Li(n,\alpha)^{3}H$. Radionuclides ^{14}C and ^{3}H for counting are isolated by fusion of the irradiated sample in a vacuum system. Data are presented on lithium and nitrogen concentrations in several terrestrial standards. The new method allows reliable measurements on 10—50-mg samples.

In most silicates and metals, the nitrogen concentration may vary between about 1 and 10^3 ppm. Nitrogen has been determined by several modifications of the two well known classical methods. In the Kjeldahl method, nitrogen is liberated as ammonia which can be easily determined. This method provides high precision and low blanks [1—3] and gives chemically bound nitrogen. In the Dumas method, total nitrogen is liberated as the gas by decomposing the sample under appropriate conditions. Moore and co-workers [4, 5] developed a modification of this method for studies of moon and meteorite samples. These classical methods suffer from one or more of the following difficulties: (i) incomplete removal of nitrogen; (ii) contamination from reagents and atmosphere; (iii) the need for large samples; and (iv) relatively high (1 ppm or more) blanks.

Some of these difficulties can be overcome by nuclear methods. Several such methods with high-energy neutrons, protons or γ-rays have been suggested [6—9], but their applications are limited by interferences and other difficulties. The most suitable activation method is to use thermal neutrons [10] where ^{14}N is converted to ^{14}C which is assayed radiochemically. The method is applicable to a wide variety of materials and can be adopted even in a laboratory quite far from a reactor facility.

This paper reports on the method for the determination of total nitrogen in silicates, metals, standards, etc. A neutron activation method for the simultaneous determination of lithium via the reaction $^{6}Li\ (n,\alpha)^{3}H$ is also described. This method, proposed over two decades ago [11, 12], has previously remained unexploited. No other satisfactory and versatile method for lithium determination is available when the concentration of lithium is less than 1 ppm. With the present technique, measurements can be made even when the lithium concentration is as low as a few ppb.

Information on the nuclear reactions involved is given in Table 1. After irradiation, the sample is fused with flux and carriers, and barium carbonate and water are isolated for the final counting.

EXPERIMENTAL

Sample preparation

As far as possible, sample preparations were carried out in a clean room to avoid contamination from laboratory fumes such as NH_3, NO, etc. With iron meteorites, any surface materials like paint, oxidation or fusion crust, or rust, were removed mechanically. Slices weighing about 1—2 g, prepared with a carborundum wheel, were further reduced to small sizes with a hacksaw, water being used as coolant. The small chips obtained were washed with benzene, etched with 4 M H_2SO_4, washed with distilled water and dried under a heat lamp. Samples of stone meteorites, silicates, and glasses were crushed in an agate mortar to appropriate sizes. The pieces were washed with distilled water and dried under the heat lamp. Monitors and lunar samples were not subjected to any washing.

Packing and irradiation

Samples were packed in a clean (washed with acetone, chromic acid, and distilled water) quartz vial (15 mm o.d., 35 mm long) having a small neck (4.5-mm diameter) to introduce samples and to facilitate sealing. To optimize the vial space, about 5 kinds of samples, e.g. stone and iron meteorites, lunar fines and rocks, tektites, and monitors, were packed together. Typically a vial contained about 5 g of total material. The monitors and any special samples were packed first in small quartz capsules (2-mm diameter) which were attached to a manifold and slowly evacuated, care being taken to avoid any powders spreading into the manifold. After about 12 h of evacuation, the capsules were sealed at about 0.04 mm Hg pressure. The external surfaces were washed and the capsules were introduced in the main quartz vial containing the other materials. This was evacuated, kept under vacuum overnight, evacuated again, and sealed under about 0.04 mm Hg pressure.

Samples were irradiated in the CIRUS reactor at Bhabha Atomic Research Centre, Bombay, for four weeks in a neutron flux of $(1—10) \times 10^{12}$ cm^{-2} s^{-1}. CIRUS is a 40-MW natural uranium, heavy water-moderated reactor.

TABLE 1

Nuclear data

Nuclide	Isotopic abundance	Neutron reaction	Cross-section (b)	Interfering reaction	Cross-sectio (b)
^{14}N	99.63	$(n,p)^{14}C$	1.82	$^{17}O(n,\alpha)^{14}C$	0.24
^{6}Li	7.42	$(n,\alpha)^{3}H$	942	$^{3}He(n,p)^{3}H$	5.33×10^{3}

Decomposition

The irradiated vials were allowed to "cool" for 2—3 months to reduce radiation hazards. They were then broken and the various samples were sorted out in a "hot" laboratory. The samples were decomposed in a vacuum system (Fig. 1) in the "hot lab" for simultaneous measurements of nitrogen and lithium. Stone and glass pieces were powdered in a stainless steel mortar. The irons were decomposed as such. The sample was mixed with the carriers ($CaCO_3$ for ^{14}C and $Ca(OH)_2$ for ^{3}H) and an oxidizing flux ($PbCrO_4$ + fused K_2CrO_4, 1:10 by mass). The mixture was placed in a porcelain combustion boat which was covered with a sillimanite guard tube and introduced into the quartz tube. The guard tube protected the quartz tube from devitrification during heating because of the sputtering of the flux. The fusion tube was evacuated and some oxygen (10—20 cm Hg) was introduced. The sample, isolated in a portion of the vacuum line, was heated at about 1050°C. The duration of heating, under static conditions was 2—3 h for stones and glasses, and 3—4 h for irons. The gases evolved were allowed to pass through a hot copper oxide layer (600°C) to convert any carbon monoxide to CO_2. Tritiated water and CO_2 were condensed in separate traps. Carbon dioxide was transferred to a flask containing ca. 2% (w/v $BaCl_2$ in 4 M NaOH where the carbonate was precipitated as barium carbonate. Tritiated water was collected in a weighed plastic container.

Purification and counting

Radiocarbon. The barium carbonate (ca. 200 mg) from the "hot lab" was purified in a "cold lab" by decomposing with 4 M HCl and bubbling the liberated CO_2 through: (i) acidified $KMnO_4$ (5% w/v) solution, (ii) chromic acid (10% w/v CrO_3 in 80% H_3PO_4), and (iii) $FeSO_4$ solution (20 g $FeSO_4 \cdot 7H_2O$ in 100 ml of 1:4, H_2SO_4:H_2O). This purification arrangeme has been taken, with modifications, from Maxwell [13]. The purified CO_2 was absorbed in 2 M NaOH containing $BaCl_2$ where it was precipitated as $BaCO_3$. Ammonium chloride solution (20% w/v) was added, and after 1—2 h, the $BaCO_3$ precipitate was filtered through a sintered glass crucible, washed with hot water and ethanol, and dried. The dried precipitate was mounted

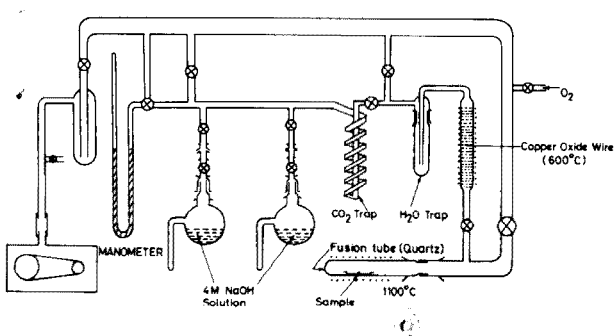

Fig. 1. Sample fusion and purification system.

on a copper planchet in the form of slurry with the aid of ethanol. Drying gave a reasonably uniform deposit. The samples were analysed with an end-window Geiger counter (Low Beta, Sharp Laboratories, La Jolla, Calif.). The counter background was steady at about 0.3 cpm. Statistical errors were kept below 3% by counting for long periods. The sample counting rates ranged from about 2 to 100 cpm. Performance of the counter was checked regularly by counting a standard ^{14}C source.

The low energy of ^{14}C β-rays makes self-absorption serious. The masses of $BaCO_3$ from the monitors and the samples were generally comparable. Experimentally determined relative self-absorption corrections were applied. The mounting geometry was essentially fixed. However, errors can be caused by non-uniform deposition of a sample. Chemical recovery factors were determined from the mass of the recovered $BaCO_3$ and the mass of the carbon present in $CaCO_3$ and $Ca(OH)_2$ carriers. The carbonate contents of $Ca(OH)_2$, mostly from atmospheric absorption, were determined in batches of carrier aliquots (stored over NaOH). In a few cases, the amount of the recovered $BaCO_3$ was more than 100%, indicating some atmospheric contamination; the chemical yield was then assumed to be 100% at the initial precipitation step.

Tritiated water. The tritiated water (ca. 150 mg) was weighed in a plastic container to calculate the chemical yield. It was diluted to about 6 ml for convenient handling and was purified by distillation. However, later results showed that the distillation was unnecessary. Samples were occasionally purified to check for any contamination. An aliquot (1 ml) of the sample solution was mixed with 10 ml of scintillation mixture [14]. The scintillation mixture contained 60 g of naphthalene, 4 g of PPO (2,5-diphenyloxazole), 0.2 g of POPOP (1,4-bis-2-(5-phenyloxazolyl)benzene) or dimethyl-POPOP, 100 ml of methanol, and 20 ml of ethylene glycol, diluted to 1 l with dioxane. The samples were counted on a Tri-Carb scintillation spectrometer (Packard Model No. 3003). The performance of the counter was routinely checked by counting standard and background (ca. 40 cpm). Quenching was proved to be absent by control experiments [14]. Sample counting rates (in cpm) were around 10^5 for tektites, 10^4 for moon samples, 10^3 for stone meteorites and 10^2 for irons.

Contamination

Radiocarbon. The ^{14}C activity in many samples was quite low. It is difficult and cumbersome to characterize ^{14}C from its radiation. Thus it is essential that the isolated ^{14}C be free from radiochemical contamination. This was established by three types of experiments: (i) absorption measurements on some samples with mylar films showed absorption curves identical to those of a standard ^{14}C source; (ii) in chemical repurification experiments, the ^{14}C activity did not change after recycling; (iii) several $BaCO_3$ samples counted after a lapse of time (a few months to a year) did not show appreciable difference, indicating an absence of short-lived radioactive contamination.

As nitrogen is abundant in the atmosphere and its compounds are often present in laboratory environments, it was important to establish the absence of such contamination. Contamination from laboratory handling must have been insignificant because excellent agreement was obtained between replicate measurements on Apollo 14 lunar fine 14163 [15] packed in different runs. Similar results were obtained [16] on other presumably homogeneous samples (stone meteorites, BCR-1, iron meteorites).

The evacuation step seems to desorb any atmospheric nitrogen. This was shown by the results on two Apollo 15 fines, 15012 and 15013 [17]. These samples were packed by the astronauts in vacuum-tight containers on the Moon (vacuum). On Earth, they were processed in a helium atmosphere at Berkeley [18] and, unlike other samples, were never exposed to atmospheric nitrogen. These soils were analysed in two sets. In one set, the fines were processed in an atmosphere of oxygen. In the other set, they were exposed to atmospheric nitrogen before packing for irradiation. The nitrogen contents of two sets did not differ significantly [17], showing an absence of appreciable adsorption. This conclusion is further supported by data on intact and powdered materials (<200 μm) of Shalka achondrite and an Apollo 14 breccia [15]. In comparison with intact pieces, the powdered samples had much larger exposed surfaces, but the nitrogen contents still did not differ significantly.

Tritium. The following three sets of experiments were done to check the possibility of contamination in tritiated samples. First, quenching of the radiation by acidic or basic impurities was checked by adding known amounts of standard solution [14]. Secondly, the samples were distilled and counted again, and the activities of the distilled and undistilled samples were the same. Thirdly, recounting after a lapse of a few months gave almost the same results.

Interfering reactions

Nitrogen measurements. The total ^{14}C measured may not be wholly from ^{14}N but also from ^{17}O (Table 1). If $^{14}C(N)$ and $^{14}C(O)$ are the amounts of carbon-14 produced from ^{14}N and ^{17}O, respectively, then for thermal neutron irradiation of a given sample containing "O" wt.-% oxygen and "N" ppm nitrogen,

$$^{14}C(O) = 0.45\ ^{14}C(N).O/N$$

For a typical sample having 40% oxygen (O = 40):

$$^{14}C(\text{total}) = ^{14}C(O) + ^{14}C(N) = ^{14}C(N).\ (N + 18)/N$$

Even if a sample has no nitrogen, its oxygen content of about 40% should give an apparent nitrogen content of about 18 ppm. This is a serious interference since quite a number of samples have nitrogen contents around or below 20 ppm. However, nitrogen values as low as ca. 10 ppm have been measured

[16, 19] for several stone meteorites (Ehole, Shalka and Paragould), which indicates that the ^{17}O contribution is certainly not as large as estimated. For a better understanding of this problem, a sample of Al_2O_3 [20] having enriched oxygen (^{17}O enriched to 20%) was irradiated and analysed for ^{14}C. Four measurements gave an apparent nitrogen value of 3700 ppm, which suggests that the reaction $^{17}O(n,\alpha)^{14}C$ contributes about 6 ppm apparent nitrogen for a sample having 40% natural oxygen. The ^{17}O contribution is about a factor of 3 lower than that calculated (6 ppm versus 18 ppm). Either the neutron cross-section values are in error, or the excitation function and the neutron energy spectrum combine to give a low production of ^{14}C from ^{17}O. The interference is clearly not serious. Iron samples have no such interference because of their low oxygen contents.

Lithium measurements. An interference in lithium determination is possible from the reaction $^{3}He(n,p)^{3}H$, particularly in samples of meteorites and moon which might contain some cosmogenic helium. In fact, this reaction has been used by Fireman and co-workers [12, 21] to measure ^{3}He in iron meteorites. For thermal neutron irradiation, the following relation is valid

$$^{3}H(He) = 2.04 \times 10^{-4}.\ ^{3}H(Li).\ (^{3}He/^{6}Li)$$

where $^{3}H(He)$ is the tritium produced from ^{3}He, $^{3}H(Li)$ is tritium from ^{6}Li, and the ^{3}He and ^{6}Li concentrations are in 10^{-8} $cm^3\ g^{-1}$ and ppm, respectively.

In most silicates, including chondrites, $^{3}He/^{6}Li$ is less than 10^2. The tritium produced from ^{3}He is thus negligible (less than 2%) compared to the ^{3}H produced from ^{6}Li. In iron meteorites, however, $^{3}He/^{6}Li$ may often be as high as 10^5, which would cause interference in the ^{6}Li determination. The technique can be used for iron meteorites with very low ^{3}He contents. In achondrites also, the $^{3}He/^{6}Li$ ratio is often high.

Errors in measurements

In the case of nitrogen measurements, the most serious errors arise from possible non-uniform deposition of the sample. In lithium measurements, the initial recovery of water might give some unreliability because some water could be adsorbed. However, blank runs after "hot" samples showed that there were no serious "memory" effects. From the spread in the data on replicate runs on samples which were believed to be fairly homogeneous, the errors appear, in both cases, to be of the order of 10% or less. A value of ±10% was therefore assumed for all cases.

Sensitivity and limits of detection

Nitrogen. In silicate materials, because of the interference from $^{17}O(n,\alpha)^{14}C$ the method is not suitable when the nitrogen contents are 10 ppm or lower. For iron meteorites or other oxygen-free materials, measurements can be made at levels of 0.5-ppm nitrogen, and much lower, with higher neutron fluxes. In the present work, silicate samples of about 20 mg and iron samples of about 100 mg were taken for measurement. The size can easily be reduced by a factor of ten if low-level gas-phase counting techniques are used for ^{14}C.

Lithium. Since the smallest lithium contents of most silicates are about 1 ppm, which is easily measured, it is more meaningful to discuss the smallest sample size. In all silicate materials, even those having high ^3He contents (like stone meteorites and lunar samples), the sensitivity is very good and samples as low as 1 mg can be measured. Irradiation at higher neutron fluxes can give still better sensitivity.

Iron meteorites have low lithium contents (10 to a few hundred ppb) [16] and serious interference from ^3He can occur. However, for samples of metal with very low ^3He contents, the technique can be used successfully on 10—50-mg samples. Again this can be further improved by using higher neutron fluxes.

RESULTS AND DISCUSSION

Nitrogen

Extensive measurements of nitrogen in a number of terrestrial standards were done in this work. To make a meaningful comparison of the present data with those of others, several features are important. The choice of a suitable standard is vital. There is evidence that the distribution of some elements in the standards often used may not be uniform [22]. Figure 2 shows the ^{14}C specific activity in BCR-1 and 33d samples from a number of different vials. The scatter in the data is much greater than the normal errors, which indicates that the distribution of nitrogen in either or both standards may not be uniform. If 33d is taken to have 110 ppm N, the value for BCR-1 becomes 39 ppm.

Some other difficulties should also be noted. Some techniques determine not the total but only the chemically bound nitrogen [1, 3]; thus the results would be systematically higher by the neutron activation method. There may be some terrestrial contamination on one hand, and incomplete removal on

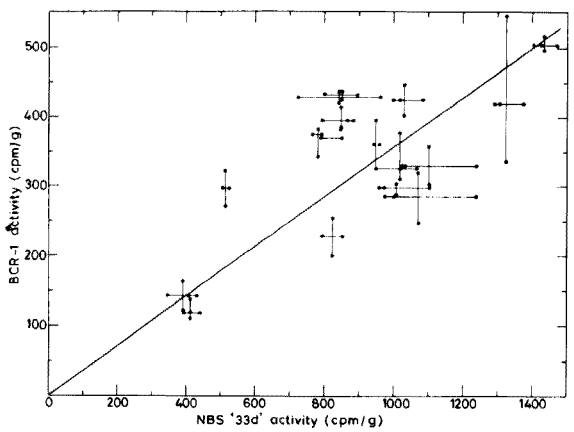

Fig. 2. Comparison of specific ^{14}C activities for NBS "33d" and BCR-1 standards in different runs. The straight line represents 39 ppm N in BCR-1 (33d ≡ 110 ppm N).

the other hand, which may result in a scatter in both directions [23]. Finally, nitrogen may not be uniformly distributed in a sample.

Figure 3 shows a comparison of the present data on samples that may be classified as reasonably homogeneous, with the data obtained by the Arizona Group. By and large, agreement is good, and there is no systematic difference. However, serious differences were found in data on carbonaceous chondrites where the Arizona values [24] are about twice as high as our values [16]. Data on standards from other laboratories are few. Such results are compared in Fig. 4. In general, lower values are reported by Müller [1, 3, 25, 26], probably because he measured only chemically bound nitrogen. Otherwise, the agreement between other data and the present data is fairly satisfactory. Further work on terrestrial standards in different laboratories is needed to obtain a better picture of these problems. Such work at Kanpur, Heidelberg and Arizona is being planned. The best nitrogen values obtained for a number of standards are given in Table 2.

Lithium

The NBS steel standard "33d" proved to be unsuitable as a reference standard because of its low lithium content. All the data obtained here were normalized for BCR-1, the lithium content of which was taken as 13 ppm. Flanagan's compilation [27] reviews the early data on various standards. Two other groups [28, 29] involved in measurements on lunar and meteoritic samples have adopted essentially the same values. Table 3 summarizes the

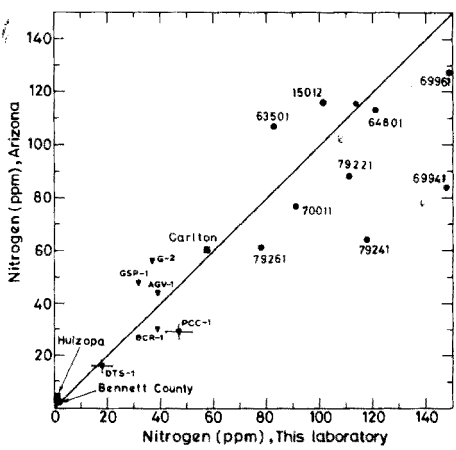

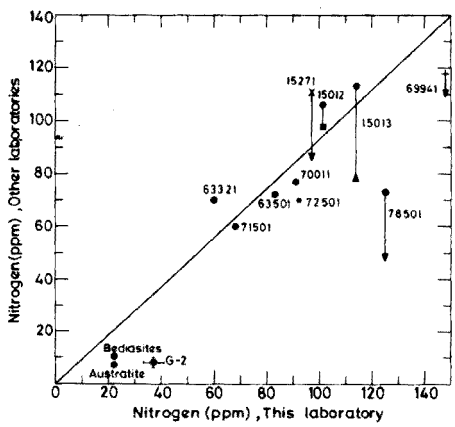

Fig. 3. Comparison of nitrogen data from this laboratory with data from the Arizona Group on samples that are probably homogeneous. Sources for the Arizona values are: DTS-1 and PCC-1, private communication; others, refs. [4, 5, 37]. • Lunar samples. ▼ USGS standards. ■ Iron meteorites (millings).

Fig. 4. Comparison of the present nitrogen data on apparently homogeneous samples with data from other laboratories (excluding the work of the Arizona Group). • Refs. 25, 26, 30. ■ Ref. 32. ▲ Ref. 33. × Ref. 34. ▼ Ref. 35. + Ref. 36.

TABLE 2

Nitrogen values for some standards[a]

Sample	Nitrogen, ppm (±10%)	
	Replicate	Mean
AGV-1, andesite	39, 38	39
BCR-1, basalt	See Fig. 2	39
DTS-1, dunite	15, 20	18
G-2, granite	36, 41, 33	37
GSP-1, granodiorite	31, 35, 29	32
PCC-1, peridotite	43, 50	47
Muscovite[b]	99, 111	105
NBS "12h"[c]	60, 57, 61, 52	57

[a]Standardized with NBS "33d" (≡110 ppm N). [b]Supplied by Professor I. R. Kaplan, UCLA. [c]Certified as 60 ppm N.

TABLE 3

Lithium values for some standards

Sample	This work, ppm (±10%)		Others (ppm)		
	Replicate	Average	Ref. 27	28	29
BCR-1, basalt	≡13		12.8	13	12.7
AGV-1, andesite	11.9, 12.1	12	12	12.5	—
DTS-1, dunite	2.1, 2.2	2.2	2	—	—
G-2, granite	26.5, 44.4, 34.7	35	34.8	40	—
GSP-1, granodiorite	30.8, 27, 46.5	34	32.1	22	—
PCC-1, peridotite	—	2.5	2	1.9	—
Muscovite[a]	320, 400	360	—	—	—

[a]Supplied by Professor I. R. Kaplan, UCLA.

present results for lithium determination in various common standards; literature values are also given. The agreement is generally good, though in some samples, there is apparently serious inhomogeneity. Further work is being done to establish the causes of these variations.

Conclusions

The neutron activation method reported here is suitable for measurements of nitrogen and lithium in a variety of samples. More sophisticated counting techniques would make it possible to determine both nitrogen and lithium on samples of less than 1 mg. A detailed study of the distribution of these elements in various minerals and phases of meteoritic and lunar material would thus be possible. Such developmental work is in progress in this laboratory.

We thank Drs. I. R. Kaplan, C. B. Moore, and O. Müller for making available the standard samples and their unpublished data. Dr. B. S. Carpenter is thanked for donating the enriched aluminum sample. This research was partly supported through an ISRO grant.

REFERENCES

1 O. Müller, Proc. Third Lunar Sci. Conf., Geochim. Cosmochim. Acta Suppl. 3, (1972) 2059.
2 W. Werner and G. Tölg, Z. Anal. Chem., 276 (1975) 103.
3 O. Müller, E. Grallath and G. Tölg, Proc. Seventh Lunar Sci. Conf., Geochim. Cosmochim. Acta Suppl. 7, (1976) 1615.
4 E. K. Gibson and C. B. Moore, Anal. Chem., 42 (1970) 461.
5 C. B. Moore and C. F. Lewis, in C. Watkins (Ed.), Lunar Science VII, The Lunar Science Institute, Houston, 1976, p. 571.
6 A. K. Berzin, K. F. Kunetsov, V. V. Sulin and V. I. Belov, Isot. Radiat. Technol., 3 (1966) 334.
7 E. Engalmann, J. Gosset, M. Loeuillet, A. Marschal, P. Ossart and M. Boisser, Nat. Bur. Stand. (U.S.) Spec. Pub. 312, Vol. II, Modern Trends in Activation Analysis, 1969, p. 819.
8 T. Nozaki, Y. Yatsurugi, N. Akiyama and I. Imai, Nat. Bur. Stand. (U.S.) Spec. Publ. 312, Vol. II, Modern Trends in Activation Analysis, 1969, p. 842.
9 S. S. Nargolwalla and E. P. Przybylowicz, Activation Analysis with Neutron Generators, J. Wiley, New York, 1973, p. 465.
10 P. S. Goel, Geochim. Cosmochim. Acta, 34 (1970) 932.
11 L. Kaplan and K. E. Wilzbach, Anal. Chem., 26 (1954) 1797.
12 E. L. Fireman and D. Schwarzer, Geochim. Cosmochim. Acta, 11 (1957) 252.
13 J. A. Maxwell, Rock and Mineral Analysis, Interscience, 1968.
14 E. Schram and R. Lombart, Organic Scintillation Detectors, Elsevier, Amsterdam, 1963.
15 P. S. Goel and B. K. Kothari, Proc. Third Lunar Sci. Conf., Geochim. Cosmochim. Acta Suppl. 3, (1972) 2041.
16 P. N. Shukla, Distribution of Nitrogen and Lithium in Samples of Moon, Meteorites, and Tektites, Ph.D. Dissertation, Indian Institute of Technology, Kanpur, 1977.
17 B. K. Kothari and P. S. Goel, Proc. Fourth Lunar Sci. Conf., Geochim. Cosmochim. Acta Suppl. 4, (1973) 1587.
18 B. R. Simoneit, J. T. Wilder, P. C. Wszolek and A. L. Burlingame, UCB Space Sciences Laboratory Organic Clean Room and Lunar Material Transfer Facilities. The transfer of Pristine Lunar Material from the Apollo 15 SESC 15012 and SESC 15013. Space Sciences Laboratory, University of California, Berkeley, 1972.
19 B. K. Kothari and P. S. Goel, Geochim. Cosmochim. Acta, 38 (1974) 1493.
20 B. S. Carpenter, D. Samuel and I. Wasserman, Radiat. Effects, 19 (1973) 59.
21 E. L. Fireman, Nature, 181 (1958) 1725.
22 C. B. Moore, Arizona State University, private communication, 1974.
23 C. B. Moore, C. F. Lewis, J. Cripe, F. M. Delles, W. R. Kelly and E. K. Gibson, Proc. Third Lunar Sci. Conf., Geochim. Cosmochim. Acta Suppl. 3, (1972) 2051.
24 E. K. Gibson, C. B. Moore and C. F. Lewis, Geochim. Cosmochim. Acta, 35 (1971) 599.
25 O. Müller, Proc. Fourth Lunar Sci. Conf., Geochim. Cosmochim. Acta Suppl. 4, (1973) 1625.
26 O. Müller, Proc. Fifth Lunar Sci. Conf., Geochim. Cosmochim. Acta Suppl. 5, (1974) 1907.
27 F. J. Flanagan, Geochim. Cosmochim. Acta, 37 (1973) 1189.

28 S. R. Taylor, P. H. Johnson, R. Martin, D. Bennett, J. Allen and W. Nance, Proc. Apollo 11 Lunar Sci. Conf., Geochim. Cosmochim. Acta Suppl. 1, (1970) 1627.
29 J. A. Philpotts, C. C. Schnetzler, M. L. Bottino, S. Schuhmann and H. H. Thomas, Earth Planet. Sci. Lett., 13 (1972) 429.
30 O. Müller, quoted in ref. 31.
31 F. Wlotzka, in Handbook of Geochemistry, K. H. Wedepohl (Ed.), Springer-Verlag, 1972, Chapter 7.
32 S. Chang, J. Smith, H. Sakai, C. Petrowski, K. A. Kvenvolden and I. R. Kaplan, in J. W. Chamberlain and C. Watkins (Eds.), The Apollo 15 Lunar Samples, The Lunar Science Institute, Houston, 1972, p. 291.
33 B. R. Simoneit, P. C. Wszolek and A. L. Burlingame, in J. W. Chamberlain and C. Watkins (Eds.), The Apollo 15 Lunar Samples, The Lunar Science Institute, Houston, 1972, p. 286.
34 H. Sakai, C. Petrowski, M. B. Goldhaber, and I. R. Kaplan, in C. Watkins (Ed.), Lunar Science-III, The Lunar Science Institute, Houston, 1972, p. 672.
35 R. H. Becker and R. N. Clayton, Proc. Sixth Lunar Sci. Conf., Geochim. Cosmochim. Acta Suppl. 6, (1975) 2131.
36 J. F. Kerridge, I. R. Kaplan, and C. Petrowski, in C. Watkins (Ed.), Lunar Science-VI, The Lunar Science Institute, Houston, 1975, p. 469.
37 E. K. Gibson and C. B. Moore, Geochim. Cosmochim. Acta, 35 (1971) 877.

Analytica Chimica Acta, 96 (1978) 271—277

DETERMINATION OF ARSENIC AND GALLIUM IN STANDARD MATERIALS BY INSTRUMENTAL EPITHERMAL NEUTRON ACTIVATION ANALYSIS

LAWRENCE E. WANGEN* and ERNEST S. GLADNEY

University of California, Los Alamos Scientific Laboratory, P.O. Box 1663, Los Alamos, New Mexico 87545 (U.S.A.)

(Received 3rd August 1977)

SUMMARY

Epithermal neutron activation analysis has been applied to the determination of arsenic and gallium in standard materials at trace concentrations. The reduction of ^{24}Na activity compared to thermal neutron activation is advantageous. Arsenic detection limits (1σ) are 0.04 and 0.015 μg for inorganic and organic materials, respectively. The corresponding gallium detection limits, for the best cases, are 0.13 and 0.29 μg. Gallium determinations with the 834-keV photopeak of ^{72}Ga suffered interferences attributed to the threshold reaction $^{54}Fe(n,p)$ ^{54}Mn; the less intense ^{72}Ga peaks at 629 and 2200 keV provided quantitative results for all samples tested. Gallium detection limits with the less intense, but more reliable 629-keV peak were 0.9 and 0.1 μg for inorganic and organic materials, respectively. Arsenic determinations are best performed with the more intense ^{76}As 559-keV line, as the 657-keV line has an unknown interference.

Arsenic and gallium are believed to be significantly introduced into the environment by coal combustion [1—4]. The results of some investigators [2, 3] indicate that arsenic and gallium are among the elements preferentially concentrated on small fly ash particles and thus not efficiently collected by the particulate control devices currently used on coal-fired power plants for the reduction of stack emissions. Other data [4] suggest that arsenic and gallium in coal ash are relatively soluble in aqueous solutions with pH values common to natural environments. Thus an evaluation of the environmental impacts of coal combustion will require the concentrations of these elements in natural ecosystems to be monitored.

Concentrations of arsenic and gallium range from low parts per billion in aquatic systems to several parts per million in soils and rocks [5], and sensitive quantitative methods for these elements are required. In addition, the variable concentration of a given trace element in natural systems usually means that many samples must be analyzed for a statistically meaningful result. Thus the rapidity of analysis is also an important criterion for an analytical method.

Several recent studies have investigated the use of epithermal neutrons for activation analysis [6—10]. Epithermal neutrons are usually defined as those

neutrons, generated by a nuclear reactor, which are not absorbed by cadmium foil. Cadmium, with an absorption cross-section for thermal neutrons of 2450 barns, is essentially opaque to neutrons with kinetic energies less than about 0.5 eV. Thus the energy range of epithermal neutrons is conveniently defined as 0.5 eV to about 1.0 MeV [11]. Epithermal neutrons offer a method of increasing the activities of those nuclides produced from isotopes with resonances in the epithermal region relative to the activities of those nuclides produced from isotopes with essentially 1/V cross-sections. Of particular utility are the increased activities of various nuclides with half-lives of the order of hours, relative to that of ^{24}Na. Sodium is present in most matrices at major element concentrations and ^{23}Na, with an isotopic abundance of 100%, has relatively few resonance absorptions in the epithermal energy region. In addition, ^{24}Na has intense γ-rays, at 2754 and 1368 keV, that dominate the analytically useful spectrum. Any procedures that reduce its activity, relative to other nuclides, can be of considerable utility for elemental analyses by instrumental neutron activation.

The theoretical advantage factor of activation by epithermal as opposed to thermal neutrons has been defined by Steinnes [10] as: $F_a = (I_0/\sigma_0)_D/(\sigma_0/I_0)_X$, where σ_0 and I_0 are absorption cross-sections for thermal and epithermal neutrons respectively, D is an element of interest, and X is a major interfering element. Advantage factors greater than unity suggest that the activity of the nuclide produced from isotope D should be enhanced relative to that of a major interfering nuclide X, such as ^{24}Na.

EXPERIMENTAL

Samples (ca. 1 g) in polyethylene vials were irradiated for 1 h in the Omega West Reactor's epithermal facility at the Los Alamos Scientific Laboratory. This is a permanent facility constructed from a 50-50 volume mixture of powdered elemental boron and aluminum, hot pressed into aluminum sleeves and accessible from an external injection port [12]. The shield wall is 2.54 cm thick and provides about 2.3 gm cm^{-2} of boron; this gives an estimated lower energy filter cutoff of 280 eV and should provide essentially total absorption of thermal neutrons [13]. Thus the theoretical advantage factors should be nearly correct except for those isotopes with resonance absorptions primarily below 280 eV. The epithermal flux in this facility was estimated to be about 5×10^{10} n cm^{-2} s^{-1}.

Arsenic and gallium standards were pipetted from solution onto filter papers that were folded into the same geometry as the samples and also placed into polyethylene vials. Nichrome wire flux monitors were irradiated in the same vial as the sample. Two sample vials were irradiated during each run, and six standards were included at various times during the irradiations. Blank filters and vials were also irradiated and counted. Samples were counted in the irradiation vials, following a 1—4-d decay period, for 60—90 min real time, with an 11.4% Ge(Li) detector with a resolution of 1.8 keV FWHM at

1332 keV and a 4000-channel analyzer. An automatic sample transfer system was used for overnight and week-end counting. Analyzer dead times were ca. 2—5% at a sample-to-detector distance of about 1 cm. Spectra were taken at a gain of 0.64 keV/channel and recorded on magnetic tape for later computerized reduction. Half-lives of both the 559-keV ^{76}As peak and the 629-keV ^{72}Ga peak were checked to ensure the identity of As and Ga.

RESULTS AND DISCUSSION

The significant nuclear reactions for the determination of arsenic and gallium and other pertinent data [14, 15] are shown in Table 1. The theoretical advantage factors, as defined above, relative to ^{23}Na, are 9.1 for the activation of ^{71}Ga and 24.5 for the activation of ^{75}As. These advantage factors suggest considerable enhancement of ^{72}Ga and ^{76}As activities relative to that of ^{24}Na upon activation by epithermal as opposed to thermal neutrons. Arsenic and gallium concentrations obtained for various standard materials are listed in Table 2; the values determined, with the 559-keV ^{76}As peak, and the 630- and 2200-keV peaks of ^{72}Ga, are in good agreement with the certified concentrations. Concentrations determined by integration of the 657-keV peak of ^{76}As and the 834-keV ^{72}Ga peak are often excessively high, suggesting interfering photopeaks.

The high arsenic concentrations determined with the 657-keV ^{76}As peak indicate a positive interference, particularly for three USGS rocks (BCR-1, AGV-1, and G-2) and the Eastman Kodak biological standard, TEG 50-C. The half-life of ^{76}As is 26.2 h. The apparent half-life of the 657-keV photopeak ranges from a low of 15 h for AGV-1 to a high of 44 h for TEG 50-C. Thus there are apparently at least two interferences in ^{76}As determinations with the 657-keV peak, a 559-keV γ-peak can be used for arsenic determinations with confidence, whereas the 657-keV peak should be used only as confirmatory identification. This is not a serious disadvantage as the 559-keV line is the more intense.

TABLE 1

Nuclear data for gallium, arsenic, and sodium isotopes [14, 15]

Reaction	Isotopic abundance (%)	Product half-life (h)	σ_0 Thermal cross section (barns)	I_0 Resonance integral (barns)	Product γ-rays[a] (keV)
^{71}Ga(n,γ)^{72g}Ga	39.6	14	4.7	25	629(26); 834(100); 2200(31)
^{75}As(n,γ)^{76}As	100	26.5	4.4	63	559(100); 657(15); 1216(10)
^{23}Na(n,γ)^{24}Na	100	15	0.53	0.31	1368(100); 2754 (100)

[a]Numbers in parentheses are relative percent peak intensities.

TABLE 2

Arsenic and gallium concentrations ($\mu g\ g^{-1}$) determined from various photopeaks[a]

Sample	Arsenic			Gallium			
	559 keV	657 keV	Accepted concentration	630 keV	834 keV	2200 keV	Accepted concentration
NBS SRM Fly Ash	54(1)	62(1)	61 ± 6	37(2)	66(1)	30(3)	38.3 ± 6.3
NBS SRM Coal	5.4(0.1)	7.0(0.3)	5.9 ± 0.6	4.8(0.2)	5.7(0.1)	4.6(0.5)	5.4 ± 0.5
NBS SRM Orchard Leaves	9.9(0.1)	9.8(0.1)	11 ± 2	⩽0.16	0.17(0.04)	⩽0.16	0.085
NBS SRM Bovine Liver	0.03(0.015)	⩽0.26	(0.055)[b]	⩽0.24	⩽0.08	⩽0.40	
TEG 50-A[c]	53(1)	56(1)	48 ± 8	55(1)	55(1)	54(2)	
TEG 50-B[c]	106(4)	110(6)		⩽0.16	⩽0.05	⩽0.18	
TEG 50-C[c]	0.09(0.04)	3.4(0.24)		55(2)	55(1)	57(1)	
GSP-1 (Granodiorite)[d]	⩽0.08	⩽0.8	0.09	20(2)	36(1)	16(3)	22
BCR-1 (Basalt)[d]	0.54(0.05)	4.9(0.5)	0.70	17(2)	68(2)	20(3)	20
PCC (Peridotite)[d]	⩽0.08	⩽0.6	0.05	⩽2.0	33(1)	⩽3.4	0.4
AGV-1 (Andesite)[d]	0.71(0.06)	4.2(0.5)	0.8	20(3)	43(2)	18(11)	22
G-2 (Granite)[d]	0.17(0.05)	11.8(0.6)	0.25	22(2)	29(1)	21(3)	22.9
NBS SRM Opal[e]	1826(73)	2092(105)	690	ND	ND	ND	

[a]Numbers in parentheses are standard deviations due to counting statistics only. [b]NBS informational value, not certified. [c]Eastman Kodak trace element gelatin standard for biological materials. [d]USGS standard rocks. [e]No Ga detection limit for opal because it was counted after decaying for 101 h so only 0.7% of the original ^{72}Ga activity remained, ND means no data.

Gallium concentrations (Table 2) were determined independently, by integration of the 629 (26%), 834 (100%), and 2200 (31%) keV γ-peaks. The concentrations found for several standard materials with the 834-keV peak are high, whereas those determined from the 630 and 2200-keV peaks are comparable with each other and with literature values. Half-lives determined for decay of the 629-keV photopeak ranged from 11.3 h to 18.5 h (mean, 14.4 h). All were within one standard deviation of 14 h, which is the half-life of ^{72}Ga. In contrast, estimated half-lives for the 834-keV photopeak activity ranged from 13.8 h to several days. Thus the 834-keV line provides analytically useful gallium determinations for some of the samples, but it is not generally reliable. The most plausible interfering γ-ray at 834-keV arises from the production of ^{54}Mn by the ^{55}Mn(n,2n) or the ^{54}Fe(n,p) reaction. γ-Spectra of these samples show no 834-keV interference in the presence of large ^{56}Mn peaks at 846, 1811, and 2112 keV but do exhibit the interference when the 1099 and 1291-keV lines of ^{59}Fe are present. Therefore the interference in gallium determinations with the 834-keV peak results principally from the reaction ^{54}Fe (n,p) ^{54}Mn. The 834-keV photopeak should be used for unconfirmed gallium determinations only in the absence of iron, unless corrections are made for the contribution of iron to peak areas. Also the possibility remains that ^{54}Mn may cause a small interference. There are apparently no interferences in gallium determinations with either the 629 or 2200-keV peaks in these materials.

Detection limits

Detection limits for elements determined by instrumental neutron activation analysis vary substantially for different samples, depending on experimental conditions and elemental composition. Irradiation and counting procedures can be optimized to minimize detection limits for a specific sample matrix, but these may not be applicable to other situations or samples. Nevertheless, it is useful to specify detection limits to enable comparison to be made with other methods. Detection limits for each peak, under the conditions of this study, are reported in Table 3. These limits were estimated by taking the square root of a nine-channel integration of the background counts under the appropriate photopeak and converting these counts to an equivalent mass of As or Ga. These detection limits seem to vary according to whether the sample matrix is predominantly organic or inorganic, thus such, more generalized, limits are also given. The lower limits for organic matrices are undoubtedly due to large quantities of carbon and hydrogen which have no product nuclides contributing to total sample activity. Thus these have significantly lower background. Several of the samples were counted at both 1 day and 2—3 days. Arsenic detection limits did not vary significantly over this time period, but those of gallium were lower by about a factor of 2 for the earlier counts. This probably results from the shorter half-life of ^{72}Ga and suggests that counting at 15—30 h after irradiation is probably the optimum for these samples and

TABLE 3

Detection limits (in μg for 1σ) for the conditions of this study

Photopeak integrated (keV)	^{76}As		^{72}Ga		
	559	657	629	834	2200
NBS Fly Ash	0.04	0.4	0.34	0.11	0.58
G-2	0.04	0.4	0.8	0.27	1.5
AGV-1	0.04	0.4	1.1	0.11	1.9
PCC-1	0.04	0.3	1.0	0.09	1.7
BCR—1	0.04	0.4	1.1	0.11	1.9
GSP-1	0.04	0.4	1.1	0.11	1.9
NBS Coal	0.017	0.15	0.14	0.039	1.17
NBS Bovine Liver	0.015	0.13	0.12	0.040	0.20
NBS Orch. Leaves	0.011	0.09	0.08	0.024	0.08
TEG 50-B	0.014	0.10	0.08	0.025	0.09
TEG 50-A	0.021	0.18	0.17	0.039	0.18
TEG 50-C	0.016	0.15	0.14	0.031	0.17
Inorganic	0.04	0.38	0.91	0.13	1.6
Organic	0.015	0.13	0.12	0.029	0.15

irradiation conditions. These limits could be improved by increasing the irradiation and/or counting times.

Arsenic detection limits with the 559-keV photopeak are an order of magnitude lower than those of the 657-keV peak. Detection limits for gallium with the three different photopeaks range from 0.13 to 1.6 μg for the inorganic matrix, and from 0.03 to 0.15 μg for organic matrices. The 834-keV peak provides detection limits which are sufficiently better to justify the simultaneous determination of iron when both are present at low concentrations.

We thank the staff at the Los Alamos Scientific Laboratory's Omega West Reactor Facility for their gracious assistance with irradiation and counting of samples. This research was supported by EPA/ERDA, E-APID No. 78BCC.

REFERENCES

1 K. K. Bertine and E. D. Goldberg, Science, 173 (1971) 233.
2 D. F. S. Natusch, J. R. Wallace, and C. A. Evans, Jr., Science, 183 (1974) 202.
3 R. C. Ragaini and J. M. Ondov, Proc. Int. Conf. Environmental Sensing and Assessment, Vol. 1, IEEE, New York, 1976, p. 17-2.
4 D. R. Dreesen, L. E. Wangen, E. S. Gladney, and J. W. Owens, Proc. Symp. Environmental Chemistry and Cycling Processes, Augusta, Georgia, U.S.A., 1976, in D. C. Adriano and I. L. Brisbin (Eds.), ERDA CONF. 760429, 1977.
5 H. J. M. Bowen, Trace Elements in Biochemistry, Academic Press, London, 1966, p. 174, 185.
6 A. O. Brunfelt and E. Steinnes, Anal. Chim. Acta, 48 (1969) 13.
7 M. Janssens, B. Desmet, R. Dams and J. Hoste, J. Radioanal. Chem., 26 (1975) 305.

8 N. V. Bagdavadze and L. M. Mosuslishvili, J. Radioanal. Chem., 24 (1975) 65.
9 R. Dams, J. Belliet, and J. Hoste, Int. J. Environ. Anal. Chem., 4 (1975) 141.
10 E. Steinnes, Anal. Chem., 48 (1976) 1440.
11 A. O. Brunfelt and E. Steinnes (Ed.), Activation Analysis in Geochemistry and Cosmochemistry, Universitetesforlaget, Oslo, 1971, p. 113.
12 C. L. Warner, Los Alamos Scientific Laboratory, internal communication, May 1974.
13 F. Rossitto, M. Terrani, and S. Terrani, Nucl. Instrum. Methods, 103 (1972) 77.
14 D. Brune and J. J. Schmidt (Eds.), Handbook on Nuclear Activation Cross Sections, IAEA, Vienna, 1974.
15 S. A. Lis, P. K. Hopke, and J. L. Fasching, J. Radioanal. Chem., 24 (1975) 125.

Analytica Chimica Acta, 96 (1978) 279—284

CALIBRATION AND USE OF A HIGH-RESOLUTION, LOW-ENERGY PHOTON DETECTOR FOR MEASURING PLUTONIUM ISOTOPIC ABUNDANCES

JOSEPH BUBERNAK

University of California, Los Alamos Scientific Laboratory, Los Alamos, New Mexico 87545 (U.S.A.)

(Received 17th August 1977)

SUMMARY

A low-energy photon detector was easily and accurately calibrated with plutonium sources of known isotopic contents after purification of the sources by anion exchange. Rapid data processing was attained by minicomputer calculations. Results obtained for plutonium abundances by γ-spectrometry and by mass spectrometry agreed within 1% for the ^{240}Pu isotope, and within 10% for ^{238}Pu and ^{241}Pu at the concentrations normally present. Alpha specific activities calculated from the abundances obtained by the two methods agreed within 0.5%.

Several regions of the spectrum of γ-rays emitted by plutonium isotopes have been investigated for possible use in measuring isotopic abundances [1—3]. A low-energy photon detector (LEPD) was suggested by Umezawa et al. [3] as being the most sensitive for measuring γ-rays of 43.5 keV for ^{238}Pu, 51.6 keV for ^{239}Pu, 45.2 keV for ^{240}Pu and 148.5 keV for ^{241}Pu. These γ-rays were used in the present work. Relative detector efficiency corrections can be made with ^{239}Pu γ-rays with energies of 38.7, 51.6, 129.6 and 203.5 keV. All of these are singlets, and accurate calculation of peak areas involves only a simple background subtraction from total counts in the peaks. A smoothed spectrum was chosen in the present work to allow greater accuracy for small peaks.

It is proposed that calibrations be based on the 51.6-keV peak of ^{239}Pu, whose specific activity is given an arbitrary value of 1 count per μg. The specific activities of all other γ-rays of interest can then be compared to that of the 51.6-keV peak by means of plutonium samples of known isotopic contents. Analyses of unknown samples are then based on a direct relationship of peak area for a given isotope to the weight of that isotope, based on the specific activity determined in the calibration. The analyses are free, therefore, of errors in γ-ray branching, half-lives, and other similar factors reported in the literature. A consistent set of γ-ray branching ratios for ^{239}Pu is required for construction of a smooth efficiency curve, and the set reported by Gunnink and Morrow [4] was used. A log-log second-order equation was found to fit the data best.

The plutonium purification procedure of Kressin and Waterbury [5] by anion exchange was used to eliminate interferences by non-plutonium isotopes. Data analyses can be carried out automatically and without intervention by the operator, by using a minicomputer interacting with the pulse-height analyzer.

EXPERIMENTAL

Equipment

A coaxial-type Ge(Li) low-energy photon detector with a 0.13-mm thick beryllium window was used for the measurements. It provided a resolution of 500 eV FWHM for the 122-keV γ-ray of ^{57}Co. The detector was coupled to a Canberra model 8700 pulse-height analyzer which in turn was interfaced with a Digital Corporation model PDP-11/20 minicomputer.

Recommended procedure

Anion exchange. Pipet an aliquot of solution containing 1—5 mg of plutonium into a 3-dram glass vial. Place the vial in a near-prone position on a ribbed watch glass inside a crystallizing dish, and evaporate the solution to near dryness under a heat lamp. Repeat the evaporation after adding 5 ml of concentrated nitric acid, to convert plutonium to the nitrate form. Adjust the plutonium solution to 8 M in nitric acid and heat with a few drops of 30% hydrogen peroxide to produce plutonium(IV). Transfer the plutonium(IV) solution to an ion-exchange column (i.d. 6 mm) containing a 6-cm bed of Dowex 1-X4 resin (50-100 mesh) in the nitrate form. Wash the column with 20 ml of 8 M nitric acid to remove ^{241}Am and ^{237}U impurities. Elute the plutonium into a new 3-dram vial with 2—4 ml of 0.35 M nitric—0.01 M hydrofluoric acids. Cap the vial and place in a plastic holder on top of the LEPD.

Calibration. Accumulate a γ-ray spectrum of a purified plutonium solution with known isotopic composition for 1000—3000 s. Calculate the areas under all the peaks of interest. Using the areas for the ^{239}Pu peaks at 38.7, 51.6, 129.6 and 203.5 keV and the abundances listed by Gunnink and Morrow [4], construct a relative efficiency calibration curve. Adjust the areas for the peaks at 43.5, 45.2, 51.6 and 148.5 keV, using the relative efficiencies interpolated from the curve. Calculate the quotients CA(43.5)/μg ^{238}Pu, CA(45.2)/μg ^{240}Pu, CA(51.6)/μg ^{239}Pu and CA(148.5)/μg ^{241}Pu, where CA represents corrected peak areas. Calculate specific activities for the isotopes relative to one count per μg ^{239}Pu by dividing each quotient by CA(51.6)/μg ^{239}Pu.

Analysis. Accumulate a spectrum of the purified sample solution. Proceed with the construction of the relative efficiency curve and calculation of corrected peak areas as above. Obtain relative weights of each isotope by dividing the proper peak area by its specific activity. Assuming the sum of ^{238}Pu, ^{239}Pu, ^{240}Pu and ^{241}Pu to represent total plutonium, calculate the weight percent of each isotope.

Computer aids

If an interactive computer program such as Canberra's SPECTRAN is available, one or more of the following routines can be implemented to speed up analysis and/or yield more accurate results.

1. Peak search. In a trial run, determine the peak channels for the 51.6- and 129.8-keV peaks of ^{239}Pu. In future runs, accumulate a spectrum such that the 51.6-keV peak occurs within ±50 channels of that obtained in the trial run. Write a program routine so that the principal peak occurring in the 100-channel region shall be designated the 51.6-keV peak. Similarly, the principal peak occurring in the ±50-channel region about the other trial run channel shall be designated the 129.8-keV peak. This process allows for analyzer gain shift. Having established the peak channels for these two γ-rays, use a two-point calibration to determine the energies of all other peaks in the spectrum.

2. Spectrum smoothing. Use the SPECTRAN smoothing function before obtaining peak areas, to allow greater accuracy for small peaks.

3. Detector efficiency. Use the SPECTRAN log-log second-order fit for efficiency data, for speed and accuracy.

RESULTS AND DISCUSSION

The anion-exchange purification procedure described provided adequate decontamination of plutonium from ^{241}Am and ^{237}U interferences. No other contaminants were present in the sources studied.

The effect of smoothing a spectrum was greatest for small peaks, as illustrated in Fig. 1, which shows the unsmoothed and smoothed 56.8-keV peak of ^{239}Pu at a gain setting of 0.0593 keV per channel. Some plutonium

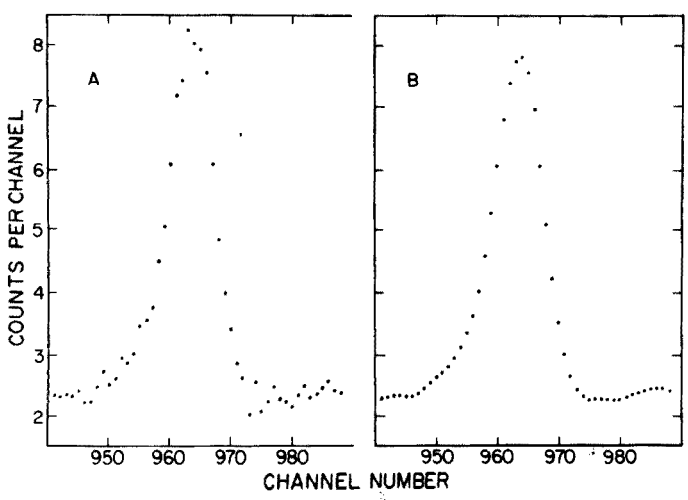

Fig. 1. Plots of raw (A) and smoothed (B) data in the 56.8-keV peak of a plutonium spectrum.

peaks used here showed smaller or greater effects on smoothing. Since peak areas are dependent on the end points for background subtraction, smoothing enabled more consistent areas to be obtained by eliminating large variations in the end points.

A log-log second order equation of the efficiency data produced a curve that fit the data well (Fig. 2). An efficiency equation must be obtained for each run, because of the low γ-ray energies and high self-attenuations involved in the measurements.

Values found for the specific activities CA(43.5)/μg ^{238}Pu, CA(45.2)/μg ^{240}Pu, and CA(148.5)/μg ^{241}Pu relative to CA(51.6)/μg ^{239}Pu = 1 were 331, 5.22 and 14.8, respectively. These were averages of 15 determinations on 5 different plutonium sources that were previously analyzed for isotopic abundances by mass spectrometry. Perhaps several determinations on one standard sample, preferably containing at least 0.1% ^{238}Pu and 3% ^{241}Pu, should suffice for the accurate calibration of a new detector system.

Determined values for plutonium isotopic abundances in several samples are shown in Table 1, and compared with mass spectrometric values in Table 2. The ^{238}Pu values in the mass spectrometric data were actually determined by α-spectrometry, which is deemed more accurate. Note that the mass spectrometric data do not total 100% because of omission of ^{242}Pu abundances. The γ-spectrometric measurements cannot include ^{242}Pu because of its lack of activity. Therefore, comparisons between the two sets of data are not exactly justified. However, the positive bias introduced into the γ-spectrometric data by the omission of (0.6%) ^{242}Pu is minimal. As expected, comparisons between mass and γ-spectrometric values show the greatest differences ($\leqslant$10%) for the low-abundance ^{238}Pu and ^{241}Pu. Agreement was within 1% for ^{240}Pu.

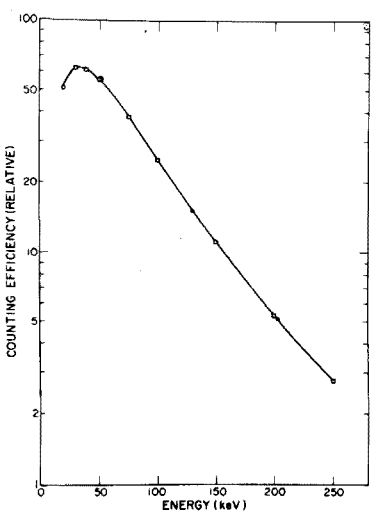

Fig. 2. Efficiency curve obtained with a log-log second-order equation. ○ Experimental point. □ Fitted point.

TABLE 1

Plutonium isotopic analyses and α-specific activities found by γ-spectrometry

Sample no.	Isotopic abundance, wt. %[a]				α-Spec. act.[a] c/m-μg
	^{238}Pu	^{239}Pu	^{240}Pu	^{241}Pu	
1	0.0168± 2.09(3)	93.68± 0.03(3)	5.874± 0.39(3)	0.422± 1.17(3)	83449± 0.13 (3)
2	0.0120± 2.10(3)	91.59± 0.08 (3)	7.987± 0.98(3)	0.410± 3.87(3)	86460± 0.23 (3)
3	0.013± 0(4)	83.35± 0.13(4)	15.42± 0.71(4)	1.21± 3.59(4)	99945± 0.23 (4)
4	0.016± 7.83(4)	77.63± 0.30(4)	20.62± 0.74(4)	1.73± 5.50(4)	109986± 0.39 (4)
5	0.243± 0.33(5)	84.05± 0.13(5)	12.30± 0.42(5)	3.39± 2.35(5)	137267± 0.17 (5)

[a]Each result is the average of several determinations with the relative standard deviation. The number of determinations is given in parentheses.

TABLE 2

Comparison of γ- and mass spectrometric results

Method	Isotopic abundances, wt. %				α-Spec. act. c/m-μg
	^{238}Pu	^{239}Pu	^{240}Pu	^{241}Pu	
γ-s.[a]	0.0168	93.68	5.874	0.422	83449
m. s.[b]	0.0154[c]	93.69	5.873	0.397	83425
Diff.[d]	+9.1	—0.01	+0.01	+6.3	+0.03
γ-s.	0.0120	91.59	7.987	0.410	86460
m. s.	0.0114[c]	91.60	7.954	0.401	86535
Diff.	+5.3	0.0	+0.41	+2.2	—0.09
γ-s.	0.013	83.35	15.42	1.21	99945
m. s.	0.013[c]	83.28	15.28	1.18	100213
Diff.	0	+0.08	+0.92	+2.5	—0.3
γ-s.	0.016	77.63	20.62	1.73	109986
m. s.	0.018[c]	77.41	20.50	1.70	110545
Diff.	—8.3	+0.28	+0.59	+1.8	—0.01
m. s.	0.243	84.05	12.30	3.39	137267
γ-s.	0.240[c]	83.71	12.19	3.29	136587
Diff.	+1.2	+0.41	+0.90	+3.0	+0.50

[a]γ-Spectrometry. [b]Mass spectrometry. [c]The ^{238}Pu is determined by α-spectrometry instead of mass spectrometry. [d](γ-s.—m. s.) × 100/(m. s.).

An important application of isotopic abundance analyses is the calculation of α-specific activities. A quick and inexpensive method is needed for determining specific activities to within ±1% accuracy, as a control over the determination of total plutonium by α-counting. As seen in Table 2, γ-spectrometry attains the desired accuracy. In Table 2, mass spectrometric values for α-specific activities included that from ^{242}Pu.

The minicomputer program written in Canberra's CLASS language and based on SPECTRAN III has been entirely satisfactory. Once the spectrum has been accumulated and the program started, the entire operation of peak searching, peak area determination, efficiency calibration and isotopic calculation is completely automatic.

This work was sponsored by the Division of Nuclear Research and Applications of the U.S. Energy Research and Development Administration.

REFERENCES

1 J. E. Cline, E. B. Nieschmidt, A. L. Connelly and E. L. Murri, A Technique for Assay of L-10 Bottles of Plutonium Nitrate, Idaho Nuclear Corporation Report IN-1433, October 1970.
2 R. Gunnink, J. B. Niday, and P. D. Siemens, A System for Plutonium Analysis by Gamma Ray Spectrometry, Part I: Techniques for Analysis of Solutions, Lawrence Livermore Laboratory Report UCRL-51517, Pt. 1, April, 1974.
3 H. Umezawa, T. Suzuki and S. Ichikawa, J. Nucl. Sci. Technol., 13 (1976) 327.
4 R. Gunnink and R. J. Morrow, Gamma-ray Energies and Absolute Branching Intensities for Plutonium-238, 239, 240, 241, and Americium-241, Lawrence Livermore Radiation Laboratory Report UCRL-51087, July, 1971.
5 I. K. Kressin and G. R. Waterbury, Anal. Chem., 34 (1962) 1598.

Analytica Chimica Acta, 96 (1978) 285—291

DETERMINATION OF TRACES OF VANADIUM IN CATALYSTS BY NEUTRON ACTIVATION ANALYSIS

H. D. BUENAFAMA* and J. A. LUBKOWITZ[§]

Instituto Venezolano de Investigaciones Científicas Centro de Petróleo y Química, Apartado 1827, Caracas (Venezuela)

(Received 11th May 1977)

SUMMARY

Determination of vanadium at very low levels in impregnated alumina-based catalysts by neutron activation analysis is reported. A pre-irradiation separation of vanadium, based on methyl isobutyl ketone extraction, yields high decontamination factors for Mo and Al. The technique is simple, precise and quantitative; recoveries of 50 ng of vanadium are obtained with a precision better than 10%. Results obtained for standard reference materials were, on average, within 3% of the reported values. The procedure can be applied satisfactorily to catalysts, metals, alloys, and geological samples. Detection limits of 5 ng can be easily achieved.

The importance of vanadium as a trace element has increased in recent years [1], and its determination has been reported in many biological and environmental samples. Vanadium is also important in metallurgical and geological samples, and in oils and catalysts. Of the many analytical techniques developed for vanadium [2—5], atomic absorption and spectrophotometry have found wide application. Neutron activation has become an important technique for vanadium at trace levels because of the detection limits generally achieved [6] and the nuclear properties of vanadium. Because of the interferences present in many samples, however, the advantage of a purely instrumental neutron activation determination cannot be fully exploited for samples containing low vanadium concentrations unless, in certain matrices, a concentration prior to irradiation is carried out to enhance the sensitivity and reduce the time required for a post-irradiation radiochemical separation.

Any treatment of the sample prior to neutron irradiation will be acceptable if a chemical separation ensures interference-free counting conditions [7—10] and blank values can be neglected or have accurately measured values.

Decomposition of samples may be done by dry ashing [8, 11, 12], wet ashing [9, 13—15], or fusion [7, 16, 17]. A complete post-irradiation separation of vanadium requires a fairly complex, lengthy separation with consequent loss of sensitivity [7, 9, 13, 15, 17].

When properly applied, solvent extraction can be recommended as a pre-irradiation separation technique because of its simplicity and the high decontamination factors achieved. Several complexing agents have been pro-

[§] Present address: Instituto Technológica Venezolano del Petróleo, Gerencia de Análicis y Evaluación, Apartado 76343, Caracas 107, Venezuela.

posed for vanadium, e.g., cupferron [9, 11, 13], 8-hydroxyquinoline [8, 10], sodium diethyldithiocarbamate [15], and *N*-benzoyl-*N*-phenylhydroxylamine [12, 16, 18–24].

The short half-life of ^{52}V implies a choice between maximum sensitivity with complete pre-irradiation separations [8, 13] and absence of blank corrections resulting from exclusively post-irradiation radiochemical separations [7, 9, 15, 17].

Chemical yields have been determined by weighing [14], by spectroscopy [9, 16], by re-irradiation or by adding tracers, e.g. ^{48}V [7, 11, 17] or ^{49}V [10] Chemical yield determinations can be avoided if quantitative, precise separations can be done.

Neutron activation analysis for trace amounts of vanadium in an alumina matrix, as in the analysis of an alumina-based petroleum hydrodesulfurization (HDS) catalyst, for which the vanadium content is of great importance, is difficult.

The present paper describes some solvent extraction methods for the determination of vanadium in alumina samples by neutron activation. Separation methods, applied directly to the solution resulting from mineralization, are proposed.

Pure alumina and virgin and spent catalysts can be analysed easily with very good detection limits and high decontamination factors.

Preliminary studies

A virgin alumina HDS catalyst (dried) has the average composition of 75.4% Al_2O_3, 16.2% MoO_3, 3.1% CoO, 0.1% Fe_2O_3, 0.34% SiO_2, 0.47% SO_3, 0.02% Na_2O. Mineralization of an alumina matrix requires drastic conditions, and care must be taken to avoid losses of vanadium through the formation of volatile halides.

An adequate mineralization procedure involves treating the sample with hot H_2SO_4–HF mixture. No losses of vanadium were detected in analyses of solutions of spiked samples.

As a result of sample mineralization and final dilution, a solution 1.4 M in H_2SO_4 is obtained; extractions are quantitative in the range 0.18–4.2 M H_2SO_4. Concentrations of HF from 0.2 M to 3.0 M do not affect the extraction yield, but it decreases to 69% when 5 M HF is used.

Several oxidizing agents were evaluated, as the actual oxidation state of vanadium in a catalyst is unknown and the extraction procedures require vanadium(V) to be present. $KMnO_4$ and $K_2S_2O_8$ were satisfactory; the latter was selected because an excess does not affect the extraction yield.

Five complexing–extracting systems were studied: *N*-benzoyl-*N*-phenylhydroxylamine (BPHA), 8-hydroxyquinoline (8-HQ), tri-n-butylamine (TBA), sodium diethyldithiocarbamate (NaDDC) and anthranilic acid. In all cases the V(V) complexes were extracted into methyl isobutyl ketone (MIBK). Further studies were not performed on NaDDC and anthranilic acid because of the low selectivity of the former and the low extraction yields from the latter.

The extraction conditions for the determination of vanadium in spent

catalysts are given under Experimental; when the catalysts are washed and dried, there are variable amounts of carbon which are difficult to destroy by mineralization, and calcination cannot be used because of possible losses of some trace elements. Under special conditions, the quantitative retention of vanadium in activated charcoal at pH 3.6 has been observed [25].

The same mineralization procedure was used for exhausted catalysts containing carbon and the final solution, with suspended carbon, was extracted. In no case did adsorption of vanadium or a decrease in extraction yield occur.

Aluminum is the only source of major interference in vanadium determinations, because of its very high concentration and nuclear properties. Molybdenum is also extracted, in some cases quantitatively in the proposed procedure, but $^{101}Mo-^{101}Tc$ activity is not a serious interference because of the low energy of their main peaks.

However, if further separation of vanadium is desired, molybdenum can be removed quantitatively on Dowex-2 resin, from 0.7—2 M H_2SO_4 solution, before the extraction step. An alternative technique for eliminating molybdenum is described below.

EXPERIMENTAL

General procedure

Samples (0.5 g) were placed in a 125-ml Teflon beaker. Sulphuric acid (2 ml, 98%) was added, followed by dropwise addition of HF (0.5 ml, 40%). When the reaction subsided, a further addition of HF (5 ml, 40%) was made. The beaker was heated for 30 min at 60—80°C. If the solution was not clear at this point (high SiO_2 content) an additional aliquot (5 ml) of HF was added. When the solution became clear, it was heated for an additional hour at 60—80°C to ensure complete removal of HF. Subsequently, distilled water was added and the solution, while still hot, was transferred quantitatively to a 50-ml volumetric flask. After cooling, the solution was diluted to volume, stored in a plastic container, and used as required for vanadium extraction.

Separation of molybdenum

If a molybdenum-free extract is desired, separation of molybdenum is necessary before the vanadium extraction. An aliquot of the solution is passed through a column containing 2—3 ml of Dowex 2-X8 (200-400 mesh) previously rinsed with 1—2 bed volumes of sulphuric acid.

A final solution of less than 50 ml, in which the vanadium concentration will be higher and a gain in sensitivity will be achieved, is possible, but the H_2SO_4 concentration will then be higher and a lower distribution coefficient for molybdenum on the resin will result. A compromise between the molybdenum and vanadium concentrations is required.

BPHA extraction

In a 20-ml stoppered tube, 5 ml of solution are treated with 50 mg of potassium peroxodisulfate and heated in a water bath for 10 min. After

cooling, 6 drops of HF and 0.7 ml of H_2SO_4 are added. The extraction is maximal at pH 1. Subsequently an equal volume of 0.02 M BPHA in MIBK is added. The mixture is stirred vigorously for 3 min and, after centrifugation, an aliquot of the organic layer is encapsulated in a plastic vial and submitted to irradiation.

Tri-n-butylamine extraction

In a 20-ml stoppered tube, 5 ml of solution are treated with 100 mg of tartaric acid and the pH is adjusted to 4. Finally 100 mg of catechol are added and the solution is extracted with 0.4 M TBA solution in MIBK.

8-Hydroxyquinoline extraction

The solution is treated as in the previous case and extracted with 0.05 M 8-HQ solution in MIBK, without the addition of catechol.

The overall separation yields for Mo, Al and V, and decontamination factors for Mo and Al, referred to vanadium for a typical HDS catalyst, are presented in Table 1.

Irradiation and counting

Samples of the organic extracts were irradiated, together with appropriate standards, in the RV-1 nuclear reactor for 5—10 min at a thermal neutron flux of 1×10^{12} n cm^{-2} s^{-1}.

Samples and standards were counted for 200—500 s, either in a Ge(Li) detector associated with a 4096-channel pulse-height analyzer or in a well-type NaI(Tl) crystal (3 × 3 in.) associated with a 1024 MCA.

Spectra of ^{52}V activity, corresponding to 54.2 ng of vanadium, are shown in Figs. 1 and 2.

Although the NaI(Tl) detector is the best choice on account of its sensitivity and counting statistics, a spectrum recorded with a Ge(Li) detector is presented to confirm the radiochemical purity of the isolated vanadium.

Treatment of data is performed with a programmable calculator, based on classical methods of peak area integration with corrections for decay and dead time losses.

TABLE 1

Separation of Mo, Al and V

Separation system	Overall separation yield (%)			Decontamination factor	
	Mo	Al	V	Mo	Al
BPHA—MIBK	97.9	0.0082	100.0	1.02	1.2×10^4
Ion exchange + BPHA—MIBK	0.037	0.0072	97.3	2.7×10^3	1.4×10^4
TBA—MIBK	100.4	0.28	98.5	0.996	357
Ion exchange + TBA—MIBK	0.038	0.26	97.8	2.6×10^3	384

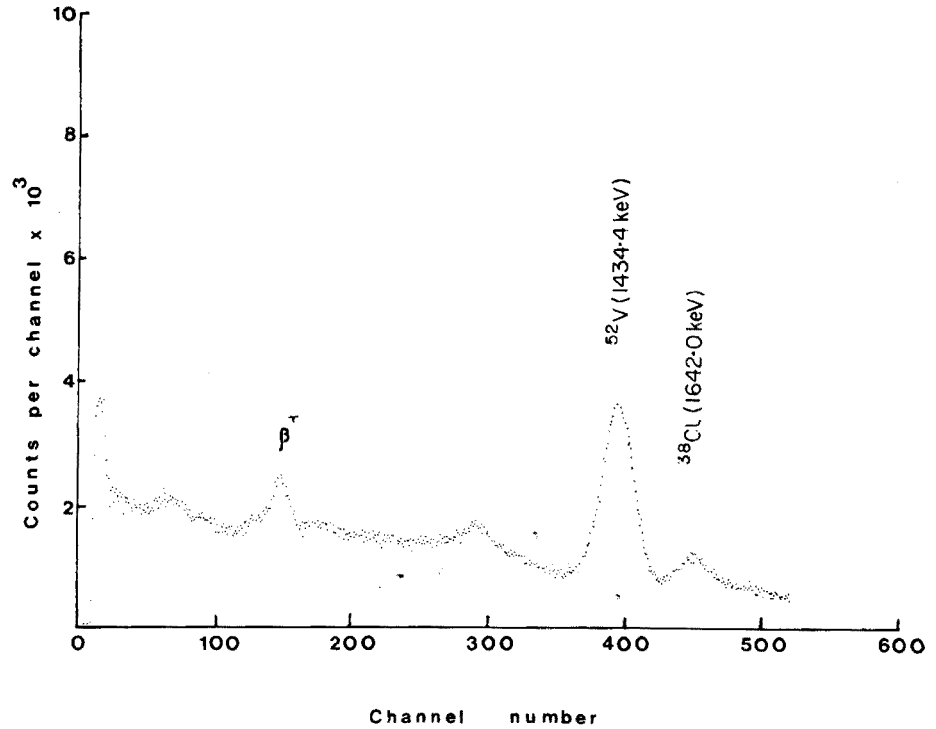

Fig. 1. γ-Spectrum for a catalyst containing 0.108 ppm V (NaI(Tl) detector).

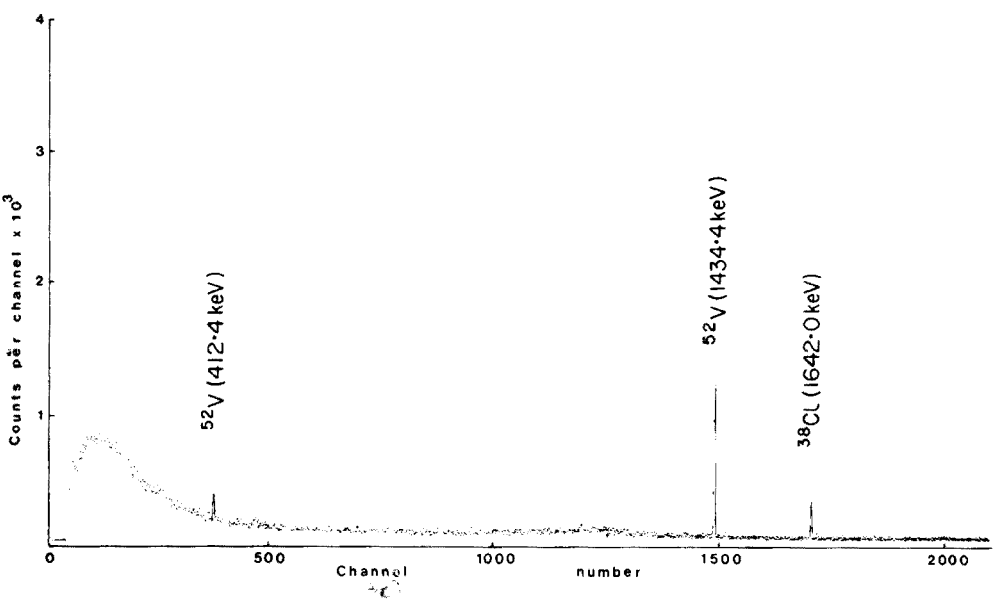

Fig. 2. γ-Spectrum for a catalyst containing 0.108 ppm V (Ge(Li) detector).

RESULTS AND DISCUSSION

As shown in Table 1, the BPHA—MIBK and CTBA—MIBK methods yield quantitative separations for Mo and V. A good decontamination factor is achieved for Al with BPHA—MIBK. Furthermore, a prior separation of Mo does not affect the extraction yield of V. The data presented in Table 1 were obtained for a catalyst of the composition mentioned under Preliminary Studies. The final solution from which V was extracted contained 654.0 μg Mo ml^{-1}, 3353.3 μg Al ml^{-1}, and 0.054 μg V ml^{-1}. Extractions with the 8-HQ—MIBK system did not show quantitative recoveries for Mo or V.

Table 2 shows the results for three standard reference materials.

A series of samples was analyzed by the standard addition method. Table 3 shows the results obtained from a spiked solution of a Al_2O_3—SiO_2 catalyst which had been previously mineralized. Vanadium is quantitatively recovered from a solution containing up to 10 μg ml^{-1} of vanadium; the curve obtained from the data shows the reliability of the method.

The overall precision of the method is better than 10% at the 5-ppm level. The data presented in Table 4 correspond to the analysis of a pure Al_2O_3 catalyst containing 15.37% MoO_3 and 76.21% Al_2O_3. In all cases the blank values were negligible.

TABLE 2

Determination of vanadium with the BPHA—MIBK method

Sample	V, found	V, reported
Valve steel	0.058 ± 0.0026%	0.058%[a]
Invar	0.00173 ± 0.00010%	0.001%[b]
Peridotite	29.16 ± 2.80 ppm	30 ppm[c]

[a] N.B.S. Certificate of analysis, July 14, 1965.
[b] N.B.S. Provisional certificate of analysis, December 6, 1972.
[c] Cf. [21].

TABLE 3

Recovery of vanadium from a solution of mineralized catalyst

V added (μg)	0	0.01	0.05	0.225	0.5	1.0	10.0
V found (μg)	0.0535	0.0697	0.128	0.289	0.54	1.09	10.16
Slope	1.01 ± 0.002						
Intercept	0.061 ± 0.007						
Corr. Coeff.	0.99						

TABLE 4

Determination of vanadium in a new catalyst by the BPHA—MIBK method

	Sample	V (ppm)
	1-0	5.4, 6.1, 6.2
	1-1	5.1, 4.8, 5.6
	1-2	4.7, 4.8, 5.3, 5.5
Mean		5.4
Std. dev.		9.8%
Std. dev. of mean		3.1%

The valuable technical assistance of H. Prieto is acknowledged.

REFERENCES

1 W. H. Zoller, G. E. Gordon, E. S. Gladney and A. G. Jones, in E. L. Kothny (Ed.), Trace Elements in the Environment, Am. Chem. Soc., Washington D.C., 1973, p. 31.
2 C. C. Butler and R. N. Kniseley, Anal. Chem., 45 (1973) 129.
3 W. A. Straub and J. K. Hurwitz, Anal. Chem., 47 (1975) 112.
4 R. V. King, Anal. Chem., 45 (1973) 169.
5 J. M. Fraser, Anal. Chem., 47 (1975) 169.
6 H. P. Yule, Anal. Chem., 37 (1965) 129.
7 D. G. Kaiser and W. W. Meinke, Anal. Chim. Acta, 29 (1963) 211.
8 H. R. Lukens, K. Heydorn and T. Choy, Trans. Am. Nucl. Soc., 8 (1965) 331.
9 H. D. Livingston and H. Smith, Anal. Chem., 37 (1965) 1285.
10 K. D. Lindstedt and P. Kruger, Anal. Chem., 42 (1970) 113.
11 R. Söremark, in D. Comar (Ed.), L'Analyse par Radioactivation et ses Applications aux Sciences Biologiques, Saclay, Presses Univ., 1964, p. 223.
12 J. P. F. Lambert, R. E. Simpson, H. E. Mohr and L. L. Hopkins, J. Assoc. Off. Agric. Chem., 53 (1970) 1145.
13 A. A. Benson, B. Marno, R. J. Flipse, H. W. Yurow and W. W. Miller, Int. Conf. Peaceful Uses Atom. Energy (Proc. Conf. Geneva, 1958) 24, U.N., New York, 1958, p. 289.
14 V. P. Guinn, in D. Comar (Ed.), L'Analyse par Radioactivation et ses Applications aux Sciences Biologiques, Saclay, Presses Univ., 1964, p. 69.
15 W. H. Strain, C. G. Rob, W. J. Pories, R. C. Childers, M. F. Thompson, J. A. Hennessen and F. J. Graber, Appl. Spectrosc., 23 (1969) 121.
16 W. H. Wahl, U. J. Molinski and H. Arino, Modern Trends in Activation Analysis, College Station, Texas A and M University, 1965, p. 44.
17 W. W. Meinke, in Radioisotopes in the Physical Science and Industry, Copenhagen, 2 IAEA, Vienna, 1962, p. 277.
18 Y. K. Chau and K. Lun-Shue-Chan, Anal. Chim. Acta, 50 (1970) 201.
19 M. Vrchlabsky and L. Sommer, Talanta, 15 (1968) 887.
20 H. A. van der Sloot and H. A. Das, RCN-75-001 Nederland, 1974.
21 F. J. Flanagan, Geochim. Cosmochim. Acta, 37 (1973) 1189.
22 V. Patrovsky, Talanta, 16 (1969) 456.
23 H. J. Crump-Wiesner and W. C. Purdy, Talanta, 16 (1969) 124.
24 M. Vrchlabsky and L. Sommer, Talanta, 15 (1968) 887.
25 H. A. Van der Sloot, H. A. DAS RCN-75-001-Nederland (1974).

Analytica Chimica Acta, 96 (1978) 293—301

AN AUTOMATED METHOD FOR THE SIMULTANEOUS DETERMINATION OF SALICYLIC ACID AND SALICYLAZOIMINOPYRIDINE IN COMMERCIAL SALICYLAZOSULPHAPYRIDINE

LARS HAGEL*

Pharmacia AB, Box 181, S-751 04 Uppsala (Sweden)

(Received 18th August 1977)

SUMMARY

An automated method for simultaneous determination of salicylic acid and salicylazoiminopyridine in salicylazosulphapyridine is presented. The components are separated from salicylazosulphapyridine on a two-layer anion and cation exchanger with a yield of almost 100%. The effluent is analyzed simultaneously for the fluorescence of salicylate and the absorbance of salicylazoiminopyridine in an Auto-Analyzer II system. The system is run at 40 samples per h with a relative standard deviation of 0.2%. The method gives, at the content of 1% of each component, a reproducibility (s_r) of 3—4%. Five commercial products from four suppliers were analyzed and found to contain 0—0.9% salicylic acid and 0—3.6% coloured impurities, expressed as salicylazoiminopyridine. Some anomalies of the automatic systems are presented and discussed. An automated method for colorimetric assay of salicylazosulphapyridine is briefly described.

The determination of salicylazosulphapyridine (I; 2-hydroxy-5[4-[(2-pyridinylamino)sulphonyl]phenylazo]benzoic acid) a drug used for the treatment of ulcerative colitis, in the presence of by-products of synthesis or degradation has become of increasing interest [1—3]. Some of these impurities are well known (e.g. salicylic acid) but some still remain to be elucidated. In the analysis of commercial salicylazosulphapyridine products for polyvinylpyrrolidone (PVP) by a previous method [4], a yellow band sometimes separated from the layer of salicylazosulphapyridine. The chromatographic and spectrophotometric behaviour of this coloured band agreed with salicylazoiminopyridine (II; 2-hydroxy-5[4-[1-(2-imino-1,2-dihydro)pyridyl]phenylazo]benzoic acid) which had earlier been identified as a component of certain commercial salicylazosulphapyridine products [5].

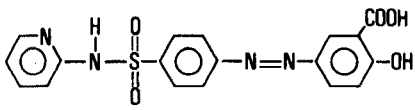

I

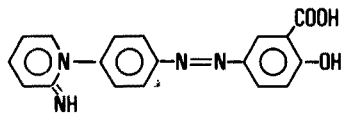

II

*Present address: Institute of Chemistry, Analytical Department, Box 531, S-751 21 Uppsala, Sweden.

The aim of this investigation was to find methods suitable for the routine analysis of salicylazosulphapyridine for salicylic acid and salicylazoiminopyridine.

The content of salicylic acid in salicylazosulphapyridine was previously determined by extraction of salicylic acid into ether, evaporation of the ether, dissolution of the residue in an iron(III)—nitric acid reagent, and measurement of the absorbance at 525 nm. The coloured complex was very pH-dependent and the reproducibility of the method was unsatisfactory. Automated methods for the determination of salicylic acid, based on the formation of this violet complex, have been described [6, 7]. These methods lack sensitivity [8], but with improved detection, a level of 5 μgml^{-1} salicylic acid was obtained [6]. A more sensitive and selective way of determining salicylic acid is to measure the fluorescence above pH 6 [9]; a sensitive method (0.02 μgml^{-1}) for the automated analysis of clinical samples has been described [8].

The previous method of analysis of salicylazosulphapyridine for salicylazoiminopyridine was based on paper electrophoresis followed by extraction of the selected spot with dimethylformamide and photometric determination at 400 nm. This method is selective but tedious. The spectrum of salicylazoiminopyridine, in neutral aqueous solution, shows a maximum at 350 nm which is displaced to 450 nm in alkaline media. Salicylazoiminopyridine can also be determined by polarographic reduction of the azo group [10].

After separation from salicylazosulphapyridine, salicylic acid and salicylazoiminopyridine can be determined by any of the proposed methods. For reasons of higher selectivity, sensitivity, and simplicity, the fluorescence approach for analyses of salicylic acid was preferred. For the determination of salicylazoiminopyridine, photometric determination at 450 nm was chosen, thus avoiding interferences of absorption from salicylic acid near 300 nm. The analyses were adapted to a Technicon Auto-Analyzer II system.

In the proposed method, salicylic acid and salicylazoiminopyridine are separated from salicylazosulphapyridine on a two-layer ion exchanger (QAE-Sephadex stratified on SP-Sephadex) with a sodium chloride solution as eluant. The effluent is analyzed simultaneously for salicylic acid and salicylazoiminopyridine in an automatic system where the sample stream is split into two parts. To one of the streams a buffer solution is added, the solutions are mixed in a coil, and the fluorescence of salicylate is measured in a fluoronephelometer. To the other stream, a sodium hydroxide solution is added and, after mixing, the amount of salicylazoiminopyridine is determined colorimetrically.

EXPERIMENTAL

Apparatus

The flow chart for the simultaneous determination of salicylic acid and salicylazoiminopyridine is shown in Fig. 1. The parts include a Technicon proportioning pump III (Tygon pump tubes), a Technicon fluoronephelometer I

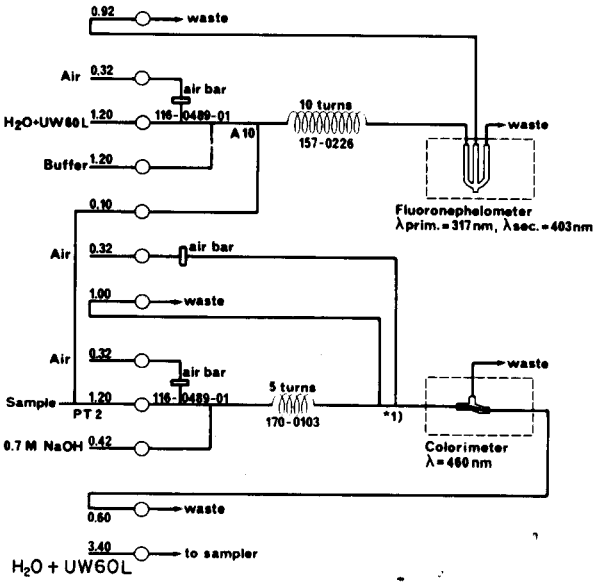

Fig. 1. Flow chart for the simultaneous determination of salicylic acid and salicylazoiminopyridine (figures represent flow rates in ml min^{-1}). (1) De-rebubbler.

with a primary filter of 317 ± 9 nm (effective bandwidth) and a secondary filter of 403 ± 7 nm, a Technicon SC Colorimeter with a 460 ± 11 nm filter, two recorders (W+W 1100, LKB-Beckman and Servograph Rec. 51, Radiometer) and a Sampletron PB 1000 sampler (Stålprodukter, Uppsala).

The equipment for the separation step is shown schematically in Fig. 2 and is to be presented in detail elsewhere [11].

Preliminary tests

A recent paper describes a step for the separation of PVP from Salazopyrin [4] which also can be used for the separation of salicylic acid and salicylazoiminopyridine from salicylazosulphapyridine by replacing water with an electrolyte as eluant. Different electrolytes were tested, including sodium hydroxide, sodium chloride, potassium chloride, potassium bromide, and ammonium chloride. Sodium chloride gave the best elution of the components of interest with retention of salicylazosulphapyridine. The concentration was varied from 0.1 to 1 M; 0.5 M sodium chloride, which gave an almost 100% yield of both salicylic acid and salicylazoiminopyridine, was chosen as eluant.

Salicylic acid fluoresces with a constant relative intensity in neutral or basic media [9]. The wavelengths for excitation and emission in the effluent solution were at 295 and 405 nm, respectively (Fig. 3). Since salicylazoiminopyridine absorbs at 405 nm (Fig. 4), the sample has to be diluted to avoid this filter effect. A 25-fold dilution, as in the automatic system, eliminated the effect from at least 5 $\mu g ml^{-1}$ of salicylazoiminopyridine, i.e. twice the expected concentration. The dilution also decreases the salt content of the

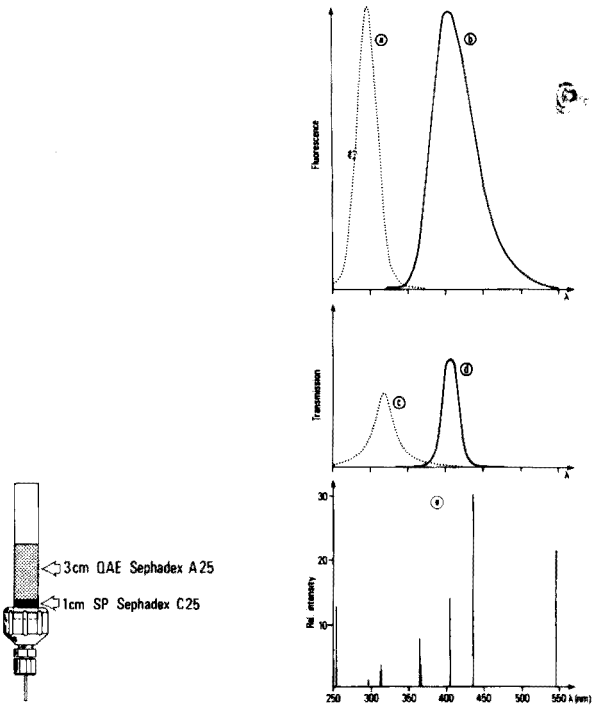

Fig. 2. Equipment for the separation step.

Fig. 3. (a) Excitation spectra of salicylic acid at λ_{em} = 405 nm, in 0.46 M sodium chloride. (b) Emission spectra of salicylic acid at λ_{ex} = 295 nm, in 0.46 M sodium chloride. (c) Transmission spectra of excitation filter (317 ± 9 nm). (d) Transmission spectra of emission filter (403 ± 7 nm). (e) Relative intensities of the emitted wavelengths from the light source (mercury lamp).

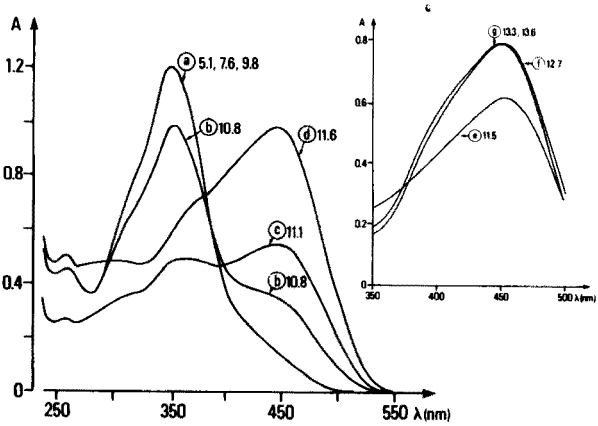

Fig. 4. Spectrum of salicylazoiminopyridine at different pH values. Concentration: 20 $\mu g ml^{-1}$, (a, b, c, d) and 10.5 $\mu g ml^{-1}$ (e, f, g), 1-cm cuvettes. Figures represent the pH of the solutions.

samples, making it possible to use water as rinsing medium in the automatic system. To ensure a suitable pH, buffers of pH 7, 9, 11, and 13 were tested with respect to filter effects from salicylazoiminopyridine. No difference between the buffers was observed; phosphate buffer (pH 7) was chosen.

The spectrum of salicylazoiminopyridine shows a maximum at 350 nm or 450 nm depending on the pH (Fig. 4). This shift is attributed to the formation of a quinoid structure when the hydroxyl group is protolyzed [12]. Since salicylic acid, in basic media, has an absorbance maximum near 300 nm but shows minimal absorption at 450 nm, this wavelength was chosen for the determination of salicylazoiminopyridine. To ensure maximum sensitivity, the final solution is made 0.2 M in sodium hydroxide, corresponding to pH 13. The analyses for salicylic acid and salicylazoiminopyridine can be made simultaneously; furthermore, the solutions for reference standards can be mixed.

Wetting agents are used frequently in Auto-Analyzer systems to prevent adsorption of components on the glass surfaces and to create a smooth flow. Some wetting agents were tested, including Triton X-100, FC-134, U(ltra)-W(et) 60L, Aerosol 22, and a mixture of FC-134 and U-W 60L (all from Technicon AB). U-W 60L was the most effective in preventing salicylazoiminopyridine from being adsorbed on the glass surfaces, and was therefore chosen.

Reagents

Ion exchangers. SP-Sephadex C-25 (sulphopropyl cation-exchanger) and QAE-Sephadex A-25 (quaternary aminoethyl anion-exchanger, Pharmacia Fine Chemicals AB) are allowed to swell for 1 h in distilled water.

The eluant is 0.5 M sodium chloride, and the buffer is 0.02 M hydrogenphosphate (pH 7.0); 0.7 M sodium hydroxide is used.

Rinse solution. Distilled water containing Ultra-Wet 60L (0.5 ml l^{-1}).

Bulk standards. (a) Salicylic acid: 15 mg of salicylic acid, exactly weighed, is dissolved in 500 ml of distilled water. (b) Salicylazoiminopyridine: 10 mg of salicylazoiminopyridine monohydrochloride monohydrate (a special laboratory product with a purity of >95% as estimated by t.l.c. [13]), exactly weighed, is dissolved in 200 ml of 0.1 M sodium hydroxide.

Working standards. For the high standard, 10 ml of bulk standard (a) plus 8 ml of bulk standard (b) plus 20 ml of 2.3 M sodium chloride solution is diluted to 100 ml with distilled water (→3 $\mu g ml^{-1}$ salicylic acid, 4 $\mu g ml^{-1}$ salicylazoiminopyridine in 0.46 M sodium chloride solution). For the low standard, 5 ml of bulk standard (a) plus 4 ml of bulk standard (b) plus 20 ml of 2.3 M sodium chloride solution is diluted to 100 ml with distilled water (→1.5 $\mu g ml^{-1}$ salicylic acid, 2 $\mu g ml^{-1}$ salicylazoiminopyridine in 0.46 M sodium chloride solution).

Procedure

Salazopyrin, 0.5 g exactly weighed, containing ca. 1% of each of salicylic acid and salicylazoiminopyridine, is dissolved in 50 ml of 0.1 M sodium hydroxide. A chromatographic column is prepared as in Fig. 2 [4]. The

column is washed with 3—5 ml of water and a sample containing 50—200 μgml^{-1} of salicylic acid and/or salicylazoiminopyridine is applied to the bed surface with a 500-μl Eppendorf pipette. The column is washed with 5 ml of water (to elute polyvinylpyrrolidone [4]) and the sample is eluted with 25 ml of 0.5 M sodium chloride. After use, the column is dismantled, the gel discarded, and new layers applied in preparation for the next sample.

The eluted samples are analyzed in the automated system at a rate of 40 samples per h with a sample-to-wash ratio of 13/2. The sample time makes it possible to measure the curves at a steady state. Between each group of calibration samples, consisting of two high and two low working standards, 10 samples are analyzed. The samples are evaluated against linear calibration curves.

Results

In the separation step, salicylic acid is eluted within 15 ml with a yield of 97.4 ± 1.6% and salicylazoiminopyridine is eluted within 24 ml with a yield of 101 ± 1%, as found by the method of standard addition at a content of 1% of each substance. The yields are independent of small variations (±0.5 cm) in the ion-exchange layers. The separation step gives no contribution (blank) to either analysis, and pure salicylazosulphapyridine is not eluted by at least 35 ml of eluant. The effluent medium, 0.46 M sodium chloride, decreases the transmittance at 460 nm. Even in the analysis for salicylic acid, the salt concentration of the samples can be critical. In order to overcome any problems caused by different salt concentrations in sample and reference solutions, the latter is made 0.46 M in sodium chloride.

In the Auto-Analyzer step, a steady state is reached after 1 min of sample time and the baseline is reached after a rinse time of 1.2 min for both analyses. At a sample rate of 40 per h, a relative standard deviation, s_r, of 0.2% (n = 10) is obtained. The repeatability of the whole method (separation, determination, and evaluation) is better than 0.9% (s_r, n = 10) for both analyses. A substance containing 1% of salicylic acid and salicylazoiminopyridine was analyzed under routine conditions over more than 1 year. Some 60 analyses on 30 occasions gave s_r = 4.2% for salicyclic acid and s_r = 3.3% for salicylazoiminopyridine.

The calibration curves are linear, passing through the origin (Fig. 5). With the specified system, the calibration solutions of salicylic acid and salicylazoiminopyridine can be mixed and no interference was found up to at least 4 μgml^{-1} for salicylic acid and 5 μgml^{-1} for salicylazoiminopyridine.

Five commercial salicylazosulphapyridine products from four different suppliers were analyzed by the proposed method; Table 1 shows that the quality of the products varies a great deal.

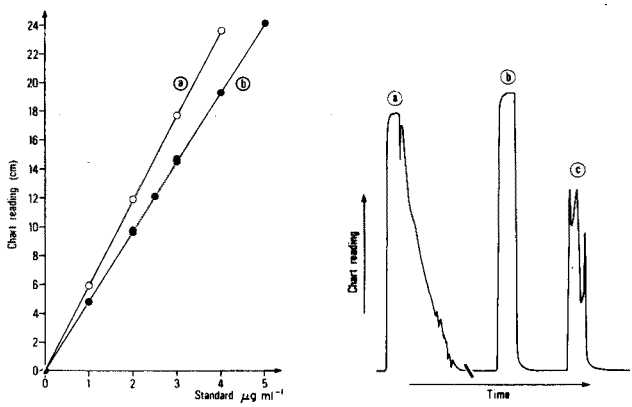

Fig. 5. Standard curves for determination of salicylic acid and salicylazoiminopyridine. (a) Salicylic acid + salicylazoiminopyridine (2.5 $\mu g ml^{-1}$) in 0.46 M sodium chloride. (b) Salicylazoiminopyridine + salicylic acid (2.0 $\mu g ml^{-1}$) in 0.46 M sodium chloride.

Fig. 6. Distortion of the salicylic acid peak from difference in density of sample and rinse solution.

	(a)	(b)	(c)	
Sample: salicylic acid (2 $\mu g ml^{-1}$) in:	0.46	0.5	0.46	M NaCl
Rinse medium:	0 (H_2O)	0.5	0.5	M NaCl

TABLE 1

Assay of salicylic acid and coloured impurities (expressed as salicylazoiminopyridine) in five commercial salicylazosulphapyridine products

Sample	Salicylic acid[a] (%)	Coloured impurities[a] (%)
A_1	not detectable	<0.1
A_2	0.9	1.5
B	—	<0.1
C	0.4	1.1
D	0.1	3.6

[a]Mean value of duplicate analysis.

DISCUSSION

In an early stage of this work, unsuccessful attempts were made to determine salicylic acid in the effluent with an Auto-Analyzer system without dilution; the rise or fall of the peaks was distorted through differences in density between the sample and rinse solutions (Fig. 6). For an eluted sample containing 0.46 M sodium chloride, the rinse solution had to be 0.45—0.47 M sodium chloride. The sample can also be rinsed with a 14.7—15.3% (w/w) solution of ethylene glycol, with almost the same density as the sample.

Losses of exciting and of emitted light through reflections caused by density gradients within the cell and at the surfaces is the most likely cause of the observed anomaly. In the automated system for analysis of salicylazoiminopyridine, adsorption effects, proportional to sample concentration, were noted when no wetting agent was used. For this system another unexpected effect was observed. Pure effluent (0.46 M sodium chloride) "absorbed" energy at 460 nm; this effect was directly proportional to the sodium chloride concentration over the range 0.1—3 M. The phenomenon might be attributed to effects from the increasing refractive index in the solution. The cuvette in the Technicon SC Colorimeter is a 15 × 1 mm barrel with spherical windows. With this design, an increase in refractive index of the solution causes losses of light through refraction and reflection of the beam in the cell.

The sample rate can be increased to 50 samples per h (10/2), but this causes a two-fold increase in s_r to 0.4—0.5%. At this sample rate a sample containing 2 μgml^{-1} was contaminated to the extent of 0.6% by a preceding sample containing 4 μgml^{-1}.

The proposed method was developed for the assay of salicylic acid and coloured impurities (i.e. salicylazoiminopyridine) at a content of 1%. Commercial upgrading of synthesis and purification of salicylazosulphapyridine, however, decreases the level of impurities to 0.01—0.1% [1]. Even at these low levels, the yield from the separation step was almost 100% for salicylic acid and 90% for salicylazoiminopyridine. Since fluorescence is a very sensitive method, the low level of salicylic acid is easily detectable. For salicylazoiminopyridine, however, the detector gain has to be increased to maximum, giving s_r = 1.8% (n = 15) for the automatic system at 0.4 μgml^{-1} of salicylazoiminopyridine. The analysis of a reference substance (containing 0.06% coloured impurities) gave s_r = 30% (n = 30) which, although high, is acceptable at these low levels.

It was also of interest to find a simple and high-capacity method for the determination of salicylazosulphapyridine, for the assay of which both polarographic [14], colorimetric [15] and l.c. and t.l.c. methods [1—3] have been described. Although the polarographic method [14] is more selective it was not chosen because of the low sample rate if automated (10 samples per h). The colorimetric method was adapted to a Technicon Auto-Analyzer system to analyse the same basic solution as used for the determination of other constituents in Salazopyrin [4]. This necessitates a large dilution step (ca. 2000 times) of the highly coloured solution. This could not be performed by the dialysis technique but was solved with two re-sampling steps (Fig. 7). The four protolytic steps of salicylazosulphapyridine [12] require careful control of the pH of the solution. For optimal conditions an acetic acid buffer (pH 4.4) is used [15] and the absorption at 352 nm is measured. The automatic system, run at 40 samples per h with a sample-to-wash ratio of 13/2, gives s_r = 0.3% (n = 9).

From a linear calibration curve, the content of salicylazosulphapyridine is obtained by subtraction of the contribution from other absorbing species (e.g. salicylazoiminopyridine).

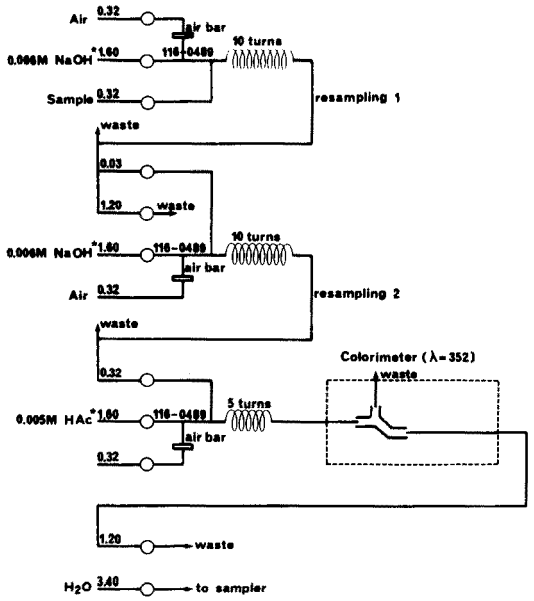

Fig. 7. Flow chart for determination of salicylazosulphapyridine. (Figures represent flow rates in ml min^{-1}).

The author expresses his gratitude to Professor Bengt Nygård and Mr. Rune Andersson for many valuable discussions. The interest of Dr. Adolf Berggren is appreciated, as well as comments on this manuscript by Mr. Martin Sandberg. For the data concerning the reference substances and Table 1 the author thanks Mr. Jan-Åke Carlsson. The author is indebted to Pharmacia AB for their support of this work.

REFERENCES

1 D. R. Powell and B. A. Burton, J. Pharm. Sci., 63 (1974) 1290.
2 J. C. Stone and R. Gorby, J. Pharm. Sci. 63 (1974) 1296.
3 L. D. Bighley and J. P. McDonnell, J. Pharm. Sci., 64 (1975) 1549.
4 L. Hagel and R. Andersson, Anal. Chim. Acta, 86 (1976) 69.
5 K. Skagius, personal communication, 1977.
6 A. Mellix, Thérapie, 28 (1973) 187.
7 L. F. Cullen, D. L. Packman and G. J. Papariello, Ann. N.Y. Acad. Sci., 153 (1968) 525.
8 J. B. Hill and R. M. Smith, Biochem. Med., 4 (1970) 24.
9 S. Udenfriend in N. O. Kaplan and H. A. Scheraga (Eds.), Fluorescence Assay in Biology and Medicine, Academic Press, New York, 1964, p. 471.
10 B. Nygård, personal communication, 1977.
11 R. Andersson, to be published.
12 B. Nygård, J. Olofsson and M. Sandberg. Acta Pharm. Suec., 3 (1966) 313.
13 H. Agback, personal communication, 1976.
14 B. Nygård, J. Olofsson and M. Sandberg, Acta Pharm. Suec., 3 (1966) 343.
15 A. Berggren and S. Hansen, Farm. Revy, 51 (1952) 537.

Analytica Chimica Acta, 96 (1978) 303—310

REINDARSTELLUNG DES 1,5-DIPHENYLCARBAZONATO-DIPHENYLBOR-CHELATES UND KONSTITUTIONSVORSCHLAG AUF GRUND SEINER SPEKTREN

BERND FRIESE und FRITZ UMLAND*

Anorganisch-Chemisches Institut der Universität Münster, Gievenbecker Weg 9, D-4400 Münster (B.R.D.)

(Eingegangen am 4 Juni 1977)

ZUSAMMENFASSUNG

Substituierte 1,5-Diphenylcarbazone reagieren mit Kationen und Diphenylborsäure wesentlich empfindlicher als die Stammsubstanz 1,5-Diphenylcarbazon. Zur gezielten Weiterentwicklung dieser Reagenzien sind Kenntnisse über die Konstitution der Chelate erforderlich. Zur Aufklärung der Konstitution dieser Chelate wurde das Diphenylborchelat des 1,5-Diphenylcarbazons (I) als Modellsubstanz gewählt. Seine Reindarstellung gelingt nur, wenn von reinem (I) ausgegangen wird. Nach den Spektren bildet das Chelat einen 5-Ring mit O—B—N-Bindung und leitet sich vom 1,5-Diphenylisocarbazon ab. Das Bor ist wahrscheinlich an das N-5-Atom der Azogruppe gebunden (XIV).

SUMMARY

Preparation of the pure 1,5-diphenylcarbazone-diphenylboron chelate and a spectroscopic study of its structure

Substituted 1,5-diphenylcarbazones react with cations and diphenylboric acid more sensitively than the original 1,5-diphenylcarbazone. Further development of these reagents requires knowledge of the constitution of the chelates. To clarify their constitution, the diphenylboron chelate of 1,5-diphenylcarbazone was chosen as a model. The pure diphenylboron chelate can be prepared only when the pure carbazone is used. The chelate forms a 5-membered ring with O—B—N bonds, and is derived from the enol form, 1,5-diphenylisocarbazone. The boron atom is probably linked to the N-5 atom of the azo group.

1,5-Diphenylcarbazon (I) gibt mit einer Reihe von Metall-Ionen intensiv farbige Chelate. Wir fanden in ersten Versuchen, daß im Phenylrest substituierte Derivate des 1,5-Diphenylcarbazons als photometrische Reagenzien gegenüber diesen Kationen noch wesentlich empfindlicher reagieren. Zur gezielten Weiterentwicklung dieser Reagenzien im Hinblick auf eine höhere Empfindlichkeit und bessere Selektivität sind Kenntnisse über die Konstitution der Chelate erforderlich. Bisher liegen nur mehr oder weniger begründete Annahmen über die Konstitution der 1,5-Diphenylcarbazon-Chelate vor.

Da sich nach Toporcer et al. [1] der Diphenylborrest wie ein einwertiges Kation mit zwei freien Koordinationsstellen verhält und seine Umsetzungen

eindeutiger als mit Metall-Kationen sind, wurde das Diphenylborchelat als Modellsubstanz zur Konstitutionsaufklärung gewählt. Die Reaktion zwischen (I) und Tetraphenyldiboroxid (II) wurde erstmalig von Neu [2] beschrieben. Er konnte hiermit organisch gebundenes Bor direkt, ohne Spaltung der Bor—Kohlenstoff-Bindung, qualitativ nachweisen. Neu [2] berichtet auch von erfolglosen Versuchen zur präparativen Darstellung des 1,5-Diphenyl-carbazonato-diphenylbor-Chelates. Thierig [3, 4] arbeitete in der Folgezeit die Farbreaktion zu einer quantitativen Bestimmungsmethode aus. Eine präparative Darstellung des Chelates gelang auch ihm nicht. Auf Grund von Analogieschlüssen in Anlehnung an andere Untersuchungen [5, 6] formulierte er das Borchelat als heterocyclischen 5-Ring (XIV), der sich von der Enol-Form von (I) 1,5-Diphenylisocarbazon (III) ableitet. Unabhängig von Thierig beschäftigte sich auch Miller [7] mit der präparativen Darstellung des Chelates. Er erhielt ein blauschwarzes Pulver von Schmp. 198°C. Im Gegensatz zu Thierig formulierte er das Borchelat als heterocyclischen 6-Ring (VI). Schließlich forderte Szonn [8] eine Resonanzstabilisierung zwischen Formazan-Grenzstrukturen (VII).

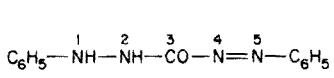

(I)

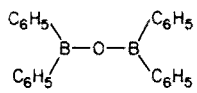

(II)

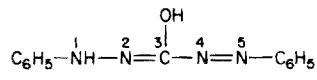

(III)

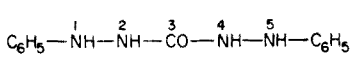

(IV)

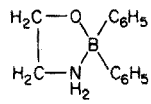

(V)

Diese widersprüchlichen Formulierungen verlangten nach einer Überprüfung. Sicher beruhen die Widersprüche zum Teil darauf, daß bisher keiner der genannten Autoren das reine Borchelat in Händen hatte. Das wiederum liegt daran, daß das bisher als Ausgangsmaterial verwendete handelsübliche (I) mit fast 50% 1,5-Diphenylcarbazid (IV) verunreinigt ist [9], worauf bereits Willems et al. [10, 11] hinwiesen.

ERGEBNISSE

Zur Synthese des 1,5-Diphenylcarbazonato-diphenylbor-Chelates

Für die folgenden Versuche wurde formelreines (I) verwendet, welches durch Oxidation von (IV) mit Chlorat und katalytischer Mitwirkung von Fe^{2+}-Ionen erhalten wurde [9]. Nach Vereinigen äquimolarer Mengen (I) und (II) bei Raumtemperatur in Eisessig schieden sich nach vorsichtigem Ausfällen mit Wasser grüne, das Licht stark reflektierende Kristalle (Schmp. 191°C) ab. Blauschwarze Produkte, wie sie Miller [7] beschrieb, wurden nur erhalten, wenn (I) mit (IV) verunreinigt war. In siedendem Eisessig bildet sich das in Lösung rote Monophenylborchelat.

Gelegentlich wurden niedriger schmelzende Produkte (Schmp. 168°C, Sintern bei 165°C) mit gleichen IR-Spektren und Elementaranalysen erhalten, die sich bei mehrmonatigem Lagern in das höher schmelzende Produkt umwandeln.

Die Umsetzung konnte auch mit Flavognost (V; Ethanolamin-Chelat der Diphenylborsäure) anstelle von (II) vorgenommen werden. Das bedeutet, daß das 1,5-Diphenylcarbazonato-diphenylbor-Chelat gegenüber dem Ethanolamin-Chelat relativ stabiler ist. Das Borchelat läßt sich ebenso gut in Ethanol oder Aceton darstellen.

Bei der Umsetzung des käuflichen [9] 1,5-Diphenylcarbazons (1:1-Molekülverbindung aus I und IV) mit (II) bildet sich zwar in Lösung das blaue Borchelat. Es konnte jedoch wegen des gleichzeitig freiwerdenden (IV) nicht in kristalliner Form isoliert werden. Andererseits läßt sich (IV) von Ammoniumperoxodisulfat zur Molekülverbindung oxidieren. Daher sollte es möglich sein, durch gleichzeitige Umsetzung von (IV) (oder der Molekülverbindung) mit Ammoniumperoxodisulfat und (V) zum Borchelat zu gelangen. Tatsächlich läßt sich das Borchelat auf diese Weise in hoher Ausbeute und Reinheit gewinnen. Diese Synthese des Borchelates hat den Vorteil, die beiden Zwischenstufen der Isolierung von Molekülverbindung und (I) zu überspringen. Die Analysenwerte zeigen, daß sich ein 1:1-Chelat gebildet hat.

Zur Konstitution

Für das Borchelat kommen die Konstitutionen (VI)—(XIV) in Frage.

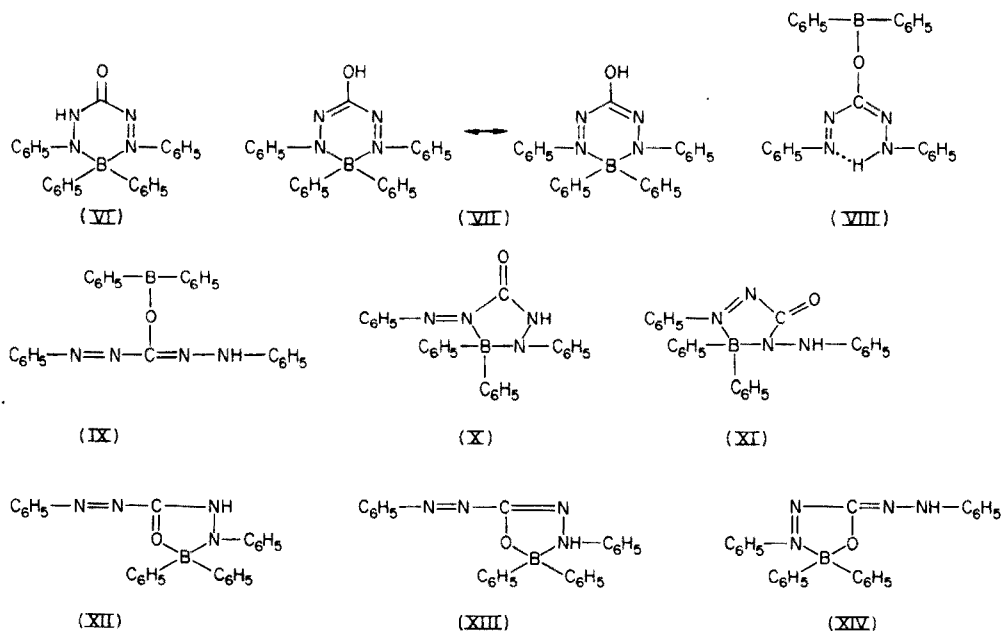

1:2-Chelate analog den sekundären Metallchelaten des Dithizons [12] werden auf Grund der Analyse von vornherein ausgeschlossen.

IR-Spektrum

Eine scharfe Bande bei 3300 cm^{-1} deutet auf eine einzelne NH-Valenzschwingung hin. Dieser Befund wurde durch Deuterierung (Aceton p.a./D_2O) erhärtet. Damit wird nochmals ein 1:2-Chelat ausgeschlossen. Sollte das Borchelat entweder eine freie oder koordinativ mit Bor verknüpfte Carbonylgruppe besitzen, so müßte die im Chelatbildner (I) bei 1705 cm^{-1} vorhandene Carbonylbande [9] im Borchelat wieder auftauchen. Das ist jedoch nicht der Fall. Die nächste Bande zu niedrigeren Wellenzahlen hin erscheint erst bei 1570 cm^{-1}. Selbst wenn man annimmt, daß der Carbonylsauerstoff eine koordinative Bindung mit dem Bor-Atom eingeht, ist eine Wellenzahlerniedrigung von 135 cm^{-1} unwahrscheinlich. Sie liegt nach Schleyerbach [13] im Bereich 30—60 cm^{-1}. Daraus muß geschlossen werden, daß die Chelatbildung zwischen dem Enol (III) und Diphenylborsäure erfolgt.

Es kommen also nur noch die Konstitutionen (VII), (VIII), (IX), (XIII) und (XIV) für die Chelatbildung in Frage. Davon lassen die Formeln (VIII) und (IX) auch die Möglichkeit der Bildung dreibindigen Bors zu.

Abel et al. [14] bestimmten die B—O-Valenzschwingung in der Diphenylborsäure und ihren Estern zu 1325 ± 2 cm^{-1}. Nach Werner und O'Brien [15] erscheint diese Bande in den Estern der Diphenylborsäure im Bereich 1340 ± 10 cm^{-1} als intensive Bande. Ihre Angaben wurden anhand des Diphenylborsäure-butylesters [16] sowie von (II) [17] bestätigt.

Im IR-Spektrum kann in dem für die B—O-Schwingung des dreibindigen Bors in Frage kommenden Bereich keine hinsichtlich der Intensität auch nur annähernd vergleichbare Bande beobachtet werden. Statt dessen findet man eine breite Bande bei 1225 cm^{-1}. Sie ist gegenüber der B—O-Valenzschwingung des dreibindigen Bors um mehr als 100 cm^{-1} nach niedrigeren Wellenzahlen verschoben. Nach Werner und O'Brien liegt demnach vierbindiges Bor vor. Es verbleiben die Formeln (VII), (XIII) und (XIV). Bei der Intensität und Breite der Bande bei 1225 cm^{-1} ist es wahrscheinlich, daß sich B—O- und C—O-Schwingungen überlagern. Hierfür spricht, daß in einigen Metallchelaten von (I) im gleichen Bereich eine ähnliche, intensive Bande auftritt.

Da im Bereich der freien OH-Valenzschwingung bei 3600 cm^{-1} und im Bereich assoziierter OH-Schwingungen um 3400 cm^{-1} keine Absorptionen auftreten, ist Formel (VII) ebenfalls auszuschließen. Diese Aussage wird dadurch gestützt, daß *C*-Ethyl-*N,N'*-diphenylformazan [18] kein Diphenylborchelat bildet [17].

Massenspektrum

Die auf Grund von Elementaranalyse und IR-Spektrum geforderte Zusammensetzung als 1:1-Chelat wird durch das MS bestätigt. So gelang es, das Molekül-Ion m/e = 404 hinsichtlich Lage und Isotopenverteilung zu bestimmen. Außerdem finden sich die in Tabelle 1 aufgeführten Fragment-Ionen im Spektrum wieder.

Die Fragment-Ionen m/e = 179 und 223 liefern Hinweise für das Vorliegen einer B—N- und B—O-Bindung wie in den Formeln (XIII) und (XIV). Weitere Schlüsse sind nicht zulässig.

TABELLE 1

Relative Intensitäten ausgewählter Fragment-Ionen des 1,5-Diphenylcarbazonato-diphenylbor-Chelates

m/e	Fragment-Ion	*I*/Base (%)	*m/e*	Fragment-Ion	*I*/Base (%)
77	C_6H_5	100	223	$M^+-(C_6H_5)_2BO$	15
91	$C_6H_5N=$	16	298	$M^+-C_6H_5NHN$	7
92	C_6H_5NH	43	299	$M^+-C_6H_5N=N$	15
105	$C_6H_5N=N$	97	312	$M^+-C_6H_5NH$	5
165	$(C_6H_5)_2B$	36	327	$M^+-C_6H_5$	81
179	$(C_6H_5)_2BN$	32	404	M^+	22

^1H- und ^{11}B-NMR-Spektren

Durch ^{1}H-NMR-Spektroskopie [17] konnte das einzige noch im Borchelat befindliche NH-Proton bei δ = 9,35 (in $CDCl_3$) identifiziert werden. Durch D_2O-Austausch wurde sichergestellt, daß es sich um ein NH-Proton handelt. Gegenüber den NH-Protonen in (I) (δ = 6,2 und 8,5) liegt das Signal bei wesentlich tieferem Feld. Man könnte daraus schließen, daß das Imino-Proton entschirmt wird, weil das N-1 entsprechend Formel (XIII) eine koordinative Bindung mit dem Bor-Atom eingegangen ist. Dieser Schluß ist jedoch nicht zwingend, da sich das Borchelat — wie nachgewiesen — von der Enol-Form (III) ableitet. Es ist nämlich zu erwarten, daß das Proton von N-1 in der Enol-Form eine andere Abschirmung als in der Keto-Form erfährt. Die Lage des Signals des Imino-Protons in (III) ist aber nicht bekannt, weil (I) — wie gezeigt [9] — fast ausschließlich in der Keto-Form existiert.

Durch Messung der ^{11}B-Kernresonanz anhand einer Reihe von Vergleichssubstanzen konnte erhärtet werden, daß das Chelat als 5-Ring mit O—B—N Koordination vorliegt. Als Vergleichssubstanzen dienten die in Tabelle 2 zusammengestellten borhaltigen 5- und 6-Ringchelate mit O—B—O-, N—B—O- und N—B—N-Koordination des Bors.

Das ^{11}B-Kernresonanzsignal des 1,5-Diphenylcarbazonatodiphenylbor-Chelates liegt bei δ = −13.4 wie das des Diphenylbor-Chelates von 8-Hydroxychinolin, bei dem nur ein 5-Ring möglich ist. Ähnlich starke Verschiebungen zu tieferem Feld finden sich nur bei 6-Ring-Chelaten mit O—B—O-Koordination. Diese ist aber mit (I) nicht möglich. Also muß ein 5-Ring mit O—B—N-Koordination vorliegen. Eine Entscheidung zwischen den noch zur Diskussion stehenden Konstitutionen (XIII) und (XIV) ist allerdings auch mit Hilfe der ^{11}B-Kernresonanz nicht möglich.

Ergänzende Versuche

Da (III) in reiner Form nicht existiert und deshalb für IR- und NMR-spektroskopische Untersuchungen zur Unterscheidung zwischen den Konstitutionen (XIII) und (XIV) nicht herangezogen werden konnte, wurden die beiden Isomeren des *C*-Ethyl-*N,N'*-diphenylformazans als Vergleichssubstanzen synthetisiert. Aus Ethanol umkristallisiert, erhält man sowohl im Tageslicht

TABELLE 2

^{11}B-Chemische Verschiebungen in Benzol bezogen auf ext. $BF_3 \cdot O(C_2H_5)_2$-Standard

Chelatbildner	Verschiebung (p.p.m.)	Koordination Ringgröße
Salicylaldehyd	−11.1	O—B—O
1-Nitroso-2-naphthol	−12.0	6-Ring
2-Nitroso-1-naphthol	−12.7	
Azomethin aus Salicylaldehyd und n-Propylamin	−5.0	O—B—N
1-Benzolazo-2-naphthol	−6.2	6-Ring
Azomethin aus o-Aminobenzaldehyd und n-Propylamin	−0.1	N—B—N
1-Benzolazo-2-naphthylamin	+0.2	6-Ring
8-Hydroxychinolin	−13.1	O—B—N
1,5-Diphenylcarbazon	−13.4	5-Ring
8-Aminochinolin	−5.6	I—B—N 5-Ring

als auch im Dunkeln die orangefarbene, offene *trans-anti*-Form (XV). Nur dann, wenn man (XV) [17, 19] aus Petrolether im Dunkeln umkristallisiert, fällt das rote *trans-syn*-Isomere (XVI) in langen roten Stäbchen an.

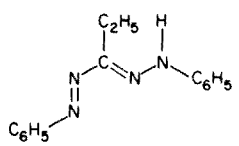

(XV)

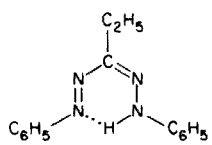

(XVI)

Das IR-Spektrum von (XV) weist bei 3250 cm^{-1} eine mittelstarke, scharfe NH-Absorptionsbande auf. Im Gegensatz dazu zeigt (XVI) im normalen NH-Valenzschwingungsbereich keine Absorption. Lediglich bei 2970 und 2940 cm^{-1} erscheinen zwei schwache Banden, die auf Grund der im Molekül vorhandenen intramolekularen Wasserstoffbrückenbindung der NH-Gruppe zugeschrieben werden könnten. Auch anderen Autoren gelang es nicht, die NH-Valenzschwingungsbande weiterer roter Formazane im NH-Valenzschwingungsbereich zu beobachten [20, 21]. Da das 1,5-Diphenylcarbazonato-diphenylbor-Chelat aber bei 3300 cm^{-1} über eine mittelstarke, scharfe NH-Valenzschwingungsbande verfügt, ist ein weiterer Beweis dafür erbracht, daß ihm auf keinen Fall die *trans-syn*-Formazanstruktur (VIII) mit intramolekularer Wasserstoffbrücke und dreibindigem Bor zukommt.

Die — verglichen mit der NH-Bandenlage der *trans-anti*-Form (XV) — bei höheren Wellenzahlen liegende Absorption der NH-Bande im Borchelat liefert ein starkes Argument für die Formel (XIV). Für Formel (XIII) wäre eine Verschiebung nach niedrigeren Wellenzahlen zu erwarten gewesen.

In [D_6]-Benzol und $CDCl_3$ lieferten sowohl (XV) als auch (XVI) übereinstimmende ^{1}H-NMR-Spektren, in denen das Signal des NH-Protons bei $\delta = 10{,}5$ durch D_2O-Austausch und Integration eindeutig festgelegt werden konnte. Diese Messung ist aber wegen der mangelhaften Lagekonstanz des NH-Signals wenig aussagekräftig. Außerdem gelang es nicht, ein unpolares Lösungsmittel mit ausreichendem Lösevermögen für die cyclische Form für Vergleichsmessungen zu finden.

Auf Grund der durchgeführten Untersuchungen ist das Diphenylborchelat ein O—B—N-5-Ring und leitet sich vom 1,5-Diphenylisocarbazon (III) ab. Einige Argumente sprechen für die Koordinierung des Bors an die Azogruppe: (1,5-Diphenylisocarbazonato-O,N^5)diphenylbor (XIV).

EXPERIMENTELLER TEIL

IR-Spektren: Perkin Elmer IR-Spektrophotometer 457 (3—5 mg Substanz/1,5 g KBr).
Massenspektren: Varian MAT Bremen, Typ CH5.
^{1}H-NMR-Spektren: Varian A-56/60, δ-Werte bezogen auf int. TMS-Standard.
^{11}B-NMR-Spektren: Varian HA-100 (32,1 MHz), Lösungsmittel Benzol, δ-Werte bezogen auf ext. $BF_3 \cdot O(C_2H_5)_2$-Standard.
Schmelzpunkte: Kupferblock, unkorrigiert.

Synthesen des 1,5-Diphenylcarbazonato-diphenylbor-Chelates

(a) 2,5 g (I) [9] und 1,8 g (II) werden jedes für sich bei Raumtemperatur in 50 ml Eisessig gelöst. Nach dem Vereinigen der beiden Lösungen läßt man unter intensivem Rühren langsam 60 ml Wasser aus einer Bürette hinzutropfen. Dabei scheiden sich feine, grünglänzende Kristalle ab. Diese werden nach 1 h abfiltriert und aus Eisessig/Wasser umkristallisiert. (Schmp. 191°C, Ausb. 3,7 g (88%). $C_{25}H_{21}BN_4O$ (403.8): Ber. 74.3% C, 5.2% H, 2.7% B, 13.9% N. Gef. 74.5% C, 5.1% H, 2.8% B, 13.9% N.).

(b) 12,1 g (50 mmol) (IV) und 11,24 g (50 mmol) (V) werden in der Hitze in Ethanol gelöst. Beim Abkühlen auf Raumtemperatur wird soviel Ethanol zugegeben, daß gerade nichts ausfällt. Dann gibt man eine gesättigte Lösung von 11,5 g (etwas mehr als 50 mmol) $(NH_4)_2S_2O_8$ zu und rührt etwa 1 h. Dabei bildet sich das in Lösung intensiv blaue Borchelat unter gleichzeitiger Abscheidung eines farblosen Niederschlages. Durch tropfenweises Zugeben von Wasser löst sich dieser wieder, und das Borchelat fällt als grüner, feinkristalliner Niederschlag aus. (Schmp. 191°C (Ethanol), Ausb. 15,2 g (75%).)

Wir danken Herrn Prof. Dr. H. Nöth für die Durchführung der ^{11}B-Kernresonanzmessungen, dem Minister für Wissenschaft und Forschung des Landes Nordrhein-Westfalen, Landesamt für Forschung, Düsseldorf, sowie dem Verband der Chemischen Industrie, Fonds der Chemie, Frankfurt/Main, für Sachbeihilfen.

LITERATUR

1 L. H. Toporcer, R. E. Dessy und S. I. E. Green, Inorg. Chem., 4 (1965) 1649.
2 R. Neu, Z. Anal. Chem., 176 (1960) 343.
3 D. Thierig und F. Umland, Z. Anal. Chem., 215 (1966) 24.
4 D. Thierig, Dissertation, Techn. Hochschule Hannover, 1966.
5 F. Umland und C. G. Schleyerbach, Angew. Chem., 77 (1965) 169, 426; Angew. Chem., Int. Ed. Engl., 4 (1965) 151, 432.
6 F. Umland und D. Thierig, Angew. Chem., 74 (1962) 388; Angew. Chem., Int. Ed. Engl., 1 (1962) 333.
7 B. Miller, Dissertation, Techn. Hochschule Braunschweig, 1964.
8 D. Szonn, Dissertation, Univ. Münster, 1968.
9 B. Friese und F. Umland, Z. Anal. Chem., 286 (1977) 107.
10 G. J. Willems, R. A. Lontie und W. A. Seth-Paul, Anal. Chim. Acta, 51 (1970) 544.
11 G. J. Willems und C. J. De Ranter, Anal. Chim. Acta, 68 (1974) 111.
12 L. I. Teternikov, A. I. Busev, V. K. Akimov und Yu. A. Mittsel', Zh. Anal. Khim., 26 (1971) 1048; Chem. Abs., 75 (1971) 122876j.
13 C. G. Schleyerbach, Dissertation, Techn. Hochschule Hannover, 1965.
14 E. W. Abel, W. Gerrard und M. F. Lappert, J. Chem. Soc., (1957) 3833.
15 R. L. Werner und K. G. O'Brien, Aust. J. Chem., 8 (1955) 355.
16 E. W. Abel, W. Gerrard und M. F. Lappert, J. Chem. Soc., (1957) 112.
17 B. Friese, Dissertation, Univ. Münster, 1975.
18 I. Hausser, D. Jerchel und R. Kuhn, Ber. Dtsch. Chem. Ges., 82 (1949) 515.
19 R. Kuhn und H. M. Weitz, Ber. Dtsch. Chem. Ges., 86 (1953) 1199.
20 A. Foffani, C. Pecile und S. Ghersetti, Tetrahedron Lett., (1959) 16.
21 D. Schulte-Frohlinde, R. Kuhn, W. Münzing und W. Otting, Justus Liebigs Ann. Chem., 622 (1959) 43.

Analytica Chimica Acta, 96 (1978) 311—317

PERJODAT-BESTIMMUNG: EINFACHE, KOLORIMETRISCHE METHODE MIT HOHER EMPFINDLICHKEIT UND SELEKTIVITÄT

H. GALLATI

Diagnostische Forschungsabteilung der F. Hoffmann-La Roche & Co. AG, Basel (Schweiz)

(Eingegangen den 17. August 1977)

ZUSAMMENFASSUNG

Durch Perjodat wird Phenol aktiviert und kondensiert mit 4-Aminoantipyrin zum roten Chinonimin-Farbstoff. Die Farbintensität zeigt eine lineare Proportionalität zum eingesetzten Perjodat im Konzentrationsbereich von 0—200 μmol l^{-1}. Diese neue Perjodatbestimmungsmethode zeichnet sich aus durch eine einfache und schnelle Testdurchführung (nach Vermischen der Probe mit der Reagenzienlösung kann die Farbintensität nach 10 Min bestimmt werden), durch hohe Sensibilität (bis 2μmol l^{-1} Perjodat), gute Selektivität und Reproduzierbarkeit (VK = 0,7%). Sie ist interessant für analytische und synthetische Arbeiten mit Perjodat als Oxydationsmittel. Es werden Beispiele für den Oxydationsverlauf von löslicher Stärke sowie verschiedenen Sephadexarten bei Anwesenheit von Perjodat gegeben.

SUMMARY

Phenol is activated by periodate and condensed with 4-aminoantipyrine to a red quinoneimine dye; the absorbance is proportional to the periodate concentration in the range 0—200 μmol l^{-1}. The procedure is simple and quick (the sample and reagent are incubated at 25°C for 10 min), shows high sensitivity (2 μmol l^{-1} periodate), and good selectivity and reproducibility (r.s.d. = 0.7%). It is useful for analytical and synthetic work when periodate is used as oxidizing agent. Examples are given for the oxidation of soluble starches as well as for various species of Sephadex.

Für die analytischen und synthetischen Arbeiten mit Perjodat als Oxydationsmittel ist es wesentlich, den Reaktionsverlauf durch wiederholte quantitative Bestimmungen der eingesetzten Reaktionspartner oder der gebildeten Reaktionsprodukte zu verfolgen. Dazu wird meistens der Verbrauch an Perjodat gemessen, indem entweder das bei der Reaktion gebildete Jodat nach einer kolorimetrischen Methode [1—5] oder das in der Reaktionsmischung noch vorhandene Perjodat titrimetrisch [6—9], photometrisch bei der Wellenlänge 222,5 nm [10—12] oder kolorimetrisch [13—15] bestimmt wird. All diese Methoden haben aber den Nachteil, dass sie in der Durchführung aufwendig und zeitraubend sind (titrimetrische und kolorimetrische Methoden), oder dass sie nur beschränkt eingesetzt werden können (photometrische Bestimmung des Perjodats bei 222,5 nm ist nur möglich, sofern keine andere Substanz der Reaktionslösung bei dieser Wellenlänge absorbiert).

In der vorliegenden Arbeit wird eine neue Methode zur Bestimmung von Perjodat beschrieben, die sich durch Einfachheit in der Durchführung, durch eine gute Reproduzierbarkeit sowie durch eine hohe Empfindlichkeit und Selektivität auszeichnet. Ueberraschenderweise hat sich gezeigt, dass Phenol durch Perjodat aktiviert wird und mit 4-Aminoantipyrin zum roten Chinonimin-Farbstoff kondensiert, dessen Farbintensität der Perjodatkonzentration direkt proportional ist. Mit der vorgeschlagenen Methode kann innerhalb von 10 Min Perjodat in einem Konzentrationsbereich von 2—200 μmol l^{-1} quantitativ bestimmt werden.

MATERIAL UND METHODEN

Die verwendeten Chemikalien waren analysenrein. 4-Aminoantipyrin (4-Amino-1,5-dimethyl-2-phenyl-3-pyrazolon, 4-Aminophenazon) wurde von Fluka, Schweiz bezogen.

Zur Bestimmung der Perjodatkonzentration in einer Reaktionsmischung wird eine bestimmte Probenmenge in 0,15 mol l^{-1} Natrium-Boratpuffer vom pH 10 mit 25 mmol l^{-1} Phenol und 2 mmol l^{-1} 4-Aminoantipyrin bei 25°C inkubiert und zwischen der 10 und 40 Min die Farbintensität photometrisch bei 500 nm gemessen. Mit Hilfe einer Perjodat-Standardkurve, einer Perjodat-Standardlösung oder eines Umrechnungsfaktors kann dann die Perjodatkonzentration in der Reaktionsmischung berechnet werden.

RESULTATE UND DISKUSSION

Spektrum der entstehenden Farblösung

Das durch Perjodat aktivierte Phenol kondensiert mit dem 4-Aminoantipyrin zu einem roten Farbstoff, dessen Spektrum (Abb. 1) identisch ist mit demjenigen des Chinonimin-Farbstoffes, der bei der "Trinder-Reaktion" [16] unter Einwirkung von Peroxidase auf H_2O_2 in Gegenwart von Phenol und 4-Aminoantipyrin entsteht. Es ist daher anzunehmen, dass bei der Bildung dieses Farbstoffs die katalytische Reaktion der Peroxidase mit H_2O_2 durch das Oxydationsmittel Perjodat ersetzt werden kann. Der gebildete Chinonimin-Farbstoff zeigt ein breites Absorptionsband mit dem Maximum bei der Wellenlänge 500 nm. Im Bereich von 400 nm bis 600 nm besteht eine lineare Proportionalität zwischen der eingesetzten Menge an Perjodat und der entstehenden Farbintensität.

Einfluss des pH-Wertes und des Puffersystems auf die Farbentwicklungskurve

Die Farbentwicklungskurve wird wesentlich vom pH-Wert der Reaktionslösung beeinflusst (Abb. 2). Unter sonst identischen Reaktionsbedingungen wird beim pH 10 nach einer Reaktionsdauer von 5—10 Min die maximale Farbintensität erreicht, die über 40 Min stabil ist, während bei tieferen-und höheren pH-Werten innerhalb der Messdauer die Farbintensität instabil bleibt. Dabei kann festgestellt werden, dass im stark alkalischen Milieu

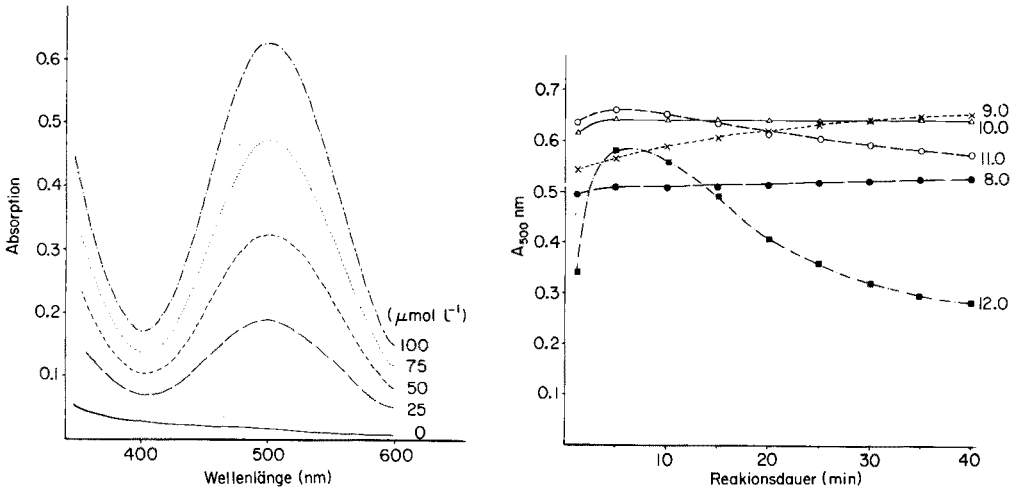

Abb. 1. Die angegebenen Mengen Perjodat werden in 0,15 mol l^{-1} Natrium-Boratpuffer vom pH 10 mit 25 mmol l^{-1} Phenol und 2 mmol l^{-1} 4-Aminoantipyrin während 10 Min bei 25°C inkubiert und anschliessend die Spektren der entsprechenden Farblösungen aufgenommen.

Abb. 2. Perjodat (100 μmol l^{-1}) werden in 0,15 mol l^{-1} Natrium-Boratpuffer der angegebenen pH-Werte mit 25 mmol l^{-1} Phenol und 2 mmol l^{-1} 4-Aminoantipyrin bei 25°C inkubiert und nach bestimmten Zeitintervallen die Absorption bei 500 nm gemessen.

(z.B. bei pH 12) langsam eine Farbveränderung von Rot nach Blau eintritt, was sich in den entsprechenden Spektren dieser Reaktionslösungen zeigt. (Abb. 3). Beim pH 12 nimmt nach 5 Min Reaktionsdauer die Farbintensität bei 500 nm langsam ab und bei 630 nm entsprechend zu. Diese Farbveränderung ist aber nach 60 Min noch nicht abgeschlossen.

Der bei pH 10 gebildete und stabile Chinonimin-Farbstoff verliert bei höheren und tieferen pH-Werten an Farbintensität und Farbstabilität.

Bei sonst identischen Reaktionsbedingungen zur Bestimmung von Perjodat ist die entstehende Farbintensität abhängig vom eingesetzten Puffersystem. Die höchste Absorption wird mit dem Puffersystem Natriumcarbonat (=100%) erzielt, gefolgt von Natrium-Borat (94%), Natriumphosphat (88%), Triethanolamin (50%) und Tris(hydroxymethyl)-aminomethan (6%). Die Resultate für die beiden letzten Puffer lassen vermuten, dass Triethanolamin und vor allem Tris [13] durch Perjodat oxydiert werden.

Die Konzentration an Natrium-Borat beeinflusst die Reaktionsgeschwindigkeit wie auch die Farbintensität. Während mit 150 mmol l^{-1} Natrium-Boratpuffer innerhalb von 5—10 Min (je nach eingesetzter Perjodatmenge) die maximale Farbintensität erreicht wird, die anschliessend über 40 Min stabil bleibt, nimmt bei geringerer Pufferkonzentration die Reaktionsgeschwindigkeit wesentlich ab, so dass die maximale Farbintensität erst nach längerer Reaktionsdauer erreicht wird. Bei höherer Natrium-Borat-

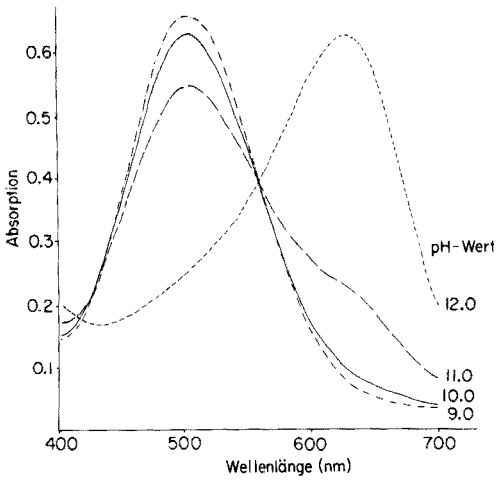

Abb. 3. Perjodat (100 μmol l^{-1}) werden in 0,15 mol l^{-1} Natrium-Boratpuffer der angegebenen pH-Werte mit 25 mmol l^{-1} Phenol und 2 mmol l^{-1} 4-Aminoantipyrin bei 25°C während 50 Min inkubiert und anschliessend die Spektren der entsprechenden Farblösungen aufgenommen.

konzentration bleibt die rasch gebildete Farbintensität nicht stabil. Auf Grund dieser Ergebnisse wurde für die Perjodat-Bestimmung eine Natrium-Boratkonzentration von 150 mmol l^{-1} gewählt.

Bestimmung des Konzentrationsoptimums für Phenol und 4-Aminoantipyrin

Die Abhängigkeit der Farbintensität von der Phenolkonzentration wurde bei Anwesenheit von 100 μmol l^{-1} Perjodat und 2 mmol l^{-1} 4-Aminoantipyrin untersucht und dabei festgestellt, dass mit 25 mmol l^{-1} Phenol die höchste Farbintensität und eine gute Farbstabilität erreicht wird. Die Unterschiede der Farbintensität im Konzentrationsbereich von 3 bis 100 mmol l^{-1} Phenol sind gering. Mit Phenolkonzentrationen unter 3 mmol l^{-1} werden wesentlich geringere Farbintensitäten erreicht.

Bei Anwesenheit von 100 μmol l^{-1} Perjodat und 25 mmol l^{-1} Phenol sind zur Erreichung einer optimalen Farbintensität minimal 300 μmol l^{-1} 4-Aminoantipyrin notwendig. Eine höhere 4-Aminoantipyrin-Konzentration hat auf die Perjodat-Bestimmung keinen negativen Einfluss, während bei Konzentrationen unter 300 μmol l^{-1} die erreichbare Farbintensität stark abnimmt.

Empfindlichkeit, Reproduzierbarkeit, Selektivität und Stabilität

Unter den vorgeschlagenen Testbedingungen besteht eine lineare Proportionalität zwischen der Absorption bei 500 nm und der in der Testlösung vorhandenen Perjodatmenge im Konzentrationsbereich von 0—120 μmol l^{-1} (A_{500nm} = 0—0,9). Die Nachweisgrenze liegt bei 2 μmol l^{-1} Perjodat. An Stelle von Perjodat kann bei entsprechend abgeänderten Testbedingungen sowohl 4-Aminoantipyrin wie auch Phenol mit gleicher Empfindlichkeit nachgewiesen

werden, sodass bezogen auf die Proportionalität der Farbintensität zur eingesetzten molaren Konzentration identische Standardkurven für Perjodat, 4-Aminoantipyrin und Phenol erhalten werden.

Die Prüfung der Reproduzierbarkeit dieser Perjodat-Bestimmungsmethode mit 20 serienmässig durchgeführten Bestimmungen [80 μmol l^{-1} $NaIO_4$] ergab einen Variationskoeffizienten von 0,7%.

Die Interferenzstudien mit verschiedenen Anionen im Konzentrationsbereich von 1—100 mmol l^{-1} haben ergeben, dass die beschriebene Perjodat-Bestimmungsmethode durch Jodid, Jodat, Chlorid, Chlorat, Perchlorat, Nitrat, Nitrit, Sulfat, Ammoniumacetat, Wasserstoffperoxyd und EDTA nicht beeinflusst wird, während Hypochlorit, Sulfit und Tris-Puffer stark interferieren.

Protein in Konzentrationen über 0,1 g l^{-1} in der Testlösung bewirken eine der Proteinkonzentration entsprechende Abnahme der Farbintensität sowie eine Verschlechterung der Farbstabilität. Diese Proteininterferenz kann dadurch erklärt werden, dass das durch Perjodat aktivierte Phenol auch mit freien Aminogruppen des Proteins kondensiert, und dass sich anderseits ein Protein-Farbstoffkomplex bildet, wodurch das Resonanzsystem des Chinonimin abgeschwächt und dadurch die Farbintensität vermindert wird.

Die Perjodat-Testlösung in der vorgeschlagenen Zusammensetzung (0,15 mol l^{-1} Natrium-Boratpuffer vom pH 10 mit 25 mmol l^{-1} Phenol und 2 mmol l^{-1} 4-Aminoantipyrin) ist in einer gut verschlossenen, braunen Glasflasche bei Raumtemperatur 7 Tage und bei 4°C 4 Wochen haltbar. Die langsam entstehende Rosafärbung hat auf die Perjodat-Bestimmung keinen Einfluss.

Eine 5 mmol l^{-1} Perjodatlösung in 50 mmol l^{-1} Natriumphosphat im pH-Bereich von 2—11 ist in einer braunen Glasflache bei Raumtemperatur aufbewahrt während mindestens 2 Wochen haltbar. Dank dieser guten Stabilität der Perjodatlösung kann die Berechnung der Perjodatkonzentration in einer Probe — neben der Benützung einer Perjodat-Standardkurve oder eines Umrechnungsfaktors — auch mit Hilfe einer mitgeführten Perjodat-Standardlösung erfolgen.

Praktische Anwendungsbeispiele der Perjodat-Bestimmungsmethode

Die Oxydation von löslicher Stärke bei 25°C durch Perjodat verläuft langsam und ist nach 24 Stunden noch nicht abgeschlossen. Für den Oxydationsverlauf der Abb. 4 wurden zu 5 mmol l^{-1} Perjodat lösliche Stärke im Konzentrationsbereich von 0—5 mmol l^{-1} (bezogen auf den Glucosegehalt) zugesetzt und nach bestimmten Zeitintervallen der Verbrauch an Perjodat gemessen.

Für die Versuche der Abb. 5 wurde die lösliche Stärke durch verschiedene Arten von Sephadex ersetzt. Daraus ist ersichtlich, dass Perjodat Sephadex bedeutend schneller oxydiert als lösliche Stärke, und dass anderseits stärker vernetzte Sephadexarten wie Sephadex G-10 oder G-15 weniger Perjodat verbrauchen als die weniger stark vernetzten Sephadexarten von G-25 bis G-200.

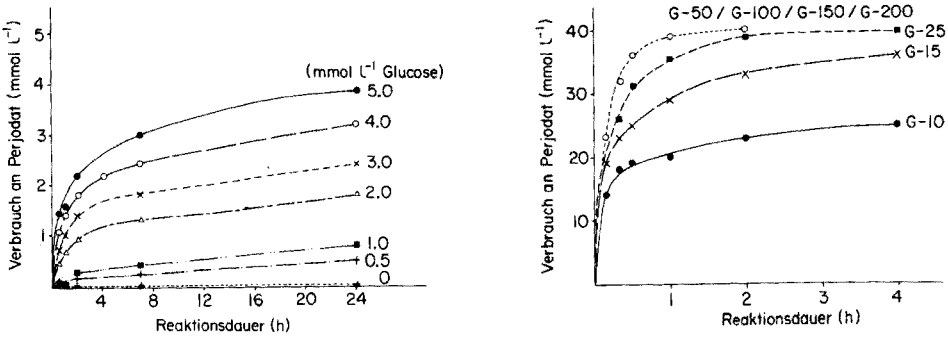

Abb. 4. Lösliche Stärke in den angegebenen Konzentrationen wird in einer wässrigen, 5 mmol l^{-1} Perjodatlösung bei 25°C inkubiert. Nach bestimmten Zeitintervallen wird nach der beschriebenen Methode die noch vorhandene Perjodatmenge gemessen.

Abb. 5. Verschiedene Arten von Sephadex (in einer auf Glucose bezogenen Konzentration von 80 mmol l^{-1}) werden in einer wässrigen, 40 mmol l^{-1} Perjodatlösung bei 25°C inkubiert. Nach bestimmten Zeitintervallen wird nach der beschriebenen Methode die noch vorhandene Perjodatmenge gemessen.

Der durch Perjodat bewirkte, zeitliche Oxydationsverlauf der Disaccharide Saccharose, Maltose und Lactose ist unterschiedlich. Am schnellsten wird Lactose oxydiert, gefolgt von der Maltose und der Saccharose. Zudem ist auch der Verbrauch an Perjodat zur Oxydation von 1 mmol l^{-1} der drei Disacchariden verschieden (Lactose: 4 mmol l^{-1}; Maltose und Saccharose: 3 mmol l^{-1} $NaIO_4$).

Von den untersuchten Monosacchariden wird die Fructose am schnellsten durch Perjodat oxydiert, gefolgt von der Glucose und der Mannose. Der Perjodatverbrauch ist auch bei diesen drei untersuchten Monosacchariden unterschiedlich: 1 M Mannose und Glucose verbrauchen 4 M Perjodat, während 1 M Fructose 3 M Perjodat benötigen.

Ethylenglycol ist in wenigen Minuten durch Perjodat oxydiert. Dabei entsteht eine lineare Proportionalität des Perjodatverbrauchs zur eingesetzten Ethylenglycolkonzentration: 1 M Perjodat vermag 1 M Ethylenglycol zu oxydieren.

Der Autor dankt Frl. H. Dettmar für die effiziente technische Hilfe bei der Durchführung der Versuche.

LITERATUR

1 D. Burnel, Compt. Rend., 261 (1965) 1982.
2 D. Burnel, B. Gournail und L. Malaprade, Compt. Rend., 261 (1965) 2117.
3 R. Belcher und A. Townshend, Anal. Chim. Acta, 41 (1968) 395.
4 G. Nisli und A. Townshend, Talanta, 15 (1968) 1377.
5 S. A. Barker, P. Peplow und P. J. Somers, Carbohyd. Res., 22 (1972) 201.
6 L. Malaprade, Compt. Rend., 186 (1928) 392.

7 L. Malaprade, Bull. Soc. Chim. Fr., 43 (1928) 683.
8 S. Hara, Jpn. Analyst, 5 (1956) 163.
9 J. Dyer, Methods Biochem. Anal., 3 (1956) 124.
10 C. Crouthamel, H. Meek, D. Martin und C. V. Banks, J. Am. Chem. Soc., 71 (1949) 3031.
11 C. Crouthamel, A. Hayes und D. Martin, J. Am. Chem. Soc., 73 (1951) 82.
12 J. Dixon und D. Lipkin, Anal. Chem., 26 (1954) 1092.
13 D. Rammler, R. Bilton, R. Haugland und C. Parkinson, Anal. Biochem., 52 (1973) 198.
14 G. Mahuzier, Anal. Chim. Acta, 76 (1975) 79.
15 P. Senise und L. Silva, Anal. Chim. Acta, 80 (1975) 396.
16 C. Allain, L. Poon, C. Chan, W. Richmond und P. Fu, Clin. Chem., 20 (1974) 470.

Analytica Chimica Acta, 96 (1978) 319—325

AUTOMATIC COULOMETRIC TITRATION WITH PHOTOMETRIC END-POINT DETECTION
Part I. A Coulometric Titrator Based on Differential Photometric Detection

ANDERS O. LINDBERG

Department of Analytical Chemistry, University of Umeå, S-901 87 Umeå (Sweden)

(Received 14th July 1977)

SUMMARY

A system for automatic coulometric titrations with photometric end-point detection is described. To compensate for errors caused by gas bubbles and turbidity, the beam is split after passing the titration cell. The intensities of the respective light beams are registered by means of two photodiodes operating in the current mode. The currents are converted to voltages and the logarithm of the quotient is taken. The measured absorbance is only slightly dependent on the variation in the intensity of the incident light. A diminution of one absorbance unit causes a relative error of less than 5%. The deviations due to carbon particles (37—75 μm) were less than 0.002 absorbance units per mg of carbon present in 10 ml of solution. The improvement with respect to errors caused by gas bubbles is illustrated. The fundamental advantage of a one-lamp system over a two-lamp system is shown.

Coulometric determinations with potentiometric (glass electrode) end-point detection are troublesome for non-aqueous acid—base titrations because of the electric field interference on the indicating electrode system; photometric end-point detection has been suggested in order to improve such titrations. The drawbacks of normal photometry, i.e., errors brought about by dilution, turbidity or by the formation of gas bubbles have been investigated. Wise et al. [1, 2] described a photometric system which compensated for errors caused by gas bubbles in coulometric acid—base titrations. The light beam was split after passing the titration cell and detected with a differential ratio-detecting photometric unit. An indicator, predominantly in its acidic form, was placed in front of the other phototube, the same indicator being present in the titration cell. Light passing through an acidic solution will pass through the filter containing the acid form of the indicator with very little attenuation but will be attenuated in the filter containing the indicator in its basic form. Such an arrangement produces a ratio of light intensities which will not be significantly affected by an overall diminution of the light transmitted through the solution being titrated, such as is caused by the formation of bubbles.

Liberti [3] described a similar photometric detector with two selenium cells in the light path after the titration cell. A filter placed in front of one of the detectors was sensitive to colour changes occurring at the end-point. The other detector was not filtered; its output compensated for changes in light intensity and interferences from the generation of gas bubbles in the titration cell.

Ringbom et al. [4] described a two photocell titrator in which light beams of different wavelengths are used. By choosing two corresponding wavelengths the end-point was determined precisely and independently of the concentration of the indicator. Accurate complexometric and acid–base titrations could be performed even when the stability constant was below 10^4, but the errors exemplified in the preceding paragraph were not discussed.

An approach to the minimization of errors from turbidity was described by van Oort et al. [5]. Two light beams of different wavelengths were passed through the cell; one of the wavelengths was chosen so that no absorption was obtained. The theoretical treatment of this system was based on the assumption that the turbidity contributes to the absorbance of the two beams by the same amount. Upon subtracting the two indicating signals, Oort et al. found a value in which the turbidity error is zero and it was shown that the error from the dilution of the solvent could be almost eliminated. However, the theory presented was based on the assumption that the sensitivity of the photocells was independent of the wavelength, which is not true. A refinement of the results was made including a correction for the difference in the relative spectral sensitivity of the detectors and for the particle size and wavelength-dependent light scattering [6]. Although this approach improves normal photometric systems with respect to the interferences mentioned above, it is not ideal since the two beams are passed through the cell in different ways; this makes adequate corrections difficult.

This paper describes a further development of a coulometric titration system with photometric end-point detection based on the passage of a single beam through the cell, the beam being split after the passage. This idea, first proposed by Wise et al. [1], has not been followed up adequately.

Fundamental principles

The photometric system is based on the principle that one light beam is split into two after passage through the cell solution; the intensities of the light beam are measured at 615 and 470 nm, for thymolphthalein as an example. One of these wavelengths corresponds to the maximum absorptivity of this indicator; the other corresponds to the minimum. It is assumed that thymolphthalein is the only absorbing species. If the superscript ′ is referred to 615 nm and superscript ″ to 470 nm, Beer's law gives

$$\log (I''/I') = \log (I''_0/I'_0) + bc(a' - a'') \qquad (1)$$

If I'_0 and I''_0 vary by the same factor, the value of $\log I''/I'$ will be independent of the overall diminution of the light transmitted through the solution. Moreover, if the values of the intensities I'_0 and I''_0, which are different for the two wavelengths, are amplified so that $I'_0 = I''_0$, eqn. (1) gives

$$\log (I''/I') = bc(a' - a'') \quad (2)$$

Maximum sensitivity in the indicating system, i.e., the maximum value of $d(\log I''/I')/dc$, is obtained for $a'' = 0$. Hence $A' = \log (I''/I') = a'bc$, i.e. $\log I''/I'$ follows Beer's law and is independent of the intensity of the light under the assumptions made above.

EXPERIMENTAL

A schematic diagram of the titration system is shown in Fig. 1. The light source was a halogen lamp (Atlas, 150 W/15 V) connected to a constant current generator. The light beam, via an i.r. filter, 6 mm, and two identical positive lenses (F = 15 mm), passes through the titration cell and through a focussing lens. After passing the beam splitter (50/50) the intensities of the two beams are measured at certain wavelengths by means of two photodiodes. The connection between the monochromator (GM 100 Schoeffel Instrument) and the photodiode (HP 4220) is provided with a small positive lens in contact with an i.r. filter. The intensity of the respective light beam (see Fig. 2) is registered by means of the photodiodes D_1 and D_2 operating in the current mode [7]. The respective currents i_1 and i_2, directly proportional to the intensities of the incident light, are converted to voltages, U_1 and U_2, and the logarithm of the quotient, A_2, is taken by means of a log module (Philbrick No. 4753). The value of this quotient is compared with a preset value A_1, which corresponds to the desired absorbance value at the end-point of the titration. The difference between the actual value and the preset, $\Delta A \rightarrow U_3$, is amplified and a current proportional to the difference is passed through the generating electrode system. The current decreases asymptotically

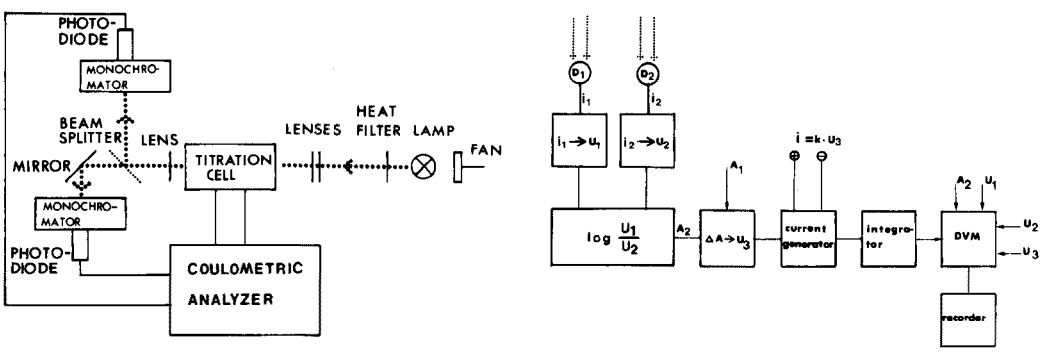

Fig. 1. Schematic diagram of the experimental arrangement.

Fig. 2. Block diagram of the coulometric analyzer.

towards zero during the titration; the uncertainty in the end-point is less than 0.001 absorbance unit. The integrator could be read down to 1×10^{-12} equivalents. The readout module was built up so that A_2, U_1, U_2 and U_3 could be studied separately with a digital panel meter. The cell is described in Part 2 of this series [8].

RESULTS AND DISCUSSION

The accuracy of the photometric system was tested by inserting filters of known absorbance values in front of one of the monochromators adjusted to 615 nm while the other was held at 470 nm. The observed values for log (U_1/U_2) agreed within 2% with the nominal absorbance of the filters, up to an absorbance value of 1.3.

The ability of the photometric system to compensate for a decrease in the intensity of the light was tested by inserting wire mesh, corresponding to various absorbance values, in front of the halogen lamp, the wavelengths of the monochromators being adjusted to 615 nm and 470 nm, respectively. The results of these experiments (Fig. 3) show that the measured absorbance $A_2 = \log (U_1/U_2)$ (see Fig. 2) is very little affected by an overall diminution of the transmitted light, e.g. the relative error caused by a decrease of as much as one absorbance unit was less than 5%.

Figure 4 shows a comparison between the photometric system described in this paper and a single beam system with regard to the problems caused by bubbles; the stability is much better in the differential photometric mode (curve A). This gain in stability contributes to the increase in sensitivity and reproducibility obtained with this system [8] compared with others reported in the literature.

Another drawback of photometric titrations based on a preset end-point absorbance value is that even slight turbidities cause errors because of the

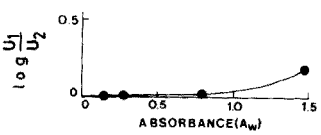

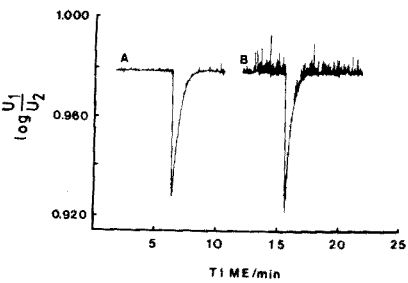

Fig. 3. Effect of a decrease in the intensity of the light on the measured signal log U_1/U_2 (= A_2, see Fig. 2) when wire mesh corresponding to the absorbance values A_w was placed in front of the light source.

Fig. 4. Comparison between titration curves (absorbance vs. time) obtained with the differential photometric system (curve A) and a single beam system (curve B). 8.9×10^{-9} mol of benzoic acid was titrated in both cases.

set-point shift caused by particle absorbance. The ability of this photometric titrator to compensate for such errors was studied for different substances giving turbidity: activated carbon (37—75 μm), quartz (37—75 μm) and alundum (1 μm and 37—75 μm, respectively). These measurements were performed with a rather strong basic solution of thymolphthalein in dimethylformamide in order to minimize errors from changes in the colour of the indicator arising from reactions with the various substances added. In order to calculate the error given by a single-beam instrument, log U_1/U_2^0 (U_2^0 is a constant and equals the value obtained before adding any substance) is plotted as a function of the amount of substance present and is inserted in Figs. 5a—d for comparison with the signal from the differential photometric system, log U_1/U_2. Figure 5a shows that the differential photometric

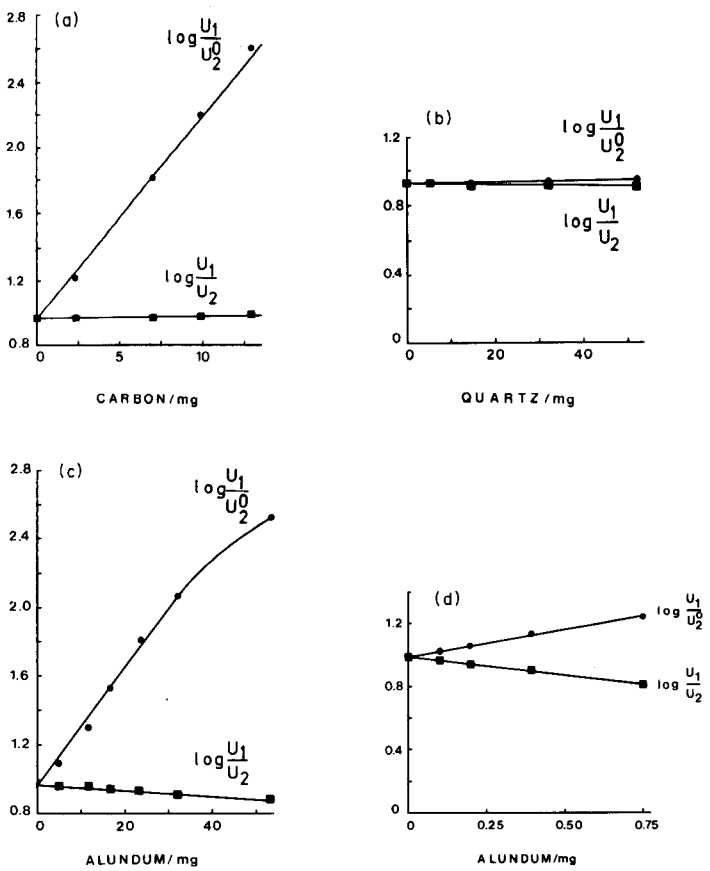

Fig. 5. Comparison between the change in the measured signal (log U_1/U_2^0 and log U_1/U_2 respectively) for a single beam system (○) and a differential beam system (■) for various amounts of substances causing turbidity added to the cell solution (10.5 ml). (a) Activated carbon, particle size 37—75 μm. (b) Quartz particles, 37—75 μm. (c) Alundum, particle size 37—75 μm. (d) Alundum, particle size about 1 μm.

system is able almost completely (the deviation is less than 0.002 absorbance units per mg of carbon) to compensate for errors caused by carbon particles of 37—75 μm size. The influence of quartz particles (37—75 μm) is shown in Fig. 5 as an example of a transparent substance giving rise to turbidity; the error from the presence of as much as 50 mg of quartz particles is very small for both systems. Finally, the effects of various particle sizes of alundum were examined; the results, represented in Figs. 5c and 5d, show that the differential photometric system is able to suppress the interferences caused by the alundum particles. However, it cannot compensate properly for very small particle sizes.

Photometric systems including two light sources have been described [4—6]. The disadvantage in using two light sources with respect to the stability of the photometric system will be shown by comparing the stability of a one-lamp system, having a certain lamp drift, with a system with two light sources, of which one has a drift characteristic identical with that of the lamp of the single beam system while the other is assumed to be ideal (i.e. zero drift). Figure 6 shows the signals, U_1 and U_2, obtained for the wavelengths 470 nm and 615 nm, respectively, when the lamp drift was simulated by means of a variation in the lamp effect. The intersection of the curves shown in Fig. 6 where $U_1 = U_2$ is called U_2^0 and represents a starting point around which the effect of the lamp was varied. The results given in Fig. 6 were used to construct the curves shown in Fig. 7. Curve A was obtained for the single-beam system in which the beam was split into two after passage through the cell and the logarithm of the signals obtained at the respective wavelength was taken. Curve B corresponds to the system with two lamps, the intensities being measured at 470 nm and 615 nm, respectively, and the logarithm of the quotient taken. One of the lamps was assumed to have zero drift, $U_2 = U_2^0$, independent of the lamp effect; the other was assumed to have a drift equal to that of the lamp of the single-beam system. The stability of the one-lamp system should be a factor of five better than the two-lamp system.

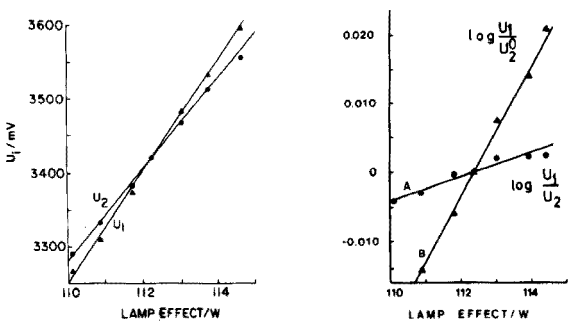

Fig. 6. U_1 and U_2 as a function of the effect of the halogen lamp.

Fig. 7. log U_1/U_2 and log U_1/U_2^0 plotted as a function of the variation of the effect of the halogen lamp.

The differential photometric system described compensates well for errors from gas bubbles and turbidity but it is difficult to make a quantitative comparison with the other photometric systems described because of the incomplete results reported earlier. Part II of this series includes a comparison between the various systems based on results obtained from titrations.

The author thanks Gillis Johansson and Anders Cedergren for valuable discussions and Lars Lundmark and Svante Jonsson for help with the construction of the apparatus. Part of this work was supported by grants from the Swedish Board for Technical Development.

REFERENCES

1 E. N. Wise, P. W. Gilles and C. A. Reynolds, Jr., Anal. Chem., 25 (1953) 1344
2 E. N. Wise, P. W. Gilles and C. A. Reynolds, Jr., Anal. Chem., 26 (1954) 779.
3 A. Liberti, Anal. Chim. Acta, 17 (1957) 247.
4 A. Ringbom, B. Skrifvars and E. Still, Anal. Chem., 11 (1967) 1217.
5 W. J. van Oort, P. C. Schalkwijk, R. A. Brandenburg and B. Griepink, Z. Anal. Chem., 276 (1975) 177.
6 W. J. van Oort, P. C. Schalkwijk, R. A. Brandenburg and B. Griepink, Z. Anal. Chem., 276 (1975) 181.
7 P. G. Witherell and M. E. Faulhaber, Appl. Opt., 9 (1970) 73.
8 A. O. Lindberg and A. Cedergren, Anal. Chim. Acta, 96 (1978) 327.

Analytica Chimica Acta, 96 (1978) 327—333

AUTOMATIC COULOMETRIC TITRATION WITH PHOTOMETRIC END-POINT DETECTION
Part II. Coulometric Determination of Nanomole Amounts of Carbon Dioxide by Non-aqueous Titration

ANDERS O. LINDBERG and A. CEDERGREN*
Department of Analytical Chemistry, University of Umeå, S-901 87 Umeå (Sweden)
(Received 14th July 1977)

SUMMARY

An improved coulometric method for the determination of carbon dioxide by non-aqueous titration is described. A titration efficiency of 100 ± 0.1% was obtained with a large generating cathode in 0.1 M potassium perchlorate solution containing 12.3 ml of dimethylformamide, 0.3 ml of monoethanolamine and 0.025 ml of an indicator solution containing 1.5 mg of thymolphthalein per ml of n-butanol. The anodic and cathodic compartments were separated by a glass membrane in contact with an ion-exchange membrane. The lowest amount of carbon dioxide which could be determined with a relative standard deviation of 10% was 0.5 nmol. Compared with other titrimetric methods, this sensitivity constitutes an improvement of about two orders of magnitude.

Trace determination of carbon dioxide is of great importance in a number of fields; carbon dioxide is easily obtained as a discrete product when a carbon-containing material is oxidized either by dry combustion at high temperature (e.g. carbon in steel) or by wet combustion. In addition, carbon dioxide is determined in connection with certain enzymatic reactions and in various decarboxylation and physiological experiments.

Determination of carbon dioxide by absorption in aqueous solution followed by titration is troublesome when carried out to an optimum pH with respect to the buffer capacity, but this disadvantage can be almost overcome if carbonic anhydrase is present in the solution [1]. With this principle, Römer et al. [2, 3] showed that, by means of coulometry, as little as 40 nmol of carbon dioxide could be determined with a precision of 5%. Because of the instability of the enzyme the titration must be performed at 0°C. Another drawback of this method is that several species affect the activity of the enzyme.

The use of a non-aqueous titration medium has therefore been investigated extensively. In 1955 Blom and Edelhausen [4] showed that the use of pyridine and acetone improved conditions for the absorption of carbon dioxide. However, the pH of the solution must be controlled by means of continuous titration. A modification of this method, including replacement

of the pyridine with dimethylformamide, was suggested by Grant et al. [5] who also showed that the method could be improved by using thymolphthalein instead of thymol blue. The method of Grant et al. [5] eliminated the need for continuous titration of the carbon dioxide. A further improvement was suggested by Jones et al. [6, 7] who showed that the absorption of carbon dioxide is very efficient if monoethanolamine is added to the dimethylformamide. Braid et al. [8] investigated important factors affecting the determination of carbon dioxide by non-aqueous titrimetry and summarized the work done up to 1966. They concluded that the changes in conditions for the determination of carbon dioxide reported up to this time had resulted from trial and error rather than from any systematic examination of the various factors involved; although they did not present a full and systematic study, most of their recommendations still hold. They concluded that ethanolamine can be used in concentrations up to 5% in dimethylformamide, and recommended the use of thymolphthalein instead of thymol blue. A typical error in their titrations was reported to be 5 μg of carbon dioxide.

Coulometry was applied to non-aqueous titrations of carbon dioxide by White [9] who showed that the titration could be carried out with 99—100% current efficiency in a titration medium containing 0.5% of methanol in acetone saturated with potassium iodide; 50 μg of carbon dioxide could be determined with an error, typically, of 1%. Similar results were reported by Boniface and Jenkins [10] who used photometric end-point detection and showed that the titration efficiency was in the range 99.5—101.5% in a titration medium containing 78 ml of dimethylformamide, 2 ml of 0.1% solution of thymolphthalein in dimethylformamide, 2 ml of water, 3 g of potassium iodide and 3 ml of monoethanolamine. The addition of water was necessary for large amounts of carbon dioxide, thereby avoiding a precipitation (probably potassium carbonate) which affected the photometric system. No problems were reported from the hydrolysis of dimethylformamide in the presence of the relatively large concentration of water, in conflict with a report by Whymark [11].

This paper reports an improved method for the determination of carbon dioxide by coulometric non-aqueous titration based on the photometric titration system already described [12].

Boniface and Jenkins [10] proposed that the following reactions take place in a titration medium similar to that used in this study. Potassium, formed at the cathode through reduction of potassium ions, reacts with monoethanolamine, and the resulting basic compound reacts completely with the monoethanolammonium ion formed by the reaction between carbon dioxide and monoethanolamine. Dimethylformamide is chosen as solvent because the monoethanolammonium ion is a stronger acid in this medium than in water.

EXPERIMENTAL

Figure 1 shows a schematic diagram of the Teflon coulometric cell, with quartz windows, constructed with special emphasis on obtaining efficient absorption of carbon dioxide. The cell path length was 5 cm. The generating electrodes were made of platinum. The area of the auxiliary electrode (anode) was 0.5 cm^2 throughout all experiments while that of the working electrode was varied. The electrodes were separated by a glass membrane (Corning Code 7930 Porous Glass) in contact with an anion-exchange resin (Permaplex A-20), the latter being in contact with the working compartment. The current will be transported between the two cell compartments almost entirely by the perchlorate ions. In this way electrical migration of the acidic products into the working compartment was minimized. The auxiliary compartment was filled with 3 ml of 0.1 M tetrabutylammonium hydroxide in toluene/methanol and the working compartment with 12.3 ml of 0.1 M $KClO_4$ solution containing 12.0 ml of dimethylformamide (BDH, spectroscopic grade), 0.3 ml of monoethanolamine (BDH, AnalaR) and 25 μl of an indicator solution containing 1.5 mg of thymolphthalein per ml of n-butanol (p.a.). In some separate experiments the volume of indicator solution added was 50 μl. During all titrations the cell was purged with a slow flow of purified (ascarite) air.

Standard samples of carbon dioxide were made with a stripping cell into which standard sodium carbonate solutions were injected. The carbon dioxide formed was stripped into the titration cell by means of a 100 ml min^{-1} flow of purified air (ascarite). The stripping solution contained sulphuric acid in distilled water (pH 3). The temperature of the stripping cell was held at 100°C. The stripping gas, after passing a reflux condenser, was chilled by an acetone—dry ice bath to remove water. No significant amount of carbon dioxide was retained.

Measurements of the titration efficiency were performed with standard solutions of benzoic acid dissolved in dimethylformamide (BDH, spectroscopic grade). This sample solution was injected into the cell with a calibrated 25-μl

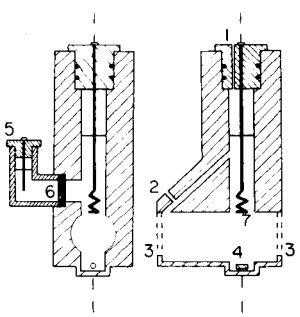

Fig. 1. Schematic diagram of the coulometric titration cell. (1) Teflon stopper with hole diameter 1.5 mm. (2) Gas inlet. (3) Quartz window. (4) Teflon-coated magnetic stirrer. (5) Auxiliary compartment with platinum anode. (6) Anion exchange and glass membranes. (7) Platinum cathode.

Hamilton syringe (r.s.d. 0.1%). The results obtained were corrected for the impurities in the dimethylformamide which were determined coulometrically to be $(0.31 \pm 0.008)10^{-9}$ mol per μl of solvent. In some experiments various amounts of air were injected with gas-tight Hamilton syringes into the titration cell.

Procedure

The electrodes were connected to the coulometric analyzer (see Part I [12]). The wavelengths of the two monochromators were adjusted to 470 (absorptivity of the indicator close to zero) and 615 nm (max. absorptivity), respectively. The pre-selected absorbance value was about half an absorbance unit for 25 μl of the indicator solution. Before addition of the first sample the titration medium was pre-titrated to the pre-selected absorbance value, and the system was allowed to equilibrate for a few hours. The integrator of the coulometer is provided with a mercury cell, which is connected to a potentiometer. When a titration is to be performed, the potentiometer is set to compensate for the residual current. A typical value for this is 1—2 μA. In this way the integrator will show a constant value. Thereafter the integrator is set to zero, the sample is introduced and the titration starts. The end-point of the titration is reached when the value of the integrator is constant within 0.05 nmol for 30 s.

RESULTS AND DISCUSSION

Stability of the dimethylformamide

The degree of hydrolysis of dimethylformamide containing various concentrations of water is shown schematically as a function of time in Fig. 2. The hydrolysis products are dimethylamine and formic acid, the latter being responsible for the increase in acidity. As indicated by the diagram, the drift of the coulometric titration system resulting from the hydrolysis is very low for concentrations of water less than about 3% (the drift in the end-point was less than 0.0002 absorbance units per min, which corresponds to less than 0.2×10^{-9} mol of carbon dioxide per min). The results given in

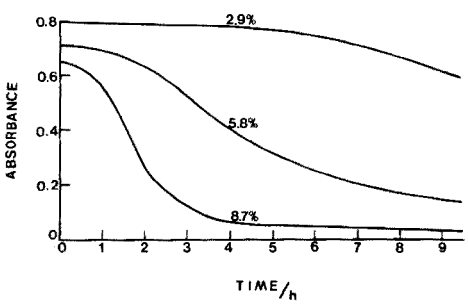

Fig. 2. Degree of hydrolysis of dimethylformamide titration solutions containing various concentrations of water.

Fig. 2 agree with those reported by Boniface and Jenkins [10]. For determinations in the range 10^{-9}—10^{-6} mol there was no need to add water to the titration solution to prevent precipitation.

Titration efficiency

Two factors were of primary importance for establishing 100% titration efficiency. (i) Separation of the anode and cathode compartment with a sintered glass disc was insufficient (large and uncontrolled drift) to prevent interference from products formed in the auxiliary compartment. This problem was overcome completely by the use of a glass membrane in contact with an ion-exchange resin. (ii) The titration efficiency was critically dependent on the concentration of the indicator, thymolphthalein. Figure 3 shows the titration efficiency for two indicator concentrations as a function of the maximum current passing through the generating electrode system during a titration of 780 nmol of benzoic acid. As can be seen, the titration efficiency is further decreased for increasing concentrations of the indicator. These results can be explained by side-reactions caused by reduction of the indicator. In these experiments the area of the cathode was 1 cm^2. These errors were eliminated by the use of a large platinum gauze cathode, 10 cm^2, and the results are shown by point A in Fig. 1 (mean value of nine determinations). Thus the side-reactions from reduction of the indicator present at a certain concentration can be controlled by the current density.

Table 1 shows the titration efficiency obtained with 25 μl of the indicator solution and a 10-cm^2 platinum gauze electrode at a maximum current of 1 mA. From the small value of the standard deviation, the titration efficiency can be considered to be very close to 100%.

The drift of the coulometric system was normally in a range corresponding to 0.5—1 nmol of carbon dioxide per min (1—2 μA). The variation in the value of the drift during short periods was always less than 0.1 nmol per min.

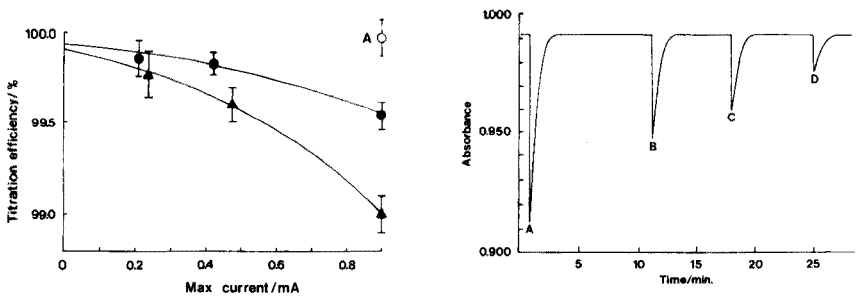

Fig. 3. Titration efficiency as a function of maximum generating current for two indicator concentrations. (▲) 50 μl of thymolphthalein, 1-cm^2 cathode area. (●) 25 μl of thymolphthalein, 1-cm^2. Point A: 25 μl of thymolphthalein, 10-cm^2 platinum gauze cathode. The height of the bars denotes twice the standard deviation.

Fig. 4. Absorbance vs. time curves for different amounts of carbon dioxide (air samples directly injected into the titration cell). (A) 13.3 × 10^{-9} mol. (B) 6.7 × 10^{-9} mol. (C) 3.3 × 10^{-9} mol. (D) 1.3 × 10^{-9} mol.

TABLE 1

Determinations of titration efficiency with benzoic acid as a standard

Taken (nmol)	Found mean value (nmol)	R.s.d. (%)	No. of detns.	Titration efficiency (%)
780.2	780.4	0.09,	9	99.9,
90.7	90.6	0.23	9	99.9

The stability of the coulometric system is illustrated in Fig. 4 for small amounts of carbon dioxide directly injected into the titration cell; the stability is good and the time required for the titrations is about 2 min.

Determination of carbon dioxide

Table 2 shows the recovery of carbon dioxide as a function of the flow rate of the stripping gas. The upper limit of the flow rate which gives an absorption efficiency of 100 ± 0.2% is 200 ml min^{-1}.

Determination of the detection limit and the absorption efficiency for very small amounts of carbon dioxide are shown in Table 3 for a stripping flow rate of 100 ml min^{-1}. The efficiency is 100% in the range 0.3—86 nmol

TABLE 2

Recovery of carbon dioxide as a function of the flow rate of the stripping gas (air). A 10-cm^2 platinum gauze electrode was used.

Flow rate (ml min^{-1})	Taken (nmol)	Found mean value (nmol)	R.s.d. (%)	No. of detns.	Recovery (%)
300	86.10	84.3	0.28	3	98
200	86.10	86.3	0.23	3	100
100	86.10	86.2	0.22	3	100

TABLE 3

Determinations of carbon dioxide produced by the stripping procedure. The flow rate of the stripping gas was 100 ml min^{-1}. A 10-cm^2 platinum gauze electrode was used.

Taken (nmol)	Found mean value (nmol)	R.s.d. (%)	No. of detns.	Recovery (%)
86.10	86.36	0.20	5	100
8.94	8.89	1.3	5	99
5.36	5.39	2.3	5	100
1.79	1.81	3.6	5	101
0.36	0.36	13	5	100

of carbon dioxide. Compared with results reported previously [2, 3], these determinations constitute an improvement in sensitivity of about two orders of magnitude.

Part of this work was supported by grants from the Swedish Board for Technical Development.

REFERENCES

1 F. J. W. Roughton and N. V. Meldrum, Brit. Patent 403, 096, p. 6, clauses 60—100 (Dec. 1, 1933).
2 F. G. Römer, P. H. van Rossum and B. Griepink, Mikrochim. Acta, (1975) 337.
3 F. G. Römer, P. H. van Rossum and B. Griepink, Mikrochim. Acta, (1975) 345.
4 L. Blom and L. Edelhausen, Anal. Chim. Acta, 13 (1955) 120.
5 J. A. Grant, J. A. Hunter and W. H. S. Massie, Analyst, 88 (1963) 134.
6 R. F. Jones, P. Gale, P. Hopkins and L. N. Powell, Analyst, 90 (1965) 623.
7 R. F. Jones, P. Gale, P. Hopkins and L. N. Powell, Analyst, 91 (1966) 399.
8 P. Braid, J. A. Hunter, W. H. S. Massie, J. D. Nicholson and B. E. Pearce, Analyst, 91 (1966) 439.
9 D. C. White, Talanta, 13 (1966) 1303.
10 H. J. Boniface and R. H. Jenkins, Analyst, 96 (1971) 37.
11 D. W. Whymark, Thesis, University of Strathclyde, 1969.
12 A. O. Lindberg, Anal. Chim. Acta, 96 (1978) 319.

Analytica Chimica Acta, 96 (1978) 335—344

A PULSE POLAROGRAPHIC INVESTIGATION OF PARATHION AND SOME OTHER NITRO-CONTAINING PESTICIDES§

MALCOLM R. SMYTH* and JANET G. OSTERYOUNG

Department of Microbiology, Colorado State University, Fort Collins, Colorado 80523 (U.S.A.)

(Received 17th August 1977)

SUMMARY

The polarographic behaviour of parathion, its major metabolites (paraoxon and *p*-nitrophenol), and of methylparathion, EPN and pentachloronitrobenzene has been studied over a wide pH range. Differential pulse polarography is used to differentiate between parathion, *p*-nitrophenol and pentachloronitrobenzene. An indirect determination of parathion in the presence of paraoxon can be based on their respective rates of hydrolysis in 0.5 M sodium hydroxide solution. The electrochemical behaviour of these compounds has also been investigated in solutions containing tetraalkylammonium salts as the supporting electrolyte.

Although there are many published methods for the determination of parathion (I), few offer the sensitivity or convenience of the polarographic method [1—6]. This compound is metabolized in vivo to give the highly toxic substances paraoxon (II) and *p*-nitrophenol.

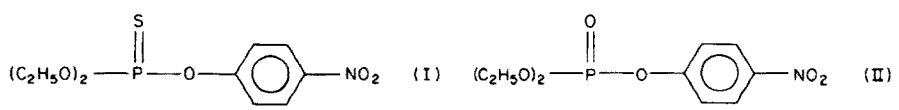

Bowen and Edwards [1] have reported that parathion could be determined in the presence of both paraoxon and *p*-nitrophenol in a supporting electrolyte containing 0.5 M KCl and 0.1 M acetic acid in 50% acetone. In this medium, parathion had an $E_{1/2}$ value of −0.39 V (vs. SCE) whereas paraoxon and *p*-nitrophenol had $E_{1/2}$ values of −0.47 and −0.68 V, respectively. Nangniot [2] has also reported a method for the determination of parathion in the presence of paraoxon; only parathion gives rise to an intense adsorption peak in linear sweep voltammetry because of the presence of the P = S moiety in its molecular structure. Parathion can be determined in the presence of *p*-nitrophenol because of the wide separation in their $E_{1/2}$ values [1, 4]. These compounds can also be determined after an ammoniacal back-extraction procedure [5]. In the study which led to official acceptance of the polaro-

§This paper was presented at the 174th ACS National Meeting in Chicago in August, 1977.

graphic method by the AOAC [3], it was reported that parathion and methylparathion (III) exhibited similar behaviour in linear sweep voltammetry. Other workers, however, have reported slight differences in the behaviour of parathion, methylparathion and EPN (IV; *O*-ethyl-*O*-*p*-nitrophenyl phenylphosphonothioate), which can be used for their differentiation in mixtures [7, 8].

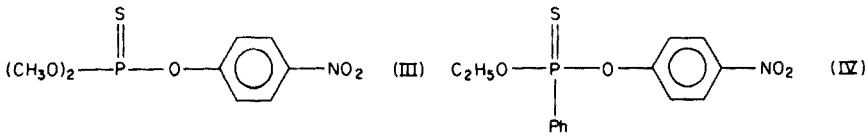

In the work described here, therefore, the polarographic behaviour of these compounds was re-examined by the normal pulse (n.p.p.) and differential pulse (d.p.p.) techniques in order to verify whether these differences in behaviour could be used for the determination of these compounds at the trace level. Pentachloronitrobenzene (PCNB) was also included in this study in order to demonstrate the selectivity offered by polarographic methods for the determination of nitro-containing pesticides.

EXPERIMENTAL

Apparatus

Polarographic curves were recorded with a PAR Model 174 Polarographic Analyser in conjunction with a three-electrode cell system having a saturated calomel reference electrode (SCE) and a platinum counter electrode. The polarograms were recorded on an Omnigraphic Model 2000 X-Y recorder. The dropping mercury electrode (DME) had a flow rate of 1.32 mg s^{-1} and a drop time of 4.6 s in 0.1 M KCl at a mercury head of 76 cm. Drop times were controlled with a PAR Model 172 drop knocker.

Reagents

Samples of parathion, paraoxon, *p*-nitrophenol, methylparathion, EPN and PCNB were obtained from the Quality Assurance Section, Environmental Toxicology Division of the Environmental Protection Agency. Stock solutions of these compounds were prepared in AnalaR methanol and stored in the dark under refrigeration. A stock Britton—Robinson (BR) buffer solution (pH 1.8) composed of a mixture of boric acid, orthophosphoric acid and glacial acetic acid, all 0.04 M, was prepared from analytical-grade reagents. From this stock solution, buffer solutions of varying pH were prepared by the addition of 0.2 M sodium hydroxide solution and measuring the pH with a glass electrode. All other compounds used were of analytical grade.

Techniques

All solutions were deaerated with oxygen-free nitrogen for 10 min before measurement. Current—potential curves were recorded in the n.p.p. and

d.p.p. modes. The solutions were blanketed by an atmosphere of nitrogen during analysis and each solution was scanned between −0.1 V and the potential of the decay of the supporting electrolyte. Scan rates of 2−5 mV s^{-1}, a drop time of 1 s (n.p.p. and d.p.p.) and a modulation amplitude of 100 mV (d.p.p.) were typically employed in most investigations.

The hydrolysis studies were carried out in a water-jacketed cell thermostatted at 25°C; 10 ml of solution (0.5 M or 1.0 M NaOH) was introduced into the cell and deaerated with oxygen-free nitrogen for 10 min. The nitrogen was then passed over the cell and the current—potential curve of the blank solution recorded in the d.p.p. mode (starting potential −0.4 V, scan rate 2 mV s^{-1}, modulation amplitude 100 mV). An aliquot (5 μl) of a 5×10^{-3} M stock solution of parathion (or paraoxon or methylparathion) was then introduced into the solution by means of a syringe and the solution mixed for 30 s. After allowing another 30 s for the solution to equilibrate, a d.p.p. curve was recorded as before. This was then repeated at various time intervals up to 30 min. Plots of log C versus t were then constructed for each of the three compounds; C is the concentration in ng ml^{-1} and t is the time (min) from the start of the scan until the E_p reaches a value of −0.625 V. The initial concentration was calculated by recording the d.p.p. curve of a 2.5×10^{-6} M solution of the compound under study in 0.01 M NaOH, in which it was assumed that negligible hydrolysis took place during the recording of the polarogram. The concentration of the compound at any time t_i was obtained by relating the peak current (i_p) to a previously prepared calibration curve.

Recommended hydrolysis procedure for the determination of parathion and paraoxon in mixtures

Take up the extract (containing parathion and paraoxon) in 4 ml of water and degas the solution for 5 min with oxygen-free nitrogen. Add 1 ml of 0.05 M NaOH and degas the solution for a further 1 min. Record the differential pulse polarogram from −0.4 to −0.8 V (drop time 1 s; scan rate 2 mV s^{-1}; modulation amplitude 100 mV). Then disconnect the cell, add a further 5 ml of 1.0 M NaOH to the solution and leave to degas for exactly 25 min. Finally, record the differential pulse polarogram in the same way as before.

RESULTS AND DISCUSSION

Effect of pH

The effect of pH on the E_p values exhibited by parathion, *p*-nitrophenol and PCNB in d.p.p. is shown in Fig. 1. Methylparathion, paraoxon and EPN all exhibit behaviour similar to that of parathion. The pK values obtained from these plots are given in Table 1. The pK_1 values for all compounds other than *p*-nitrophenol, relate to the pH at which the hydroxylamine intermediate in the electrochemical reduction of the nitro group is no longer protonated and therefore cannot be reduced. Up to this pH two waves are seen for these compounds corresponding to:

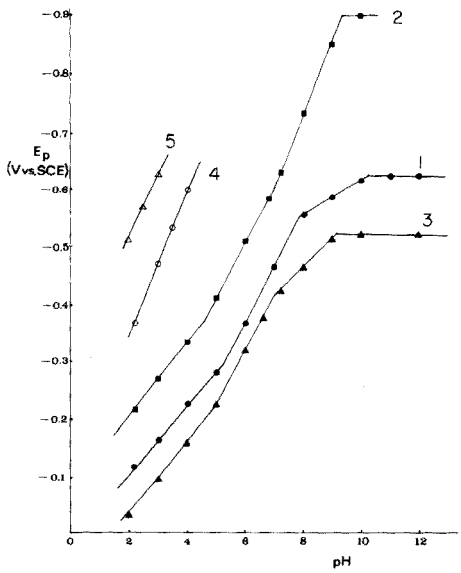

Fig. 1. Plots of E_p versus pH for the reduction of the nitro group in parathion (1, ●), *p*-nitrophenol (2, ■) and PCNB (3, ▲) and for the reduction of the hydroxylamine intermediate in parathion (4, ○) and PCNB (5, △).

TABLE 1

pK Data obtained from plots of E_p versus pH

Compound	pK_1	pK_1'	pK_2
Parathion	5.2	7.8	—
Paraoxon	5.0	8.0	—
p-Nitrophenol	4.6	—	7.0
Methylparathion	5.2	7.8	—
EPN	4.9	7.4	—
PCNB	5.0	7.0	—

(i) $R{-}NO_2 + 4e^- + 4H^+ \rightarrow R{-}NHOH + H_2O$; $R{-}NHOH + H^+ \rightleftharpoons R{-}NHOH_2^+$

(ii) $R{-}NHOH_2^+ + 2e^- + 2H^+ \rightarrow R{-}NH_3^+ + H_2O$

The pH at which $i_{H_2A^+} = i_{HA}$ (i.e. the pK_a' value) occurs several pH units above the corresponding pK_a value [9].

A further break in the E_p versus pH plot was observed for these compounds at pH values above 9—10. At higher pH values, the process was independent of pH and the d.p.p. peaks became well defined with half-peak widths of 50—55 mV. This sharpness is usually associated with a reversible electrode process, but plots of $E_{d.e.}$ versus log $i/(i_d - i)$ for the d.c. wave exhibited by

these compounds in solutions of pH over 10 exhibited two linear portions whose slopes were not equal to $59.15/n$ [10]. This indicates that the sharpness of the d.p.p. peaks in this pH region may be due to adsorption effects. The change in electrochemical behaviour is therefore probably due to the mechanism:

$$R{-}NO_2 \xrightarrow{e^-} R{-}NO_2^- \xrightarrow[\text{fast}]{3e^-,\,3H_2O} R{-}NHOH + 4OH^-$$

In the case of *p*-nitrophenol, only one wave is observed up to its pK_1 value; this corresponds to the well-known $6e^-$ reduction of the nitro group to the amine [9]. At pH values between 4.6 and 7.0, *p*-nitrophenol is reduced in a $4e^-$ process to the hydroxylamine. The break in the E_p versus pH plot at pH 7.0 (i.e. pK_2) reflects phenolic dissociation and is in good agreement with the published value of 7.15 for *p*-nitrophenol [11]. Above pH 7.0, the influence of phenolic dissociation markedly affects both the peak height and shape of the nitro reduction waves, and the waves obtained in this pH region are not suitable for analytical purposes.

The effect of pH on the n.p.p. behaviour of paraoxon is shown in Fig. 2. The maxima shown in both the $NO_2 \rightarrow NHOH$ and $NHOH_2^+ \rightarrow -NH_3^+$ reduction processes indicate reactant adsorption [12]. The n.p.p. behaviour of paraoxon differs from that of the other S-containing nitro pesticides in that the peak current obtained from the plateau region of the waves obeys the Cottrell equation. For parathion, methylparathion and EPN, the n.p.p. current is nearly completely depressed thus giving rise to a peaked wave form. This difference in behaviour is attributed to the strong adsorption properties of the sulfur moiety in these three compounds. A severe depression of the n.p.p. wave was also observed for PCNB, while the effect was less pronounced with *p*-nitrophenol.

The best defined waves for analytical purposes were obtained for parathion, methylparathion and EPN at pH $< pK_1$ and in the pH range 9—12. In contrast, paraoxon gave rise to well defined d.p.p. peaks over the pH range 2—12 while *p*-nitrophenol showed the most ideal behaviour in solutions of pH 10—12.

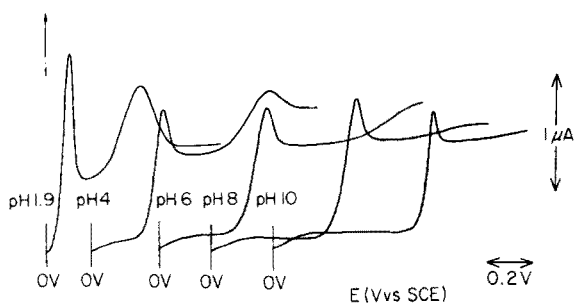

Fig. 2. Effect of pH on n.p.p. behaviour of paraoxon (19.5 μg ml^{-1}).

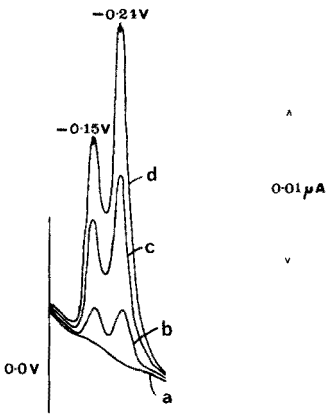

Fig. 3. D.p.p. determination of parathion (I) and *p*-nitrophenol; a, BR buffer pH 3; b, 7.5 ng ml^{-1} each of I and *p*-nitrophenol; c, 22.5 ng ml^{-1} each of I and *p*-nitrophenol; d, 37.5 ng ml^{-1} each of I and *p*-nitrophenol. Conditions: scan rate 1 mV s^{-1}, drop time 2 s, modulation amplitude 100 mV. E_p is −0.15 V for I and −0.24 V for *p*-nitrophenol.

Accordingly, *p*-nitrophenol is best differentiated from parathion in acid solution. This is illustrated in Fig. 3 for the d.p.p. determination of trace quantities of these compounds in BR buffer, pH 3. PCNB, however, is best resolved in alkaline solution where it has an E_p of −0.52 V compared to the E_p of −0.625 V for parathion. Although small differences were observed in the E_p values and wave shapes of parathion, paraoxon, methylparathion and EPN across the pH range, these cannot be used for quantitative purposes. In addition, it was not possible to achieve any differentiation between parathion and paraoxon by d.p.p. in the medium reported by Bowen and Edwards [1].

With the waves outlined above, it was possible to determine these nitro-containing pesticides down to 1×10^{-8} M by the d.p.p. technique; linear calibration plots were obtained over the range 1×10^{-5}—1×10^{-8} M for each of the compounds studied. This technique, therefore, offers a sensitive and convenient method of analysis for these compounds. In the case of a mixture containing parathion and *p*-nitrophenol (2×10^{-8}—5×10^{-6} M) each species can be determined in mixtures containing up to an eight-fold excess of either compound. In the case of mixtures containing parathion and PCNB, a fifteen-fold excess can usually be tolerated.

Effect of tetraalkylammonium salts

Since parathion and paraoxon exhibit different adsorption properties at the DME, it was decided to investigate their behaviour in solutions containing tetraalkylammonium salts as the supporting electrolyte.

The effect of varying tetrabutylammonium bromide (TBAB) concentration on the n.p.p and d.p.p. behaviour of parathion is shown in Fig. 4. At concentrations of TBAB between 1×10^{-1} and 5×10^{-2} M, parathion shows two waves in both n.p.p. and d.p.p., which begin to merge on lowering the concentration

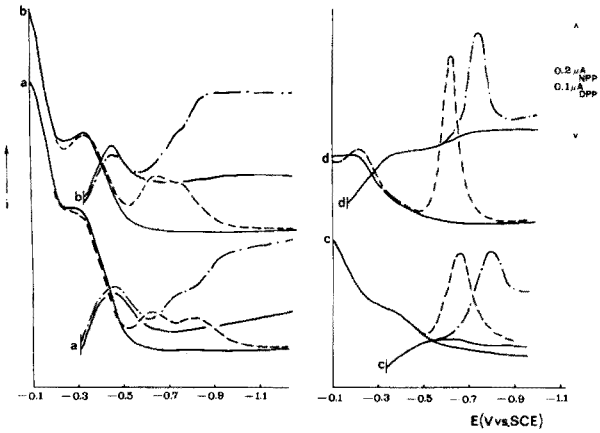

Fig. 4. The n.p.p. (—•—•—) and d.p.p. (— — —) behaviour of 1.5 μg ml^{-1} of parathion in (a) 1×10^{-1} M TBAB, (b) 5×10^{-2} M TBAB, (c) 1×10^{-2} M TBAB, and (d) 1×10^{-3} M TBAB. Conditions: scan rate 5 mV s^{-1}, drop time 1 s, modulation amplitude (d.p.p.) 100 mV; blank currents represented by unbroken lines.

of TBAB. In particular, the n.p.p. waves are well defined and exhibit none of the effects of reactant adsorption shown by parathion in BR buffer solutions. At lower concentrations of TBAB (about 10^{-2} M), the n.p.p. waves again take on a peaked wave form, but in 10^{-3} M TBAB, the current peak is nearly completely depressed. On lowering the concentration of TBAB, the d.p.p. wave becomes better defined, indicating that the adsorption of parathion in this media causes an enhancement of the response. Similar experiments were carried out with other tetraalkylammonium salts as the supporting electrolyte. In solutions containing 10^{-1}—10^{-2} M tetraethylammonium chloride (TEAC) or tetraethylammonium hydroxide (TEA—OH), parathion exhibited behaviour similar to that shown in 10^{-3} M TBAB. In tetrapropylammonium bromide (TPrAB) double-wave behaviour was exhibited at the 10^{-1} M TPrAB level, which was replaced by a single wave at concentrations of 5×10^{-2} M and lower. Although parathion exhibited similar behaviour in TBAB and tetrapentylammonium bromide (TPeAB), the limiting currents were much lower in the latter electrolyte. Polarographic investigations in TBAB therefore showed the greatest variation in response, for studying the different adsorption properties of parathion and paraoxon.

The effect of varying TBAB concentration on the n.p.p. and d.p.p. behaviour of paraoxon was similar to that exhibited by parathion except that the double-wave behaviour persisted for concentrations of TBAB down to 10^{-2} M. At the 10^{-3} M level paraoxon exhibited behaviour similar to that of parathion. The greatest difference in response between parathion and paraoxon was therefore shown in 10^{-2} M TBAB. The effect of varying paraoxon concentration on the d.p.p. wave of parathion in this medium is shown in Fig. 5; it can be seen that increasing the concentration of paraoxon produces a double

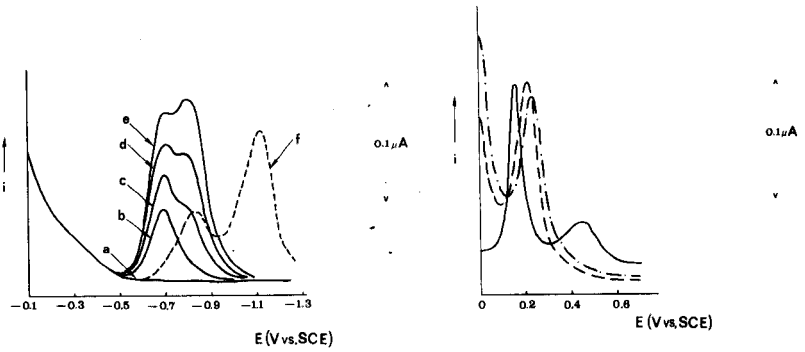

Fig. 5. Effect of varying concentration of paraoxon on d.p.p. wave of parathion in 10^{-2} M TBAB. a, 10^{-2} M TBAB; b, 1.9 μg ml^{-1} parathion; c, b + 1.5 μg ml^{-1} paraoxon; d, b + 3 μg ml^{-1} paraoxon; e, b + 4.5 μg ml^{-1} paraoxon; f, 1.5 μg ml^{-1} *p*-nitrophenol.

Fig. 6. D.p.p. of 1.9 μg ml^{-1} parathion in BR buffer pH 3 (——) in the presence of 1×10^{-3} M (— — —) and 2×10^{-3} M (—•—•—) TBAB. Conditions: scan rate 5 mV s^{-1}, drop time 1 s, modulation amplitude 100 mV.

peak which changes in magnitude depending on the concentrations of both parathion and paraoxon. This is therefore of little use for determining parathion in the presence of paraoxon. In addition, further interference is caused by the presence of *p*-nitrophenol.

The effect of TBAB on the d.p.p. behaviour of parathion in BR buffer pH 3 is shown in Fig. 6; it can be seen that TBAB shifts the $-NO_2 \rightarrow -NHOH$ reduction of parathion to more negative potentials with a resulting decrease in peak height and broadening of the $4e^-$ reduction wave. TBAB also had the effect of inhibiting the $-NHOH_2^+ \rightarrow -NH_3^+$ reduction indicating that adsorption plays a role in this electrode process. The addition of tetraalkylammonium salts to decrease the background current in d.p.p. [13] is therefore not recommended for the determination of these compounds.

Hydrolysis studies

A recent paper [14] has reported significant differences in the rates of hydrolysis of parathion and paraoxon in strongly alkaline media. These compounds (as well as methylparathion and EPN) are hydrolyzed under these conditions to form the corresponding phosphoric acid derivative and *p*-nitrophenol. It was decided, therefore, to investigate whether this property could be used for the indirect determination of paraoxon in the presence of parathion. Since the products of this hydrolysis do not give rise to a wave in alkaline media, the rates of hydrolysis were obtained by monitoring the decrease in peak height of the parent compound.

In 1 M NaOH, paraoxon was hydrolyzed to *p*-nitrophenol almost instantaneously whereas parathion was hydrolyzed according to a second-order rate reaction (k = 0.018 min^{-1} at 25°C). In this same medium methylparathion

had a second-order rate constant $k = 0.675\ \text{min}^{-1}$. In 0.5 M NaOH the rates of hydrolysis were much slower than in 1 M NaOH but did not agree with the data supplied by Ramakrishna and Ramachandran [14]. In this medium paraoxon was nearly completely hydrolyzed in 25 min whereas 37.5 ± 2.5% of the parathion had been hydrolyzed in the same time. These results on the rates of hydrolysis of parathion in alkaline media are in good agreement with those reported by Ketelaar [15].

It is possible, therefore, to use the hydrolysis procedure recommended in the Experimental part to determine parathion and paraoxon in mixtures provided that compounds such as methylparathion and EPN are known not to be present. The total concentration of parathion and paraoxon is obtained from measurement of the d.p.p. peak recorded after the first addition of sodium hydroxide. The concentration of parathion is then obtained after the complete conversion of paraoxon to *O,O'*-diethylphosphoric acid and *p*-nitrophenol. After allowing for the percent of parathion that has hydrolyzed in 25 min (37.5 ± 2.5%), the concentration of paraoxon may be obtained by difference.

This hydrolysis procedure can be used for the determination of parathion and paraoxon in mixtures (provided that paraoxon is not present in greater than three-fold excess) in the range $5 \times 10^{-8} - 1 \times 10^{-6}$ M with a relative precision of ±8%. At higher concentrations, the relative precision is of the order of ±5%.

Conclusions

This study has shown that pulse polarography (in particular d.p.p.) offers a convenient and sensitive method of analysis for parathion and various other nitro-containing pesticides. Although pulse polarography can differentiate between different structural classes of compounds, i.e., between parathion, *p*-nitrophenol and pentachloronitrobenzene, it cannot differentiate between the nitrophenyl esters of related structure. Although parathion and paraoxon can be differentiated in mixtures by a hydrolytic procedure, this method of analysis suffers from a loss in sensitivity and lack of precision compared to a direct d.p.p. procedure. For trace determination of nitrophenyl esters of related structure in mixtures, chromatographic separation would be required prior to analysis.

This work was funded in part through NSF Grant Number MPS 75-00322.

REFERENCES

1 C. V. Bowen and F. I. Edwards, Anal. Chem., 22 (1950) 706.
2 P. Nangniot, Anal. Chim. Acta. 31 (1964) 166.
3 R. J. Gajan, J. Assoc. Off. Anal. Chem., 52 (1969) 811.
4 A. Ichim, Igiena, 21 (1972) 225.
5 M. Zietek, Mikrochim. Acta, (1975) 463.
6 M. Zietek, Mikrochim. Acta, (1976) 549.
7 K. Hasegawa, Kagaku Keisatsu Kenkyusho Hokoku, 15 (1962) 62.

8 H. Yamano, T. Matsumara and K. Fukado, Kagaku Keisatsu Kenkyusho Hokoku, 15 (1962) 65.
9 P. Zuman, The Elucidation of Organic Electrode Processes, Academic Press, New York, 1969.
10 L. Meites, Polarographic Techniques, 2nd edn., Interscience, 1965, p. 203.
11 CRC Handbook of Chemistry and Physics, 55th edn., 1974—75, p. D129.
12 J. B. Flanagan, K. Takahashi and F. C. Anson, J. Electroanal. Chem., to be published.
13 J. G. Osteryoung and K. Hasebe, Rev. Polarogr. (Jpn.), 22 (1976) 1.
14 N. Ramakrishna and B. V. Ramachandran, Analyst, 101 (1976) 528.
15 J. A. Ketelaar, Rec. Trav. Chim., 69 (1950) 649.

Analytica Chimica Acta, 96 (1978) 345—351

POLAROGRAPHIC DETERMINATION OF FOLIC ACID IN PHARMACEUTICAL PREPARATIONS

E. JACOBSEN* and M. WIESE BJØRNSEN

University of Oslo, Institute of Pharmacy, P.O. Box 1068 Blindern, Oslo 3 (Norway)

(Received 3rd October 1977)

SUMMARY

A.c. polarograms of folic acid recorded from acetate buffer pH 5.5 exhibit a very well-defined wave at the dropping mercury electrode. The current is diffusion-controlled and proportional to the concentration; the optimal range of measurement is 0.2—4 $\mu g\ ml^{-1}$. Two electrons and two hydrogen ions are involved in the reduction. With the phase-sensitive a.c. polarographic method, the calibration graph is linear in the 2×10^{-8}—2×10^{-6} M range. The method proposed for the determination of folic acid in tablets is very simple and rapid, and does not involve time-consuming separation of iron salts and insoluble constituents in the tablets.

Many methods for the determination of folic acid have been described in the literature. Fluorimetric [1], microbiological [2] and spectrophotometric [3—7] methods have been proposed. The interference from iron salts in the photometric assay of folic acid has been overcome by complexing agents [5] and by precipitation with sulphide [4] or phosphate [6, 7]. Folic acid is reduced at the dropping mercury electrode and the drug has also been determined by d.c. polarography [8—12].

The object of the present work was to study the electro-reduction of folic acid and to investigate the application of a.c. polarography to rapid determination of the drug in tablets containing large amounts of iron salts.

EXPERIMENTAL

Instrumentation

A.c. and d.c. polarograms were recorded with a Metrohm E261 Polarecord connected to a Metrohm E393 a.c. modulator. An Ag/AgCl/saturated KCl electrode served as reference electrode and a tungsten electrode was employed as auxiliary electrode. All a.c. polarograms were obtained with an amplitude of 10 mV r.m.s. Differential pulse and phase sensitive a.c. polarograms were recorded with a Metrohm Polarecord E506 connected to an E505 polarographic stand.

Cyclic voltammetry and coulometry were performed with a versatile solid-state instrument constructed in this laboratory to the design of Goolsby and

Sawyer [13]. A Moseley 7030AM X-Y recorder and a Honeywell Electronic 194 strip-chart recorder were used in conjunction with the instrument. A three-electrode assembly was used for all measurements. A Metrohm E410 hanging mercury drop was used as working electrode for the cyclic voltametric experiments, and a mercury pool was employed for the controlled potential coulometric experiments. The reference electrode and the auxiliary electrode (platinum coil) were isolated in glass tubes with fine-porosity glass frits. The shield tubes were filled with the supporting electrolyte used in the sample solution.

All experiments were performed at 25 ± 0.1°C. Dissolved air was removed from the solutions by bubbling oxygen-free nitrogen through the cell for 15 min and passing it over the solution during the electrolysis.

Chemicals

Folic acid (pharmaceutical grade) and "Pregnifer" tablets were obtained from Weiders Farmasøytiske A/S, Oslo. "Foli-fer" tablets were obtained from Nyegaard and Co. A/S, Oslo. A 0.15 M stock solution of diethylenetriaminepentaacetic acid (DTPA; Geigy Chemical Corp., New York) was prepared by dissolving 60 g of DTPA in sodium hydroxide, adjusting to pH 8 by addition of more sodium hydroxide and diluting to 1 l with distilled water. A 1 mM stock solution of folic acid was prepared by dissolving 0.1104 g of the drug in 6 ml of 0.1 M sodium hydroxide and diluting to 250 ml with distilled water. All other chemicals were of reagent grade and were used without further purification.

Recommended procedure for the analysis of tablets

Transfer one tablet (equivalent to 30—60 μg of folic acid) to a 50-ml volumetric flask and add 10 ml of 0.15 M DTPA solution with pH 8. Crush the tablet with a glass rod, shake the flask for 5 min, and dilute to the mark with 0.1 M acetate buffer pH 5.5. Transfer 20 ml to a polarographic cell, deareate with pure nitrogen for 5 min and record an a.c. polarogram with start potential −0.4 V, phase angle 0°, a.c. amplitude 28 mV and scan rate 6mV mm^{-1} ($\Delta V = -1.5$ V, 1 mm/t_{drop} and t_{drop} = 1 s, rapid). Measure the peak current and determine the amount of folic acid from a standard curve prepared by the same procedure and with the same amount of iron and constituents in the tablet or by the standard addition method.

RESULTS AND DISCUSSION

Polarographic study

Folic acid gives polarographic waves over the entire pH range 3.8—10. Two d.c. waves are observed on polarograms recorded from acidic media. As shown in Fig. 1, the first d.c. polarographic step is accompanied by a very well-defined a.c. polarographic wave.

The effect of pH on the polarographic waves was investigated by recording

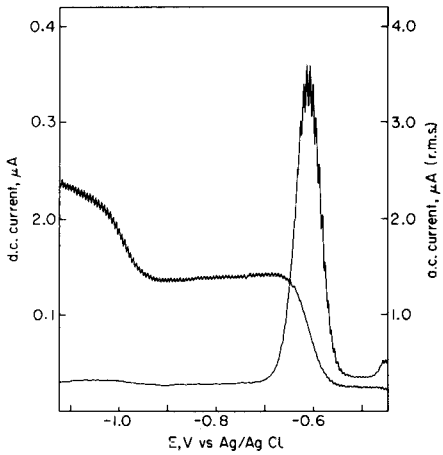

Fig. 1. D.c. and a.c. polarograms of 0.02 mM folic acid in 0.1 M acetate buffer pH 5.5.

d.c. and a.c. polarograms of the drug in various supporting electrolytes. The peak potential, and the half-wave potential of the first d.c. wave, were shifted —65 mV per pH unit to more negative values with increasing pH of the electrolyte. Above pH 6, the a.c. peak current decreased and the width of the wave at half-height increased, indicating a more irreversible electrode reaction. Hence, 0.1 M acetate buffer with pH 5.5 was chosen as supporting electrolyte for subsequent experiments.

The effect of drop time was investigated by recording d.c. polarographic curves of 0.2 mM folic acid at various heights of the mercury column. The value $i\,h^{-\frac{1}{2}}$, where h is the height of the column after correction for the "back pressure", was constant, indicating that the current is diffusion-controlled. The height of the a.c. peak was practically independent of the mercury column height. The temperature coefficient (determined in the range 20—50°C) of the d.c. wave was + 1.2% per degree; this again implies that the current is essentially diffusion-controlled.

Polarograms recorded from 0.1 M acetate buffer with various amounts of folic acid present, showed that the d.c. current increases linearly with concentration in the range 0.01—0.2 mM (Table 1). Electrocapillary curves showed that the presence of folic acid causes a large decrease in drop time in the potential range 0 to —1.1 V, which indicates that the drug is strongly adsorbed on the electrode surface. This adsorption is probably responsible for the non-linear increase in the height of the a.c. wave at concentrations above 0.01 mM. The diffusion current constant $I = i_d/Cm^{2/3}t^{1/6}$, calculated from the data in Table 1, is 2.61 μA mM^{-1} mg$^{-2/3}$s$^{1/2}$. As indicated in the Table the a.c. current is almost 30 times higher than the d.c. current. Hence, a.c. polarography is the best method for the determination of small amounts of the drug (0.2—4 μg ml^{-1}).

Coulometric reduction at controlled potential of folic acid in acetate buffer

TABLE 1

Polarographic data for the reduction of various amounts of folic acid in 0.1 M acetate buffer pH 5.5

Conc. (mM)	i_d (μA)	$-E_{\frac{1}{2}}$ (mV)	i_d/C (μA mM^{-1})	i_p (μA r.m.s.)	$-E_p$ (mV)	i_p/C (μA mM^{-1})
0.200	1.20	0.600	6.00			
0.100	0.60	0.610	6.00	1.965	0.620	19.6
0.075	0.455	0.614	6.06	2.750	0.620	36.7
0.050	0.300	0.620	6.00	5.150	0.620	103
0.025	0.148	0.628	5.92	3.800	0.624	152
0.020	0.117	0.630	5.90	3.100	0.630	155
0.010	0.060	0.636	6.00	1.610	0.630	161
0.0050	0.027	0.646	5.40	0.810	0.622	162
0.0025				0.435	0.626	174
0.0010				0.175	0.638	175
0.0005				0.0085	0.638	170

was performed to determine the number of electrons involved in the overall electron-transfer reaction. The experiments were performed in the absence of air in a small electrolysis cell with a mercury pool as the cathode. The potential of the working electrode was controlled at −0.75 V. The reduction of 2.265×10^{-5} mol of folic acid required 4.20 coulombs, which yields the value $n = 1.92$ and clearly demonstrates that 2 electrons are involved in the overall reaction. The shift in half-wave potentials (−65 mV per pH unit) indicates that two hydrogen ions are consumed in the electrode reaction.

Cyclic voltammetric experiments were performed at a hanging mercury drop electrode. Reproducible waves were obtained provided that the mercury drop was changed between each potential sweep. Voltammograms recorded from acetate buffer pH 5.5 exhibited cathodic peaks at potentials corresponding to the d.c. polarographic steps and a third peak at more negative potentials (Fig. 2). A small anodic peak resulting from re-oxidation of the reduction

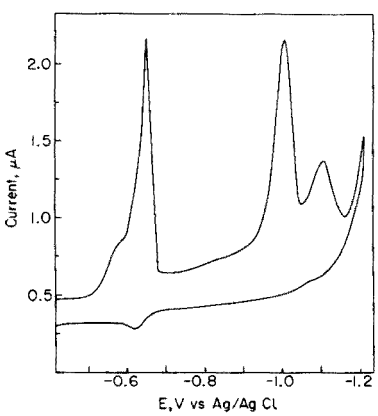

Fig. 2. Cyclic voltammogram of 0.02 mM folic acid in 0.1 M acetate buffer pH 5.5. Scan rate 0.1 V s^{-1}.

product of the first cathodic wave, indicates a reversible step in the overall electrode reaction. The cathodic peaks showed an increase in symmetry with increased scan rate and decreased bulk concentration of folic acid. Moreover, the current function $i_p/C\nu^{\frac{1}{2}}$ increased with increasing scan rate and decreasing concentration of the depolarizer. This is a characteristic feature of surface-active depolarizers [14] and implies that the drug is strongly adsorbed at the electrode surface.

The polarographic and voltammetric data given above indicate that the first wave is due to reduction of the C=N group to 7,8-dihydrofolic acid, as has been suggested by Asahi [11].

Analytical applications

It is evident from the data given above that a.c. polarography is a very sensitive method for the determination of folic acid. A polarographic method for the determination of folic acid in tablets containing large amounts of iron salts was therefore studied. The folic acid content in some tablets is only 30 μg. Hence, the polarographic peak from a single tablet will be very small and the precision of the method rather poor. Consequently, a Metrohm Polarecord E506 phase-sensitive a.c. polarograph was used. The sensitivity of the method is increased about 20 times by using phase-sensitive a.c. polarography, and concentrations of folic acid down to a few ng per ml can easily be determined. The calibration graph is linear in the concentration range 2×10^{-8}—2×10^{-6} M.

Most folic acid tablets contain large amounts of iron salts. Hence, in order to prevent precipitation of hydrated iron oxide and possible coprecipitation of folic acid, a strong complexing agent for iron must be incorporated in the supporting electrolyte. Diethylenetriaminepentaacetic acid (DTPA) proved to be very useful even at pH 5.5. Because folic acid is more soluble in alkaline media, it is preferable to dissolve the tablet in a DTPA solution at pH 8 before adding the supporting electrolyte with pH 5.5.

These experiments led to the procedure outlined in the Experimental part.

A polarogram of a "Foli-fer" tablet is given in Fig. 3. It is interesting to

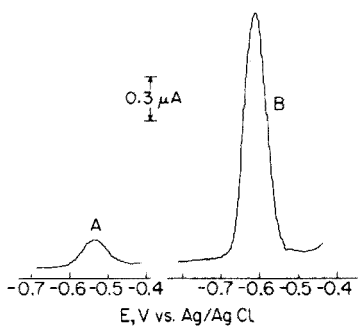

Fig. 3. Differential pulse (curve A) and phase-sensitive a.c. (curve B) polarograms of a "Foli-fer" tablet in 0.1 M acetate/0.03 M DTPA buffer at pH 5.5. The declared amount of folic acid is 34 μg and that of iron(II) fumerate is 115 mg.

note that a differential pulse polarogram of the same solution recorded with the same settings on the apparatus gives a peak which is only about 1/10 of the a.c. peak. Obviously, phase-sensitive a.c. polarography is by far the most sensitive polarographic method for the determination of folic acid.

A.c. polarographic waves are often distorted by the presence of even small amounts of surfactants and a decrease in peak height or even a complete inhibition of the electrode reaction may occur [15]. The a.c. polarographic wave of folic acid was found to be distorted by the presence of carbowax (polyethylene glycol), and the peak height decreased in the presence of some other surfactants like methylcellulose. Consequently, if the tablets contain surfactants (the amount of which may vary from one tablet to another) the most reliable results are obtained by the standard addition method.

The results of a few determinations of folic acid in "Foli-fer" tablets and "Pregnifer" tablets by the recommended procedure are given in Table 2.

The proposed method is very simple and gives satisfactory accuracy for the determination of folic acid in tablets. Moreover, because the removal of insoluble matter and the separation from iron salts are unnecessary, the present method is also much faster than previous methods.

TABLE 2

Phase-sensitive a.c. polarographic determination of folic acid in "Foli-fer" and "Pregnifer" tablets; all data obtained by the standard addition method

Foli-fer tablets[a]		Pregnifer tablets[b]	
Tablet no.	Folic acid found (μg)	Tablet no.	Folic acid found (μg)
1	33.3	1	63.6
2	36.1	2	63.0
3	34.4	3	60.4
4	35.4	4	63.0
5	34.4	5	59.6
6	35.0	6	60.7
7	33.9	7	62.0
8	35.8	8	59.1
9	35.0	9	59.8
10	33.9	10	65.5
	Mean 34.7		Mean 61.6

[a]Declared amount of folic acid 30 μg + 12% excess = 34 μg and 115 mg of iron(II) fumerate.
[b]Declared amount of folic acid 60 μg + 5% excess = 63 μg and 200 mg of iron(II) sulphate.

The authors wish to thank cand.pharm. B. Nielsen, Weiders Farmasøytiske A/S, Oslo and cand.real. T. Jacobsen, Nyegaard and Co. A/S, Oslo, for valuable discussions and for supplying the drugs and tablets used.

REFERENCES

1 V. Allfrey, L. J. Teply, C. Greffen and C. G. King, J. Biol. Chem., 178 (1949) 465.
2 L. J. Teply and C. A. Elvehjem, J. Biol. Chem., 157 (1945) 303.
3 The United States Pharmacopeia, XVIIIth Revision, Mack Publ. Co., Easton, Pa., 1970, p. 270.
4 S. K. Ganguly and H. Bhattacharya, Indian J. Pharm., 18 (1956) 361.
5 E. Häberli, E. Béguin and G. Schenk, Z. Anal. Chem., 155 (1957) 415.
6 R. C. Shah, S. B. Gandhi and V. S. Kanetkar, Indian J. Pharm., 20 (1958) 180.
7 G. Kanjilal, S. N. Mahjan and G. Ramana Rao, Analyst, 100 (1975) 19.
8 W. J. Mader and H. A. Frediani, Anal. Chem., 20 (1948) 1199.
9 M. Brezina and P. Zuman, Polarography in Medicine, Biochemistry and Pharmacy, Interscience, New York, 1958, p. 394.
10 A. H. I. Ben-Bassat, G. Frydman-Kupfer and M. Ben-Bassat, in "Polarography 1964", vol. 2, Macmillan, London, p. 993.
11 Y. Asahi, Rev. Polarog. (Japan), 8 (1960) 1; 11 (1963) 176.
12 I. E. Kruze, Farmatsiya (Moscow), 18 (1969) 59. C. A. 71 (1969) 116574 k.
13 A. D. Goolsby and D. T. Sawyer, Anal. Chem., 39 (1967) 411.
14 R. H. Wopschall and I. Shain, Anal. Chem., 39 (1967) 1514.
15 N. Gundersen and E. Jacobsen, Anal. Chim. Acta, 45 (1969) 346; J. Electroanal. Chem. Interfacial Electrochem., 20 (1969) 13.

Analytica Chimica Acta, 96 (1978) 353—358

POLAROGRAPHIC MAXIMA IN THE COBALT—8-HYDROXYQUINOLINE SYSTEM

SUDARSHAN LAL*

The Thomas Hunt Morgan Institute of Genetics, 628 North Broadway, Lexington, Kentucky 40508 (U.S.A.)

P. S. JAIN

J.K. Synthetic Works, Kota (Rajasthan) (India)

(Received 15th April 1977)

SUMMARY

The behavior of the polarographic maximum of the cobalt—8-hydroxyquinoline system in ammonia—ammonium chloride buffer has been studied with regard to general morphology, effect of mercury flow rates, current—time curves and streaming patterns under carefully controlled conditions. The maximum appears to be an adsorption-controlled catalytic maximum. Current—time curves and streaming observations provide useful information in its characterization. Difficulties in distinguishing the first-kind negative maxima from catalytic maxima are discussed.

Streaming polarographic maxima [1] are commonly caused either by an uneven polarization of the mercury drop (first kind) or by a rapid flow of mercury from the glass capillary (second kind). First-kind maxima appear on both the positive and negative sides of the electrocapillary zero, the solution streaming downwards and upwards, respectively, whereas maxima of the second kind appear over a wide potential range and always exhibit upward streaming. The behavior of a few typical systems of each kind has been studied in detail by Lal, Bauer and co-workers [2—6]. In addition to these maxima, other types such as maxima of the third kind [7], adsorption maxima, catalytic maxima and maxima on anodic waves have also been mentioned in the literature [8]. Schwaer and Suchy [9], and Hans and Stackelberg [10] reported an unusual and uncharacterized maximum at −1.29 V in the reduction wave of tellurite to tellurium in an ammoniacal buffer solution.

It is necessary to study systems with maxima under stringently controlled conditions such as mercury flow-rate, solution purity, and three-electrode circuitry in order to unravel their true behavior. Ivanov [11] has published a sketchy report on the cobalt wave in the presence of 8-hydroxyquinoline (HQ). These studies were conducted at fairly high mercury flow-rate (3.65 mg s^{-1}) in solutions of unknown purity, conditions that are conducive to the appearance of a second-kind maximum. Hence, the cobalt—8-hydroxyquinoline system has been re-investigated systematically

*Present address: Halen Research and Development Corp., 33 Industrial Ave., Little Ferry, N.J. 07643 (U.S.A.).

to study the characteristics of the maximum: the streaming patterns, dependence on concentration of 8-HQ and on mercury flow-rate, and current—time curves.

It has been found that cobalt(II) in the presence of 8-hydroxyquinoline in ammoniacal buffer yields three polarographic steps, the first step corresponding to the uncomplexed cobalt, the second to the cobalt complex, and the third, presumably, to an adsorption-initiated catalytic maximum.

EXPERIMENTAL

Current—voltage curves of cobalt in ammonia—ammonium chloride buffer pH 9.4 were recorded with a Princeton Applied Research Electrochemistry System Model 170, in the three-electrode mode. The current—time curves were monitored with a 502 Tektronix oscilloscope attached to a C-12 camera. The capillary constant of the d.m.e. was 2.25 $mg^{2/3}\ s^{-\frac{1}{2}}$ in open circuit. Deaeration was accomplished by a steady flow of Linde prepurified nitrogen, passed through chromium(II) sulfate and presaturated with the vapors of a solution of the same composition as that used in the polarographic cell. All measurements were made at 25 ± 0.1°C. Streaming of the solutions was observed with a stereo-microscope (Anchor Optical Co. magnification 4—10×) in the presence of suspended particles of charcoal (Norit A. Fisher, Sci. Co.). All chemicals used were A.R. grade and an ethanolic solution of 8-hydroxyquinoline was used.

RESULTS AND DISCUSSION

Nature of the polarographic wave and effect of 8-hydroxyquinoline

Cobalt(II) (4×10^{-3} M) in 0.2 M ammonia—ammonium chloride gave a sharp acute negative maximum (Fig. 1A) with upward streaming at low flow rate (<1 mg s^{-1}). In the presence of low concentrations of 8-HQ, the d.c. polarogram showed a mixture of three steps (Fig. 1B). The first maximum appeared at −1.25 V, a diffuse wave appeared at about −1.40 V to −1.50 V, and the second maximum at −1.59 V. The shapes of these maxima were different, the first being a typical spiked negative maximum of cobalt and the other being due presumably to catalytic or adsorptive activity of the cobalt complex. The first two steps were drawn out, showing irreversible character, and the third showed a maximum.

The presence of three steps was also confirmed by derivative pulse polarography with peaks at −1.145 V, −1.305 V and −1.53 V, respectively. Cyclic voltammetry also indicated the presence of three steps. Anodic sweep gave only one peak corresponding to the oxidation of cobalt whereas the cathodic sweep showed three distinct peaks. The absence of two peaks in the anodic sweep gives evidence for the adsorption process and irreversibility.

With increasing concentrations of 8-HQ, the first cobalt maximum was suppressed considerably, disappearing at a concentration of 5×10^{-4} M.

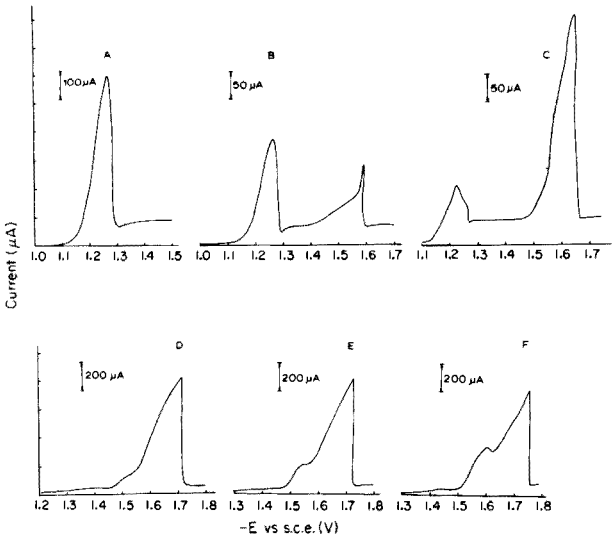

Fig. 1. Current—voltage plots of 4×10^{-3} M Co(II) in 0.2 M NH_3—NH_4Cl in pure solutions at varying concentrations of 8-hydroxyquinoline: (A) 0 (B) 10^{-5} M (C) 5×10^{-5} M (D) 5×10^{-4} M (E) 10^{-3} M (F) 2×10^{-3} M.

The present studies have been focussed mainly on the second maximum in the potential range −1.5 V to −1.7 V. This maximum increased in height with increasing concentration of 8-HQ and appeared to split into two steps at 5×10^{-4} M (Fig. 1D). The maximum of the third step showed the concentration-dependence typical of catalytic currents: the maximum increased linearly with increasing concentration of 8-hydroxyquinoline, reached a limiting value and finally decreased with further increase in 8-HQ concentration at a given concentration of cobalt.

Effect of mercury height on second maximum

The variation of peak height with changing mercury height is presented in Table 1. The plot of i_{max} vs. h was linear with two segments, each corresponding to high and low flow rates, respectively; the i_{max} vs. $h^{1/2}$ plot was a typical curve characteristic of an adsorption or catalytic process [12].

TABLE 1

10^{-5} M 8-hydroxyquinoline with 4×10^{-3} M Co(II) in ammonia buffer

h (cm)	m (mg s^{-1})	Second maximum	
		i_{max} (μA)	$-E_{max}$ (V)
110.6	4.73	135	1.600
90.6	3.95	130	1.585
60.6	2.65	125	1.580
40.6	1.81	102	1.565
30.6	1.40	95	1.550
20.6	0.98	90	1.535

The maximum shifted to less cathodic potentials with decrease in mercury flow rate.

Current—time behavior

Sporadic attempts to employ i—t curves in describing maximum formation at the d.m.e. have been described [13—20]. Recently, Lal [21] reported in detail the behavior of i—t patterns under varying conditions favorable for maximum formation for nitrobenzene. A detailed analysis of i—t plots obtained with a d.m.e. can provide useful information about the processes occurring at the electrode.

Values of the exponent α in the relationship $i = kt^{\alpha}$ were determined (Table 2); i—t curves are depicted in Fig. 2. The curves at —1.25 V and —1.53 V show humps which indicate an adsorption process and are analogous to the curves obtained when surfactants influence a faradaic process [22]. The current increases early in the drop-life because of upward swirling, followed by adsorption in the later part of the drop-life which lowers the current. When swirling starts to subside, excessive current caused by convection decreases, and the current tends to become diffusion-controlled. In the earlier parts of the drop-life, α values are about 0.4 which is slightly higher than the exponents obtained for adsorption (0.33). The exponents appear to be potential-dependent; at potentials of —1.49 V and —1.53 V, values

TABLE 2

Values of α obtained in the 3-electrode mode from i—t curves for 4×10^{-3} M cobalt and 5×10^{-5} M 8-HQ in ammonia buffer pH = 9.4 at the indicated potentials

Potential (V vs. s.c.e.)	α values at varying intervals in drop-life
—1.20	0.42 (0.5 s), 0.25 (~2.3 s)
—1.25	0.38 (0.5 s), 0.23 (~2.0 s)
—1.30	0.40 (0.5 s), 0.18 (~2.0 s)
—1.49	0.60 (0.2 s), 0.20 (>0.5 s)
—1.53	0.25 (0.6 s), 1.4 (~1.0 s), 0.25 (>1.5 s)
—1.70	0.41 (0.6 s), 0.3 (~1.8 s)

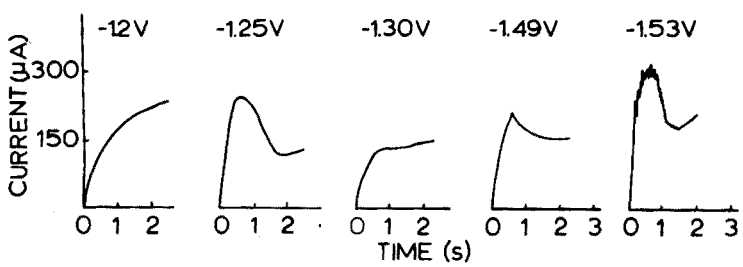

Fig. 2. Current—time curves for 4×10^{-3} M Co(II) in 0.2 M NH_3—NH_4Cl and 5×10^{-5} M 8-hydroxyquinoline (m = 2.60 mg s^{-1}) at the indicated potentials.

of 0.6 and 1.4 are obtained, respectively, which suggest the possibility of catalytic currents preceded by adsorption. It appears that adsorption of the cobalt complex triggers streaming, which consequently transports more depolarizer to the electrode. The uneven electrode coverage could possibly cause differences in interfacial tension at the neck and bottom of the drop, and produce streaming similar to first-kind maxima. The maximum, however, was suppressed by Triton X-100, which was probably due to displacement of the complex from the interface by the more adsorptive surfactant. Deformation of the electrocapillary curve was also noticed, which suggests adsorption in that potential range. The incisions and fluctuations in some i—t curves are probably due to turbulent streaming in solution.

Streaming patterns

At low flow rate (0.98 mg s^{-1}), at the foot of the wave, an upward motion was noticed which developed into a strong upward motion with vortices at a potential of —1.25 V. This upward motion subsided after the region of the cobalt maximum until at —1.55 V, a moderate upward motion was observed which was due to the presence of the cobalt complex.

At a moderate flow rate (2.65 mg s^{-1}), upward streaming initiated from the foot of the first step which intensified at —1.25 V and seemed to be a function of drop growth, achieving its fullest extent at the maturity of the drop size, until the whole motion ceased some moments before the fall of the drop. Some motion appeared to originate from the sides and then moved upward tangentially towards the periphery of the drop. Pulsation of the drop was also observed. The motion subsided in the vicinity of —1.4 V and again initiated at —1.50 V which developed into a vigorous upward motion around —1.6 V. The pattern and nature of the streaming were similar to a negative maximum of the first kind. However, it seems difficult to differentiate the catalytic maximum from a first-kind maximum which requires a clearly defined system producing such effects. The data on variations with mercury flow-rate and dependence on HQ concentration, lend support to the suggestion of an adsorption-controlled catalytic maximum. The laminar upward streaming did not stop at higher negative potentials greater than —1.60 V. The motion appeared to be violent and qualitatively stronger than that for a negative maximum. This streaming was not only directed to the neck of the drop, but also towards different places on the drop with some irregular whirls. Distinction between negative maxima of the first kind and catalytic maxima may be achieved by determining the streaming velocities in well defined systems, but this remains to be done.

The authors are grateful to Prof. Henry Bauer for helpful discussions and facilities, and to Mr. V. B. Dixit for technical assistance.

REFERENCES

1 H. H. Bauer in A. J. Bard (Ed.), Electroanalytical Chemistry, Vol. VIII, M. Dekker, New York, p. 169.
2 S. Lal and H. H. Bauer, Anal. Lett., 9 (1976) 13.
3 S. Lal and H. H. Bauer, J. Electroanal. Chem., 51 (1974) 319.
4 S. Lal, T. W. Holt and H. H. Bauer, J. Electroanal. Chem., 42 (1973) 429.
5 S. Lal, A. Kumar and H. H. Bauer, J. Electroanal. Chem., 42 (1973) 423.
6 F. M. Hawkridge, T. W. Holt and H. H. Bauer, Anal. Chim. Acta, 58 (1972) 203.
7 A. N. Frumkin, E. V. Stenina and N. V. Fedorovich, Sov. Electrochem., 6 (1970) 1516.
8 J. Heyrovsky and J. Kuta, Principals of Polarography, Academic, New York, 1966, pp. 430, 458.
9 L. Schwaer and K. Suchy, Collect. Czech. Chem. Commun., 7 (1935) 25.
10 W. Hans and M. v. Stackelberg, J. Elektrochem., 54 (1950) 62, 65.
11 I. D. Ivanov, Russ. J. Phys. Chem., 34 (1960) 1187.
12 J. Heyrovsky and P. Zuman, Practical Polarography, Academic, New York, 1968, p. 33.
13 D. Ilkovič, Collect. Czech. Chem. Commun., 8 (1936) 13.
14 T. A. Kryukova, Zh. Fiz. Khim., 21 (1947) 365.
15 A. B. Ershler, D. I. Dzhazaridze and G. A. Tedoradze, Russ. J. Phys. Chem., 37 (1963) 344.
16 H. J. Antweiler, Z. Elektrochem., 44 (1938) 888.
17 R. Brdicka, Collect. Czech. Chem. Commun., 8 (1936) 419.
18 E. Verdier and M. Bourdin, J. Chim. Physicochim. Biol., 65 (1968) 1375.
19 T. A. Kryukova, Zavod. Lab., 9 (1940) 691; 14 (1948) 511.
20 K. Micka, Collect. Czech. Chem. Commun., 21 (1956) 940.
21 S. Lal, Z. Naturforsch. Teil B., 31 (1976) 51.
22 R. W. Schmid and C. N. Reilly, J. Am. Chem. Soc., 80 (1958) 2087.
23 M. v. Stackelberg and H. Fassbender, Z. Elektrochem., 62 (1958) 834.

Analytica Chimica Acta, 96 (1978) 359—365

PYROLYSIS-GAS CHROMATOGRAPHY OF BUTADIENE CO-POLYMERS

TATSUHISA SHIMONO, MINORU TANAKA and TOSHIYUKI SHONO*

Department of Applied Chemistry, Faculty of Engineering, Osaka University, Yamada-kami, Suita, Osaka 565 (Japan)

(Received 17th August 1977)

SUMMARY

Pyrolysis-gas chromatographic investigations have been carried out on five kinds of butadiene (BD) co-polymers with a Curie-point pyrolyzer. In the pyrolysates, the yield of vinylcyclohexene (VCH) formed from successive BD units in the co-polymer shows the different sequential structures of these co-polymers. Assuming that the probability of the BD unit in the center of each triad degrading to products other than BD and VCH is constant, the VCH/BD molar ratio, Q, is related to the run number, R, and the BD mole%, X, in the equation $Q = [k_1(X - R/2)^2 + k_2R(X - R/2)]/[(1 - k_1)(X - R/2)^2 + (1 - k_2)R(X - R/2) + R^2/4]$. The run number of each co-polymer is then calculated by means of Q and X obtained from the pyrogram.

With progress in polymerization techniques, many polymers having controlled sequential structures have been produced. Some of these polymers have specific properties resulting from their unique microstructures. Typical examples are the alternating vinyl co-polymers. The alternating isobutylene—alkyl acrylate co-polymer is superior to acrylic rubbers in its resistance to hydrolysis and heat [1]. Further, the alternating styrene—acrylonitrile co-polymer has a high softening point and excellent mechanical properties compared with the random co-polymers [2]. It is therefore important to investigate the microstructures of polymers. Pyrolysis-gas chromatography (p.g.c.) is one of the most powerful methods for the investigation of microstructures; p.g.c. has been applied successfully to the analysis of chain branching in polyethylene or poly(vinyl chloride) and shown to be an effective method of determining the short-chain branch content [3, 4].

The pyrolysis-gas chromatographic behaviours of polybutadienes [5] and butadiene—acrylonitrile [6] co-polymers have been reported. In this work, the relationships between the pyrolysis products and the microstructures for butadiene co-polymers (co-monomer = acrylonitrile, methacrylonitrile, methyl methacrylate, methyl acrylate, and methyl vinyl ketone) were investigated by p.g.c. and the run number of each co-polymer was evaluated.

EXPERIMENTAL

Materials

Alternating co-polymers of butadiene (BD) with methyl methacrylate (MMA) [7], methyl vinyl ketone (MVK) [8], methyl acrylate (MA) [9], methacrylonitrile (MAN) [10], and acrylonitrile (AN) [10] were synthesized by complexed co-polymerization with Lewis acids. Random co-polymers with different composition were prepared in low yield by radical polymerization with azobisisobutyronitrile as initiator.

Table 1 shows the co-polymer compositions calculated from elemental analysis.

Apparatus

A Curie-point pyrolyzer (Nippon Bunseki Kogyo JHP-2) was coupled directly to a gas chromatograph (Shimazu GC-4BM) equipped with a dual flame-ionization detector. Samples of 30—60 μg and a stainless steel column (2 m × 3 mm i.d.) packed with 20% DOP on 60-80 mesh Celite 545 support were used. The column temperature was 80°C. The flow rate of nitrogen was 40 ml min^{-1}; the hydrogen and air pressures were 0.5 kg cm^{-2} and 1.0 kg cm^{-2}, respectively. A column (5 cm × 3 mm i.d.) packed with a mixture of K_2CO_3 and Diasolid H (60-80 mesh, 1 + 2, w/w) was placed between the pyrolyzer and the separation column to precut acidic products from nitrile co-polymers.

The peak areas were measured by a digital integrator (Shimazu ITG-4A). Identification of the peaks was carried out by comparison with the retention data of known substances.

TABLE 1

Composition of BD co-polymers
(A: alternating co-polymer, R: random co-polymer.)

Co-polymer	Co-monomer of BD (mole %)				
	MMA—BD	MVK—BD	MA—BD	MAN—BD	AN—BD
A	50.1	53.6	53.0	48.6	50.5
R_1	5.8	17.8	19.4	26.6	28.0
R_2	19.3	43.7	24.1	33.0	37.3
R_3	28.2	51.0	47.2	37.5	42.2
R_4	30.4	51.5	57.1	41.3	47.3
R_5	54.8	67.7	61.3	41.4	56.0
R_6	80.6	92.3		47.6	59.4
R_7				70.0	
R_8				71.2	

RESULTS AND DISCUSSION

The BD monomer and the cyclic BD dimer, 4-vinylcyclohexene (VCH), obtained from successive 1,4-BD units are well known as the main pyrolysis products of polybutadienes; the BD units are mostly linked 1,4 in polybutadienes prepared by conventional radical polymerization. The relationship between the pyrolysis products (mainly VCH, BD, and co-monomer of BD) and the monomer sequence distribution in some co-polymers is reported in this paper.

Pyrogram and composition

Figure 1 shows the pyrograms of MMA—BD co-polymers at the pyrolysis temperature of 590°C. Under the p.g.c. conditions used, lower hydrocarbons, BD, MMA, and VCH were the main pyrolysis products. There is a difference between the pyrograms of alternating and random co-polymers; the VCH peak is barely detectable in the pyrogram of the alternating co-polymer. Most of the MMA units in MMA—BD co-polymers pyrolyze into MMA monomer as in poly(methyl methacrylate). The yield of MMA at 590°C was plotted against the MMA content of the co-polymer, where the yield is taken as the MMA mole fraction in the pyrolysis products, i.e., MMA/(MMA + BD + 2VCH) as one mole of VCH corresponds to two moles of BD. A very good linear relationship was obtained; this MMA yield therefore indicates the composition of MMA—BD co-polymers, including the alternating one. From least-squares regression analysis, the regression line of the MMA content of co-polymer (y) on the MMA yield described above (x) was $y = 1.06x - 9.93$, and the error variance (V_{yx}) was 7.02.

The pyrolysis-gas chromatographic behaviour of MAN—BD and MMA—BD co-polymers are closely similar. The yield of MAN, MAN/(MAN + BD + 2VCH), indicated the composition of the co-polymers. In MVK—BD co-polymers, a small quantity of acetone was formed in addition to lower hydrocarbons, BD, MVK, and VCH.

Polyacrylonitrile exhibits complicated pyrolytic reactions, i.e., elimination of hydrogen cyanide or cyclization involving the C≡N group. Large quantities

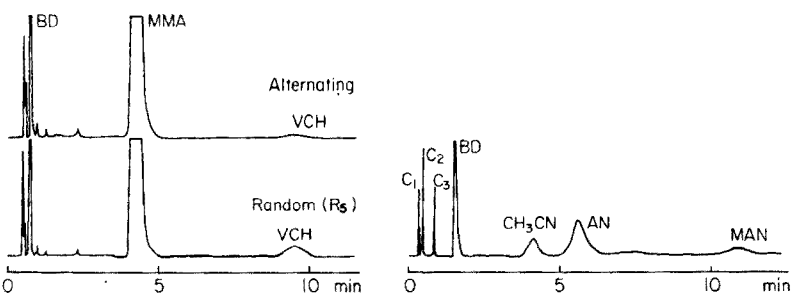

Fig. 1. Pyrograms of MMA—BD co-polymer at 590°C.

Fig. 2. Pyrogram of alternating AN—BD co-polymer with Porapak N column.

of both acetonitrile and lower hydrocarbons and quantities of the monomers were formed on the pyrolysis of AN—BD co-polymers. Figure 2 shows the pyrogram of the alternating AN—BD co-polymer at 590°C. Porapak N was used as a column packing, because the separation of AN from acetonitrile was impossible with the DOP column. The mole fraction (AN + acetonitrile)/(AN + acetonitrile + BD + 2VCH) in the degradation products indicated the composition of these AN—BD co-polymers.

MA—BD co-polymers gave the monomers, and also a great deal of methanol from scission of the side-chain. This phenomenon is especially notable at the low pyrolysis temperature. Figure 3 gives the pyrograms of the alternating MA—BD co-polymer pyrolyzed at 590 and 710°C. The production of methanol decreased greatly at 710°C; the yield MA/(MA + BD + 2VCH) at 710°C indicated the composition of both the alternating and the random MA—BD co-polymers.

Table 2 shows the results of regression analysis for five BD co-polymers, where y is a co-monomer content of BD co-polymer and x is a co-monomer yield on pyrolysis. It is reasonable that the MA—BD co-polymer, with the high tendency to undergo side-chain scission, has the large error variance, V_{yx}.

VCH/BD molar ratio and run number

Figure 4 shows the VCH/BD molar ratio in the degradation products of each MMA—BD co-polymer pyrolyzed at 386, 590, and 710°C. The other four BD co-polymers also gave the same tendency as the MMA—BD co-polymer. The VCH/BD molar ratio changes with the pyrolysis temperature and the co-polymer composition in the case of random co-polymers. The fact that in the case of the alternating co-polymers the values of the VCH/BD

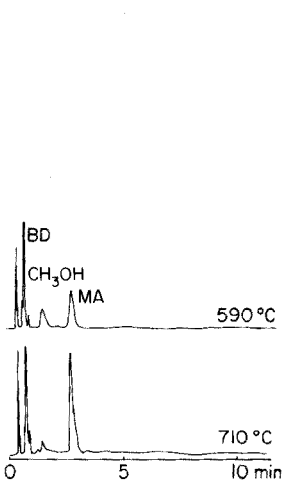

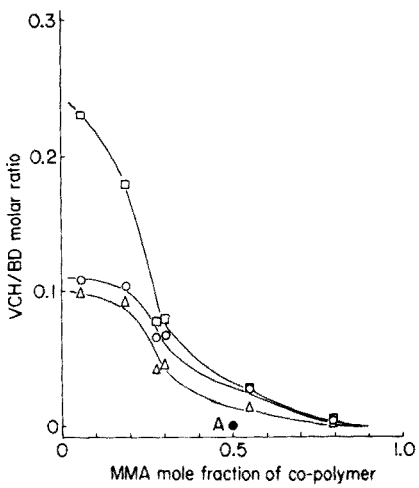

Fig. 3. Pyrograms of alternating MA—BD co-polymer at 590 and 710°C.

Fig. 4. VCH/BD molar ratio of MMA—BD co-polymers. □ 386°C; ○ 590°C; △ 710°C.

TABLE 2

Regression analysis for co-monomer-content (y) and -yield (x) at the pyrolysis temperature of 590°C

Co-polymer	a[a]	b[a]	V_{yx}
MMA—BD	1.06	−9.93	7.02
MVK—BD	1.19	3.87	10.3
MA—BD[b]	0.875	0.83	18.4
MAN—BD	0.862	−0.44	2.09
AN—BD	1.11	2.88	0.968

[a] $y = ax + b$. [b] Pyrolyzed at 710°C.

molar ratio are nearly zero may be interpreted as follows. The pyrolysis temperature dependence of the VCH/BD molar ratio results from the number of sites where a random chain scission occurs. The number of random chain scissions increases with increase in pyrolysis temperature. Consequently, the higher the pyrolysis temperature, the smaller the probability of VCH production. The dependence on the co-polymer composition is a result of the difference in BD sequence distribution. Because the number of successive BD units decreases with decreased BD content in the random co-polymer, the lower the BD content, the smaller the probability of VCH production. The alternating co-polymer contains only BD-co-monomer units in its chain, and has a VCH/BD ratio of nearly zero.

The relationship between this VCH/BD molar ratio and the BD sequence distribution was further investigated. Let P_{BBB}, P_{BBM}, P_{MBB}, and P_{MBM} represent the probabilities of a BD unit in the center of triads BD—BD—BD, BD—BD—M, M—BD—BD, and M—BD—M, respectively, where M is a co-monomer. If the probability of the BD unit in the center of each triad degrading to products other than BD and VCH is constant, and if the BD units in the center of BD—BD—BD, BD—BD—M, and M—BD—BD triads degrade to VCH and BD in the ratio $k_1/(1-k_1)$, $k_2/(1-k_2)$, and $k_2/(1-k_2)$, respectively, the VCH/BD molar ratio, Q, can be given as

$$Q = [k_1 P_{BBB} + k_2(P_{BBM} + P_{MBB})] / [(1-k_1)P_{BBB} + (1-k_2)(P_{BBM} + P_{MBB}) + P_{MBM}] \quad (1)$$

In this equation, each P value is calculated from the monomer reactivity ratios shown in Table 3 and the monomer feed ratio [11], and Q is estimated from the pyrograms. The values of k_1 and k_2 can therefore be calculated. For the pyrolysis of MMA—BD co-polymers at 590°C, the calculated Q values when $k_1 = 0.11$ and $k_2 = 0.067$ in eqn. (1) agreed very well with the Q values obtained from the pyrograms; the correlation coefficient was 0.997. Table 3 gives the values of k_1 and k_2 for five BD co-polymers. All the k_1 values are nearly 0.1, as is k_1 for polybutadiene obtained by conventional radical polymerization. The value of k_2 decreases in the order MMA—BD >

MAN—BD > AN—BD > MVK—BD > MA—BD; this order may result from the stability of the radical produced after chain scission at position (1) shown below.

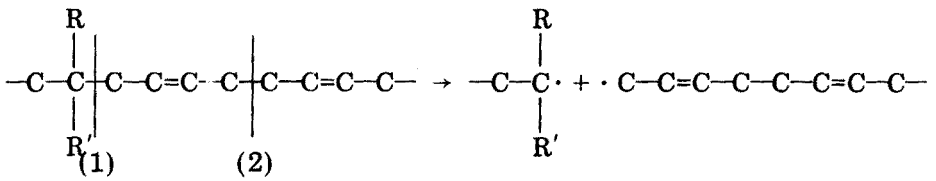

where R = CH_3, H, and R′ = —C≡N, —C(=O)—O—CH_3, or —C(=O)—CH_3.

The tertiary radical is produced in the cases of MMA— and MAN—BD co-polymers (R = CH_3) and the secondary radical in the other three co-polymers (R = H). Therefore, the scission at this position is easier in the former and the k_2 values (the probability of the dimer formation) become larger than in the latter.

The run number is a parameter [12] for characterizing sequence distribution in co-polymers. The run number is 1 for a homopolymer and 100 for a completely alternating co-polymer; eqn. (1) can be rewritten as

$$Q = \frac{k_1(X - R/2)^2 + k_2R(X - R/2)}{(1 - k_1)(X - R/2)^2 + (1 - k_2)R(X - R/2) + R^2/4} \qquad (2)$$

where R = run number, and X = BD mole%. When the values of k_1 and k_2 are known in eqn. (2), the run number of a BD co-polymer can be calculated by using the values of Q and X obtained from the pyrogram. The run numbers of five BD co-polymers are shown in Table 4. Each alternating co-polymer has an R value near 100 and the alternating sequential structure of each is confirmed; the difference between the alternating co-polymer and the random one with the composition of ca. 50 mole% is obvious.

As described above, the VCH/BD molar ratio in the pyrolysis products of BD co-polymers indicates the sequence distribution of co-polymers, and the run number can be determined from it; the run numbers obtained were reasonable for the co-polymers studied.

TABLE 3

k_1 and k_2 values for BD co-polymers
(r is a monomer reactivity ratio)

Co-polymer	k_1	k_2	r_{BD}	r_M
MMA—BD	0.11	0.067	0.60	0.17
MVK—BD	0.10	0.012	0.30	0.14
MA—BD	0.12	0.0090	2.2	0.13
MAN—BD	0.092	0.028	0.50	0.20
AN—BD	0.11	0.013	0.51	0.072

TABLE 4

Run numbers of BD co-polymers

Co-polymer	MMA–BD	MVK–BD	MA–BD	MAN–BD	AN–BD
A	99	94	95	96	99
R_1	10	25	32	57	45
R_2	35	31	43	68	62
R_3	54	65	74	66	75
R_4	52	64	69	79	84
R_5	71	64	65	78	85
R_6	38	16		81	81
R_7				60	
R_8				58	

REFERENCES

1 M. Hirooka, K. Mashita, S. Imai and T. Kato, Paper No. 16, 103rd Meeting of Rubber Division, ACS, May 1973.
2 M. Hirooka and T. Kato, J. Polym. Sci., Polym. Lett. Ed., 12 (1974) 31.
3 M. Seeger and E. M. Barrall II, J. Polym. Sci., Polym. Chem. Ed., 13 (1975) 1515.
4 D. H. Ahlstrom and S. A. Liebman, J. Polym. Sci., Polym. Chem. Ed., 14 (1976) 2479.
5 T. Shono and K. Shinra, Anal. Chim. Acta, 56 (1971) 303.
6 T. Shono, M. Tanaka, K. Terashita and K. Shinra, Bunseki Kagaku, 21 (1972) 326.
7 J. Furukawa, E. Kobayashi and Y. Iseda, Bull. Inst. Chem. Res., Kyoto Univ., 47 (1969) 222.
8 S. Pasynkiewicz, T. Diem and A. Korol, Makromol. Chem., 137 (1970) 61.
9 J. R. Ebdon, J. Macromol. Sci. Chem., 8 (1974) 417.
10 W. Kuran, S. Pasynkiewicz, R. Nadir and B. Kowalewska, Makromol. Chem., 177 (1976) 1293.
11 K. Ito and Y. Yamashita, J. Polym. Sci., Part A, 3 (1965) 2165.
12 H. J. Harwood and W. M. Ritchey, J. Polym. Sci., Part B, 2 (1964) 601.

Analytica Chimica Acta, 96 (1978) 367—381

THE UPTAKE OF METAL IONS AND ORGANIC COMPONENTS BY CO-POLYOXAMIDES

SIDNEY SIGGIA*

Department of Chemistry, University of Massachusetts, Amherst, MA 01003 (U.S.A.)

ALLEN H. BEEBER and O. VOGL

Polymer Science and Engineering, University of Massachusetts, Amherst, MA 01003 (U.S.A.)

(Received 28th July 1977)

SUMMARY

The interaction of metal ions and of certain organic components in aqueous solution with water-insoluble co-polyoxamides was examined. Studies were performed with one-plate batch equilibrations and percentage uptake was determined spectrometrically. The metal ions investigated were Pb(II), Cu(II), Zn(II), Cd(II), Ni(II), Cr(III), Ag(I), Ca(II), and Li(I). Studies performed included variations of metal ion concentrations, pH, temperature, ionic strength, competitive uptake with other metal ions, degree of aromatic content of the resin, time, surface area, physical form of resin (whether particle or film), and comparison studies on uptake by sand particles. The results indicate the discovery of a resin whose mechanism of uptake can be converted from complexation at slightly acidic pH values to ion exchange at high base strengths or vice versa. Investigations into the uptake of aromatic acids and bases by co-polyoxamides have shown that percentage uptake is increased as the aromatic content of either the polymer or of the low-molecular-weight organic compounds is increased.

Several investigations indicate that many amides coordinate with metals through the oxygen atom [1]. However, there are some amides, notably diamides (I), in which the close proximity of the two amide groups changes the coordination behavior so that it is now through the nitrogen atom. Oxamides, malonamides, and their sulphur analogs are such compounds.

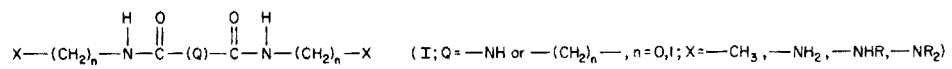

Many diamides have been known for some time. Few studies into their complexation behavior were carried out until 20 years ago.

Oxamide itself ($H_2NCOCONH_2$) can act as a bidentate ligand. It may coordinate through either or both the oxygen and nitrogen atoms depending on the solution environment. In non-aqueous solvents such as dichloromethane, 1:1 complexes may be formed between oxamide and $TiCl_4$, where the oxygens of the carbonyl group are the donor atoms. However, in the case of dithiooxamide the donor atoms appear to be the nitrogens. The reversal appears to be due to electronegativity and steric differences [1].

The complexes are weak since they are rapidly hydrolyzed in water, hence the use of non-aqueous solvents in many cases.

Replacing the amine hydrogens with alkyl groups leads to several changes. Working with *N,N'*-dimethyloxamide, Kruss and Ziegler [2] reported complexes with $SnCl_4$ involving N,O-bonding. This was later confirmed by Izakenaite et al. [3]. Desseyn et al. [4] found that with Hg(II), Pd(II) and Ag(I) in 50% alcoholic solutions there was metal-to-sulphur bonding when *N,N'*-monosubstituted dithiooxamides were employed. However, in Cu(II) and Ni(II) complexes the bonding was between the metal and nitrogen.

Good and Siddall [5] have studied the bonding of Cu(II) and Ni(II) with tetramethyleneoxamide (II) in nitromethane. They established that bonding

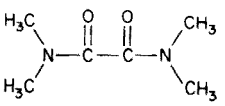

(II)

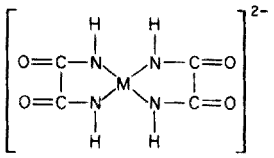

(III)

occurred through the carbonyl oxygens. Note that there are no hydrogens on the nitrogens. The malonamide analog showed stronger bonding, apparently because of the formation of a less-strained six-membered ring rather than a five-membered one. The effect is not as great with metal ions of larger ionic radii, such as Mn(II), Pb(II), and Cd(II). This appears to be due to better accommodation of the larger ions in the ring. Hart et al. [6] found that tetraethyldithiooxamide would coordinate with various divalent transition metals through the sulphur atoms in non-complexing solvents.

In highly polar, alkaline media, whether it be aqueous or in DMSO, the bonding is very different and much simpler. Several workers, notably Kuroda et al. [7], Armendarez and Nakamoto [8], and Bour and co-workers [9], have concluded that in highly alkaline aqueous solutions, the complex with Cu(II), Ni(II), and Pb(II) is a square planar diimido structure (III).

Investigations into dithiooxamide showed that in alkaline media it would react with divalent transition metals to form neutral, inner 1:1 complexes (IV), each nitrogen losing one hydrogen. This effect appears to be due to the lower electronegativity of sulphur atoms [6].

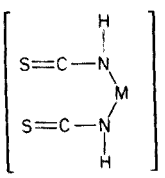

(IV)

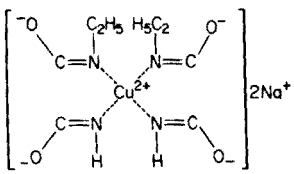

(V)

N,N'-diethyloxamide undergoes the biuret reaction to form a complex (V), whereas *N,N*-diethyloxamide (unsymmetrical) and *N,N,N'*-triethyloxamide show no reaction [10]. This shows that the diimido structure must be formed in order for there to be complexation through the nitrogens in aqueous media

Jacobs and Yoe [11] synthesized *N,N'*-bis(3-dimethylaminopropyl)dithiooxamide and found that it was a better chelating agent than the simple dithiooxamide. Zuberbuhler and Fallab [12] were the first of a number of investigators to study the chelating ability of diamine-diamides in depth. They began with the reaction of *N,N'*-diglycyl-1,2-diaminoethane (whose close analog, triethyltetraamine, was a well-known complexing agent) and higher homologs with $CuSO_4$ in alkaline solutions.

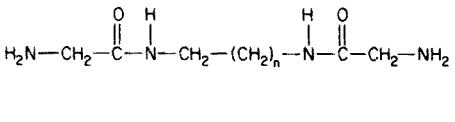

(VI; n=1-5)

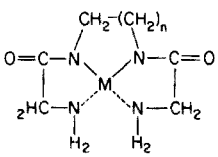

(VII; n=1-5)

These diamines-diamides (VII) formed 5-, 6-, 7-, 8-, and 9-membered rings between the two amide groups. There was no evidence of binuclear species.

Greisser and Fallab [13] worked with analogous diamides (VIII), except that the —CO—NH— order was reversed. Along with other investigators [14],

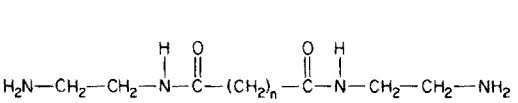

(VIII; n=1-3)

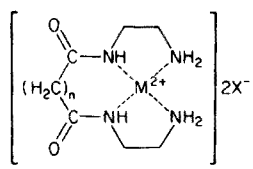

(IX)

they found that oxamide ($x = 0$) and malonamide ($x = 1$) compounds formed tridentate mononuclear chelates in slightly acidic media. The malonamide derivative (IX) exhibited greater stability. These compounds were more stable in alkaline media because the amide hydrogens were abstracted, resulting in a strong electron donor (X).

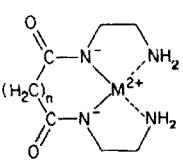

(X)

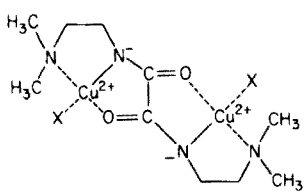

(XI; X=H_2O or OH^-)

If the concentration of Cu(II) ions was high, a bidentate dinuclear chelate (XI) was formed, as illustrated in the case of *N,N'*-bis(2-dimethylaminoethyl)oxamide shown above [15].

Several variations have been made by replacing the amino group with groups such as 2-pyridylmethyl [16—18], but otherwise there is little new in the literature regarding metal chelation or complexation by oxamides.

Wang and Bauman [19] measured the ionization constants of *N,N'*-bis(2-aminoethyl)oxamide in 1.0 M KNO_3 solution at 25°C and determined that pK_{a_1} = 8.30 and pK_{a_2} = 9.54 for the oxamide hydrogens.

There is only one report pertaining to organic complexation with oxamides. In studies with *o*-, *m*-, and *p*-nitrophenols with oxamide, *N,N'*-dimethyloxamide, and *N,N,N',N'*-tetramethyloxamide in aqueous systems, Tronov et al. [20] found that the stability of the complexes decreases with increasing number of methyl groups.

There have been very few reports in the literature regarding the complexation behavior of polyoxamides, and more specifically, of regular co-polyoxamides of the general formula XII, where R can be aliphatic, aromatic or heteroaromatic and n can vary from 0, 2, 3, 4, ... , 12, although indication of complexing behavior has been qualitatively obtained [21]. A large effort

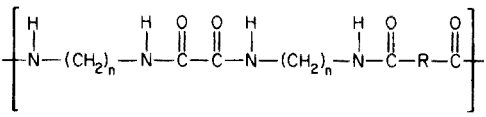

(XII)

has been made in these laboratories on the synthesis and characterization of co-polyoxamides [21—28]. Recent work by Mourey et al. [29] indicates that many polyamides have good potential for removing aromatic organics from aqueous solutions because of the many amide groups present and this provided an impetus to the present study.

The present study investigates the uptake of a number of alkaline and transition earth metals and several aromatic acids and bases from aqueous solutions by several water-insoluble co-polyoxamides.

EXPERIMENTAL

Resins

Altogether four different co-polyoxamides were used. The regular co-polyoxamide of m-2-2-2 and isophthaloyl chloride, designated p-2-2-2-I (see Table 1), was prepared by interfacial polymerization of the diamine-diamide *N,N'*-bis(2-aminoethyl)oxamide with isophthaloyl chloride. Similarly, p-2-2-2-*cis*-1,4 and p-2-2-2-*trans*-1,4 were prepared by interfacial polymerization of *N,N'*-bis(2-aminoethyl)oxamide with the respective acid chlorides. These regular co-polyoxamides were selected for their good mechanical strength and wetability. To prepare each polymer for the uptake studies, it was first ground to 60/80 mesh size. Each was then magnetically stirred in a large volume of distilled, deionized water for at least 6 h, first at pH 10.6 (NH_4OH), then at pH 1.4 (HCl), and finally in plain distilled, deionized water. After each washing step, the polymer was filtered through a coarse glass-sintered funnel and washed with large amounts of water. For the organic uptake studies, further washing with distilled, deionized water in a Soxhlet apparatus was necessary to lower the absorbance of a solution of

TABLE 1

Abbreviation nomenclature of co-polyoxamides of the general formula:

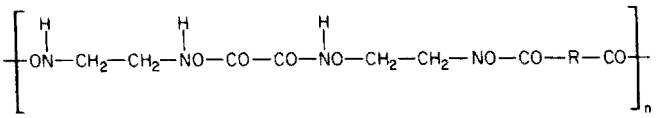

(XV)

Full name	Abbreviation
Poly(iminoethyleneiminooxalylimimoethyleneiminoisophthaloyl)	p-2-2-2-I
Poly(iminoethyleneiminooxalylimimoethyleneimimocarboxyl-2,6 naphthylene-carbonyl)	p-2-2-2-2,6N
Poly(iminoethyleneimimooxalylimimoethyleneimimocarbonyl-*cis*-1,4 cyclohexenecarbonyl)	p-2-2-2-*cis*-1,4
Poly(iminoethyleneimimooxalylimimoethyleneimimocarbonyl-*trans*-1,4-cyclohexylenecarbonyl)	p-2-2-2-*trans*-1,4

just polymer plus distilled water to below 0.1. The water was renewed every 12 h over a period of two days. Films of p-2-2-2-I were cast from 5—10% trifluoroacetylacetone solutions, dried for 1 min in the hood, and then gelled by quickly placing them in a tray filled with ice water. Each resin was then dried at 100°C overnight at 0.01-mm pressure before the equilibration studies were begun. This washing procedure caused little hydrolytic degradation.

Reagents

Lead, silver, chromium, nickel, copper, calcium, and zinc acetate and lithium chloride (Fisher Scientific Co.) and cadmium acetate (J. T. Baker Chemical Co.) were used as received. Other reagents used as received were: trichloromethylsilane (PCR Inc.); pyridine, aniline, sodium chloride, and glacial acetic acid (technical grade; Fisher Scientific Co.), phenol and sea sand (purified; J. T. Baker Chemical Co.) and β-naphthol (Eastman Kodak). Toluene (Fisher Scientific Co.) was dried over $CaCl_2$ before use. Acetic anhydride (Eastman Kodak) was distilled under nitrogen before use.

The metal stock solutions were prepared by weighing the appropriate amount of dried metal salt and dissolving it in a 1-l volumetric flask to yield an aqueous solution (distilled, deionized water) which contained 1000 mg l^{-1} (ppm) of the metal ion. The stock solutions were stored in polyethylene bottles. The lower concentrations used for the standards and test solutions were prepared fresh for each analysis by making appropriate dilutions with A-type glassware. A similar procedure was followed in preparing the organic solutions.

The silanization solution consisted of 10 parts toluene, 1 part trichloromethylsilane, and 0.4 parts pyridine. The test tubes used were filled with the solution and allowed to sit for 10 min. They were then emptied, washed with methanol, then distilled water, and dried before use.

Instrumentation

A double-beam Perkin-Elmer 403 atomic absorption spectrometer was employed for the metal analyses, for both absorption and emission. For the competition studies, lamps were chosen which included both elements in order to minimize the time required to change from analyzing for one element to another. Both a Beckman Acta MVI double-beam ultraviolet spectrophotometer and a Heath modular double-beam scanning spectrophotometer, model EU-707, equipped with a Heath-805A DVM, were used for the organic analyses. All values were taken from the digital readouts. An AO Model 02156 Water Bath Shaker (American Optical Corp.) was used for elevated temperature studies. Infrared measurements were made on a Warkus Flat Film Pinhole Camera used in the wide angle mode, at a 5-in. sample-to-film distance, with Cu K_α radiation at 35 kV and 20 mA. Scanning electron microscopy (s.e.m.) was performed on an Etec Autoscan scanning electron microscope at an accelerating voltage of 20 kV. Surface area measurements were performed by Cabot Corp., Concord Rd., Billerica, Mass. Standard 6-in Pyrex test tubes were used to contain the resin plus the solution. To decrease the amount of metal leaching and/or absorption with the walls of the test tubes, they were all silanized.

Procedure

A one-plate batch equilibration technique was used for investigating the metal uptake by the resins. This involved weighing out 50 (±5) mg of sieved, dried resin and adding it to a 6-in silanized test tube. To this was added by volumetric pipet 10 (±0.02) ml of the aqueous solution of interest. The pH values were adjusted with minimum amounts of HCl and NH_4OH; usually a Cenco pH meter (Catalog No. 21690) was used with Cenco glass and saturated calomel electrodes. In the investigations with silver, HNO_3 was used in place of HCl, and care was taken to minimize exposure to light. The test tubes were then sealed closed with a double layer of Parafilm. Usually there were three test tubes without resin (designated the "Standard") and three test tubes with resin (designated the "Sample"). An average value plus a standard deviation was then calculated for each point.

The sealed test tubes were shaken horizontally in plastic test tube shipping trays for a specified period of time, usually 24 h, on the mechanical shaker at a moderate speed at room temperature (unless otherwise noted). After this equilibration period, the tubes were placed vertically in racks for several minutes. Aliquots were then carefully pipetted from these solutions into silanized 4-in test tubes, centrifuged, and then analyzed after making the appropriate dilutions if necessary.

All metal ions except lithium were measured by atomic absorption; lithium was measured by atomic emission. Since there were no interfering ions present in the solutions, no precautions were necessary to guard against them. All analyses were made within the linear working range of the instruments. Most of the investigations were made on p-2-2-2-I sieved particles unless otherwise noted.

RESULTS AND DISCUSSION

Percentage uptake vs. metal concentration

At high copper concentrations the white resin turned progressively greener with time, a strong indication of complexation. The only other metal ion to give a color change was Ag(I), which turned the resin brown. The highest percentage uptake of Cu(II) and Ni(II) occurred at low concentrations (Table 2). Further investigations were confined to test solutions whose concentrations were never greater than 6 ppm.

Percentage uptake vs. pH for the various metal ions

The results are listed in Table 3. In general, the relative uptake of p-2-2-2-I at slightly acidic pH values was: Pb(II) > Cu(II) > Ag(I) > Cd(II) > Zn(II) > Cr(III) > Ni(II) > Ca(II) > Li(I). Transition metals were taken up better than alkali metals, behavior which is characteristic of weak acid cation-exchange resins. Atomic number was influential in that the heavier metal ions were generally taken up more readily: Cd(II) > Zn(II), Ca(II) > Li(I), and Pb(II) > all others. Bonding with the soft metals, such as Cu(II) and Ag(I), was more favorable than with the hard metals, such as Cr(III), because the "*d*" orbitals of the former two were more hybridized. Bonding with Ca(II) and Li(I) could only be ionic since there were no '*d*' orbitals available for bonding.

Even slight changes in concentration could have significant effects on uptake. For example, a 2.0-ppm copper solution gave an uptake of approximately 40%, while a 4.0-ppm solution shows only a 30% uptake at the same pH.

Increasing the basicity of the solution almost invariably led to greatly increased uptake, sometimes as high as 100%. The reason for this behavior is that the mechanism by which uptake occurs changes with the rise in hydroxide concentration. In slightly acidic solutions a metal ion approaches an oxamide group in which both hydrogens are essentially non-ionized.

TABLE 2

Percentage uptake vs. metal concentration

Cu^{2+} Initial conc. (ppm)	Uptake (%)	Ni^{2+} Initial conc. (ppm)	Uptake (%)
1000	5.5	1000	0.6
700	10.4	800	16.3
400	10.6	400	19.1
200	11.8	200	19.1
100	15.0	100	17.0
50	18.5	20	22.5
10	28.0	2	32.5
1	65.0		

TABLE 3

Percentage uptake vs. pH for Cu^{2+}, Zn^{2+}, Cd^{2+}, Pb^{2+}, Ni^{2+}, Cr^{3+}, Ag^{+}, Ca^{2+}, and Li^{+}

Metal	pH	Standard	Sample	Uptake (%)
Cu^{2+}	5.51	0.072 ± 0.004	0.043 ± 0.001	40.3
(2.0 ppm)	7.40	0.059 ± 0.008	0.002 ± 0.000	96.6
	10.00	0.068 ± 0.002	0.000 ± 0.000	100.0
Zn^{2+}	5.84	0.191 ± 0.000	0.153 ± 0.027	19.9
(1.0 ppm)	7.95	0.056 ± 0.006	0.039 ± 0.011	75.5
	9.87	0.051 ± 0.004	0.000 ± 0.000	100.0
Cd^{2+}	5.78	0.286 ± 0.004	0.210 ± 0.009	26.5
(2.0 ppm)	7.97	0.284 ± 0.002	0.086 ± 0.005	69.7
	10.05	0.224 ± 0.000	0.000 ± 0.000	100.0
Pb^{2+}	5.20	0.040 ± 0.002	0.019 ± 0.004	52.5
(4.0 ppm)	7.80	0.015 ± 0.003	0.008 ± 0.002	46.7
	10.03	0.037 ± 0.004	0.014 ± 0.003	62.2
Ni^{2+}	5.70	0.068 ± 0.001	0.065 ± 0.001	4.4
(6.0 ppm)	7.60	0.069 ± 0.001	0.063 ± 0.001	8.7
	10.15	0.035 ± 0.000	0.008 ± 0.004	77.1
Cr^{3+}	4.60	0.046 ± 0.001	0.042 ± 0.000	8.7
(4.0 ppm)	7.80	0.036 ± 0.001	0.031 ± 0.000	13.9
	10.03	0.042 ± 0.000	0.042 ± 0.000	0.0
Ag^{+}	5.00	0.177 ± 0.008	0.099 ± 0.013	44.1
(4.0 ppm)	7.80	0.178 ± 0.008	0.085 ± 0.006	52.3
	10.03	0.178 ± 0.003	0.041 ± 0.003	77.0
Ca^{2+}	5.70	0.231 ± 0.001	0.228 ± 0.005	1.3
(4.0 ppm)	7.80	0.235 ± 0.001	0.213 ± 0.003	9.4
	10.10	0.218 ± 0.014	0.074 ± 0.005	66.1
Li^{+}	5.97	1.969 ± 0.042	1.974 ± 0.003	0.0
	7.60	1.976 ± 0.002	1.928 ± 0.005	2.7
	10.05	1.993 ± 0.019	1.730 ± 0.008	13.2

For complexation to occur, the two hydrogens must be displaced in favor of the metal ion. Formation of the ring is favorable in terms of energy considerations.

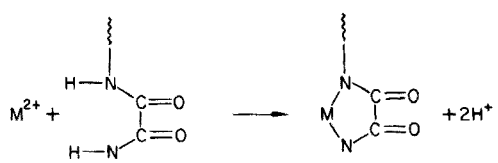

(XIII)

Those metal ions which naturally tend to form stronger amine or amide complexes will tend to complex more strongly with the oxamide group, as expected. However, with increasing hydroxide concentration the hydrogens

of the oxamide unit begin to ionize. Wang and Bauman [19] found that the ionization constants for *N,N'*-bis(2-aminoethyl)oxamide were $pK_{a_1} = 8.30$ and $pK_{a_2} = 9.54$. Therefore, at high pH values the oxamide unit becomes a dianion.

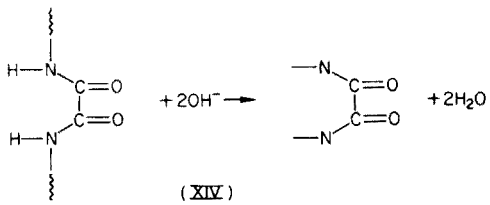

(XIV)

Whereas at slightly acidic pH values the mechanism was one of complexation, it now becomes one of (stronger) ionic bonding. Therefore, the alkali metals are taken up in highly basic solutions, and almost all metal ions show better uptake. This unique ability of co-polyoxamides to undergo conversion from a specific complexing resin to a general cation-exchange resin and vice-versa does not seem to have been previously reported.

One problem which was encountered in these studies was that hydroxide formation interfered with the uptake by the resin. Many metal ions, e.g. Zn(II) and Pb(II), form hydroxide precipitates in slightly basic solutions. Results were better for solutions adjusted with ammonia solution than with sodium hydroxide. The ammonium ions aided in solvation of the metal ions, and an amphoteric effect with NH_4OH was clearly evident in some cases, as can be seen in the variation of the standard values. Though the presence of the ammonium ions was helpful, one cannot be sure in which form the metal ion was being taken up as, whether by itself, as a hydroxide, or as an ammonium solvated species. The abnormal behavior of lead and chromium at high hydroxide concentrations may be due to solubility problems. Both metals appear to be in solution at high pH values, which indicates that the ammine complexes may be stronger than the oxamide ones.

Further investigations demonstrated that there was no uptake of Cu(II) by the resin at low pH values. Also, absorbed metal ion could be stripped off the resin by treatment with strong acid. In this way the resin was shown to be easily renewable, and could thus be recovered and re-used for subsequent studies.

Percentage uptake vs. ionic strength and temperature

Ca(II) and Cu(II) solutions of ionic strength 0.17 were made by addition of appropriate amounts of sodium chloride or glacial acetic acid. Sodium chloride had neutral or negative effects on uptake by the resin for both calcium and copper. Calcium uptake was negligibly affected by the additional acetate, but the uptake of copper was significantly increased (Table 4). At pH 5.60, the uptake would normally be approximately 30%. Again, solubility plays an important role. Chloride salts are less soluble than acetate salts, especially of transition metals. Also, the increased ionic strength has two

TABLE 4

Effect of ionic strength on percentage uptake for 4.0 ppm copper(II)

Conditions	pH	Standard	Sample	Uptake (%)
Acetate	4.18	0.181 ± 0.001	0.167 ± 0.005	7.7
μ = 0.17	5.60	0.176 ± 0.001	0.102 ± 0.001	42.1
	7.90	0.044 ± 0.009	0.001 ± 0.000	97.7
	10.05	0.067 ± 0.003	0.001 ± 0.001	98.5
Chloride	5.60	0.149 ± 0.001	0.107 ± 0.001	28.2
μ = 0.17	7.80	0.017 ± 0.005	0.008 ± 0.003	52.9
	10.03	0.016 ± 0.011	0.002 ± 0.002	87.5

other effects [30]. First, ion-pair formation, e.g. $Cu^{2+}(X^-)_2$ (X^- = acetate in this case) is promoted. Since the anions must accompany the cations onto the resin, adsorption of the metals by the resin is increased because electroneutrality is more readily preserved in solutions of higher ionic strength. Secondly, the activities of the metal ions are decreased, an effect which is favorable to metal—amide complexation.

Uptake was significantly increased by raising the temperature at which the equilibrations were performed (Table 5).

Competitive uptake studies

In competition with another metal ion, the metal which exhibits the higher uptake separately will be taken up preferentially by the resin (Table 6).

*Percentage uptake of Cu(II) and Cd(II) on p-2-2-2-2,6N and p-2-2-2-*cis*-1,4 resins*

Both resins exhibited poorer uptake than p-2-2-2-I (Tables 7 and 8). Changing the aromatic content did not have a large effect on percentage uptake. Rather, the results are explained by the fact that the 2,6-naphthyleney and *cis*-1,4-cyclohexyl acid residues are less hydrophilic than the isophthaloyl residue and therefore less wettable. Hence, interaction of the aqueous phase with the polymer surface interface was reduced, and this resulted in a less favorable environment in which complexation could occur.

TABLE 5

Percentage uptake vs. temperature for 4.0 ppm copper(II) at pH 5.60.

Temp (°C)	Standard	Sample	Uptake (%)	Diff.
R.T.[a]	0.155 ± 0.001	0.108 ± 0.001	30.3	9.4
37.5	0.156 ± 0.003	0.094 ± 0.009	39.7	
R.T.	0.151 ± 0.004	0.108 ± 0.003	28.5	15.3
50.0	0.146 ± 0.002	0.082 ± 0.001	43.8	

[a]Room temperature, ca. 25°C.

TABLE 6

Competitive uptake study: Cu^{2+} vs. Zn^{2+} or Ag^{+} at pH 5.75

Metals	Standard	Sample	Uptake (%)	Metals	Standard	Sample	Uptake (%)
Cu^{2+} vs. Zn^{2+}				*Cu^{2+} vs. Ag^{+}*			
Cu^{2+} (2.0 ppm)	0.075 ± 0.002	0.038 ± 0.001	49.3	Cu^{2+} (4.0 ppm)	0.167 ± 0.002	0.116 ± 0.003	30.5
Zn^{2+} (1.0 ppm)	0.154 ± 0.001	0.104 ± 0.005	32.5	Ag^{+} (4.0 ppm)	0.164 ± 0.002	0.128 ± 0.003	22.0
Cu^{2+} (2.0 ppm)	0.075 ± 0.001	0.041 ± 0.001	45.3	Cu^{2+} (4.0 ppm)	0.169 ± 0.003	0.115 ± 0.003	32.0
Zn^{2+} (1.0 ppm)	0.171 ± 0.002	0.165 ± 0.002	3.5	Ag^{+} (4.0 ppm)	0.184 ± 0.002	0.165 ± 0.005	11.5

TABLE 7

Percentage uptake of Cu^{2+} and Cd^{2+} on p-2-2-2-*cis*-1,4 resin

	pH	Standard	p-2-2-2-I	U (%)	p-2-2-2-*cis*-1,4	U (%)
Cu^{2+} (4.0 ppm)	5.50	0.152 ± 0.001	0.103 ± 0.003	32.2	0.129 ± 0.003	15.1
Cd^{2+} (2.0 ppm)	5.45	0.245 ± 0.000	0.177 ± 0.002	30.3	0.252 ± 0.003	1.0

TABLE 8

Percentage uptake of Cu^{2+} and Cd^{2+} on p-2-2-2-2-6N resin

	pH	Standard	p-2-2-2-I	U (%)	p-2-2-2-2,6N	U (%)
Cu^{2+} (4.0 ppm)	5.75	0.275 ± 0.005	0.172 ± 0.005	37.5	0.189 ± 0.003	31.3
Cd^{2+} (2.0 ppm)	5.65	0.252 ± 0.002	0.159 ± 0.007	36.9	0.203 ± 0.013	19.4

Percentage uptake on silanized sand

Studies involving silanized sand showed that it exhibited significant uptake even at slightly acidic pH values (Table 9). Apparently, the macroscopic structure of the sand particles acted as a filtration bed and/or nucleation sites for hydroxide precipitates. Therefore, some of the uptake by the co-polyoxamides is partly due to this surface effect; it is not solely due to complexation, as might have been assumed. With increasing hydroxide concentration, "uptake" is greater. Very soluble cations, such as calcium, are less affected by this since their hydroxides are still very soluble at high pH values.

TABLE 9

Percentage uptake on silanized sand for 4.0 ppm copper(II)

pH	Standard	p-2-2-2-I	Uptake (%)	Sand	Uptake (%)
5.60	0.151 ± 0.003	0.103 ± 0.005	31.8	0.141 ± 0.003[a]	6.6
5.70	0.151 ± 0.004	0.108 ± 0.003	28.5	0.145 ± 0.003[b]	4.0
5.95	0.131 ± 0.002	0.089 ± 0.002	32.1	0.133 ± 0.008[b]	12.8
7.85	0.012 ± 0.010	—	—	0.007 ± 0.001[b]	58.3
10.05	0.018 ± 0.004	—	—	0.008 ± 0.008[b]	44.4

[a]Sieved sand (60/80). [b]Unsieved sand.

Percentage uptake of particles vs. films

Gelled films of p-2-2-2-I had a much higher surface area (5.8 $m^2 g^{-1}$) than did 60/80 mesh size particles (4.0 $m^2 g^{-1}$), measured by a nitrogen gas absorption technique. This was the reverse of what was expected. This anomaly was explained by taking SEM pictures of the film interior. They showed many tubular structures whose interior surface area was much larger than the surface area of the outside of the films. Hence, the relatively high surface area obtained for the films can be explained if one assumes that the nitrogen gas permeates the interior of the films. However, though the films possessed a higher overall surface area, they did not take up metal ions as well as the particles (Table 10). One must conclude that complexation occurs on the outer surface of the materials. The 60/80 mesh size particles, which had the larger external surface area, exhibited the greater uptake.

TABLE 10

Percentage uptake of 60/80 mesh particles vs. films

Metal	pH	Standard	Particles	Uptake (%)	Film	Uptake (%)
Cu^{2+} (4.0 ppm)	5.03	0.182 ± 0.001	0.133 ± 0.003	26.9	0.153 ± 0.001	15.9
Zn^{2+} (1.0 ppm)	5.70	0.191 ± 0.008	0.141 ± 0.009	26.2	0.187 ± 0.001	2.1
Ca^{2+} (4.0 ppm)	5.70	0.188 ± 0.008	0.183 ± 0.001	2.7	0.208 ± 0.007	0.0
Li^{+} (2.0 ppm)	5.97	1.969 ± 0.042	1.974 ± 0.003	0.0	2.037 ± 0.004	0.0
Pb^{2+} (4.0 ppm)	5.68	0.069 ± 0.006	0.038 ± 0.003	44.9	0.053 ± 0.004	23.2
Cd^{2+} (2.0 ppm)	5.80	0.215 ± 0.013	0.168 ± 0.002	21.9	0.214 ± 0.001	0.0

Percentage uptake vs. time and surface area

Time studies involving slightly basic solutions again displayed the problem of hydroxide precipitation (Table 11). The standard values showed great fluctuation and no definite trend was observed. Further investigations were then carried out at slightly acidic pH values with Cu(II), Cd(II), and Pb(II), where this problem was minimized. Again, it was observed that percentage uptake was highly dependent on concentration and on pH, especially. Materials of smaller mesh size exhibited greater uptake, as would be expected because of the greater surface area. Renewed p-2-2-2-I resin exhibited increased uptake over fresh resin, and unlike the latter, percentage uptake would increase with time. Renewed resin appeared to degrade mechanically more rapidly than virgin material during the washing procedure. This led to increasing surface area as time progressed, and is the most likely explanation for the observed increase in uptake.

Miscellaneous studies involving metal ion complexation

Infrared measurements indicated that the amount of amine and/or carboxylic end groups was low and that endcapping with acetic anhydride did not have a negative effect on uptake. Accurate infrared investigations of the metal oxamide were not possible because of the obscuring effect exhibited by the polymeric structure of the material. Wide-angle x-ray studies showed that films of the co-polyoxamides had little crystallinity, whether complexed or not.

Organic acid and base uptake studies

Increasing the degree of aromatic character of the acids (e.g. phenol to 2-naphthol) and the bases (e.g. pyridine to aniline) resulted in increased organic uptake by the p-2-2-2-I (Table 12). In the case of the p-2-2-2-2,6N

TABLE 11

Percentage uptake vs. time and surface area for 4.0 ppm copper(II)

Conditions	Time (h)	Standard	Sample	Uptake (%)
pH 7.87	0.8	0.071 ± 0.041	0.022 ± 0.002	69.0
Fresh resin,	2.0	0.130 ± 0.011	0.064 ± 0.005	50.8
60/80 mesh	4.0	0.045 ± 0.016	0.004 ± 0.001	91.1
	7.0	0.060 ± 0.001	0.000 ± 0.001	100.0
	10.5	0.072 ± 0.006	0.000 ± 0.001	100.0
	24.0	0.042 ± 0.014	0.000 ± 0.001	100.0
pH 5.60	5.5	0.171 ± 0.005	0.132 ± 0.000	22.8
Fresh resin	24.0	0.166 ± 0.003	0.120 ± 0.004	27.7
<60/80	48.0	0.172 ± 0.003	0.115 ± 0.004	33.1
mesh	72.0	0.172 ± 0.003	0.115 ± 0.003	33.1
pH 5.60	24.0	0.165 ± 0.000	0.110 ± 0.001	33.3
Renewed	48.0	0.187 ± 0.000	0.115 ± 0.001	38.5
resin, 60/80	72.0	0.171 ± 0.001	0.094 ± 0.004	45.0
mesh				

TABLE 12

Percentage uptake by p-2-2-2-I and p-2-2-2-2,6N
(Phenol and pyridine showed almost zero uptake over the pH range 2.0—10.5 on p-2-2-2-I.)

Compound	p-2-2-2-I		Compound	p-2-2-2-2,6N	
	pH	% Uptake		pH	% Uptake
2-Naphthol	2.3	42.2 ± 0.4	Phenol	1.99	13 ± 1
	4.5	41.0 ± 1.3		4.07	13 ± 1
	5.8	41.8 ± 0.0		5.90	13 ± 1
	7.0	42.2 ± 0.5		8.41	13 ± 1
	9.2	36.7 ± 1.8		10.69	11 ± 1
	10.5	29.3 ± 1.7	Aniline	4.00	50 ± 2
	12.0	3.0 ± 1.7		7.90	48 ± 2
Aniline	4.0	47 ± 2		10.11	35 ± 4
	5.8	24 ± 2			
	8.0	20 ± 1			
	10.3	22 ± 3			
	12.0	17 ± 1			

(Table 12), the uptake of phenol and aniline was greater than for the p-2-2-2-I resin, the latter polymer having a smaller degree of aromatic character. The p-2-2-2-*cis*-1,4 and p-2-2-2-*trans*-1,4 materials both exhibited some uptake of phenol and aniline, also. Uptake appears to be more influenced by the degree of aromatic content within the polymer chain than how polar or wettable the resin is. The binding mechanism is probably charge transfer between the amide bonds and the unsaturated molecule [29]. As expected, the organic acids were taken up better in their non-ionized forms. However, the organic bases showed better uptake in their protonated form, and uptake appeared to level off quickly. This behavior is puzzling and warrants further investigations. Studies on silanized sand showed no uptake whatsoever.

In summary, then co-polyoxamides demonstrate the potential for separating a wide range of metal ions from one another and of separating molecules which vary in their degree of aromatic content.

We are grateful to R. Cohen and B. Beauchemin for their help in the organic uptake studies, and S. Bacyek and P. Gilmore for technical assistance in the x-ray and electron microscopy studies, respectively. This work was in part supported by a grant of the Office of Saline Water, The Department of Interior and the National Science Foundation.

REFERENCES

1 S. C. Jain and R. Rivest, J. Inorg. Chem., 29 (1967) 2787.
2 Von B. Kruss and M. L. Ziegler, Z. Anorg. Allg. Chem., 401 (1973) 89.
3 A. Izakenaite, L. T. Koslova and S. N. Mel'nik, Chem. Abstr., 84: 173157u.

4 H. O. Desseyn, W. A. Jacob and M. A. Herman, Spectrochim. Acta, Part A, 25 (1969) 1685.
5 M. L. Good and T. H. Siddall, III, J. Inorg. Nucl. Chem., 30 (1968) 2679.
6 D. M. Hart, P. S. Roles and J. M. Kessinger, J. Inorg. Nucl. Chem., 32 (1970) 469.
7 Y. Kuroda, M. Kato and K. Sone, Nippon Kagakukai, 34 (1961) 877.
8 P. X. Armendarez and K. Nakamoto, Inorg. Chem., 5 (1966) 790.
9 J. J. Steggerda, J. J. Bour and P. J. M. W. L. Birker, Inorg. Chem., 10 (1971) 1201.
10 M. M. Rising, J. S. Hicks and G. A. Moerke, J. Biol. Chem., 89 (1930) 1.
11 W. D. Jacobs and J. H. Yoe, Anal. Chim. Acta, 20 (1959) 435.
12 A. Zuberbuhler and S. Fallab, Helv. Chim. Acta, 50 (1967) 889.
13 R. Greisser and S. Fallab, Chimia, 22 (1968) 90.
14 H. Ojima and K. Yamada, Nippon Kagaku Zasshi, 89 (1968) 490.
15 A. Zuberbuhler and Th. Kaden, Helv. Chim. Acta, 51 (1968) 1805; Chimia, 23 (1969) 418.
16 A. Zuberbuhler and U. P. Buxtorf, Helv. Chim. Acta, 56 (1973) 524.
17 H. Ojima and K. Yamada, Nippon Kagakukai, 43 (1970) 1601; 3018.
18 J. J. Steggerda and J. J. Bour, Proc. Symp. Coord. Chem., 3rd., 1 (1970) 273.
19 J. C. Wang and J. E. Bauman, Jr., Inorg. Chem., 4 (1965) 1613.
20 B. V. Tronov, A. P. Izakenaite and V. D. Gol'tsev, Chem. Abstr. 66:32413r.
21 H. J. Chang, Ph.D. Thesis, University of Massachusetts, Amherst, Mass., 1974, p. 128.
22 H. J. Chang, D. Stevenson and O. Vogl, Abstr. 4th NERM, Hartford, Conn., 1972, p. 139; Polym. Prepr., ACS Polym. Div., 15 (1974) 417.
23 H. J. Chang and O. Vogl, Abstr., 6th NERM, 1974, p. 163.
24 D. Stevenson, R. A. Gaudiana and O. Vogl, Polym. Prepr., ACS Polym. Div., 15 (1974) 426.
25 D. Tirrell and O. Vogl, Abstr., 18th Can. High Poly. Forum, 32, Hamilton, Ont., 1975; J. Polym. Sci., Poly. Chem. Ed., in press.
26 H. J. Chang and O. Vogl, J. Polym. Sci., Poly. Chem. Ed., Parts I and II, in press.
27 D. Stevenson, R. Gaudiana, A. Beeber and O. Vogl, J. Macromolecular Sci. Chem., (in press).
28 H. J. Chang, R. Gaudiana and O. Vogl, Macromol. Synth., in press.
29 T. Mourey, A. P. Carpenter, Jr., and S. Siggia, Anal. Chem., 48 (1976) 1592.
30 J. F. Dingman, Ph.D. Thesis, University of Massachusetts, Amherst, Mass., 1972, p. 113.

Analytica Chimica Acta, 96 (1978) 383—390

DETERMINATION OF GAS PHASE—LIQUID PHASE (OR OTHER) DISTRIBUTION COEFFICIENTS BY ANALYSIS OF ONE PHASE ONLY

CYRUS FELDMAN

Oak Ridge National Laboratory, Oak Ridge, Tennessee 37830 (U.S.A.)

(Received 8th August 1977)

SUMMARY

In measuring inter-phase distribution coefficients ($k_{I/II}$) it is often convenient, and sometimes necessary, to obtain all of the analytical data from one phase. A rigorous formula, applicable to both low and high $k_{I/II}$ values has been derived; measurements of the distribution of mercury, methylmercury and $^{67}Cu^{2+}$ between various pairs of phases with this formula gave $k_{I/II}$ values similar to those obtained from other approaches.

The distribution coefficient of a chemical species between two phases is usually determined by measuring the concentration of the species in both phases, or by measuring the concentration in one phase and calculating it in the other by difference. However, these methods may be unreliable or inconvenient in individual cases under any one or more of the following conditions: (1) one phase may be difficult to sample, or to analyze for the species of interest; (2) the concentration of the species in the phase not analyzed may be difficult to calculate by difference, because of chemical or physiochemical equilibria existing in the system; (3) the total quantity of the species in the system may not be known. In such cases, it would be convenient to be able to determine the distribution coefficient by analyzing only the more easily analyzed phase. This can be accomplished by means of a method of successive equilibrations.

THEORY

For the sake of concreteness, the derivation given below will first be phrased in terms of a liquid phase/gas phase distribution equilibrium; however, the formulae obtained apply equally well to the distribution of any species between any two phases, provided that the concentration of that species is not affected by competing reactions in either phase. This case will be referred to below as the ideal case. The effects of some types of non-ideal behavior will be treated at the end of the theoretical section.

Let us assume that a closed container is partially filled with a liquid, the remainder of the volume being a gas. The solute may originally be entirely in either phase, or distributed between the two. The container is shaken until

concentration distribution equilibrium is attained between the phases. The concentration of the distributed species is then determined in the phase that is the easier to analyze, assumed here to be the gas phase. The analytical results may be expressed in arbitrary units if desired. The original gas phase is now replaced by an equal amount of the same gas, not containing the species of interest. The equilibration is repeated and the concentration of the species again measured in the gas phase. Since the total quantity of this species originally present in the system is finite, its concentration in the gas phase decreases with each equilibration. The equilibration and measurement may be repeated as many times as desired or possible. This type of procedure, in which the phase voided after each equilibration (the gas phase, in this case) is the phase analyzed will be called Procedure A. The opposite type of procedure, in which the phase that is retained after each equilibration (the liquid phase, in this case) is the phase analyzed will be called Procedure B.

Ideal case, Procedure A

It will first be shown that, under the conditions of Procedure A, the ratio of the concentration of the distributed species in the gas phase after any one equilibration to its concentration in the gas phase after the next equilibration is a constant, defined as $R_{n/n+1}$, and that this ratio is directly related to the distribution coefficient of the species between the two phases. In the equations below, the C's represent concentrations, the V's volumes, L and G the liquid and gas phases, respectively, and n the running number of the equilibration.

After any given nth equilibration, the quantity of the species of interest in the liquid phase is $C_{L_n} V_L$. The gas phase is now replaced, and the $(n + 1)$th equilibration performed. Mass balance requires that:

$$C_{L_n} V_L = C_{G_{n+1}} V_G + C_{L_{n+1}} V_L \tag{1}$$

If $k_{G/L}$ is defined as the gas/liquid distribution coefficient of the species of interest, then

$$C_{L_n} = C_{G_n}/k_{G/L} \text{ and } C_{L_{n+1}} \equiv C_{G_{n+1}}/k_{G/L} \tag{2}$$

Substituting the appropriate statements of eqn. (2) into eqn. (1) and rearranging gives

$$C_{G_n}/C_{G_{n+1}} = (k_{G/L} V_G/V_L) + 1 \tag{3}$$

Since V_G and V_L are constant in a given series of measurements, and $k_{G/L}$ is assumed to be constant, the right side of eqn. (3) is constant; i.e., the ratio of any two successive values of C_G should be constant for a given system, regardless of the value of $k_{G/L}$.

Rearrangement of eqn. (3) gives

$$k_{G/L} = [V_L/V_G]/[(C_{G_n}/C_{G_{n+1}}) - 1] \tag{4}$$

Since we have already defined

$$C_{G_n}/C_{G_{n+1}} = R_{n/n+1} \tag{5}$$

eqn. (4) can be written

$$k_{G/L} = (V_L/V_G)\,(R_{n/n+1} - 1) \tag{6}$$

Ideal case, Procedure B

When the phase analyzed is the phase which is not replaced after each equilibration, (the liquid phase, in this case), the derivation of the formula for $k_{G/L}$ again starts with eqn. (1). In the present case, however, the substitution made is $C_{G_{n+1}} \equiv k_{G/L}C_{L_{n+1}}$. Straightforward algebraic rearrangement again leads to eqn. (6), in which $R_{n/n+1}$ now represents the ratio of the concentration of the species in the liquid phase after a given equilibration to its concentration in the liquid phase after the next equilibration. Thus the formula for $k_{G/L}$ is the same, regardless of whether the phase analyzed is the phase voided after each equilibration of the phase retained. In each case, $R_{n/n+1}$ refers to the phase which is analyzed.

The subscripts G and L can be replaced by "Phase I" and "Phase II", respectively, without any loss of generality, Phase I always being the phase which is replaced after equilibration. Thus, in more general form, eqn. (6) may be restated as

$$k_{I/II} = (V_{II}/V_I)\,(R_{n/n+1} - 1) \tag{7}$$

The value of $R_{n/n+1}$ for a given system is the same, regardless of which phase is analyzed. This is made evident by rearranging eqn. (7)

$$R_{n/n+1} = (k_{I/II}\,V_I/V_{II}) + 1 \tag{8}$$

since all of the quantities on the right side of eqn. (8) are the same regardless of which phase is analyzed.

The validity of this approach, termed the single phase-successive concentration ratio (SP—SCR) method, can be checked in two ways; the first way is by comparing the $k_{G/L}$ value obtained by it with the value obtained by directly measuring the concentrations in the two phases (when possible). The latter method is called the 2P—CR method in Table 2.

The second way of checking the SP—SCR method is as follows: $\Sigma_{n=1}^{\infty} C_{G_n} V_G$ can be measured experimentally; the result is the total quantity of the species in the system, expressed in arbitrary units. Subtracting $C_{G_1} V_G$ from this total gives the quantity of the species remaining in the liquid phase after the first equilibration, or $(\Sigma_{n=1}^{\infty} C_{G_n} - C_{G_1})V_G$. The concentration of the species in the liquid phase is then $C_{L_1} = (\Sigma_{n=1}^{\infty} C_{G_n} - C_{G_1})V_G/V_L$, and thus

$$k_{G/L} \equiv \frac{C_{G_1}}{C_{L_1}} = \frac{C_{G_1} V_L}{(\sum_{n=1}^{\infty} C_{G_n} - C_{G_1})V_G} \tag{9}$$

This is referred to in Table 2 as the single phase-summation (SP-S) method.

Non-ideal case: effects of adsorption

Under actual working conditions, the species whose distribution coefficient is desired may be adsorbed by the walls of the container, or by small, possibly invisible, amounts of suspended matter.

Returning to the gas phase—liquid phase case, it is assumed that a small amount of solid or colloidal matter, capable of adsorbing the distributed species, is suspended in the liquid phase. After the $(n + 1)$th equilibration, part of the distributed species in the liquid phase is in solution, and the rest is adsorbed on the suspended solids. If it is assumed that the quantity adsorbed is proportional to C_L and to the mass of adsorbent M_S, a mass balance equation analogous to eqn. (1) can be written

$$C_{L_n}V_L + C_{L_n}k_{S/L}M_S = C_{G_{n+1}}V_G + C_{L_{n+1}}V_L + C_{L_{n+1}}k_{S/L}M_S \qquad (10)$$

where $k_{S/L}$ is the adsorption coefficient for the distributed species on the suspended solids. As before, the left side of eqn. (10) represents the mass of the distributed species left behind in the system when the gas is vented after the nth equilibration, and the right side represents the distribution of this same mass between the phases after the $(n + 1)$th equilibration. By a mathematical procedure identical with that used above, the present case gives

$$R_{n/n+1} = C_{G_n}/C_{G_{n+1}} = [k_{G/L}V_G/(V_L + k_{S/L}M_S)] + 1 \qquad (11)$$

in place of eqn. (3), and

$$k_{G/L} = [(V_L + k_{S/L}M_S)/V_G]\ [R_{n/n+1} - 1] \qquad (12)$$

in place of eqn. (6).

Equation (11) shows that when suspended matter is present, the ratio of the concentration of the species in the gas phase after the nth equilibration to its concentration in the same phase after the $(n + 1)$th equilibration is again a constant. Equation (12) indicates that $k_{G/L}$ can still be measured under these conditions by the SP—SCR method, but that the product $k_{S/L}M_S$ will have to be known, as well as V_L and V_G.

It is evident from the forms of eqns. (10), (11), and (12), that the SP—SCR method can be used in the presence of any reaction which competes for the distributed species in the liquid phase, provided that the total mass of the species adsorbed or otherwise sequestered from solution is a linear function of C_L. Other cases must be investigated individually.

Thus, the fact that the same value of $R_{n/n+1}$ is obtained experimentally for a number of successive equilibrations does not in itself prove the absence of any reactions competing with the interphase distribution. It is usually possible to check for such reactions by measuring $k_{I/II}$ under various sets of experimental parameters, or by analyzing the suspended solids.

EXPERIMENTAL

To verify the above formulae, measurements of distribution coefficients were made with Hg or $(CH_3)_2Hg$ as the distributed species, argon or air as the gas phase (phase I), and water, various acid solutions or brine as the liquid phase (phase II). The liquid phase was treated with an amount of the distributed species which was insufficient to saturate it. This mixture was transferred to the equilibration cell; the remaining space was filled with the appropriate gas. All openings in the cell were closed, and the cell was agitated vigorously for 2—5 min. The gas phase (phase I) was then analyzed by connecting the cell to a cold vapor atomic absorption (c.v.a.a.) unit or conventional absorption (u.v.) photometer, or by sampling the gas phase with a gas syringe and using gas chromatography (g.c.). After each equilibration and measurement, the gas phase was replaced.

Measurements of solid phase—gas phase equilibria were made by observing the distribution of carrier-free $^{67}Cu^{2+}$ tracer between Dowex 50-X1 resin (phase II) and aqueous 0.1 M HCl (phase I). After each equilibration, the phases were separated by centrifugation, and the activity of the supernatant liquid (phase I) was counted with a well-type scintillation counter (s.c.). The liquid phase was then replaced and the operation repeated.

In measuring distribution coefficients, it was necessary to be sure that the system had been agitated long enough to achieve equilibrium. This is achieved by continuing the agitation until the concentration of the species in one phase reaches a limiting value.

As a confirmatory test for the attainment of equilibrium, all $R_{n/n+1}$ values should be the same for a given series of extractions. If they show an increasing or decreasing trend, the period of agitation should be increased. This test is particularly sensitive when the species of interest is injected into phase I, and phase I is analyzed and replaced after each equilibration (Procedure A). In this case, equilibrium is approached from one direction in the first equilibration (material transferred from phase I to phase II) and from the other direction in all subsequent equilibrations (material transferred from phase II to phase I). Thus if equilibrium has not been attained, $R_{1/2}$ in phase I will be greater than its equilibrium value, and greater than the subsequent $R_{n/n+1}$ values.

Low $k_{I/II}$ values (which would give $R_{n/n+1}$ values only slightly above 1) can best be measured by making several successive extractions (e.g., 5) and taking the 4th root of $R_{1/5}$.

RESULTS AND DISCUSSION

Table 1 shows the $k_{I/II}$ values obtained for 11 gas—liquid distributions and one solid—solid distribution. All symbols have the same meaning as in the text; n_{max} represents the total number of equilibrations performed in each case. $R_{n/n+1}$ is the arithmetic mean of the $n_{max} - 1$ values of R calculated

TABLE 1

Determination of gas–liquid and solid–liquid distribution coefficients by the single phase–successive concentration ratio method

Solute	Phase I	Phase II	V_I (ml)	V_{II} (ml)	T (°C)	n_{max}	$R_{n/n+1}$	$k_{I/II}$ (eqn. 7)	Analytical technique
Hg^0	Ar (g)	H_2O (l)	40	40	29	10	1.19 ± 2.4%	0.19 ± 12%	c.v.a.a.
Hg^0	Ar (g)	H_2O (l)	60	20	28	3	1.54 ± 3.8%	0.18 ± 11%	c.v.a.a.
Hg^0	Ar (g)	H_2O (l)	35	55	25	10	1.12 ± 4.0%	0.19 ± 37%	c.v.a.a.
Hg^0	Ar (g)	10% $HClO_4$ (l)	38	42	24	7	1.26 ± 3.7%	0.29 ± 18%	c.v.a.a.
Hg^0	Ar (g)	10% $HClO_4$ (l)	40	40	26	5	1.34 ± 5.4%	0.34 ± 21%	c.v.a.a.
Hg^0	Ar (g)	8% H_2SO_4(l)	40	40	25	3	1.56 ± 1.6%	0.56 ± 4.5%	c.v.a.a.
Hg^0	Ar (g)	10% HCl (l)	32	48	25	5	1.28 ± 2.6%	0.42 ± 12%	c.v.a.a.
Hg^0	Ar (g)	2.7% NaCl (l)	40	40	25	5	1.35 ± 1.3%	0.35 ± 5.0%	c.v.a.a.
$(CH_3)_2Hg$	Ar (g)	H_2O (l)	59	21	25	3	1.82 ± 1.8%	0.29 ± 4.0%	u.v.
$(CH_3)_2Hg$	Air (g)	H_2O (l)	17.5	5.0	25	5	2.1 ± 9.0%	0.31 ± 17%	g.c.
$(CH_3)_2Hg$	Air (g)	H_2O (l)	17.5	5.0	0	4	1.49 ± 1.6%	0.14 ± 4.9%	g.c.
$^{67}Cu^{2+}$	0.1 M HCl (l)	Resin (s)	40	0.050	23	4	4.74 ± 2.5%	2990. ± 3.2%	s.c.

from a given series of extractions. The arithmetic mean deviations listed in the $k_{I/II}$ column are greater than the corresponding deviations in the $R_{n/n+1}$ column. This is due to the subtraction of 1 in eqn. (7).

The following conclusions can be drawn from Table 1.

(1) $R_{n/n+1}$ behaves as a constant through as many as ten successive extractions; in all cases but one, its relative mean deviation is 5% or less.

(2) The $k_{I/II}$ value obtained by the SP—SCR method is (as it should be) independent of V_I and V_{II}, and of the analytical technique used.

(3) Because of the subtraction of 1 in eqn. (7), the relative mean deviation of the $k_{I/II}$ value obtained decreases as $R_{n/n+1}$ increases. Equation (8) shows that $R_{n/n+1}$ increases as V_I/V_{II} increases. Precision can thus be improved by using higher values of V_I/V_{II}. However, $R_{n/n+1}$ values which are too high restrict the number of successive extractions which can be made, because of the difficulty of measuring low concentration values.

In a few cases, the values obtained by the SP—SCR method were compared with those obtained for the same system by the 2P—CR method and the SP—S method (eqn. 9). The results are shown in Table 2.

Table 2 indicates that the $k_{I/II}$ values obtained by the SP—SCR method are essentially the same as those obtained by other methods.

CONCLUSIONS

The single phase—successive concentration ratio method for obtaining distribution coefficients is recommended in cases where one phase is easier to analyze or sample than the other, or where the total amount of the species in the system is not known accurately. It is also useful in determining distribution coefficients when the identity of the substance is unknown, but its concentration can be determined in arbitrary units in one of the phases (e.g., by gas chromatography or absorption colorimetry).

TABLE 2

Comparison of $k_{I/II}$ values obtained by various methods

Solute	Phase I	Phase II	$k_{I/II}$		
			Method of measurement		
			SP—SCR	2P—CR	SP—S
Hg^0	Ar (g)	H_2O (l)	0.19		0.19
$(CH_3)_2Hg$	Air (g)	H_2O (l)	0.31	0.33	0.31
$(CH_3)_2Hg$	Ar (g)	H_2O (l)	0.29		0.29

The author expresses his gratitude to Yair Talmi for obtaining the gas chromatographic data in Tables 1 and 2. This research was supported by the NSF-RANN program under NSF Interagency Agreement No. 40-237-70, and performed at the Oak Ridge National Laboratory, operated by Union

Carbide Corporation under contract with the U.S. Atomic Energy Commission. Parts of this paper were presented at the 17th Colloquium Spectroscopicum Internationale in Florence, Italy, September 21, 1973.

Analytica Chimica Acta, 96 (1978) 391—394

Short Communication

DETERMINATION OF CHROMIUM(VI) AS PERCHROMIC ACID BY SOLVENT EXTRACTION AND ATOMIC ABSORPTION SPECTROMETRY§

N. ICHINOSE*

Department of Chemistry, Hamamatsu University, School of Medicine, Hamamatsu City (Japan)

T. INUI and S. TERADA

Shizuoka Prefectural Industrial Research Institute, Shizuoka City (Japan)

(the late) T. MUKOYAMA

Department of Applied Chemistry, Faculty of Engineering, Yamanashi University, Kofu City (Japan)

(Received 28th June 1977)

The atomic absorption spectrometric (a.a.s.) determination of chromium(VI) can be made more sensitive by extracting chromium as its pyrollidinedithiocarbamate (APDC) [1, 2] or diethyldithiocarbamate (DDTC) [3] complex into methyl isobutyl ketone (MIBK) and spraying the extract into the flame. However, the procedures tend to be complicated and their applications are limited by the instability of the reagents in acidic solutions.

The present communication reports a determination of traces of chromium(VI) in which perchromic acid, formed by reaction with hydrogen peroxide in dilute acidic solutions [4—7], is extracted into MIBK, which is then sprayed into an air—acetylene flame. The distribution ratio of chromium as perchromic acid between MIBK and the aqueous phases was studied by measuring the ^{51}Cr γ-activity.

Experimental

Apparatus. The scintillation counter comprised a Nippon Musen Model NDW-451 (NaI(Tl)) detector and a Nippon Musen Model TDC-102 scaler. The Shimadzu Model-AA-610 atomic absorption spectrometer used was equipped with a chromium hollow-cathode lamp (357.8 nm). An air—acetylene flame was used with a 10-cm slot burner.

Reagents. A standard chromium(VI) stock solution (1.000 g Cr ml^{-1}) was prepared by dissolving 0.325 g of potassium dichromate (>99.99% purity) in 1 l of water. Radioactive chromium(VI) solution was prepared by diluting

§ This paper was read at the 36th Annual Meeting of the Chemical Society of Japan, Osaka, April, 1977.

ca. 2 mCi of ^{51}Cr activity (Japan Atomic Energy Research Institute) to 100 ml with water. Chromium tracer solution ($\leqslant$1 mg Cr ml^{-1}) was made by mixing various amounts ($\leqslant$100 mg Cr^{6+}) of the standard chromium(VI) stock solution with ca. 20 μCi of ^{51}Cr tracer and diluting to 100 ml with water. Other reagents used were of analytical-reagent grade.

General extraction procedure. Hydrogen peroxide solution (1 ml) was added to 9 ml of dilute sulfuric acid solution containing a 1-ml aliquot of the chromium tracer solution. The solution was shaken vigorously (240 shakes/min) with an equal volume of MIBK in a 50-ml separatory funnel. The ^{51}Cr γ-activity in each aliquot was counted with a well-type NaI(Tl) scintillation counter (1250 V). No temperature control was exercised, but the ambient temperature was fairly constant at 10 ± 2°C.

Results and discussion

Extraction of chromium(VI). The effects of shaking time, and of the concentrations of hydrogen peroxide and acids (sulfuric acid, hydrochloric acid, nitric acid) and chromium(VI) concentration on the distribution of chromium (2×10^{-3} M Cr^{6+}) between aqueous solution and MIBK, and the stability of the violet species (perchromic acid) developed in the organic phase, were studied by using ^{51}Cr tracer. Plots of log D vs. pH for the extraction of chromium(VI) in the concentration range 2×10^{-3}—2×10^{-5} M (Fig. 1) indicate that the maximal distribution ratio occurs at pH 1.7 for sulfuric acid solutions. Hydrochloric and nitric acid solutions gave similar results. Later results obtained by a.a.s. were in good agreement with these radiotracer measurements.

Atomic absorption measurement of chromium. With an air—acetylene flame, the optimal air and acetylene flow rates were 10 l min^{-1} and 1.2 l min^{-1} respectively. Better sensitivity was obtained with a fuel-rich flame. The optimal optical path was 5—10 mm above the burner head (lamp current, 10 mA); below 3 mm, the sensitivity and the linear range decreased.

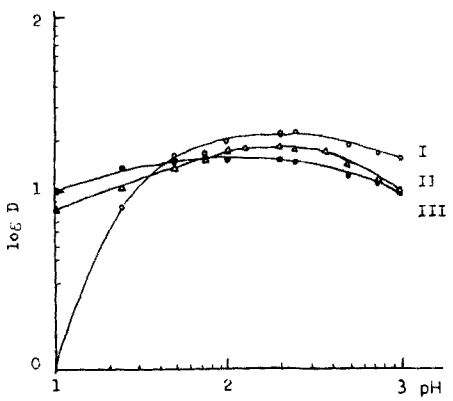

Fig. 1. Plots of log D vs. pH in sulfuric acid solutions containing 0.03 M H_2O_2. I, ca. 2×10^{-3} M Cr. II, ca. 2×10^{-4} M Cr. III, ca. 2×10^{-5} M Cr.

Esters and ketones are the best extraction solvents, because they can be burned completely, and provide a stable flame which does not absorb radiation at the relevant wavelength. MIBK, ethyl acetate, methyl propionate and isopropyl acetate extracted the perchromic acid, but methyl propionate was unsatisfactory in that centrifuging was needed for phase separation; ethyl acetate was too soluble in water, and did not give a stable flame. MIBK is relatively insoluble in water and gives a stable flame. Calibration curves were linear for the range 0—5 ppm Cr (in the solvent).

Effects of experimental variables. Essentially quantitative extraction of chromium (1 ppm) into MIBK from sulfuric, hydrochloric or nitric acid solutions containing 0.03 M H_2O_2 was possible in the pH range 1.2—2.5. To study the effect of hydrogen peroxide concentration, a fresh solution of hydrogen peroxide, prepared from 30% solution, was standardized against potassium permanganate. Known volumes of this solution were added to aqueous solutions containing chromium and 0.01 M sulfuric acid (pH 1.7). The perchromic acid formed was extracted into MIBK and determined by atomic absorption spectrometry. Maximum absorbance for chromium was obtained when the concentration of hydrogen peroxide in the aqueous solution was from 0.015—0.05 M. Above this concentration the absorbance of chromium decreased gradually.

In a study of the effect of shaking time on the extraction from various acidic solutions, there was no perceptible change in the absorbances for shaking times from 20 s to 25 min.

Stability of perchromic acid. Several solutions were extracted as described under the recommended procedure, and the separatory funnels were left under diffuse daylight. The absorbances of the organic phase were measured at different times after extraction. The absorbances of chromium (2, 1 and 0.5 ppm) in extracts from sulfuric, hydrochloric or nitric acid solutions were constant for 25—30 min and then decreased gradually.

Interferences. Under the recommended conditions, iron(III), cadmium, zinc, manganese(II), nickel, copper(II), lead, mercury(II) and chromium(III) did not interfere in 1-mg amounts. Aluminum interfered with the extraction into MIBK (Table 1).

Recommended procedure and analysis of samples

Shake 30 ml of a dilute acidic solution (pH 1.7 with sulfuric, hydrochloric or nitric acid) containing 0.03 M hydrogen peroxide and 0.5—50 μg of chromium, for about 1 min with 10 ml of MIBK in a 100-ml separatory funnel. Separate the phases and measure the absorbance of chromium in the supernatant extract against a reagent blank.

TABLE 1

Interference of aluminum

Al added (μg)	0	200	500	1000
Cr(VI) found (μg)	10.0	10.0	9.3	7.9

Under these conditions, calibration graphs were linear in the range 0—5 ppm chromium in MIBK. Chromium(VI) in the waste waters from organic detergents for glassware was determined. After the sample had been decomposed with sulfuric acid and nitric acid, the solution was adjusted to pH 1.7 with ammonia solution, and chromium(VI) was determined as described above. The results obtained agreed closely with the results of spectrophotometry with diphenylcarbazide.

REFERENCES

1 R. E. Mansell and H. W. Emmel, At. Absorpt. Newsl., 4 (1965) 365.
2 C. E. Mulford, At. Absorpt. Newsl., 5 (1966) 88.
3 J. Nix and T. Goodwin, At. Absorpt. Newsl., 9 (1970) 119.
4 D. G. Tuck, Anal. Chim. Acta, 27 (1962) 296.
5 V. I. Evans, J. Chem. Soc., 4013 (1957).
6 R. K. Brookshier and H. Freund, Anal. Chem., 23 (1951) 1110.
7 A. Glasner and M. Steinberg, Anal. Chem., 27 (1955) 2008.

Analytica Chimica Acta, 96 (1978) 395—399

Short Communication

BARIUM DETERMINATION BY ISOTOPE DILUTION AND NEUTRON ACTIVATION METHODS: A COMPARISON OF MARINE SEDIMENT ANALYSES

TSAIHWA J. CHOW* and JOHN L. EARL
Scripps Institution of Oceanography, La Jolla, California 92093 (U.S.A.)
JOHN H. REED, NICHOLAS HANSEN and VICTOR ORPHAN
Science Applications, Incorporated, La Jolla, California 92037 (U.S.A.)
(Received 3rd June 1977)

Barite (barium sulfate) is commonly used as a weighting agent in oil- and gas-well drilling mixtures; therefore, studies of the barium content in sediments near drilling sites may provide an indicator of anthropogenic chemical contamination from these operations. The purposes of this report are to describe two different methods of barium determination and to compare the results of analyses for Southern California Bight sediments.

Sediment sampling sites and procedures are described elsewhere. The processed samples were split and their barium content was determined by an isotope dilution method and neutron activation analysis.

Isotope dilution method

Dissolution. The pulverized sediments (8 g) were weighed into Pyrex beakers and heated in a muffle furnace at 325°C for 24 h to destroy the organic matter. After cooling, the sample was transferred to a 100-ml Teflon beaker. Double-distilled 70% $HClO_4$ (1 ml), distilled concentrated HNO_3 (6 ml), and 48% HF (12 ml) were added to the beaker, which was covered with a Teflon lid, and the mixture was refluxed on a hot plate at about 90°C for 24 h. The temperature was then reduced to 60°C, the beaker uncovered, and the solution evaporated nearly to dryness. This procedure was repeated once or twice in order to decompose the silicate minerals. The temperature was then raised to 90°C until $HClO_4$ fumes stopped evolving from the dried cake.

After the cake had been evaporated to dryness, about 50 ml of 0.5 M HCl was added to the beaker, the mixture stirred with a Teflon rod, and the slurry transferred to a 250-ml volumetric flask containing about 100 ml of 0.5 M HCl and a Teflon-coated magnetic stirring bar. The flask was placed on a magnetic-stirring hot plate, the temperature raised to 90°C, and the mixture stirred until all of the slurry dissolved. The clear solution was

cooled to room temperature, the stirring bar was removed, and the solution was made up to 250 ml with 0.5 M HCl. Usually a few mineral grains remained undissolved in each sediment sample. Based on gross physical aspects the minerals appeared to be chiefly zircon, chromite and spinel.

Mass spectrometry. Barium carbonate, enriched in ^{135}Ba, was obtained from Oak Ridge National Laboratory and dissolved in 5% nitric acid to make up a spike solution containing 283 μg Ba ml^{-1}. The isotopic composition of common barium and the spike barium are given in Table 1.

A portion (2 ml) of the sediment solution was mixed with 100 μl of ^{135}Ba spike solution. The mixture was evaporated to dryness in a Teflon beaker, taken up with 5 drops of double distilled water, and about 10 μl of the solution was placed and dried on a pre-baked tantalum filament.

The filament was then inserted into a solid-source 30-cm radius mass spectrometer equipped with an electron multiplier. After the pressure had been reduced to 10^{-7} mm Hg, the filament current was slowly raised to about 1.8 A, corresponding to a temperature of 1000°C. At this temperature the Ba^+ isotopic spectrum was observed. The charged Ba^+ ions, which arrived at the collector, passed through a 50% transmittance grid and impinged on the conversion dynode of an electron multiplier which had a gain of 10^5. The signal was further amplified by passing the collected ion current through a 10^8-ohm resistor connected to the input of a vibrating reed electrometer. The changes in the $^{135}Ba/^{138}Ba$ atom ratio, precisely measured to ±0.1%, were used to compute the barium concentration of sediment samples. The atomic weight correction was incorporated in the calculation as well as the square root of mass ratio correction to compensate for the velocity discrimination in the electron multiplier.

Reproducibility. An indication of the reproducibility of the individual barium analyses was obtained by measuring the variations in apparent concentration of a standard reference material. The standard employed was the U.S. Geological Survey Diabase W-1 which has an accepted barium concentration of 160 ppm [1]. Two vials of this standard were available. One aliquot of the standard was weighed out and processed, along with a chemical blank, with each batch of sediment samples. Altogether six determinations were made on the U.S.G.S. standard — three determinations from each of the two vials. The mean barium concentration of the standard, analyzed by the isotope dilution method, was 157 ppm with a standard deviation of ±1.0 ppm.

TABLE 1

Isotopic composition of common and spike barium (in atom %)

Isotope	130	132	134	135	136	137	138
Common Ba	0.10	0.10	2.42	6.59	7.81	11.32	71.66
Spike Ba							
Oak Ridge	0.1	0.1	0.36	93.6	1.61	0.87	3.56
This paper	0.001	0.005	0.454	93.47	1.629	0.885	3.560

Neutron activation method

Irradiation. Special care was taken to avoid contaminating the samples from the environment, reagents and laboratory utensils. Specimen preparation was carried out in a clean chemical laboratory. All plastic and glass wares were cleaned with detergent and hot tap water, rinsed with deionized water and placed in polypropylene tanks containing 3 M HNO_3 for 24 h. After rinsing three or more times with deionized water, the materials were placed on a laminar flow bench to dry and wrapped in polyethylene sheets.

The total barium determination by instrumental neutron activation was based on the ^{131}Ba activity, which is virtually free from all yield and blank errors [2]. The most serious interference for the 11.7-day ^{131}Ba activity in marine specimens is ^{24}Na which has a half-life of 15 h. Since the barium content of these sediments is relatively high (see Fig. 1), barium assays were successfully performed, without removing the sodium, by "cooling" the irradiated samples for at least 10 days, thus permitting the short-lived ^{24}Na to decay to an acceptable level.

Each sediment sample (1 g) was weighed into 2/5-dram vials which were heat-sealed with an aluminum jacketed soldering iron. After sealing, each vial was tested for leaks by immersing in deionized water and squeezing with stainless steel forceps. These sample vials were in turn placed in 2-dram vials which were also heat-sealed to provide double containment for each

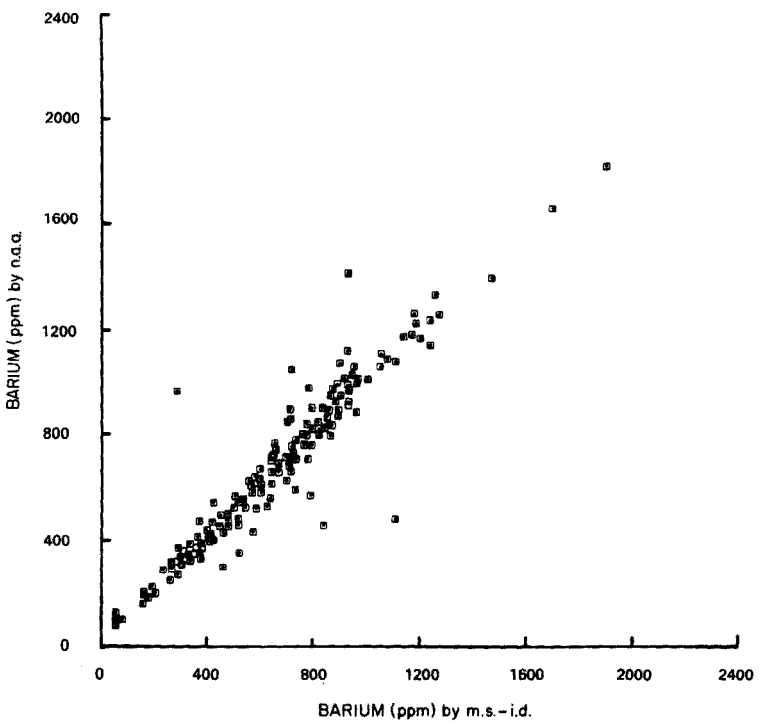

Fig. 1. Barium determinations by m.s.i.d. vs. n.a.a.

sediment sample. These sealed containers were rinsed with deionized water before being placed in the reactor. Up to 65 samples together with 15 blanks, standards and reference materials were irradiated for 14 h in a neutron flux of 2.5×10^{12} n cm^{-2} s^{-1} in the "Triga Mark I" reactor at the University of California at Irvine. After 10- to 12-day "cooling", post-irradiation decontamination of all containers was effected by scrubbing the external surfaces of the vials with detergent and rinsing with deionized water.

Counting. The irradiated samples were assayed for ^{131}Ba by counting the 496-keV γ-rays with a Ge(Li) detector coupled to a minicomputer-based multichannel analyzer (Nuclear Data Model ND-4420). The detector was surrounded with lead (4-in. thick) to reduce the γ-ray background. The inside of the lead shield was lined with tin and copper sheets to absorb x-rays produced by sample γ-ray bombardment of the lead shield. Accurately positioned in front of the detector was a lucite sample holder which also effectively absorbed any β-particles emanating from the sample. Samples to be counted were placed on an inclined sample rack installed over a baffled hole in the lead shield. Each sample was positioned in the sample holder for a 2-h counting period by an automatic sample changer controlled by the analyzer minicomputer.

The Nuclear Data 4,096-channel pulse height analyzer recorded the following data on magnetic tape: γ-ray spectra, live time, time at the end of the irradiation, time at the start of the count, counting time, and sample identification number. The data were subsequently transferred to a central processing computer (SAI DEC-10) for print-out and analysis.

Data processing. The data print-out was qualitatively checked by hand to assure that the proper channels for barium were selected for the quantitative analysis by computer and to search for any spectral interferences. The digital spectra were processed with a modified SAMPO program [3] which located all significant peaks, and calculated the peak energies and areas for barium as well as the predesignated interferences. The results of the SAMPO analysis were provided to the program, ASSAY, that calculated the barium concentration (in ppm) based on the 496-keV ^{131}Ba γ-ray and on the normalization factor determined by the analysis of several barium standards irradiated concurrently with each group of samples.

The root mean square (r.m.s.) error associated with the peak areas used were automatically evaluated in the modified SAMPO program. The r.m.s. error in the normalization factor derived from the barium standards included in each irradiation was also estimated. These errors were combined in the program ASSAY to provide a total estimated r.m.s. error for the barium determination.

Quality control. Blank samples, determined with each irradiation, contained less than 2 μg of barium. Standards totalling 10% of the number of sediment samples to be determined were included in each batch of assays. All systematic errors of any given barium determination were found to be less than 3%.

The barium concentration of the Diabase W-1 standard, analyzed by the neutron activation method, was 140 ± 40 ppm. The estimated precision included uncertainty from counting statistics and all systematic errors.

Comparison of methods

Both the isotope dilution and the neutron activation analyses gave the total barium concentration of the sediments. The barium content of some 208 sediment samples from Southern California coasts ranged from 43 to 1899 ppm. The results of these two different methods were compared by plotting a linear regression line of their respective concentrations in the sediments (Fig. 1). Calculated from the slope of the regression line, the correlation coefficient of these two sets of data was 0.923. The mean barium concentration of these samples was 653 ppm by isotope dilution and 675 ppm by neutron activation analysis. The difference between the two means was about 3%.

We thank A. Soutar and D. Straughan for the collection of sediment samples, and C. B. Snyder for laboratory assistance. The help of V. P. Guinn in planning the neutron activation analysis is acknowledged. This work was supported by the U.S. Bureau of Land Management-Pacific OCS No. 08550-CT5-52 and the Marine Chemistry Program of the National Science Foundation.

REFERENCES

1 F. J. Flanagan, Geochim. Cosmochim. Acta, 37 (1973) 1189.
2 V. P. Guinn, Chapter 98, Activation Analysis, in I. M. Kolthoff and P. J. Elving (Eds.), Treatise of Analytical Chemistry, Part 1, Vol. 9, J. Wiley, New York, 1971.
3 J. T. Rutti, SAMPO — A Fortran IV Program for Computer Analysis of Gamma Ray Spectra from Ge(Li) Detectors, and for Other Spectra with Peaks, Lawrence Radiation Laboratory, University of California, Berkeley, UCRL-19452, 1969.

Analytica Chimica Acta, 96 (1978) 401—404

Short Communication

EFFECT OF REDUCING AGENTS OF PHARMACOLOGICAL IMPORTANCE ON THE CHEMILUMINESCENCE OF TRIS-(2,2'-BIPYRIDINE)RUTHENIUM(II)

WILLIAM K. NONIDEZ** and DONALD E. LEYDEN*

Department of Chemistry, University of Georgia, Athens, Georgia 30602 (U.S.A.)

(Received 11th May 1977)

In 1966, Hercules and Lytle [1] reported that the reduction of tris-(2,2'-bipyridine)ruthenium(III) ($Ru(bipy)_3^{3+}$) in 0.05 M H_2SO_4 solution, upon the addition of hydroxide ion or hydrazine, resulted in intense light emission at 600 nm. Other reducing agents tested, such as Na_2SO_3, $Na_2S_2O_3$, and $SnCl_2$, did not produce chemiluminescence. The reduction causes chemiluminescence as a result of the production of excited-state tris-(2,2'-bipyridine)ruthenium(II) ($Ru(bipy)_3^{2+}$) which relaxes to the ground state with light emission. $Ru(bipy)_3^{2+}$ is known to be a strongly phosphorescent compound [2]. The use of $Ru(bipy)_3^{2+}$ as a sensitizer in photo-reactions [3—6], and quenching studies of the luminescence of this complex by other molecules [7—10] have been reported.

The results of Hercules and Lytle [1] suggested the utilization of $Ru(bipy)_3^{3+}$ as a selective analytical reagent for the generation of chemiluminescence in the presence of some reducing agents of pharmaceutical importance. The theoretical criteria for light emission in these reactions are: (1) fast reaction rates, (2) sufficient reaction energy to produce an excited state, (3) presence of an emitter to release the excitation energy and the presence of a species capable of forming an excited electronic state, and (4) the absence of quenchers in the reaction mixture. The $Ru(bipy)_3^{2+}$ complex fulfills requirement (3); the question of whether a given reducing agent will cause chemiluminescence depends on whether the remaining criteria are met. These criteria are difficult to predict a priori. Therefore, the feasibility of a given reaction resulting in light emission is usually determined empirically.

A well known antihypertensive agent, hydralazine (1-hydrazinothalazine), can be considered as a substituted hydrazine and is known to be a good reducing agent [11]. Preliminary tests confirmed that hydralazine does reduce $Ru(bipy)_3^{3+}$ with the emission of light. However, this communication shows that the reaction is not as selective as earlier results indicated it may be.

*Author to whom reprint requests should be sent. Present address: Department of Chemistry, University of Denver, Denver, CO. 80210.

**Present address: Department of Chemistry, West Georgia College, Carrolton, GA.

Experimental

Apparatus. Light intensities were measured with a Hamamatsu R818 high-cathode-sensitive photomultiplier, with spectral sensitivity in the 185—850-nm range powered at 1100—1250 V by a Kepco Model ABC 2500 M regulated power supply. The signal was amplified by a Keithley Solid-State 610C electrometer and recorded on a Hewlett-Packard Model 7172A potentiometric strip chart recorder.

Steady-state chemiluminescence was observed by using the flow cell shown in Fig. 1. A Masterflex Model 7545-10 peristaltic pump equipped for two-channel operation with pump head Models 7013 and 7013-20 was used to pump simultaneously the tris-(2,2′-bipyridine)ruthenium(III), and sulfuric acid into the flow cell from their respective containers. This allowed a background luminescence to be established. The sample, which was an aqueous solution of hydralazine, was introduced into the flow cell via a three-way valve to allow pumping from either the solvent or sample container. All lines in the flow system were constructed of either Teflon or Tygon tubing except the lines utilized in the peristaltic pump which were of silicone rubber.

The oxidized (3+) state of the ruthenium chelate was produced by controlled potential electrolysis. The U-shaped Pyrex electrolysis cell used was fitted with a fine glass frit between the anode and cathode chambers which were 100 ml and 30 ml, respectively. The anode was a cylindrical platinum gauze. The controlled anode potential was +1.10 V versus a saturated calomel electrode. The potentiostat circuit was constructed from operational amplifiers (Analog Devices Corporation, Model 118A) which allow a maximum current of 5 mA. Voltage was regulated by measuring the potential between the reference electrode and the working electrode and the extent of the electrolysis was monitored by measuring current decay. This method proved to be an efficient way to produce and maintain the $Ru(bipy)_3^{3+}$ in solution.

Dissolved oxygen was removed from all solutions by nitrogen bubbling, which also ensured constant mixing in the electrolytic cell. In all cases,

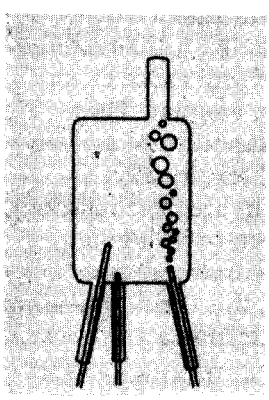

Fig. 1. Diagram of flow cell.

extra-high purity nitrogen was used; any oxygen present was removed by passing through copper turnings packed in a quartz tube (1-in. diameter, 2 ft long) which was placed in a Lindburg furnace Type 55035-A at 500°C. The oxidized copper was regenerated periodically by passing Selox hydrogen at 500°C. Before the nitrogen was passed into the solutions, it was bubbled through distilled water to insure that it was cooled and equilibrated with water vapor.

Reagents. $[Ru(bipy)_3]Cl_2 \cdot 6H_2O$ (G. F. Smith Chemical Co.) was used without further purification to prepare 1×10^{-2} M solutions. The acidity of these solutions was controlled by adding concentrated sulfuric acid. The hydralazine hydrochloride was obtained from Sigma Scientific Co.

Hydrochlorothiazide was supplied as a powder. Reserpine was received as an aqueous solution (1 mg ml^{-1}) preserved with 1% propylene glycol. These compounds were obtained from the University of Georgia School of Pharmacy.

All other reagents (Fisher Scientific Company) were either reagent or analytical grade. All solutions were prepared from distilled water passed through a mixed bed ion-exchange resin D5040 Standard Cartridge (Scientific Products Co.).

Procedure. A solution 3×10^{-4} M in tris-(2,2′-bipyridine)ruthenium(II) and 1 M in H_2SO_4 was prepared by pipetting 6 ml of chelate stock solution and 1.1 ml of 18 M H_2SO_4 into a 200-ml volumetric flask and diluting to the mark with distilled water. An aliquot (20 ml) of this solution was placed in the cathode compartment of the electrolytic cell and the remainder in the anode compartment. The electrodes were then put in place and the solution was deoxygenated for 30 min by passing purified nitrogen. The current was switched on and the electrolysis allowed to proceed for 40 min. When the chelate was completely oxidized, the peristaltic pump was started at a pumping rate of 3.6 ml min^{-1}, pumping the chelate and blank solution simultaneously into the flow cell. As soon as the baseline had settled to a constant value, adjustments of the nitrogen stirring rate in the flow cell could be made to lower the noise level in the system. Samples were then introduced for 20-s periods. This will introduce 1.2 ml of sample which is sufficient to allow steady-state readings.

Discussion

Demos et al. [12] have reported the excited-state quenching of the $Ru(bipy)_3^{2-}$ species by molecular oxygen in both methanol and water. This phenomenon was found to have a bimolecular quenching constant which approached the diffusional controlled limit, indicating that a large fraction of collisions result in deactivation of the excited state. This phenomenon was indeed found to cause quenching in the system described here. It was observed that the sensitivity and detection limit for hydralazine were affected by the amount of oxygen present.

The problem created by the quenching of the chemiluminescence by

oxygen was not inordinately difficult to minimize. Deoxygenation with high-purity nitrogen provided sufficient reproducibility for an analytical method. In a typical run, thirteen solutions of hydralazine (5.41×10^{-7}–2.86×10^{-5} M) resulted in a linear response with a linear least-squares fit to give the expression: Relative Response = 4.0×10^{4} [hydralazine] + 3.46×10^{-3}, with a correlation coefficient of 0.9999. If the detection limit is defined as the concentration of hydralazine which gave a signal three times the standard deviation of the background noise, the lower limit of detection was found to be 9.6×10^{-9} M. A concentration of $Ru(bipy)_3^{3+}$ at least 22 times the concentration of hydralazine was required to insure linearity.

The method reported appears to show considerable potential. However, a number of organic substances present in samples such as urine or blood are reducing agents. Because these compounds must be able to reduce the chelate with rapid kinetics and large energy production, it was hypothesized that relatively few compounds would be able to produce light in this system. It was surprising to find that various compounds reduced the chelate with the production of chemiluminescence. Ascorbic acid quenched the reaction. Chlorothiazide gave a very strong response; strong responses also appeared with hydralazine and reserpine, the latter with high noise. Hydrazine sulfate caused a weak chemiluminescence (non-linear with concentration) whereas the weak signal from oxalic acid was linear with concentration. Glucose caused a very weak response, and ethylene glycol gave none.

Several of these compounds are expected to be present in biological fluids. Reserpine is frequently compounded with hydralazine when the latter is administered as an antihypertensive agent. The lack of selectivity of the reaction reported here creates serious limitations to its analytical usefulness. There may, however, be potential if the method were employed as a chemiluminescence detector for a separation technique such as liquid chromatography.

This work was supported in part by research grant MPS 73-08675 0A2 from the National Science Foundation.

REFERENCES

1 D. M. Hercules and F. E. Lytle, J. Am. Chem. Soc., 88 (1966) 4745.
2 D. M. Hercules and F. E. Lytle, J. Am. Chem. Soc., 91 (1969) 253.
3 J. N. Demas and A. W. Adamson, J. Am. Chem. Soc., 93 (1971) 1800.
4 P. Natarajan and J. R. Endicott, J. Phys. Chem., 77 (1973) 971.
5 H. D. Gofney and A. W. Adamson, J. Am. Chem. Soc., 94 (1972) 8238.
6 G. S. Laurence and V. Balzani, Inorg. Chem., 13 (1974) 2976.
7 G. Navon and N. Sutin, Inorg. Chem., 13 (1974) 2976.
8 F. Boletta, M. Maestri and L. Moggi, J. Phys. Chem., 77 (1973) 861.
9 J. N. Demas, D. Diemente and E. W. Harris, J. Am. Chem. Soc., 95 (1973) 6864.
10 I. Fiyeta and H. Koboyashi, Ber. Bunsenges. Phys. Chem., 76 (1972) 115.
11 S. Fallab, Helv. Chim. Acta, 45 (1962) 1957.
12 J. N. Demos, D. Diemente and E. W. Harris, J. Am. Chem. Soc., 95 (1973) 6864.

Analytica Chimica Acta, 96 (1978) 405—409

Short Communication

DOSAGE DES SULFATES DANS LES EAUX NATURELLES A L'AIDE D'UNE ELECTRODE SELECTIVE AU BARYUM

GÉRALD OUZOUNIAN et GIL MICHARD*

Groupe de Géochimie des Eaux (LA 196), Université Paris 7, Tour 54-53, 2, place Jussieu 75221 Paris Cedex 05 (France)

(Reçu le 25 juillet 1977)

Parmi les problèmes qui peuvent conduire les géochimistes à s'intéresser à l'analyse des sulfates dans les eaux naturelles, les plus intéressants nécessitent souvent des mesures immédiates. L'un de ces problèmes est la réduction progressive des sulfates dans les eaux interstitielles des sédiments actuels, où d'après Berner [1] le gradient vertical de disparition des sulfates permet une estimation de la vitesse de sédimentation. L'autre concerne les sources thermales sulfureuses; ces sources contiennent à la fois sulfures, sulfates et thiosulfates. Le rapport sulfate/sulfure ainsi que les rapports isotopiques $^{32}S/^{34}S$ de ces deux espèces sont des paramètres dont on espère pouvoir tirer des renseignements quant à l'origine et à la température profonde des eaux thermales [2]. Dans ces deux cas, il serait très intéressant de pouvoir doser les sulfates sur le terrain. Généralement en effet, on mesure les autres espèces sur place et on obtient le sulfate par différence après une mesure du soufre total au laboratoire sur une solution que l'on oxyde au moment du prélèvement.

Les méthodes classiques de dosage des sulfates telles que gravimétrie, colorimétrie ou absorptiométrie ne sont pas adaptables à ce problème. Plusieurs auteurs [3—6] ont proposé l'utilisation d'électrodes spécifiques mais celles-ci sont soit peu sélectives, soit difficilement utilisables en titration. Nous avions pensé dans un premier temps décationiser nos échantillons, puis précipiter le sulfate de baryum et enfin mesurer l'excès de baryum en solution à l'aide d'une électrode à ions divalents. Levins en 1971 [7] propose l'utilisation directe d'une électrode sensible au baryum. Nous avons légèrement modifié l'électrode de Levins principalement pour utiliser des produits aisément disponibles dans le commerce, et nous avons pu montrer que l'électrode ainsi préparée permettait des mesures dans les conditions que nous rencontrons fréquemment dans les analyses d'eaux naturelles, dans une marge d'erreur inférieure à 1% pour les milieux relativement concentrés.

Partie expérimentale

Préparation des électrodes. Le corps de l'électrode de mesure utilisé pour ce travail est commercialisé par Orion pour le dosage des ions divalents: Orion,

modèle 92-32. Le liquide de remplissage externe est un échangeur de baryum basé sur les propriétés électriques et stériques de l'ion Ba^{2+}. Il est préparé par dissolution d'une solution saturée en chlorure de baryum dans du Triton N101 (*p*-nonylphenoxypolyethoxyethanol, réactif de scintillation Koch-Light) et par précipitation de l'ion oxonium ainsi obtenu par du tétraphenylborate de sodium en excès. Le précipité est bien lavé à l'eau, filtré et séché dans un dessiccateur sous vide à moins de 50°C. Ce précipité repris à saturation dans du *p*-nitroéthylbenzène (réactif Koch-Light) constitue la solution de remplissage externe de l'électrode. Le liquide de remplissage interne est une solution de chlorure de baryum 10^{-1} M saturée en chlorure d'argent. La membrane, compatible avec les alcools et les solutions aqueuses, est en triacétate de cellulose et a une porosité de 0,45 μm (Gelman, Metricel GA-6). L'électrode de référence est une électrode double-jonction Orion modèle 90-02-00 dont le remplissage externe est effectué avec une solution de trichloroacétate de lithium 3 M. Avant la mesure, les électrodes doivent être conditionnées pendant 1—2 h dans une solution de chlorure de baryum 10^{-3} M.

Conditions d'utilisation de l'électrode. La réponse de l'électrode est linéaire, quasi Nernstienne, jusqu'à une concentration de $3 \cdot 10^{-5}$ M de baryum. Sa pente est de 25 mV par décade entre 10^{-1} et $3 \cdot 10^{-5}$ M (Fig. 1). Cette droite d'étalonnage a été obtenue par passage de l'électrode dans des solutions de chlorure de baryum de plus en plus diluées. La même droite a été tracée par ajouts successifs d'EDTA à une solution de baryum. L'équilibre est atteint en moins d'une minute sur toute la gamme de concentrations, et le potentiel est stable plusieurs heures. Une légère dérive de 1—2 mV peut être observée en 2—3 jours; chaque remplissage de l'électrode permet de travailler environ 5 jours. Nous avons en effet constaté quelques pertes de liquide externe, ce qui limite sa durée d'utilisation. Par ailleurs, la solution n'étant pas très stable, il est préférable de conserver le complexe sous forme solide

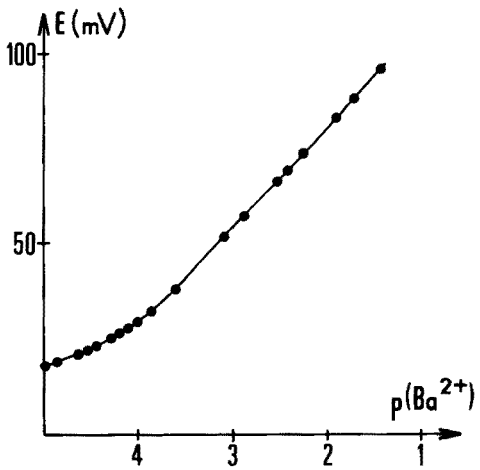

Fig. 1. Réponse de l'électrode à l'ion Ba^{2+}.

et de le dissoudre dans le *p*-nitroéthylbenzène juste avant le remplissage de l'électrode.

Nous avons recherché les conditions d'utilisation les plus précises et les mieux adaptées au dosage des sulfates dans les eaux naturelles. Plusieurs possibilités ont été envisagées et seule la titration directe du sulfate par le baryum a été retenue. L'électrode mesurant l'activité du baryum en solution [7], il faudrait une analyse complète de l'échantillon pour déterminer de façon précise la concentration en baryum. Les méthodes rapides développées par analogie avec celle qu'utilisent Culberson et al. [8] pour la détermination de la réserve alcaline sont donc rendues imprécises dans le cas d'une eau naturelle par les incertitudes sur le coefficient d'activité de l'ion Ba^{2+} et son degré de complexation. La méthode de Gran [9] souvent conseillée pour les mesures à faible concentration peut également entrainer des incertitudes si la pente de l'électrode est mal connue ou peu reproductible. Elle peut en effet varier de 1 ou 2 mV d'un remplissage de l'électrode à un autre.

Aux faibles teneurs en sulfates, la précipitation du sulfate de baryum étant lente, nous l'avons initiée par addition d'un peu de $BaSO_4$ solide, et nous avons favorisé cette précipitation en travaillant en milieu 40% méthanol. La stabilisation du potentiel est ainsi rapide et par conséquent le dosage également. Etant donné l'insensibilité de l'électrode aux ions H^+, elle peut être utilisée dès pH 2, afin d'éviter la précipitation du carbonate de baryum.

Tenant compte de ces considérations, la courbe de titration a été tracée pour chaque échantillon. Le saut de potentiel est de l'ordre de 60 mV pour une solution de sulfate $4 \cdot 10^{-4}$ M. La précision obtenue est meilleure que 1% pour les solutions étalons.

Exemples d'utilisation

Nous avons dosé le sulfate dans une eau de mer par titration directe (Fig. 2A) et nous avons comparé le résultat à ceux obtenus par la méthode gravimétrique après décationisation et filtration. Les deux méthodes ont respectivement donné $2{,}796 \cdot 10^{-2}$ M (s = 0,53%, n = 5) et $2{,}820 \cdot 10^{-2}$ M (s = 0,1%, n = 2) de sulfates en moyenne. L'écart entre les deux résultats n'est que de 0,85%. Parmi toutes les espèces dissoutes dans l'eau de mer, aucune ne perturbe le dosage. A moins de 10^{-5} M de baryum, la réponse de l'électrode n'est pas modifiée par la présence d'autres cations aux concentrations décrites dans le Tableau 1. Les valeurs maximales des constantes de sélectivité sont reportées dans ce même tableau. L'électrode a également été utilisée pour le dosage des sulfates dans les cendres du volcan La Soufrière (Guadeloupe). Les mesures ont été effectuées après lessivage des cendres à l'eau déminéralisée à 50°C pendant 2 h. La reproductibilité du dosage sur une première eau de lessivage est de 0,10 pour une teneur de $1{,}96 \cdot 10^{-3}$ M de sulfates. Le premier lessivage permet d'extraire 97% des sulfates contenus dans ces cendres; au second lessivage, le reste des sulfates est passé en solution.

Nous avons aussi utilisé cette électrode pour le dosage des sulfates dans 60 eaux thermales sulfurées des Pyrénées Orientales et de la Corse (France).

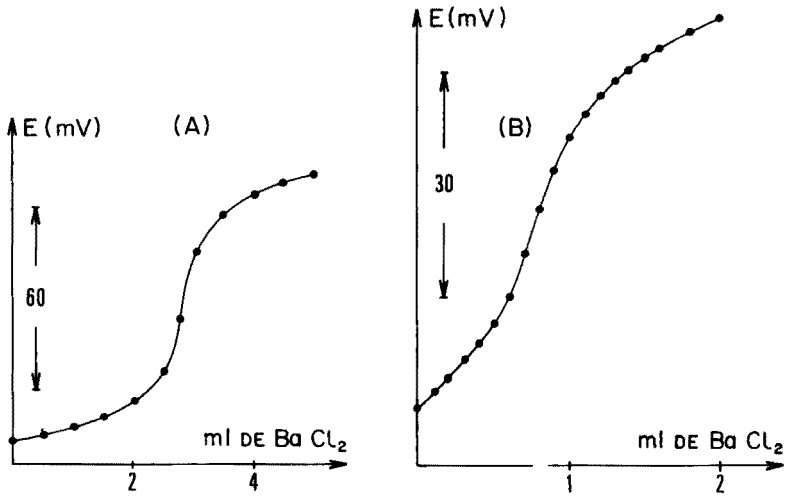

Fig. 2. A. Dosage des sulfates dans 10 ml d'eau de mer par $BaCl_2$ 10^{-1} M. B. Dosage des sulfates dans 50 ml d'eau de La Goccia (Guagno, Corse) par $BaCl_2$ $5 \cdot 10^{-2}$ M, après élimination des sulfures par acidification.

TABLEAU 1

Concentrations c des cations M^{z+} dans l'eau de mer et valeurs maximales des constantes de sélectivité K_{Ba-M}

M^{z+}	Concentration c (M)	K_{Ba-M}
Na^+	$4{,}81 \cdot 10^{-1}$	$2{,}1 \cdot 10^{-5}$
K^+	$10{,}17 \cdot 10^{-3}$	$9{,}8 \cdot 10^{-4}$
Ca^{2+}	$1{,}06 \cdot 10^{-2}$	$9{,}4 \cdot 10^{-4}$
Mg^{2+}	$5{,}46 \cdot 10^{-2}$	$1{,}8 \cdot 10^{-4}$

Ces eaux contiennent des sulfates, des sulfures et des thiosulfates. Les sulfures ont été chassés à l'émergence par acidification et les sulfates dosés dans les heures qui suivent le prélèvement. Les thiosulfates ne s'oxydant que très lentement ne faussent pas du tout le dosage. Un tel traitement sur les solutions artificielles a permis une mesure des sulfates à 0,4% près. Le sulfite est aussi totalement chassé par acidification lorsqu'il intervient dans le composition d'une eau. La Fig. 2B représente une courbe de dosage tracée pour l'eau de La Goccia (Guagno-Corse). Sa teneur en sulfates est de $7{,}6 \cdot 10^{-4}$ M: l'ensemble de ces mesures a donné des résultats compris entre $1{,}8 \cdot 10^{-4}$ M et $2{,}22 \cdot 10^{-3}$ M de sulfates.

Conclusion

L'utilisation d'une telle électrode permet d'obtenir des résultats rapides et précis dans une gamme de concentrations où les autres méthodes n'étaient pas toujours satisfaisantes. Sa facilité d'emploi rend possible le dosage des

sulfates sur le terrain dans le cas d'eaux contenant des espèces réduites du soufre, ce qui est particulièrement intéressant.

BIBLIOGRAPHIE

1 R. A. Berner, Earth Planet. Sci. Lett., (1977), sous presse.
2 B. W. Robinson, Earth Planet. Sci. Lett., 18 (1973) 443.
3 G. A. Rechnitz, Z. F. Lin et S. B. Zamochnick, Anal. Lett., 1 (1967) 29.
4 E. B. Buchanan, Jr. et J. L. Seago, Anal. Chem., 40 (1968) 517.
5 G. A. Rechnitz, G. H. Fricke et M. S. Mohan, Anal. Chem., 44 (1972) 1098.
6 M. Mascini, Analyst, 98 (1973) 325.
7 R. J. Levins, Anal. Chem., 43 (1971) 1045.
8 C. P. Culberson, R. M. Pytowicz et J. E. Hawley, J. Mar. Res., 28 (1970) 15.
9 G. Gran, Analyst, 77 (1952) 661.

Analytica Chimica Acta, 96 (1978) 411—415

Short Communication

BIAMPEROMETRIC DETERMINATION OF MICROGRAM AMOUNTS OF TELLURIUM(IV) WITH COULOMETRICALLY GENERATED SILVER(I)

Z. MARCZENKO* and T. KOWALSKI

Department of Analytical Chemistry, Technical University, Warsaw (Poland)

(Received 7th August 1977)

Microgram amounts of tellurium, one of the principal components of semiconductor materials of the $A^{II}B^{VI}$ type, are generally determined by spectrophotometric methods. Most of these are based on colour reactions of tellurium(IV) with organic reagents [1]. Coulometric methods have also been used for the determination of microgram amounts of tellurium. Agasyan et al. [2] determined 25—100 μg of tellurium by a potentiostatic coulometric method in which tellurium(IV) was reduced to the elemental state on a platinum electrode in phosphate buffer medium. The error of the determination was 10—3%. In another method [3], 100—500 μg of tellurium(IV) was oxidized with potassium permanganate, and the excess of permanganate was back-titrated with coulometrically generated iron(II); the error of this determination was 10—5%. Similar results were obtained when potassium dichromate [4] was used. Methods based on reduction of tellurium(IV) by coulometrically generated tin(II) and titanium(III) have also been developed; in the tin(II) method [5], 30—150 μg of tellurium was determined with an error of 7—0.7%, but the results obtained by the titanium(III) method [6] were considerably worse.

In the method described here, microgram amounts of tellurium(IV) are titrated with coulometrically generated silver(I). The method is based on precipitation of sparingly soluble silver tellurite [7]. A silver electrode, polarized anodically in 0.05 M sodium sulphate solution and 0.01 M borate buffer, is used as the silver(I) source. Obviously, the supporting electrolyte should not contain ions that form stable compounds with tellurium(IV) or silver(I), and a buffer is needed because tellurium(IV) occurs in several forms which remain in equilibrium [8].

$$TeO_3^{2-} \underset{OH^-}{\overset{H_2O}{\rightleftharpoons}} HTeO_3^- \underset{H_2O}{\overset{H^+}{\rightleftharpoons}} TeOOH^+$$

The formation of tellurite is accompanied by liberation of protons.

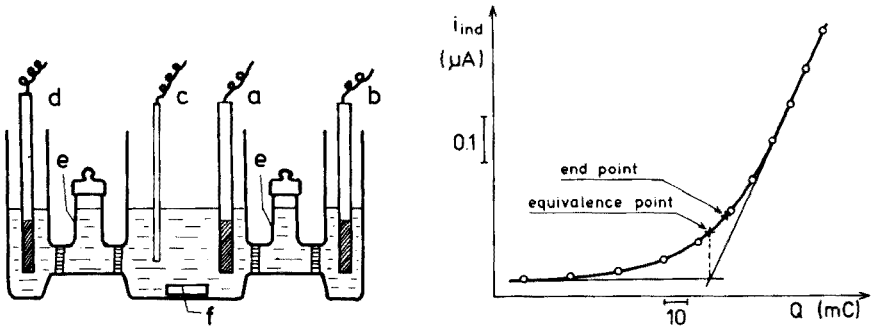

Fig. 1. Coulometric cell. (a) Generator electrode, (b) auxiliary electrode, (c) indicator electrode, (d) reference electrode, (e) salt bridges, (f) stirrer.

Fig. 2. Biamperometric end-point in the titration of tellurium(IV) with electrogenerated silver(I).

Experimental

Apparatus. A universal coulometric analyser (OH-404, Radelkis, Hungary) was used. To increase the sensitivity, the standard coulometric cell provided with the coulometer was replaced by a smaller cell (Fig. 1). The central compartment of the cell contained the supporting electrolyte, the test solution and the generating (silver electrode with an area of ca. 2 cm^2) and indicator (silver wire) electrodes. The auxiliary (platinum) and reference (SCE) electrodes were mounted in the side compartments. The salt bridges were filled with 0.5 M sodium sulphate solution. The small cell allowed titrations of solution of 20-ml volume.

Aliquots of tellurium solutions (standard and sample) were measured by means of weight pipettes.

Reagents. Analytical-grade reagents were used. Twice-distilled water was used for preparation of the solutions.

Tellurium(IV) standard solution (1 mg Te ml^{-1}). Dissolve 100 mg of tellurium (99.9%) in 1 ml of 18 M sulphuric acid by heating. Dilute the solution with about 50 ml of water and adjust to pH 10—11 with 5 M and 0.5 M sodium hydroxide solutions. Dilute to 100 ml with water.

End-point detection. The coulometer OH-404 is designed for titrations to a pre-set point by potentiometric and amperometric techniques; titration is terminated when the electrode potential or indicator current attains a pre-set value. The OH-404 coulometer is provided with a system which permits accurate detection of end-points.

Preliminary examination of the suitability of potentiometric, amperometric and biamperometric techniques showed that the biamperometric method with two silver indicator electrodes provided the best results. The end-point i.e. the value of the indicator current at which the titration was terminated, was chosen on the basis of a coulometric titration curve of tellurium(IV) with

silver(I). The end-point was taken slightly beyond the equivalence point, on the steeper section of the titration curve (Fig. 2), because accurate detection on the flatter section was difficult. This choice of end-point can give rise to positive errors in single titrations. Such errors could be avoided by series analysis: successive portions of tellurium(IV) solution were added to the same supporting electrolyte and each was titrated to the same end-point. For such titrations, the volume of the titrated solution should be constant, the distance between the end-point and equivalence point should not be excessive, and the properties of the indicator electrodes should not change during successive titrations. In this work, the volumes of the tellurium(IV) solution added to the coulometric cell were small (ca. 0.1 ml) compared to the volume of the supporting electrolyte (ca. 20 ml), and the position of the end-point was carefully selected. The small scatter of the results obtained in series of measurements suggests that the properties of the indicator electrodes were unaffected.

Procedure. Aliquots (0.1—0.2 ml) of standard tellurium(IV) solution were successively added to the supporting electrolyte (0.05 M sodium sulphate solution and 0.01 M borate buffer). Tellurium was then titrated with silver(I) generated at a current of 75 μA. When a higher generating current was used, the response of the system to changes in reagent concentration was too slow. Titrations were carried out at exactly 5-min intervals to ensure similar conditions during titration of successive portions. The titrations were terminated when the indicator current attained the pre-set value. Each measuring series comprised seven determinations, of which the first two results were discarded. Both aqueous and aqueous ethanol (1 + 1) media were tested. The indicator electrodes were polarized at 300 mV.

Results and discussion

The course of the titration curves for tellurium(IV) and therefore the precision of the results, depends significantly on the pH of the titrated solution. As the pH decreases, the titration curves become flatter because of the increased solubility of silver tellurite (Fig. 3). Better relative standard deviations (s_r) were obtained at higher pH values in aqueous media (Table 1). The systematic positive error obtained in aqueous medium is presumably due to a side-reaction with formation of basic silver tellurite.

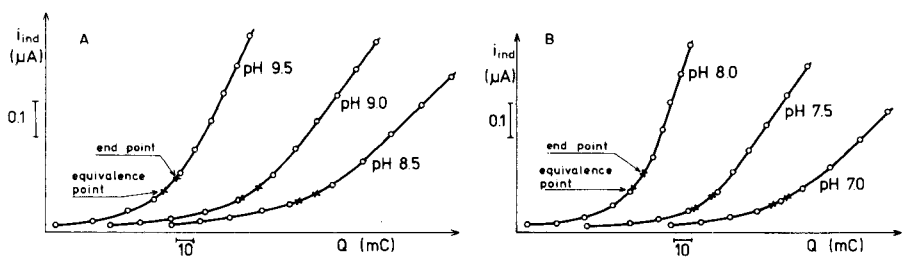

Fig. 3. Titration curves for the biamperometric titration of tellurium(IV) with electrogenerated silver(I). A, Aqueous solution. B, Aqueous ethanol (1+1) solution. Indicating electrode system, 300 mV applied to a double silver wire electrode. Generating current, 75 μA.

TABLE 1

Results of coulometric determination of tellurium(IV) in aqueous and aqueous ethanol (1 + 1) media

Aqueous media				Aqueous ethanol media			
Te(IV) added (μg)	Te(IV) found (μg)	Recovery factor[a]	s_r (%)	Te(IV) added (μg)	Te(IV) found (μg)	Recovery factor[a]	s_r (%)
pH 8.5				*pH 8.0*			
21.46	22.08	1.029		22.19	22.39	1.009	
22.17	22.17	1.000		22.49	22.51	1.001	
22.82	23.82	1.044	0.78	20.17	20.01	0.992	0.39
22.51	22.64	1.006		21.04	20.81	0.989	
23.43	24.02	1.025		21.95	22.08	1.006	
pH 9.0							
23.10	24.62	1.066		45.82	45.87	1.001	
22.47	23.17	1.031		43.90	44.38	1.011	
22.49	23.82	1.059	0.67	46.09	46.37	1.006	0.24
23.05	24.29	1.054		45.70	45.65	0.999	
22.25	22.98	1.033		44.11	44.55	1.010	
pH 9.5							
22.13	23.92	1.081		92.08	92.36	1.003	
20.73	22.16	1.069		91.73	92.10	1.004	
20.49	22.38	1.092	0.48	91.89	91.89	1.000	0.15
22.50	24.01	1.067		91.73	92.19	1.005	
21.24	23.15	1.090		92.40	92.12	0.997	

[a]The recovery factor is based on the amount of Te(IV) found per 1 μg Te(IV) added.

Because of the generally lower solubility of ionic compounds in partly non-aqueous media, the titrations were re-examined in water—ethanol (1+1) solutions. The titration curves in this medium were steeper than in aqueous medium (Fig. 3B). The results of such titrations at pH 8.0 (Table 1) showed increased precision and accuracy compared to the results obtained for aqueous media.

Conclusions

The proposed biamperometric coulometric titration of tellurium(IV) allows the determination of microgram amounts with higher precision than that of earlier methods. The method is suitable for the determination of 20—100 μg of tellurium (1—5 μg Te ml^{-1}) with a relative standard deviation of 0.40—0.15% (5 results). Titrations are possible in aqueous medium at pH 8.5—10.0 or in aqueous ethanol medium at pH 7.0—9.0.

Tellurium can be determined in the presence of anions that do not yield sparingly soluble or poorly dissociated complexes with silver. Because of the low solubility of most metal tellurites, only alkali metal cations can be present. Prior separation of tellurium is therefore essential for practical samples.

REFERENCES

1 Z. Marczenko, Spectrophotometric Determination of Elements, Ellis Horwood, Chichester, 1976.
2 L. B. Agasyan, A. G. Yurchenko and P. K. Agasyan, Zh. Anal. Khim., 22 (1967) 229.
3 P. K. Agasyan, A. N. Denisova, L. B. Agasyan and E. V. Nikolaeva, Zavod. Lab., 34 (1968) 129.
4 V. K. Khakimova and P. K. Agasyan, Uzb. Khim. Zh., (1960), No. 6, s. 21; cited in: Zavod. Lab., 34 (1968) 129.
5 L. B. Agasyan, E. V. Nikolaeva, P. K. Agasyan and Z. M. Lebedeva, Izv. Vyssh. Ucheb. Zav., Khim. Khim. Tekhnol., 12 (1967) 1315.
6 L. B. Agasyan, E. V. Nikolaeva and P. K. Agasyan, Zh. Anal. Khim., 22 (1967) 904.
7 W. Wawrzyczek and W. Wiśniewski, Chem. Anal. (Warsaw), 8 (1963) 395.
8 Gmelin Handbuch der Anorganischen Chemie, Teil B1, Ergänzungsband, Springer Verlag, Berlin, 1976, p. 86.

Analytica Chimica Acta, 96 (1978) 417—420

Short Communication

ELECTROCHEMICAL BEHAVIOR OF THE TUNGSTEN ELECTRODE IN THE PRESENCE OF IRON(III)

C. C. LIU

Department of Chemical and Petroleum Engineering, University of Pittsburgh, Pittsburgh, PA 15260 (U.S.A.)

V. A. KIMSTACH** and J. F. COETZEE*

Department of Chemistry, University of Pittsburgh, Pittsburgh, PA 15260 (U.S.A.)

(Received 21st June 1977)

Many ligands form sufficiently stable complexes with iron(III) to suggest the possibility of quantitative titrimetric determination. However, the lack of a satisfactory indicator electrode has generally ruled out potentiometry for such purposes, although in some cases a little iron(II) may be added to establish the iron(III)—(II) redox couple and thus allow potentiometric titration at a platinum electrode [1]. Yet, the fluoride ion may be titrated with iron(III) without adding iron(II) if a tungsten electrode is used [2, 3].

The purpose of this communication is to clarify the "anomalous" response of the tungsten electrode in the presence of iron(III) and to show that this response is analytically useful in a number of complexiметric titrations with iron(III).

Experimental

Materials. All chemicals were reagent grade. The tungsten wire electrode was of 1.6-mm diameter. It was cleaned with emery paper, washed with distilled water, and then immersed in 0.1 M hydrochloric acid for 5 min before each experiment.

Apparatus. Potentiostatic measurements were made with a Princeton Applied Research Model 170 Electrochemical System. The reference electrode was a saturated calomel electrode. All potentials reported are reduction potentials and refer to the saturated calomel electrode, except where otherwise noted.

Results and discussion

Potentiostatic polarization curves of the tungsten electrode in solutions containing varying concentrations of iron(III) chloride and 0.1 M hydrochloric

**IREX scholar, on leave of absence from Department of Chemistry, Rostov State University, Rostov-on-Don, U.S.S.R.

acid as supporting electrolyte are shown in Fig. 1. With the supporting electrolyte alone, considerable anodic currents are obtained. It seems likely that the anodic process responsible for these currents is formation of tungsten hemipentoxide, W_2O_5 [4]. The standard reduction potential of the W_2O_5—W couple is —0.04 V vs. NHE or —0.28 V vs. SCE, so that the thermodynamic potential of the couple in 0.1 M HCl will be —0.34 V vs. SCE. However, formation of W_2O_5 is expected to be highly irreversible electrochemically and to occur at much more positive potentials than the thermodynamic value. When up to 10^{-4} M iron(III) chloride is added, the polarization curves remain very similar to the background curve, but at higher concentrations the expected reduction of iron(III) is observed.

Figure 2 shows that, in a 10^{-2} M solution of iron(III) chloride, the behavior of the tungsten electrode is quite different from that of the platinum electrode. Whereas the potential of the platinum electrode at zero current is unpoised, the corresponding potential of the tungsten electrode is sufficiently poised to suggest the presence of not only iron(III), but also iron(II), at the electrode surface. The iron(II) must be produced by reactions such as $10Fe^{3+} + 2W + 5H_2O \rightarrow 10Fe^{2+} + W_2O_5 + 10H^+$, or $6Fe^{3+} + W + 3H_2O \rightarrow 6Fe^{2+} + WO_3 + 6H^+$, which are both thermodynamically possible since the standard reduction potentials of the Fe^{3+}—Fe^{2+}, W_2O_5—W and WO_3—W couples are +0.77, —0.04 and —0.01 V vs. NHE, respectively [5].

Potentiostatic polarization curves of the tungsten electrode in different concentrations of iron(III) chloride are shown in Fig. 3. Limiting anodic currents should be proportional to the concentrations of iron(II) generated by chemical reduction of iron(III), while the corresponding cathodic currents should be proportional to the concentrations of remaining iron(III). The relationship between equilibrium potentials (where $I = 0$) and the ratios of cathodic to anodic currents is given by curve C in Fig. 4, and is significantly non-Nernstian. Likewise, the relationship between equilibrium potentials and concentrations of total iron is non-Nernstian, as shown in Fig. 5. While this rules out the use of the tungsten electrode in direct

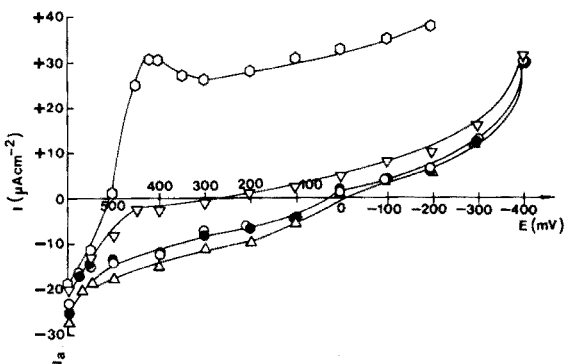

Fig. 1. Potentiostatic polarization curves of the tungsten electrode in solutions of different concentrations of iron(III) chloride in 0.1 M HCl. • 0.1 M HCl. △, ○, ▽ and ◊ apply to 10^{-5}, 10^{-4}, 10^{-3} and 10^{-2} M $FeCl_3$, respectively. $V = 0.5$ mV s^{-1}.

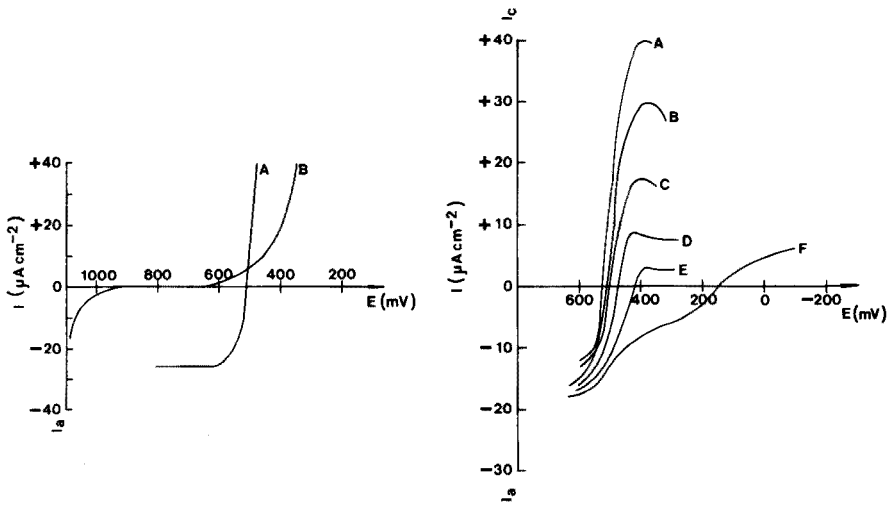

Fig. 2. Comparison of potentiostatic polarization curves of tungsten (A) and platinum (B) electrodes in 10^{-2} M iron(III) chloride.

Fig. 3. Potentiostatic polarization curves of the tungsten electrode in solutions of different concentrations of iron(III) chloride. A, B, C, D, E and F apply to 10, 8, 5, 3, 2 and 1 mM $FeCl_3$, respectively. $V = 0.5$ mV s^{-1}.

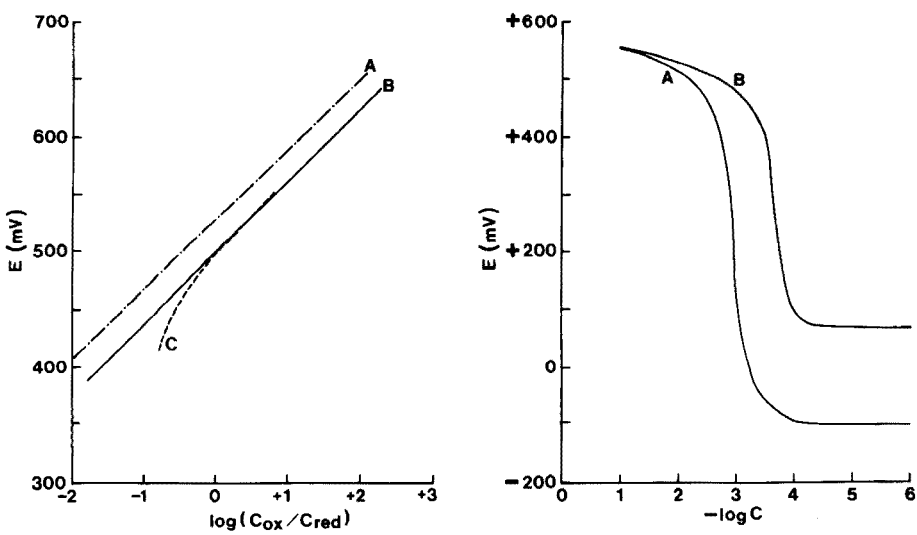

Fig. 4. Variation of equilibrium potential with the ratio C_{ox}/C_{red}. A, calculated from Nernst equation. B, corresponding experimental curve for Pt electrode. C, experimental curve for W electrode based on Fig. 3.

Fig. 5. Variation of equilibrium potential of tungsten electrode with total concentration of iron. A, quiet solution. B, stirred solution.

TABLE 1

Potentiometric titration of 5.03 mg of iron(III) at the tungsten electrode

Titrant	pH	$\bar{X}$ (mg)	$(\bar{X}-a)$ (%)	s (mg)	Confidence limit (95%)
NaF	2.0—2.3	5.06	0.59	0.04	0.06
$K_4Fe(CN)_6$	(1.5 M HCl)	4.96	−1.59	0.10	0.16
N-Benzoylphenyl-hydroxylamine	2.2—2.5	5.11	5.59	0.04	0.06
N-Nitrophenyl-hydroxylamine	2.0—2.8	5.15	2.39	0.07	0.10
EDTA	2.0	5.02	−0.20	0.00	0.00

potentiometry, the super-Nernstian response in the region 10^{-3}—10^{-4} M total iron is actually advantageous in potentiometric titrations. Typical results of such titrations are given in Table 1. It can be concluded that the tungsten electrode offers analytical advantages in allowing complexiметric titrations with iron(III).

REFERENCES

1 Sh. T. Talipov and T. L. Teodorovich, Zavod. Lab., 15 (1949) 529.
2 Z. I. Ivanova and V. A. Kimstach, in Metody Ctrimicheskogo Anal. Stokov Predpr. Chim. Prom., RGU, Rostov-on-Don, 1971, p. 108.
3 Z. I. Ivanova and V. A. Kimstach, in Electrochim. Metody Anal. Materialov, Metal., Moskow, 1971, p. 187.
4 N. R. Stalica, Ph.D. thesis, The Pennsylvania State University, 1963.
5 W. M. Latimer, The Oxidation States of the Elements and their Potentials in Aqueous Solution, 2nd edn., Prentice Hall, Englewood Cliffs, N.J., 1952.

Analytica Chimica Acta, 96 (1978) 421—426

Short Communication

REDOX—EXTRACTION CHROMATOGRAPHY: ISOLATION OF SOME ACTINIDE ELEMENTS BY USING 2,5-DI-TERT-PENTYLHYDROQUINONE AND VARIOUS ORGANIC EXTRACTANTS IN THE STATIONARY PHASE

A. DELLE SITE* and V. MARCHIONNI

Medical and Radiotoxicological Service, C.S.N. Casaccia, CNEN, Rome (Italy)

(Received 7th August 1977)

Separations of neptunium and plutonium from other actinide elements have been obtained recently by means of redox—extraction chromatography; the stationary phase, which showed simultaneous reducing and extracting properties, was an organic solution of an extractant, tri-n-octylphosphine oxide, and of a reducing compound, 2,5-di-tert-pentylhydroquinone [1, 2]. Both the extractant and the reductant are retained well by the solid support; furthermore, the hydroquinone can be oxidized on the column to the quinone form with strong oxidizing systems. Tri-n-octylphosphine oxide was chosen for its good extraction features, but it shows some interactions with the hydroquinone in the organic phase, which hinder its extracting capability at low acidities [2].

In the work described here, other established extractants such as tri-n-butylphosphate, di(2-ethylhexyl)phosphoric acid and tri-n-octylamine were employed together with 2,5-di-tert-pentylhydroquinone on redox—extraction columns. The kinetic aspects of neptunium and plutonium retention were also studied in order to obtain rapid separations of actinide elements.

Experimental

Equipment and reagents. Liquid scintillation counting was used to measure α- and β-activities [2]. α-Spectrometry was performed as already described [2]; the radionuclides were electroplated on stainless steel disks (1.5-cm diameter) from ammonium sulphate solution. The chromatographic columns made of Perspex had an internal diameter of 1 cm. Microthene-710 (microporous polyethylene, 50-100 mesh; Columbia Organic Chem.) was used as the inert support in the redox—extraction columns.

2,5-Di-tert-pentylhydroquinone (DPHQ; Eastman Kodak) was employed as the redox reagent. Tri-n-octylphosphine oxide (TOPO; Eastman Kodak), tri-n-butyl-phosphate (TBP, Fluka), di(2-ethylhexyl)phosphoric acid (HDEHP, K and K) and tri-n-octylamine (TOA, Fluka) were used as the extractants without further purification.

The actinide elements (Amersham Radiochemical Centre) were the same

as used in the earlier work [1, 2]. All other reagents were of analytical grade (C. Erba).

Preparation of extractant—DPHQ columns. The following solutions were used as the stationary phases: 0.1 M TOPO and 0.1 M DPHQ in cyclohexane; 1 M TBP and 0.1 M DPHQ in xylene; 1 M HDEHP and 0.1 M DPHQ in xylene; 0.2 M TOA and 0.1 M DPHQ in xylene. They were yellow except for the HDEHP—DPHQ solution, which was dark red. The appropriate solution (2 ml) was added dropwise to 3 g of Microthene, and the slurry was stirred for 30 min with the conditioning hydrochloric acid solution to obtain a homogeneous product and to remove floating particles. Then the slurry was transferred to a chromatographic column with 40 ml of the same hydrochloric acid solution as used for the subsequent experiment. Repeated washing of these columns demonstrated that the retention of the redox—extractant solution on the solid support is generally better than that of the extractant solution alone.

Preparation of TOPO—DPQ column. Vanadium(V) (10 ml of 0.1 M in 4 M HCl) was passed through a TOPO—DPHQ column to achieve quantitative oxidation of the hydroquinone to quinone. The column was then washed with 40 ml of 1 M HCl and conditioned with 20 ml of hydrochloric acid. This procedure is faster than the previous one with cerium(IV) sulphate, which required an accurate washing procedure with 1 M H_2SO_4 to eliminate cerium(IV) from the column. In fact, vanadium(V) is not extracted at low concentrations of hydrochloric acid [3] and can therefore be easily washed out. In both cases the excess of oxidant can be titrated to check the quantitative oxidation of DPHQ. An analogous procedure can be used to oxidize DPHQ to DPQ on the other extractant—DPHQ columns.

Actinide retention and separation experiments. Aliquots (20,000 dpm) of each radionuclide were used for each retention experiment. The nitric acid solution of the radionuclide (10—25 μl) was completely evaporated and the residue was dissolved with 1 ml of hydrochloric acid at the desired concentration. This solution was fed to the column which was then washed with 45 ml of hydrochloric acid at a flow rate of 0.1—1.5 ml min^{-1}. Elution with 1 M HF was employed to determine the percentage of radionuclide retained on the column; only the retention of uranium on HDEHP—DPHQ column was determined by elution with 9 M HCl. The two fractions were evaporated (the HF fraction in a Teflon beaker) and their activity was determined by liquid scintillation counting.

The same procedure was used to obtain the isolation of one actinide element from a mixture of three of four; in this case, α-spectrometry was used to determine the distribution of each element between the two fractions. When uranium-233 and neptunium-237 were used in the same feed solution, spectrometric analysis was impossible because the α-peaks overlapped; therefore, their retention was assumed to be the same as that obtained for the single radionuclides.

TABLE 1

% Retention of plutonium and neptunium on extraction and redox—extraction columns

Radionuclide	HCl (M)	Extraction		Redox—extraction	
		Column	Retention (%)	Column	Retention (%)
Plutonium	6	TOPO	23	TOPO—DPHQ	<0.1
	8	TBP	37	TBP—DPHQ	<0.1
	1	HDEHP	92	HDEHP—DPHQ	2
	8	HDEHP	2	HDEHP—DPHQ	<0.1
	7	TOA	99	TOA—DPHQ	3
	8	TOA	35	TOA—DPHQ	2
	0.5[a]	TOPO	63	TOPO—DPHQ	1
Neptunium	6	TOPO	85	TOPO—DPHQ	>99
	8	TBP	86	TBP—DPHQ	>99.9
	8	HDEHP	95	HDEHP—DPHQ	>99.9
	7	TOA	87	TOA—DPHQ	99
	8	TOA	99	TOA—DPHQ	>99
	6	TOPO	85	TOPO—DPQ	99

[a]0.5 M HNO_3.

Results

The retention of neptunium (Np(IV) + Np(V) + Np(VI)) and plutonium (Pu(III) + Pu(IV) + Pu(VI)) on redox—extraction columns was compared with their retention on the corresponding extraction columns (Table 1). The concentrations of the extractant in the organic phase and of the aqueous hydrochloric acid were chosen on the basis of the liquid—liquid extraction behaviour of each radionuclide in the various valence states [4—6]. Table 1 also shows the retention of plutonium on a TOPO—DPHQ column when 0.5 M HNO_3 was used as the aqueous medium. The flow rate for these experiments was very low (0.1 ml min^{-1}) in order to ensure the best conditions for complete redox reactions.

The same experiments were then repeated at various flow rates ranging between 0.1 and 1.5 ml min^{-1}. The results (Table 2) show that the TBP—DPHQ column can be used at 1.5 ml min^{-1}, whilst the other extractant—DPHQ columns require lower flow rates to give complete reduction of both elements at 25 ± 2°C. The reduction of plutonium on the TOA—DPHQ column is satisfactory only at a flow rate of 0.1 ml min^{-1}, but when the temperature of the column is increased to 40°C, almost complete reduction of plutonium occurs at a flow rate of 1 ml min^{-1}.

No relevant effects of flow rate were found for the retention of thorium and uranium on redox—extraction columns.

All these results were used to predict a series of interesting separations. Table 3 summarizes the conditions necessary to obtain selective elution or retention of a single element from a solution containing three or four actinide elements.

TABLE 2

Effect of the flow rate on the % retention of neptunium and plutonium on redox—extraction columns at room temperature
(Mobile phase: 6 M HCl for TOPO—DPHQ columns; 8 M HCl for TBP—DPHQ and TOA—DPHQ columns; 1 M HCl (A) and 8 M HCl (B) for HDEHP—DPHQ columns.)

Flow rate (ml min^{-1})	TOPO—DPHQ		TBP—DPHQ		HDEHP—DPHQ			TOA—DPHQ	
	Pu	Np	Pu	Np	Pu(A)	Pu(B)	Np(B)	Pu	Np
0.10	<0.1	>99	<0.1	>99.9	2	<0.1	>99.9	2	>99
0.25	<0.1	96	<0.1	—	—	<0.1	>99.9	44	—
0.50	<0.1	97	<0.1	>99.9	3	—	>99	39	—
1.00	0.2	77	<0.1	>99.9	3	0.2	75	32 2[a]	>99 >99[a]
1.50	0.1	—	<0.1	97	1	0.2	—	—	99

[a]At 40°C.

TABLE 3

Experimental conditions for the isolation of Th, U, Np, Pu and Am by redox—extraction chromatography

Column	HCl (M)	Flow rate (ml min^{-1})	Retention (%)				
			Th	U	Np	Pu	Am
TBP—DPHQ	8	1.0	<1	>99	>99.9	—	—
HDEHP—DPHQ	1	1.0	>99	—	—	3	1
HDEHP—DPHQ	8	1.0	>99.9	<1	—	<1	<0.1
TOA—DPHQ	8	1.0	<1	99	>99	—	—
TOPO—DPHQ	6	1.0	—	>99	—	<1	<1
TBP—DPHQ	8	1.0	2	>99	—	1	1
HDEHP—DPHQ	1	1.0	—	>99	—	3	<1
HDEHP—DPHQ	8	0.5	>99.9	<1	>99	—	—
TOA—DPHQ	8	0.1; 1.0[a]	1	99	—	3	<1
TOPO—DPHQ	6	0.5	—	—	96	<0.1	<1
TBP—DPHQ	8	1.0	1	—	99	2	1
HDEHP—DPHQ	8	0.5	—	<1	>99	<1	<0.1
TOA—DPHQ	8	0.1; 1.0[a]	0.1	—	>99	2	0.1
TOPO—DPHQ	6	0.5	—	>99	97	0.1	—
TBP—DPHQ	8	1.0	—	>99	>99.9	<0.1	—
HDEHP—DPHQ	1	1.0	>99	>99	—	3	—
HDEHP—DPHQ	8	0.5	99	—	99	0.1	—
TOA—DPHQ	8	0.1; 1.0[a]	—	99	>99	1	—
TOPO—DPHQ	6	0.5	—	>99	97	—	<1
TBP—DPHQ	8	1.0	—	>99	>99.9	—	<0.1
HDEHP—DPHQ	1	1.0	99	99	—	—	3
HDEHP—DPHQ	8	0.5	>99.9	—	99	—	<0.1
TOA—DPHQ	8	1.0	—	99	>99	—	1
TOPO—DPQ	6	0.5	—	>99	99	—	1

[a]At 40°C.

Discussion

The preliminary results (Table 1) show that other systems besides TOPO—DPHQ and TOPO—DPQ can be employed in redox—extraction chromatography: the presence of DPHQ produces a remarkable decrease in plutonium retention and a corresponding increase in neptunium retention. The redox reactions involved in such redox—extraction processes have been discussed previously [1, 2]; it was suggested that plutonium is reduced by DPHQ to Pu(III) and neptunium to Np(IV), while DPQ oxidizes Np(IV) and Np(V) to Np(VI) at high acidities.

As far as the behaviour of the TOPO—DPQ column is concerned, further experiments showed that the previous results [2] require some revision. The behaviour of neptunium, which seemed not to be retained on a TOPO—DPQ column at low concentrations of hydrochloric acid [2], is not reproducible; it varies when the neptunium stock solution is changed. A satisfactory explanation of this problem is difficult, without a precise knowledge of the distribution of the neptunium ionic species in the feed solution.

The effect of flow rate on the retention of plutonium and neptunium was considered in establishing the best conditions for their separation from other actinide elements. The retention of plutonium is not affected by flow rate (Table 2), except for the TOA—DPHQ column, on which plutonium is reduced appreciably only at a flow rate of 0.1 ml min^{-1}; however, a small increase in column temperature to 40°C, gives satisfactory reduction even at 1 ml min^{-1}. The different behaviour of plutonium on TOPO—DPHQ columns found previously [1] could also be explained on this basis. A good control of column temperature seems essential for a better understanding of this problem.

The retention of neptunium does not generally depend on the flow rate; only the TOPO—DPHQ and HDEHP—DPHQ systems give an appreciably decreasing retention as the flow rate changes from 0.5 to 1.0 ml min^{-1}.

The results in Table 3 confirm that redox—extraction chromatography is useful in obtaining effective separations and selective isolations of actinide elements. An analogous result has been reported by Coleman and Weaver [7], who used DPHQ for quantitative stripping of plutonium from an organic solution of HDEHP containing a mixture of plutonium, transplutonium elements and zirconium by means of a solvent extraction technique.

As far as the mobile phase is concerned, nitric acid can be used only when its concentration is less than 1 M. At higher concentrations, it rapidly oxidizes DPHQ to DPQ; in any case, small volumes of nitric acid can be added to the hydrochloric feed solution without any oxidizing effect on DPHQ.

The authors thank Prof. C. Testa for helpful discussions.

REFERENCES

1 A. Delle Site and C. Testa, Anal. Chim. Acta, 72 (1974) 155.
2 A. Delle Site and G. De Angelis, Anal. Chim. Acta, 87 (1976) 365.

3 J. C. White and W. J. Ross, Separations by Solvent Extraction with Tri-n-octylphosphine oxide, Nat. Acad. Sci., Nat. Res. Council Publ., NAS-NS 3102 (1961).
4 Y. Marcus and A. S. Kertes, Ion Exchange and Solvent Extraction of Metal Complexes, Wiley—Interscience, New York, 1969.
5 G. H. Coleman, The Radiochemistry of Plutonium, Nat. Acad. Sci., Nat. Res. Council Publ. NAS-NS 3058 (1965).
6 E. Akatsu, JAERI Report 1099 (1965).
7 C. Coleman and B. S. Weaver, U.S. Patent 3,580,705, May 25, 1971.

Analytica Chimica Acta, 96 (1978) 427—428

Short Communication

BENZYLTHIOURONIUM CHLORIDE AS AN ALKALIMETRIC STANDARD IN NON-AQUEOUS TITRIMETRY

J. V. KRISHNA REDDY and K. S. BOPARAI*

School of Studies in Chemistry, Vikram University, Ujjain, 456 010 (India)

(Received 19th April 1976)

In non-aqueous titrimetry, solutions of alkali metal alkoxides in benzene—methanol are the most popular basic titrants. Benzoic acid is used for their standardization, but it has the shortcoming of forming a gelatinous precipitate [1] in solutions titrated with sodium methoxide or potassium methoxide; this precipitate may interfere with the colour change of the indicator. Benzylthiouronium chloride is easily prepared and readily purified and is available in a state of high purity [2]. It was, therefore, considered worthwhile to study its use as an alkalimetric standard. Visual titrations in benzene—methanol with thymol blue as indicator have been carried out against benzoic acid and benzylthiouronium chloride. The standard deviation of the mean molarity obtained with benzylthiouronium chloride is less than that obtained with benzoic acid. The procedure, therefore, merits recommendation.

Standardization of sodium methoxide against benzoic acid (BA) and benzylthiouronium chloride (BC)

The solution of sodium methoxide (ca. 0.1 M), prepared in benzene—methanol [1], was standardized against benzoic acid (BDH, AR) and benzylthiouronium chloride (BDH, OAS) dissolved in benzene—methanol (3 + 1, v/v, 25 ml), with thymol blue (two drops, 0.3% w/v in methanol) as indicator. The titration was carried out until the yellow solution became clear blue. Blank determinations, carried out with the same volume of solvent, were deducted from the actual determinations. Table 1 records the 1st, 7th, 13th, 19th, and 25th of the set of 25 measurements made, from which mean molarities, standard deviations, and confidence limits [3] have been calculated, as shown in Table 2.

TABLE 1

Standardization of sodium methoxide

Wt. of BA (mg)	CH_3ONa consumed (ml)	Molarity of CH_3ONa	Wt. of BC (mg)	CH_3ONa consumed (ml)	Molarity of CH_3ONa
40.25	3.21	0.10268	71.44	3.44	0.10247
85.38	6.80	0.10283	133.24	6.40	0.10274
128.86	10.30	0.10248	194.44	9.35	0.10263
170.47	13.58	0.10282	247.37	11.90	0.10260
204.89	16.34	0.10269	298.63	14.35	0.10272

TABLE 2

Results from data obtained (N = 25)

	Titration with BA	Titration with BC
Mean molarity	10258×10^{-5}	10261×10^{-5}
Standard deviation	14.083×10^{-5}	8.6723×10^{-5}
90% confidence limit	$\pm 4.8192 \times 10^{-5}$	$\pm 2.9677 \times 10^{-5}$
95% confidence limit	$\pm 5.8135 \times 10^{-5}$	$\pm 3.5800 \times 10^{-5}$
99% confidence limit	$\pm 7.8780 \times 10^{-5}$	$\pm 4.8513 \times 10^{-5}$

The authors are grateful to C.S.I.R. (India) for the award of a research fellowship to J. V. Krishna Reddy.

REFERENCES

1 J. Kucharsky and L. Šafářik, Titrations in Non-aqueous Solvents, Elsevier, Amsterdam, 1965, pp. 99 and 109.
2 Anon., Analyst, 87 (1962) 304.
3 W. J. Youden, Statistical Methods for Chemists, Wiley, New York, 1961.

Analytica Chimica Acta, 96 (1978) 429—434

Short Communication

VISUAL AND OLFACTORY INDICATION OF END-POINTS IN CATALYTIC TITRATIONS. USE OF *p*-DIMETHYLAMINOBENZALDEHYDE AND *p*-TOLUIDINE FOR COMPLEXIMETRIC DETERMINATION OF MANGANESE(II)

SHIGEKI ABE*, SHUNICHI KON and TSUTOMU MATSUO

Department of Applied Chemistry, Yamagata University, Yonezawa (Japan)

(Received 6th July 1977)

In recent years, interest in metal ion-catalyzed reactions has increased markedly, and various types of analytical application have been reported. The use of catalytic reactions for end-point indication in titrimetric analysis — catalytic or catalymetric titrations [1] — has become well known. Weisz et al. [2—4] have described the technique and its advantages, and have worked out numerous examples. General reviews of catalytic titrations have been presented [5, 6]. The characteristic feature is that kinetics is not involved in the main stoichiometric titration reaction but only in the indication of the end-point. There are two approaches to end-point indication: visual and instrumental. The visual (indicator) method offers great potential for routine analysis because it is inexpensive and simple. Chromogenic oxygen acceptors such as aromatic amines and phenols have been employed for the catalytic titration of manganese(II) and other metal ions [7, 8]. In principle, other senses besides sight can be used. An attractive alternative is the use of an olfactory indicator, although there are often difficulties in obtaining suitable indicator systems. To date, few applications have been reported. The study by Rancke-Madsen and Krogh [9] of the titration of sodium hydroxide with hydrochloric acid is an example of the use of smell indicators.

The present communication describes two new types of visual and olfactory indication based on catalytic oxidation of aromatic amines, and their applications to the complexiметric titration of manganese(II). The characteristic end-point signals are obtained from catalytically oxidized intermediates of *p*-dimethylaminobenzaldehyde and *p*-toluidine.

Experimental

Reagents and apparatus. All chemicals were of analytical-reagent grade; deionized distilled water was employed for the preparation of solutions, which were stored in polyethylene bottles. The manganese(II) sulfate solution (0.01 M) was standardized against 0.01 M EDTA with eriochrome black T indicator. *p*-Dimethylaminobenzaldehyde (*p*-DMAB) and *p*-toluidine hydro-

chloride (Tokyo Chemical Co., Japan) were used as received. Indicator solutions of *p*-DMAB were prepared by dissolving the reagent in 50% ethanol. Hydrogen peroxide solutions were prepared daily from a stock solution (30%, w/v) by dilution, and were standardized iodimetrically.

A Hitachi Model 124 double-beam spectrophotometer and a Hitachi Model 139 spectrophotometer equipped with a titration cell were used for kinetic measurements.

Visual titration. To about 50 ml of 0.4 M sodium hydrogencarbonate solution containing known amounts of EDTA, were added 1 ml of 0.2% *p*-DMAB and 1 ml of 3% hydrogen peroxide solution. This mixture was titrated with manganese(II) solution under magnetic stirring. At the end-point, the solution turned deep red, because of catalytic oxidation of *p*-DMAB. This colored intermediate disappeared within a few seconds.

Olfactory end-point detection. The procedure was the same as for the visual method except that, at the beginning of the titration, 1 ml of 0.2% *p*-toluidine solution was added instead of *p*-DMAB, and 1,2-diaminocyclohexanetetraacetic acid (DCyTA) was used as the titrant. At the end-point, the solution turned deep orange and an intermediate product emitting a strong carbylamine-like odor indicated the equivalence point. All titrations were performed at room temperature.

Results and discussion

Visual indication with p-*dimethylaminobenzaldehyde.* The precision obtainable with any titrimetric method largely depends on the sharpness of the end-point, i.e. on the indicator color change or the change in instrumental response. Schematic patterns of visual indication may be considered to fall into three classes, analogously to instrumental procedures: sigmoidal curves (increase of color or absorbance), reversed sigmoidal curves (decrease of color or absorbance) and differential curves showing a peak at the end-point. While the first two are well known in visual titrations, the third type of indicator reaction has been little used.

When *p*-DMAB and hydrogen peroxide solution were mixed in the presence of traces of manganese(II), a very strong absorption band appeared near 500 nm. The spectrophotometric response of the colored products was almost instantaneous. These colored intermediates disappeared within a few seconds and gave a characteristic signal, passing a sharp maximum at the equivalence point (Fig. 1). This catalytic indication system proved to be suitable for visual titration of manganese(II) with EDTA. The results of manganese(II) titrations are shown in Table 1. Each value reported is the average of at least three individual titrations. The relative error of the assay indicates that this catalytic method has acceptable accuracy for titrimetric analysis.

The effect of the hydrogencarbonate concentration on the manganese(II)-catalyzed reaction has previously been discussed [10]; this ion plays an important role in manganese(II)-catalyzed reactions, and titrations were

TABLE 1

Catalytic titration of manganese(II) with *p*-DMAB indicator

0.009675 M EDTA taken (ml)	Titer of Mn^{2+} (ml)		Relative error (%)
	EBT method[a]	Catalytic method	
5.00	5.34	5.36	+0.37
7.00	7.48	7.52	+0.53
10.00	10.68	10.67	−0.09
15.00	16.03	16.03	±0.00
20.00	21.36	21.39	+0.14

[a]Eriochrome black T as metal indicator.

possible at hydrogencarbonate concentrations above 0.3 M. A satisfactory color change was observed at pH values between 8.4 and 9.7. In some experiments, a pale red color appeared near the end-point of the titration, then changed quite sharply through deep red to colorless at the equivalence point. Results taken at the point of disappearance of the intense red color were reproducibly precise. Preferably, *p*-DMAB indicator may be added during the course of the titration to obtain much sharper end-point signals. Diethylaminobenzaldehyde (*p*-DEAB) also gave a sharp colorless to red end-point signal in manganese(II) titrations, and can be used as a catalytic indicator.

Titration in non-aqueous media proved to be unsuccessful. The presence of large amounts of organic solvent impaired the sharpness of the end-point. With 10% ethanol present, the color change was quite obscure, and manganese(II) could not be determined.

Olfactory indication with p-*toluidine*. The olfactory indication method is based on the formation of intermediates which give a carbylamine-like odor. Preliminary experiments showed that the manganese(II)-catalyzed reaction could be followed by the odor with *p*-toluidine hydrochloride indicator, whereas the sodium salt of *p*-toluidine-*m*-sulfonic acid gave no carbylamine-like odor at the equivalence point. The *m*- and *o*-toluidine hydrochlorides did not give distinct end-points for either visual or olfactory purposes, because of their higher redox potentials, as in the case of 2,4-dimethylaniline hydrochloride. The effects of substituent groups on the catalytic oxidation of the indicator substrate and the criteria for selection of indicator reactions have been discussed for some aminophenol derivatives [8]. Substituted *p*-toluidines such as *N,N*-dimethyl-*p*-toluidine are unsuitable because they are already odorous.

The data obtained with the olfactory end-point with *p*-toluidine are shown in Tables 2 and 3. As a working medium, sodium hydrogencarbonate solution was preferred to ammonium carbonate solution, which emits ammonia.

In principle, catalytic indication systems have much larger end-point signals than do chemically equilibrated systems, and so provide greater sensitivity.

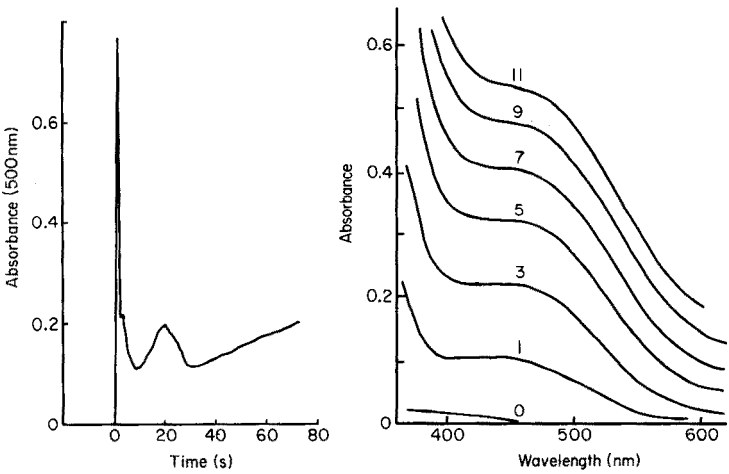

Fig. 1. Spectrophotometric response of *p*-DMAB. Manganese(II) (25 μg) was added to 75 ml of 0.4 M $NaHCO_3$ solution containing 0.004% *p*-DMAB and 0.06% H_2O_2.

Fig. 2. Absorption spectra of *p*-toluidine and its oxidation products. The numbers on the curves indicate the time elapsed (in min) after addition of Mn^{2+}. Recording speed, 100 nm/25 s. Experimental conditions: 4 μg of Mn^{2+} was added to 50 ml of 0.4 M $(NH_4)_2CO_3$ solution containing 0.012% of *p*-toluidine and 0.06% H_2O_2.

TABLE 2

Catalytic titration of manganese(II) with olfactory indication

0.010095 M DCyTA taken (ml)	Titer of Mn^{2+} (ml)		Relative error (%)
	EBT method[a]	Catalytic method	
2.00	2.13	2.17	+1.88
5.00	5.34	5.39	+0.94
10.00	10.67	10.72	0.43
15.00	16.01	16.07	+0.37
20.00	21.34	21.40	+0.28

[a]Eriochrome black T as metal indicator.

Earlier applications of olfactory indication involving equilibrium measurement in thermodynamically stable systems [9] are less favorable from the viewpoint of the Weber—Fechner law, $S = k \cdot \log X$, where S is the intensity of the odor, X is the concentration of the odorous substance and k is a constant. No difficulty was found in locating the end-point with *p*-toluidine indicator. For comparison, some results with other catalytic indicators are presented in Table 4. The main advantage of the olfactory method compared with a visual method is that a turbid or colored solution can be titrated with-

TABLE 3

Catalytic titration of manganese(II) with olfactory indication
(Initial conditions: 0.4 M $NaHCO_3$ solution containing 10.00 ml of 0.01008 M DCyTA. Amounts of *p*-toluidine and hydrogen peroxide were varied as described.)

p-Toluidine concn. (%)	H_2O_2 concn. (%)	Mn^{2+} concn. (mg ml^{-1})
0.012	0.06	0.5091
0.004	0.06	0.5091
0.0012	0.06	0.5082
0.004	0.30	0.5143
0.004	0.06	0.5091
0.004	0.03	0.5091

TABLE 4

Comparison of visual and olfactory indication method

Catalytic indicator	Indication	Mn^{2+} concn. (mg ml^{-1})		
p-Phenetidine	Visual[a]	0.5136		
m-Aminophenol	Visual[a]		0.5108	
Acid blue 45	Visual[b]	0.5183		
p-Toluidine	Olfactory	0.5159		
p-DMAB	Visual[c]		0.5044	0.5260
p-DEAB	Visual[c]			0.5265
(Eriochrome black T			0.5101	0.5281)

[a] Analogous to *S*-shaped titration curve.
[b] Analogous to reversed *S*-shaped titration curve.
[c] Analogous to differential titration curve.

out difficulty. This olfactory method was successfully applied to the indirect catalytic titration of zinc and cadmium by adding a known excess of DCyTA and back-titrating with standard manganese(II) solution.

The absorption spectra of *p*-toluidine and its oxidation products are shown in Fig. 2. Details of the reaction mechanism are still under investigation, but the very disagreeable carbylamine-like odors suggests the formation of isocyanides, which are sometimes called isonitriles or carbylamines. Because of their strong odor, the "carbylamine test" is a highly sensitive test for $R\text{-}NH_2$ [11]. These catalytic oxidation processes involving *p*-DMAB and *p*-toluidine with manganese(II) catalyst are irreversible, and may occur through formation of a complex compound of manganese, hydrogen peroxide and hydrogencarbonate, yielding final products of the quinoneimine type, as has been reported for other aromatic amines [7].

REFERENCES

1 K. B. Yatsimirskii and T. I. Fedorova, Dokl. Akad. Nauk. USSR, 143 (1962) 143.
2 H. Weisz and U. Muschelknautz, Z. Anal. Chem., 215 (1966) 17.
3 H. Weisz and T. Janjic, Z. Anal. Chem., 227 (1967) 1.
4 H. Weisz and S. Pantel, Anal. Chim. Acta, 62 (1972) 361.
5 H. A. Mottola, Talanta, 16 (1969) 1267.
6 T. P. Hadjiioannou, Rev. Anal. Chem., 3 (1976) 82.
7 S. Abe, K. Takahashi and T. Matsuo, Nippon Kagaku Kaishi, (1973) 963.
8 S. Abe and S. Kon, Bunseki Kagaku, 25 (1976) 846.
9 E. Rancke-Madsen and J. A. Krogh, Acta Chem. Scand., 10 (1956) 495.
10 S. Abe, K. Takahashi and T. Matsuo, Anal. Chim. Acta, 80 (1975) 141.
11 J. D. Roberts and M. C. Caserio, Basic Principles of Organic Chemistry, Benjamin, New York, 1965.

Analytica Chimica Acta, 96 (1978) 435—443

Book Reviews

Edward Maslowsky Jr., *Vibrational Spectra of Organometallic Compounds*, John Wiley, New York, 1977, xiv + 528 pp., price £18.75, U.S. $31.70.

The publication of L. J. Bellamy's book "The Infrared Spectra of Complex Molecules" in 1954 helped to make possible the development of infrared spectroscopy as perhaps the most important technique available for the qualitative analysis of organic compounds. Before that, anyone wanting to find out about characteristic infrared frequencies had to make up his own correlation tables; this was a considerable task, for although less work was published, there were fewer annual surveys available. Now the situation is rather different; although there is no book comparable to Bellamy's dealing with organometallic compounds, there are collections like the Chemical Society's specialist periodical reports on the spectra of organometallic compounds from which information can be collected without a huge amount of trouble. It is therefore unlikely in my opinion that Maslowsky's book will prove as important as Bellamy's did.

Nevertheless, this book will certainly be very useful to a lot of research workers. It is sensibly organized, in terms of ring systems and functional groups; there are plenty of tables of characteristic frequencies, and the text contains usefully summarized accounts of particular features in particular systems. This kind of material is not at all easy to collate; the organometallic chemist sometimes deals with small systems for which a complete or nearly complete vibrational analysis is appropriate, and at others is concerned with no more than the crudest and most qualitative of "fingerprinting". Maslowsky has managed to combine material for both of these extreme approaches and for a wide range of intermediate treatments in a very sensible way, and with considerable success. Though because of the typesetting there is rather less on each page than at first appears, the book contains a very great deal of useful information. It is extremely expensive, but nowadays most such books are; any practising organometallic chemist will be glad to have access to it, though perhaps not many will be able to afford a personal copy. Specific sections of the book would also be of considerable value in advanced undergraduate coursework, apart from any applications in connection with laboratory classes. All in all, this book is certainly to be recommended.

E. A. V. Ebsworth

William G. Schrenk, *Analytical Atomic Spectroscopy*, Plenum Press, New York, 1975, pp. xvii + 375, price $39.00.

For the last decade or more, analytical atomic spectroscopy has been one of the most important and rapidly growing areas of analytical chemistry. The provision of a book which covers the whole of this field in a reasonably detailed and up-to-date way, as this does, is therefore very welcome. The book begins with a brief history of atomic spectroscopy, followed by the historical development of the theory of atomic spectra, and the currently acceptable wave mechanical interpretation, energy level diagrams and derivation of spectroscopic terms. This is generally acceptable, but it could be argued that the inclusion of out-dated theories is a confusing and counter-productive complication for the intended readership. It is a pity, too, that there is almost no further reference to the spectroscopic terms (or indeed to much of the spectral theory) in the further sections of the book; this absence gives the erroneous impression that the practice of analytical spectroscopy has no use for these aspects. Also included in these chapters are brief descriptions of laser action (without describing what laser action is) and molecular spectra.

The next chapters, all very clearly written, concern the optical components and construction of optical spectrometers of all types, arc and spark accessories (including a brief section on plasmas), and methods of measurement of emissions (solar blind phototubes, vidicon detectors and direct reading spectrographs are briefly mentioned). This is followed by an equally acceptable treatment of qualitative, semi-quantitative and quantitative emission spectrochemical analysis.

The remaining 40% of the text is a very readable account of modern flame atomic analytical techniques (emission, absorption and fluorescence) dealt with in conventional style, but including topics such as the electrodeless discharge lamp, ultrasonic nebulizer, Delves' cup, electrothermal atomizers, vapour generation systems and laser excitation sources. The book concludes with author and subject indexes and various appendices. They include tables of spectral lines arranged by wavelength and by element, spectral charts, Seidel functions and detection limits. Less necessary are the tables of atomic weights, logarithms, absorbance—transmittance conversions, and a periodic table.

The book is clearly written, illustrated and presented. The author has obviously paid a great deal of attention to detail, and very few errors were detected (the Meeker (sic) burner was a glaring exception). The book is highly recommended to final year undergraduates and postgraduates, and to the non-specialist analytical chemist, but can they afford to buy it?!

A. Townshend

Hugh E. Malone, *The Analysis of Rocket Propellants*, Academic Press, London, 1976, x + 148 pp., price £6.50, U.S. $14.25.

This book is Vol. 12 in the series "The Analysis of Organic Materials". It is well known that information on special research projects performed or supported by governments is often difficult to obtain. When exotic materials such as chlorine pentafluoride become operational and are produced commercially, the original specifications, which include recommended methods of analysis, are often only to be found by tedious searches of government reports.

This book succeeds in delineating sources of such information: many of the references cited are to U.S. military specifications or reports by personnel of specialised chemical companies or aerospace agencies. Generally, sufficient detail is given for skilled chemists to carry out analyses without having to refer to obscure and highly specialised literature that is difficult to locate and obtain. Many of the methods of analysis described can be carried out in a modest laboratory without the necessity for sophisticated apparatus.

Many books concern themselves only with the analysis of the sample after it reaches the laboratory. Malone introduces the reader early in this book to the various techniques for sampling fuels and oxidisers; he continually stresses the guidelines essential for the safe storage of such materials and describes clearly the safety precautions essential during their sampling and analysis. A chapter on field methods is included.

The text is fairly evenly divided between the analysis of fuels, fuel mixtures, and oxidisers. The treatment of the analysis of high energy oxidisers containing fluorine is particularly good. More emphasis, however, has been placed on the hydrazine-based fuels; these are far more widely used than the high energy oxidisers and much more work has been published on their analysis. This book is intended for the practical chemist and will be used in all laboratories dealing with the analysis of propellants, exotic and conventional.

B. L. Tuffly

E. Bishop in C. L. Wilson and D. W. Wilson (Eds.), *Comprehensive Analytical Chemistry Vol. IID, Coulometric Analysis*, Elsevier, Amsterdam, 1975, xxviii + 673 pp., price Dfl. 240.00 (US $99.95).

Coulometric analysis has few more enthusiastic advocates than Professor Bishop, and none who has devoted so much time to its theoretical development. This book has been long in the making, and the result is a treatise which merits deep study by anyone interested in electroanalytical chemistry.

The first part of the book (170 pages) contains the theory and principles from Faraday's Laws onwards, with discussions of electrode processes,

solvent and solvent-ion reactions, mass transfer, charge transfer, parameter effects, behaviour patterns, background reactions, efficiencies, etc. Part II (67 pages) deals with practical aspects: apparatus, power supplies, measurement of quantity of electricity and automatic instrumentation. Part III (113 pages) contains excellent discussions of the Faraday constant, coulometry as an investigational tool, and relaxation methods; various special methods such as electrochromatography and stripping are also considered. In Part IV (247 pages), potentiostatic and amperostatic procedures for the determination of elements are considered in detail. Finally, there are 2444 references, and a computer program.

The price of the book puts it outside the range of private buyers, which is a pity because it is a book to browse on rather than consult quickly. This volume is strongly recommended; it will certainly be the standard work on coulometric analysis for many years to come.

G. Svehla (Ed.), *Wilson and Wilson's Comprehensive Analytical Chemistry, Volume VIII*, Elsevier, Amsterdam, 1977, xvi + 589 pp., price Dfl. 190.00 (US $77.75).

Volume VIII of this treatise covers four aspects of analytical chemistry. The first chapter — on enzyme electrodes by G. G. Guilbault — contains discussions of general principles, immobilization methods, electrode construction, performance characteristics, and analytical applications. The applications cover not only enzyme electrodes per se for assays of glucose, urea, amino acids, etc., but substrate electrodes for assay of enzymes such as urease and cholinesterase. There is a very useful comparison of different types of enzyme electrode, and the text is illuminated by many practical hints based on the author's extensive experience in this field. This is a very good account of an expanding field, and is marred only by the reference list which ends in 1974, apart from one or two of Guilbault's own papers.

The second chapter covers molecular fluorescence spectroscopy and is also by G. G. Guilbault. This is a straightforward account of the theory and practice of luminescence and phosphorescence, with discussions on the determination of inorganic ions and organic compounds, especial attention being given to the assay of drugs and enzymes.

Photometric titrations are discussed (183 pp.) by M. A. Leonard, who provides a stout defence of their use in routine situations. Essentially, this is a monograph, starting with basic principles and ending with industrial applications. There are useful tables of the procedures available for different species, and the coverage is generally well-balanced.

In the fourth chapter (155 pp.), W. Nebe provides a minor monograph on the analytical applications of interferometry. The theoretical background is dealt with in considerable detail, as is the available instrumentation. Interferometric analysis of homogeneous substances is discussed theoretically

and practically, with emphasis on the suitability of the technique for explosive and toxic gases and vapours, and gases of biological and clinical interest. Solution analysis in water and other liquids, and measurements of optical glasses and thin layers are also considered. Analysis of inhomogeneous (e.g. stratified) substances, sedimentation studies, characterization of macromolecules and other chemical applications of interferometry are reviewed, with emphasis on the theoretical aspects.

The contents of this Volume are a somewhat heterogeneous collection. The standard of treatment is generally good, but there has been a publication delay somewhere along the line. Only Dr. Nebe offers a disclaimer for anything that happened after 1972, but the other chapters contain few references after 1970, and even the chapter on enzyme electrodes contains few references after 1973. Thus the main bugbear of multi-author books has not been overcome, and there is a strong argument for producing smaller volumes as manuscripts become available. Nonetheless, this is a very useful book which should be on the shelves of every library.

A. M. G. Macdonald

K. Venkataraman (Ed.), *The Analytical Chemistry of Synthetic Dyes*, J. Wiley, New York, 1977, pp. xxii + 591, price £31.90, $54.00.

Venkataraman, who retired from the Directorship of the Indian National Chemical Laboratory at Poona around 10 years ago, has continued to work actively on projects such as this, in which he has had the assistance of 6 European and 16 American authors, of whom 7 belong to the Research and Development Division of E.I. du Pont de Nemours and Co. This book is therefore an authoritative and comprehensive treatise which will be welcome in a specialised field which, over the years, has suffered from a lack of enthusiastic editors and authors.

This book is self-contained in the sense that, before the specialised chapters that deal with the analysis of a particular class of dyestuffs, or particular application of dyestuffs, there are several chapters that deal with the basic analytical techniques applied most frequently in this field. These chapters, on paper, thin layer, gas and high pressure liquid chromatographies, infrared, n.m.r. and mass spectroscopy, are particularly good examples of concise, up-to-date introductions. There follow chapters that give examples of structure determinations of dyestuffs, and the book concludes with a brief but useful chapter on the ecological and toxicological monitoring of dyestuffs.

The literature coverage is broad and up-to-date; most of the major chapters give references to work published in journals in 1975. The text is free from trivial errors, the production is first class throughout, and Venkataraman is to be congratulated on welding together the individual contributions of so many authors to give a uniform and unique text.

D. M. W. Anderson

J. Urbanski, W. Czerwinski, K. Janicka, F. Majewska, and H. Zowall, *Handbook of Analysis of Synthetic Polymers and Plastics*, Ellis Horwood, Chichester, 1977, 494 pp., price £25.00, $47.50.

This is the English edition of a co-edition with Wydawnictwa Naukowo-Techniczne, Warsaw. The translator, Andrzej Skup, and the translation editor, Dr. G. G. Cameron, have both carried out their tasks competently. The Polish printers have done well but the quality of the paper is not up to the standard expected in an expensive text, and the stitching and canvas backing of the spine have unfortunately already parted company in the reviewer's copy.

Although this book is attributed to a team of authors, Urbanski has contributed what appears to be around 85% of the text, which opens with several chapters that give introductions to the essential, basic analytical techniques, viz., chemical methods, i.r., u.v., n.m.r., chromatography, and polarography. Separate chapters are then devoted to each of the different classes of polymers; short chapters on cellulose derivatives and silicones are included.

The foreword to this edition points out that communication is one of today's major problems in science and that translations such as this make available a range of literature that would otherwise be inaccessible to many readers. Allowance must always be made for the time required by translators to complete their work; notwithstanding, this book appears to be just a little too long in the tooth for it to be welcomed unreservedly — it is splendid as far as the pre-1970 literature goes, but it is difficult to detect references to work published more recently than 1972/73.

W. W. Wendlandt and L. W. Collins (Eds.), *Thermal Analysis*, Dowden, Hutchinson and Ross (distributed by Halsted Press), Stroudsburg, Pennsylvania, 1976, pp. ix + 337, price £26.20, U.S. $43.20.

This second volume of "Benchmark" papers in analytical chemistry deals with the historical development of thermal analysis. There are in all 36 papers, reprinted in their entirety from the original journals or reports. The editors who are responsible for the selection of the papers included in this volume have arranged the contents into two parts; the first and larger is devoted to differential thermal analysis (25 papers) and the second to thermogravimetry (11 papers). Each part contains a short editorial commentary by way of an introduction to the collection of papers.

As an educational exercise, this type of presentation has much to commend it and those scientists interested not only in the genesis of these thermal methods, but also in the overall development and sophistication of the techniques will find this a valuable compilation. Here, in one volume, the reader has immediate access to the originals from the classical contributions

of Le Chatelier (here especially translated from the original French publication of 1887) and Roberts-Austen (1899), to the differential scanning calorimeter of Watson, O'Neill, Justin and Brenner (1964) of the Perkin-Elmer Instrument Corporation.

Similarly in the section devoted to thermogravimetry, the papers of Honda (1915), Chevenard (1944) and Duval (1951) lead the reader via papers such as Simons and Newkirk's (1964) study of calcium oxalate monohydrate to the highly sophisticated automatic devices as exemplified by the work of Bradley and Wendlandt (1971).

Curiously, the selection does not include any papers from Eastern Europe, which is surprising especially in view of the major contributions of the Hungarian chemists and physicists to the development of thermal methods of analysis, particularly with regard to automatic instruments capable of simultaneously recording TG-, DTG- and DTA-curves (Derivatograph). This may arise from commercial rather than scientific reasons, but it does rather tend to create the impression that the large volume of work done in these Communist countries is only of secondary importance.

Nevertheless, this is a worthy successor to *Ion-Exchange Chromatography*, the first volume in this series. Students of analytical chemistry will find this a particularly valuable source of primary information on these two major techniques of thermal analysis. Unfortunately, there will be very few who have the resources to purchase this book and thus will have to rely on their college library for access to it.

W. I. Stephen

L. S. Bark (Ed.), *Selected Annual Reviews of the Analytical Sciences, Vol. 4*, Chemical Society, London, 1976, 73 pp., price £9.50.

This thin paperback contains two reviews. Advances in voltammetric techniques are reported by B. Fleet and R. D. Jee; particularly useful are the tabulated summaries of developments. There are now about 40 varieties of voltammetric and polarographic techniques, and even specialists become confused over exactly which electrical modification is applied and what is measured; the table here helps to clarify matters. Voltammetric methods offer many advantages for routine analysis, particularly now that versatile, compact and reliable instrumentation is available. This review provides a good guide to the recent literature.

In the second review, B. L. Sharp discusses high-frequency electrodeless plasma spectrometry. The aspects dealt with are classification of plasma types, emission spectrometry, nebulizers, the inductively-coupled r.f. plasma torch and the microwave plasma. The decision to include theoretical considerations of a quite general nature seems rather ill-advised; where does one stop? However, this review is again very useful in indicating recent developments in this important field.

In both reviews, addenda are provided to bring the literature coverage into 1976. The authors are to be congratulated on the speed with which they have amalgamated their reviews from an often confusing literature.

C. W. Fuller (Ed.), *Annual Reports on Analytical Atomic Spectroscopy, Vol. 5*, Chemical Society, London, 1976, viii + 267 pp., price £15.00.

This Report covers the 1975 literature; the magnitude of the task facing the reporters is indicated by the 1573 references listed. The organization is along the same lines as in previous volumes, and there are many useful tables which summarize experimental conditions for the analyses described. This is a worthwhile series, providing, in reasonably digestible form, a survey of a tremendous bulk of original literature.

Achtes Kolloquium über metallkundlicher Analyse mit besonderer Berücksichtigung der Elektronenstrahl-und Ionenstrahl Mikroanalyse, (Mikrochimica Acta, Supplementum VII), Springer-Verlag, Wien, 1977, vii + 596 pp., price DM 232.

This paper-bound supplement to Mikrochimica Acta contains the texts of 41 papers read at the Eighth Colloquium on metallurgical analysis, held in Vienna in October 1976. Most of the papers are in German. Electron microprobe analysis predominates, but there are also papers dealing with s.i.m.s., x.r.f., s.e.m., ESCA and Auger spectroscopy. These biennial meetings serve a useful purpose in bringing together industrial and academic workers in this field, but it is doubtful if their formal deliberations are worth the outrageous price asked for this volume.

Proceedings of the Second International Symposium on Nitrite in Meat Products, Centre for Agricultural Publishing and Documentation, Wageningen, 1977, 326 pp., price Dfl. 65.

This 4-day Symposium was held in the Netherlands in September, 1976, and attracted participants from Western Europe, America and Japan. The 36 papers in this paperback are divided into sections on microbiology, technology, epidemiology and chemistry; the chemical sessions — the bulk of the proceedings — deal with reactions of nitrite, and with the formation, occurrence, carcinogenicity and determination of nitrosamines. Condensed discussions are given after most of the papers, but there are no proper reference lists. The lack of reliability of current techniques for the trace determination of N-nitroso compounds is evident, and there is much of interest for analytical chemists in this book. The book ends with a note on SI units and on ISO and IUPAC recommendations, but the editor has understandably boggled at the task of converting all the papers in this volume to these usages.

R. S. Porter and J. F. Johnson (Eds.), *Analytical Calorimetry, Volume 4*, Plenum Press, New York, 1977, pp. ix + 251.

This volume contains, in part, papers presented before the Division of Analytical Chemistry at the Fourth Symposium on Analytical Chemistry, at the 172nd National meeting of the American Chemical Society during August 29th—September 3rd, 1976. It contains 21 contributions in all, covering a broad area of quantitative thermal analysis. The application of thermal methods to a wide range of materials is now very well-established and the work described in this present volume admirably reflects not only the sophistication of the techniques but their continuing development in an ever-widening field of chemical technology. The papers in the present volume include quantitative thermal data on a variety of materials from gun propellants to dental guttapercha, and will provide interesting reading for all concerned with the development of thermal methods on a quantitative basis.

Analytica Chimica Acta, 96 (1978) 444—446

Announcements

1978 PITTSBURGH CONFERENCE ON ANALYTICAL CHEMISTRY AND APPLIED SPECTROSCOPY

The 1978 Pittsburgh Conference will be held on February 27—March 3, 1978 in the Cleveland Convention Center, Cleveland, Ohio, U.S.A. The Theme of the Conference will be "Service to Humanity through Analytical Chemistry and Applied Spectroscopy".

The following Symposia have been arranged.

Keeping up with computer interfacing and microcomputers I and II: arranged by Frank Plankey, University of Pittsburgh and John Rombough, USS Chemicals (Follow-up of the successful "Getting Started in Digital Electronics and Computer Interfacing" symposium at the 1977 Conference).

Biomedical applications of ion-selective electrodes I and II: arranged by Henry Freiser, University of Arizona.

Laboratory Automation I — computerization — some case studies: arranged by Gerst Gibbon, PERC/ERDA.

Laboratory Automation II — computer information handling in clinical laboratories: arranged by Robert Megargle (ASTM E-31), Cleveland State University.

Coal liquefaction products — a new separations challenge for liquid chromatography — arranged by Peter Talarico, Waters Associates.

Analytical chemistry and OSHA: arranged by John Frohliger, University of Pittsburgh and Oswald Wilkinson, Alcoa.

Toxicology in industry — arranged by Joseph Feldman, Duquesne University and Rita Windisch, Pittsburgh Mercy Hospital.

Speedy spectroscopy — how fast is fast?: Advances in Time Resolved Spectroscopy — arranged by Peter Castle and Gerald Carlson, Westinghouse Research Laboratories.

Advances in applied surface analysis I — arranged by N. S. McIntyre (ASTM E-42), Atomic Energy of Canada, Ltd.

Advances in applied surface analysis II — arranged by David Hercules, University of Pittsburgh.

Glass capillary gas chromatography for routine analysis — arranged by William Suits, Varian.

Chemical analysis as applied to the steel industry — arranged by Bruce LaRue, National Steel Corporation.

Automatic analysis comes of age — arranged by James Foreman, Laboratory of the Government Chemist, London U.K., and coordinated by William Straub, United States Steel Corporation.

The British are coming — what's new in spectroscopy — arranged by William Fateley, Kansas State University.

Fourier transform spectroscopy group — arranged by James Durig, University of South Carolina.

Coblentz award and symposium — symposium arranged by Jack Koenig, Case Western Reserve University.

A critical evaluation of procedures employed for airborne contaminants — arranged by Robert Freedman, U.S. Bureau of Mines.

1978 SACP, SSP and Stephen Dal Nogare awards symposium — (Society for Analytical Chemists of Pittsburgh, Spectroscopy Society of Pittsburgh, Chromatography Forum of Delaware Valley) — arranged by Harold Sweeney, Koppers Company, Robert Baudoux United States Steel Corporation and Lyle Phifer, Chem. Services Inc., respectively.

The 1978 Conference will again be the site for the premier exhibition of equipment used in analytical chemistry and spectroscopy. In 1977, the Exposition involved some 350 companies which used 693 booths and 18 seminar rooms.

Further information from: Pittsburgh Conference on Analytical Chemistry and Applied Spectroscopy, 4400 Fifth Avenue, Pittsburgh, PA 15213, U.S.A.

INTERNATIONAL CONFERENCE ON COMPUTERS AND OPTIMIZATION IN ANALYTICAL CHEMISTRY

Amsterdam, April 5—7, 1978

An International Conference on Computers and Optimization in Analytical Chemistry will be organised in Amsterdam under the auspices of the Royal Netherlands Chemical Society, Analytical Division. The scientific program will include invited plenary lectures, invited and submitted research papers, as well as discussion sessions.

The topics will be: Design and use of computer systems for data acquisition and processing; Computer controlled analysis and application of microprocessors; Data retrieval, pattern recognition and artificial intelligence; Development and application of formal techniques for design, optimization and evaluation of analytical procedures and results; Application of systems theory, operations research, information theory, mathematics, statistics and other chemometric techniques in analytical chemistry.

The number of participants will be limited to 200. Further information from: The Secretary, Computers and Optimization in Analytical Chemistry, Laboratory for Analytical Chemistry, Nieuwe Achtergrachte 166, Amsterdam, The Netherlands.

12TH INTERNATIONAL SYMPOSIUM ON CHROMATOGRAPHY

The 12th International Symposium on Chromatography will be held in Baden-Baden (Federal Republic of Germany) on 25—29th September 1978.

To be included in the programme are discussion-papers in all fields of chromatography and related techniques as well as a number of invited plenary lectures and reviews. Lectures may be held in English, French or German; in order to facilitate communication however, it is recommended that English be used where possible.

The symposium is jointly organised by the "Chromatography Discussion Group", the "Groupement pour l'Avancement des Methodes Spectroscopiques et Physicochimique d'Analyse" (G.A.M.S.) and the "Arbeitskreis Chromatographie der Fachgruppe 'Analytische Chemie' der Gesellschaft Deutscher Chemiker".

In conjunction with the symposium, an exhibition of instruments and accessories is planned. This exhibition is to be of a new and concentrated form.

Further information from: Geschäftsstelle der Gesellschaft Deutscher Chemiker Abteilung Fachgruppen, Postfach 900440, 6000 Frankfurt/Main 90, B.R.D.

CONFERENCE BRIEFS — NATIONAL BUREAU OF STANDARDS MARCH—JULY 1978

March 13—15 *Construction documentation conference*, NBS Gaithersburg, MD; sponsored by NBS, the Construction Specifications Institute, and the Guide Specifications Committee of the Federal Construction Council; contact, Roger Rensburger, A151 Technology Building, National Bureau of Standards, Washington, D.C. 20234, 301/921-3126.

March 22—24 *28th IEEE vehicular technology conference*, Denver, Colo; sponsored by NBS and the Institute of Electrical and Electronic Engineers; contact, John Shafer, National Bureau of Standards, Boulder, Colo., 80302, 303/499-1000, ext. 3185.

April 10—13 *Trace organic analysis: a new frontier in analytical chemistry*, NBS, Gaithersburg, MD; sponsored by NBS; contact, Harry S. Hertz, A105 Chemistry Building, National Bureau of Standards, Washington, D.C. 20234, 301/921-2153.

April 17—20 *Acoustic Emission Working Group Meeting*, NBS, Gaithersburg, MD; sponsored by NBS and the AEWG; contact, John Simmons, B118 Materials Building, National Bureau of Standards, Washington, D.C. 20234, 301/921-3355.

April 23—26 *American nuclear society topical conference on computers in activation analysis and gamma ray spectroscopy:* Mayaguez, Puerto Rico; sponsored by NBS, American Chemical Society, American Nuclear Society, Energy Research and Development Administration, U. of Puerto Rico, Puerto Rico Nuclear Center; contact, B. S. Carpenter, Bldg. 235, NBS, Washington, D.C. 20234, 301/921-2167.

May 8—10 *Symposium on real-time radiographic imaging*, NBS, Gaithersburg, MD; sponsored by NBS and the American Society for Testing and Materials; contact, Donald A. Garrett, A106 Reactor Building, National Bureau of Standards, Washington, D.C. 20234, 301/921-3634.

June 19—21 *Gas kinetics conference*, NBS, Gaithersburg, MD; sponsored by NBS, Committee on Chemical Kinetics of the National Academy of Sciences/ National Research Council; contact, David Garvin, B154 Chemistry Building, National Bureau of Standards, Washington, D.C. 20234, 301/ 921-2771.

June 26—29 *Conference on precision electromagnetic measurements*, Ottawa, Ontario, Canada; sponsored by Institute of Electrical and Electronics Engineers, U.S. National Committee-International Union of Radio Science, and NBS contact, Dee Belsher, National Bureau of Standards, Boulder, Colo., 80302, 303/499-1000, ext. 3981.

July 17—20 *Fourth annual conference of the American Association for Crystal Growth*, NBS, Gaithersburg, MD; sponsored by NBS and AACG; contact, Robert L. Parker, B164 Materials Building, National Bureau of Standards, Washington, D.C. 20234, 30/921-2961. (777-5)

Analytica Chimica Acta, 96 (1978) 447

Erratum

R. G. Smith, J. C. van Loon, J. R. Knechtel, J. L. Fraser, A. E. Pitts and A. E. Hodges, A Simple and Rapid Hydride Generation — Atomic Absorption Method for the determination of arsenic in Biological, Environmental and Geological Samples, Anal. Chim. Acta, 93 (1977) 61—67.

Table 1, page 66 was printed incorrectly; the correct version is as follows:

TABLE 1

Results for arsenic in standard samples (ppm unless otherwise noted)

Sample	Digestion procedure	Mean value[a]	Standard deviation	Accepted value
NBS 1571 (Orchard Leaves)	acid	10.2	±0.2	11±2
NBS 1633 (Fly Ash)	fusion	59	±3.5	61±6
Incinerated Sludge[b]	fusion	38	±4.2	34[c]
Sludge D[b]	fusion	15	±0.6	12[d]
USGS-W1	fusion	2.3	±0.2	2.4
GSC-SY2	fusion	19.4	±0.9	18[d]
GSC-SY3	fusion	19.3	±1.2	16[d]
GSC-SU1	fusion	524	±29.3	510[d]
GSC-MP1	fusion	0.83%	±0.06%	0.79%

[a]This mean was calculated from the preferred value of each laboratory.
[b]From the Wastewater Technology Centre. P.O. Box 5050, Burlington, Ontario, Canada.
[c]No accepted value. The value used is the average of results obtained from several laboratories.
[d]No accepted value. The value used is that obtained colorimetrically.

ANALYTICA CHIMICA ACTA, VOL. 96 (1978)

AUTHOR INDEX

ANALYTICA CHIMICA ACTA, VOL. 96 (1978)

SUBJECT INDEX

(continued from page 4 of cover)

Short Communications

PRINTED IN THE NETHERLANDS

CONTENTS

(continued on inside page of the cover)